

If

*If you can keep your head when all about you
Are losing theirs and blaming it on you;
If you can trust yourself when all men doubt you,
But make allowance for their doubting too;
If you can wait and not be tired by waiting,
Or, being lied about, don't deal in lies,
Or, being hated, don't give way to hating,
And yet don't look too good, nor talk too wise;*

*If you can dream - and not make dreams your master;
If you can think - and not make thoughts your aim;
If you can meet with triumph and disaster
And treat those two imposters just the same;
If you can bear to hear the truth you've spoken
Twisted by knaves to make a trap for fools,
Or watch the things you gave your life to broken,
And stoop and build 'em up with worn-out tools;*

*If you can make one heap of all your winnings
And risk it on one turn of pitch-and-toss,
And lose, and start again at your beginnings
And never breathe a word about your loss;
If you can force your heart and nerve and sinew
To serve your turn long after they are gone,
And so hold on when there is nothing in you
Except the will which says to them: "Hold on";*

*If you can talk with crowds and keep your virtue,
Or walk with kings - nor lose the common touch;
If neither foes nor loving friends can hurt you;
If all men count with you, but none too much;
If you can fill the unforgiving minute
With sixty seconds' worth of distance run -
Yours is the Earth and everything that's in it,
And - which is more - you'll be a Man my son!*

by Rudyard Kipling

Rational Design and Synthesis of
Receptors for Carboxylates

by

Graham M. Kyne

Doctor of Philosophy

University of Southampton

Faculty of Science

Department of Chemistry

October 2000

UNIVERSITY OF SOUTHAMPTON

ABSTRACT

FACULTY OF SCIENCE

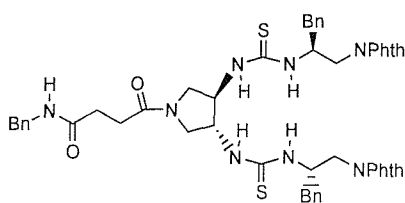
DEPARTMENT OF CHEMISTRY

Doctor of Philosophy

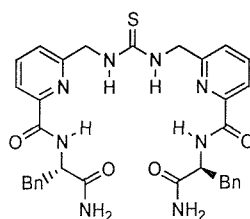
Rational Design and Synthesis of Receptors for Carboxylates

by Graham Michael Kyne

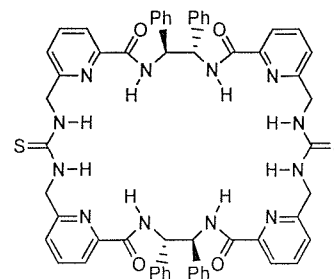
This thesis is concerned with the synthesis and subsequent investigation of the properties of thiourea based receptors for amino acid carboxylate derivatives. Chapter two describes the synthesis of novel bithiourea pyrrolidines such as **123**, which were found to form tightly bound dimers and were consequently unsuitable for the complexation of carboxylate salts. Chapter three describes the synthesis of pyridyl thiourea tweezer receptors, which were found to form well defined complexes with a range of carboxylates. Attention is also given to the level of conformational control (preorganisation) present in the receptor. Both the thiourea and amide hydrogens present in **161** were involved in forming hydrogen bonds to the carboxylate *syn* and *anti* lone pairs and receptor **161** bound a range of chiral carboxylates with enantioselectivities of up to 2:1. Having probed the properties of tweezer based receptors, chapter four goes on to describe the synthesis of a novel bithiourea based macrocycle **193** and examines its behaviour with the *N*-Boc protected dicarboxylate salts of glutamate and aspartate.



123



161



193

Contents

Preface		i
Acknowledgements		ii
Abbreviations		iii
<u>Chapter One</u>	Introduction	1
1.1	Molecular Recognition	1
1.2	Enantioselective Receptors for Amino Acid Carboxylates	1
1.3	Review of Synthetic Receptors for Carboxylates and Carboxylic Acids	3
1.3.1	Guanidinium Receptors for Carboxylates	3
1.3.2	Amidopyridine Receptors for Carboxylic Acids	16
1.3.3	Urea and Thiourea Receptors for Carboxylates	22
1.3.4	Polyaza and Crown Ether Receptors for Carboxylates	30
1.3.5	Miscellaneous Receptors for Carboxylates	36
1.4	Aims of the Project	41
<u>Chapter Two</u>	Synthesis of Pyrrolidine Based Bisthiourea Tweezers	
2.1	Literature Precedent and Receptor Design	42
2.2	Synthesis of Bisthioureas 118 and 123	45
2.3	Binding and Dimerisation Properties of Bisthioureas 118 and 123	48
2.4	Synthesis of Bisguanidiniums	54
2.5	Attempted Catenation of Bisthioureas 118 and 123	56
2.6	Conclusions	57

Chapter Three Synthesis of Dipyridyl Based Thiourea Tweezers

3.1	Receptor Design	58
3.2	Synthesis of Amino Hydrochloride 151	61
3.3	Synthesis of Achiral Pyridyl Tweezer 144	62
3.4	Synthesis of Achiral Benzo Tweezer 145	63
3.5	Binding Studies of Achiral Pyridyl Tweezer 144 and Achiral Benzo Tweezer 145	64
3.6	Synthesis of Chiral Pyridyl Tweezer 161	70
3.7	Synthesis of Chiral Benzo Tweezer 162	70
3.8	Binding Properties of Chiral Tweezers 161 and 162 : Optimisation of Enantioselectivity	71
3.9	Binding Properties of Chiral Thiourea 161 : Investigation of the Preorganisation Hypothesis	75
3.10	Design Concept of Second Generation Tweezer Receptor 183	76
3.11	Synthesis of Second Generation Tweezer Receptor 183	77
3.12	Binding Properties of Tweezer Receptor 183	80
3.13	Conclusions	81

Chapter Four Synthesis of a Novel Bisthiourea Macrocycle

4.1	Receptor Design	83
4.2	Synthesis of Macrocycle 193	85
4.3	Binding Properties of Bisthiourea 193	87
4.3.1	Binding in DMSO-d ₆	88
4.3.2	Binding in Chloroform	91
4.4	Conclusions and Outlook	95

Chapter Five **Experimental**

5.1	General Experimental and Instrumentation	96
5.1.1	General Experimental	96
5.1.2	Instrumentation	96
5.2	Experimental for Chapter Two	97
5.3	Experimental for Chapter Three	113
5.4	Experimental for Chapter Four	127
5.5	Experimental for Binding Studies	130

<u>References</u>	178
--------------------------	------------

Preface

The research described in this thesis was carried out under the supervision of Prof. Jeremy D. Kilburn at the University of Southampton between October 1994 and October 2000. No part of this thesis has been submitted at this or any other University except where specific acknowledgement has been made.

Acknowledgements

My sincere thanks and gratitude go to my supervisor Prof. Jeremy Kilburn who has given me invaluable advice, encouragement and inspiration throughout my project.

I would also like to thank Joan Street and Neil Wells for the numerous times they have either run spectra for me or helped me to sort out the problems that invariably crop up when using NMR spectrometers. Thanks are also due to Dr Jon Essex for his constructive help and advice on molecular modeling and to Dr John Langley and Julie Herniman for their help with mass spectrometry.

Thanks are also due to the dedicated volunteers who proof read my thesis, thanks to Emma Shepherd, Matthew Lucas, Jon Underwood, Faye Watson, Neil Wells and Jed Long. I would especially like to thank both Matthew Lucas, Emma Shepherd and Jed Long for their help at very short notice and for their help way beyond the call of duty, I owe you guys big time!

During my time in Southampton I have made some good friends, who have all given me their trust, support and most importantly their friendship. The space on this page is too small to describe what this has really meant to me, but I would like to mention a few things. Cheers to my housemates Jed Long (for his expertise on alcoholic beverages), Neil Wells (for top class banter) and Jon Griffiths (for numerous 'lively debates'). I would also like to thank members of the Kilburn group past and present. I am particularly indebted to Emma Shepherd for putting up with the 'occasional' moan when my chemistry didn't quite do what it's supposed to do, and also to Faye, Mariangela, David, Tobias, Sara, Jon, Rossella, Lee, Alex, Guillaume and Anawat for their friendship and support.

I would finally like to thank James and Simon Parker, Nigel Senior, Evan Thompson, Malcolm Walker, the Rag committee, Mum, Dad, Stephanie and Peter.

You have all eased the passage over the last few years and I can honestly say you've all really made the difference.

Abbreviations

Boc	<i>tert</i> -butyloxycarbonyl
Bn	Benzyl
CBS	Carboxylate binding site
COSY	Correlated spectroscopy
CPK	Corey, Pauling and Kultan
DCC	<i>N,N'</i> -Dicyclohexylcarbodiimide
DCM	Dichloromethane
DIPEA	<i>N,N'</i> -Diisopropylcarbodiimide
DMAP	4-Dimethylaminopyridine
DME	1,2-Dimethoxyethane
DMF	<i>N,N'</i> -Dimethylformamide
DMSO	Dimethylsulfoxide
DPPA	Diphenylphosphoryl azide
EDC	1-(3-Dimethylaminopropyl)-3-ethylcarbodiimide hydrochloride
ES ⁺ MS	Positive electrospray mass spectrometry
FAB	Fast atom bombardment
FT-IR	Fourier transform infrared
HOBt	1-Hydroxybenzotriazole
HRMS	High resolution mass spectrometry
m.p.	Melting point
n.O.e	Nuclear Overhauser effect
NMR	Nuclear magnetic resonance
NOESY	Nuclear Overhauser effect spectroscopy
obsc.	Obscured
ppm	parts per million
pyr	pyridyl
quant.	Quantitative
Tf	Triflate
TFA	Trifluoroacetic acid
THF	Tetrahydrofuran
TLC	Thin layer chromatography

TMS	Trimethylsilyl
Ts	Tosyl

Amino Acids

Ala	Alanine
Asp	Aspartic acid
Gln	Glutamine
Glu	Glutamic acid
Gly	Glycine
His	Histidine
Ile	Isoleucine
Leu	Leucine
Phe	Phenylalanine
Ser	Serine
Thr	Threonine
Trp	Tryptophan
Tyr	Tyrosine
Val	Valine

Chapter One

Introduction

1.1 Molecular Recognition

The study of the interactions between molecules has been a longstanding venture within science. Early pioneers, including Lehn,¹ Cram² and Pedersen,³ first generated new artificial receptors, which allowed investigations into the fundamental principles governing intermolecular interactions to be performed. These studies led to the birth of supramolecular chemistry. Within supramolecular chemistry, processes such as the binding and selection of a substrate (molecular recognition), transformation of bound species into products, and the translocation of substrates through different media are the principle areas of interest. From the outset, an important goal within supramolecular chemistry has been to emulate and eventually exceed the substrate selectivity observed in biological systems such as enzymes. In nature, important biochemical processes such as protein assembly and genetic information processing rely on molecular recognition processes. Non-covalent interactions are of fundamental importance to all biological processes and this has been the inspiration for efforts made by supramolecular chemists to understand complexation phenomena. The non-covalent interactions involved in the formation of molecular complexes that contribute to the overall binding energy are: hydrogen-bonding, dipole-dipole, electrostatic, van der Waals and hydrophobic interactions. These interactions can be utilised when rationally designing synthetic host-guest systems. The rational design of host-guest systems is motivated by the prospect that advances in the areas of biomimetics, asymmetric catalysis, separation technology and the development of new nanoscale devices can be made.

1.2 Enantioselective Receptors for Amino Acid Carboxylates

One area of interest within the Kilburn group is separation technology. In order to separate racemic mixtures, we hope to synthesise receptors that are: (i) enantioselective, (ii) capable of binding their substrates with sufficient power to draw them across phase boundaries and (iii) able to facilitate transport between separated phases (e.g. in an aqueous-organic-aqueous system). This concept is illustrated schematically in figure 1.1.

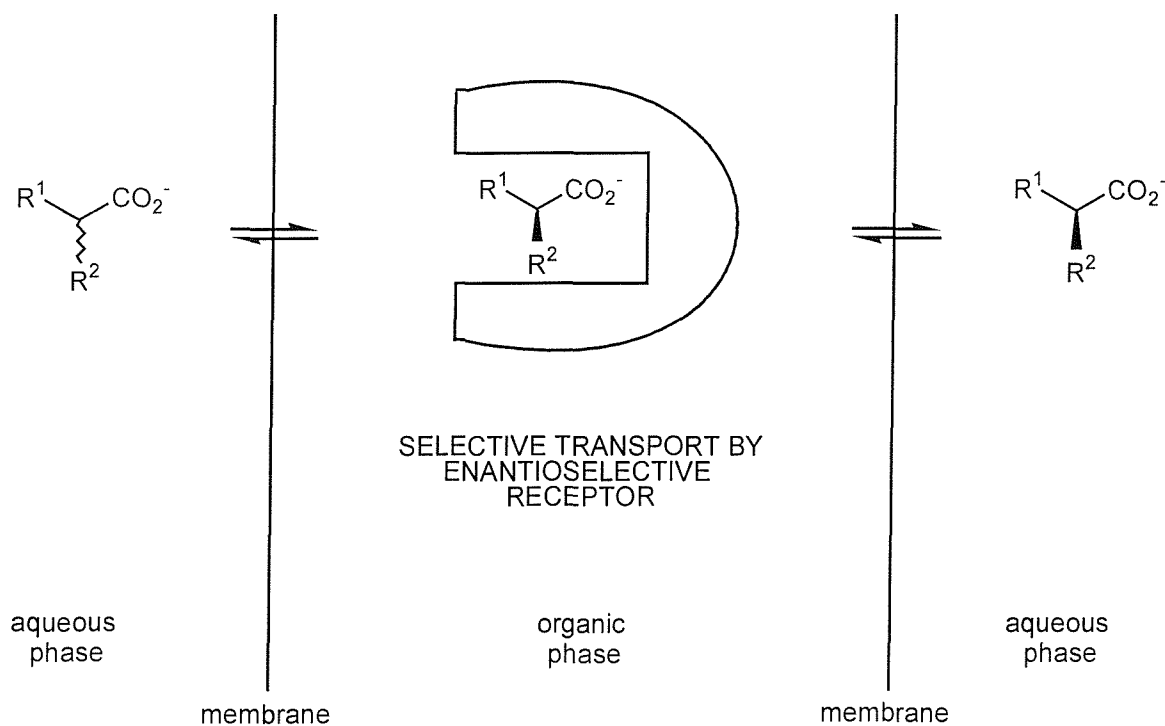


Figure 1.1: Membrane separations of racemic mixtures

Provided the receptor is enantioselective, resolution will be effected. If the receptor is both non-stoichiometric (*i.e.* catalytic in action) and reasonably versatile, then the method could be readily adapted to new challenges faced by industry.

Carboxylic acid derivatives are suitable substrate targets for our separation methodology because they are usually soluble in water as carboxylate salts, can be extracted into organic phases by agents which quench the charge and hydrophilic character of the carboxylate groups, and many important chiral molecules contain the carboxyl group (*e.g.* amino acids).

Before the separation technology outlined above becomes industrially viable, synthetic receptors capable of high levels of enantioselective recognition and transport need to be developed. Below is a review highlighting the major contributions that have been made to the field of carboxylate and carboxylic acid recognition by synthetic receptors. Particular attention is paid to the enantioselective binding of substrates.

1.3 Review of Synthetic Receptors for Carboxylates and Carboxylic Acids

The following review is divided into sections relating to the site within the receptor to which the carboxylate or carboxylic acid group is bound (*i.e.* the carboxylate or carboxylic acid binding site or CBS). Within each section, examples of the way in which the CBS has been used are given, and consideration is given to the strength and selectivity observed between different receptors and substrates. The number of examples given within each section reflects the degree to which each CBS moiety has been utilised in receptor design.

1.3.1 Guanidinium Receptors for Carboxylates

The guanidinium group as a carboxylate binding moiety possesses several useful features. Firstly, it remains protonated over a much wider pH range than the ammonium group due to its high pK_a (which for guanidinium itself is 13.5). The group can also form characteristic pairs of zwitterionic hydrogen-bonds, which provide binding strength due to their charge and structural organisation (as evidenced from the crystal structures of many guanidinium salts). The binding of carboxylate salts involves a bidentate hydrogen-bonding pattern 1 (figure 1.2).

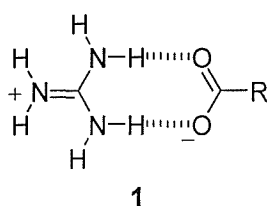


Figure 1.2: Bidentate guanidinium hydrogen-bonding pattern to carboxylates

The guanidinium group of arginyl amino acid residues has an important function in maintaining the tertiary structure of proteins *via* internal ‘salt bridges’ with carboxylate groups. It is also involved in the binding and recognition of anionic substrates by enzyme receptor sites and antibodies.⁴⁻⁶ Lehn was the first to utilise the guanidinium group in the complexation of carboxylates by synthesising a series of structurally different guanidiniums and measuring their association constants with carboxylate salts.⁷ Figure 1.3 shows a

selection of the guanidiniums prepared and lists the association constants with acetate and maleate in a 9:1 methanol/water mixture measured by pH-metric titration experiments.

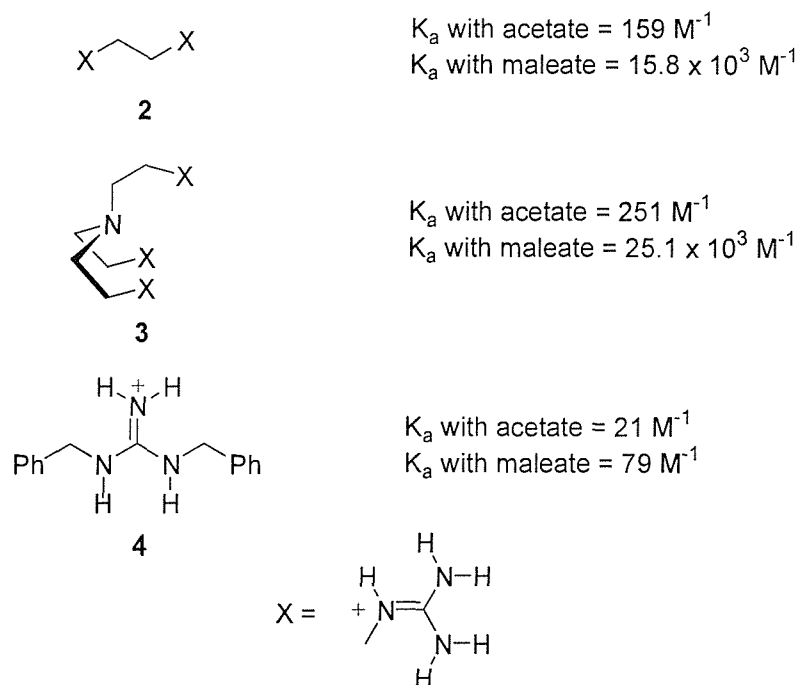


Figure 1.3: Association constants of a series of guanidinium salts 2-4 with acetate and maleate in a 9:1 methanol/water mixture

The association constant for diguanidinium **2** with acetate was 159 M^{-1} and $15.8 \times 10^3 \text{ M}^{-1}$ with maleate. The significant increase in the association constant for maleate with bisguanidinium **2** reflects the fact that there are two guanidinium-carboxylate interactions. The situation was the same for trisguanidinium **3**, which gave an association constant of 251 M^{-1} with acetate and $25.1 \times 10^3 \text{ M}^{-1}$ with maleate, again reflecting the two guanidinium-carboxylate interactions. Monoguanidinium **4** gave an association constant of 25 M^{-1} with acetate and 79 M^{-1} with maleate. The association constant for monoguanidinium **4** with acetate is of the same order of magnitude as **2** and **3**, and is significantly lower than that observed for bisguanidinium **2** and trisguanidinium **3** with maleate, due to only having one guanidinium-carboxylate interaction.

Hamilton has synthesised guanidinium **5** ($pK_a \sim 14$) and found the stabilisation of complementary charges led to exceptionally strong binding between guanidinium **5** and acetate forming complex **6** giving an association constant of $12,000 \text{ M}^{-1}$ in DMSO-d_6 (figure 1.4).⁸

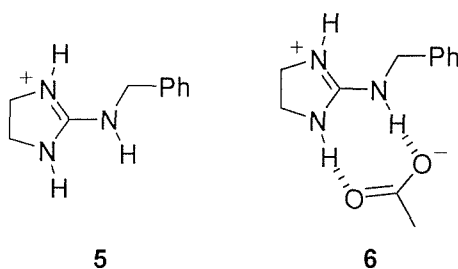


Figure 1.4: Guanidiniums such as **5** exhibit exceptionally strong binding

Lehn and Mendoza have extended simple guanidiniums **2-5** by synthesising chiral receptor **7**, which contained a rigid bicyclic guanidine and two naphthoyl units.⁹ Bicyclic guanidine **7** was found to bind *p*-nitrobenzoate **8** as shown in figure 1.5. The ¹H NMR spectrum of the host-guest complex revealed significant shifts for most signals of both host and guest. The N-H guanidinium protons showed a 1.78 ppm downfield shift in the complex relative to the free host. Most aromatic protons of the host and guest shifted upfield. In a separate experiment, sodium *p*-nitrobenzoate **8** was quantitatively extracted from water by a chloroform solution of **7**. This data strongly supported the formation of complex **9**, which has a well-defined geometry involving double recognition of the guest by the guanidinium cation (zwitterionic hydrogen-bonds with the carboxylate function) and the naphthoyl side arms (π - π stacking with the *p*-nitrophenyl moiety). The association constant with *p*-nitrobenzoate **8** in CDCl₃ was measured to be 1609 M⁻¹.

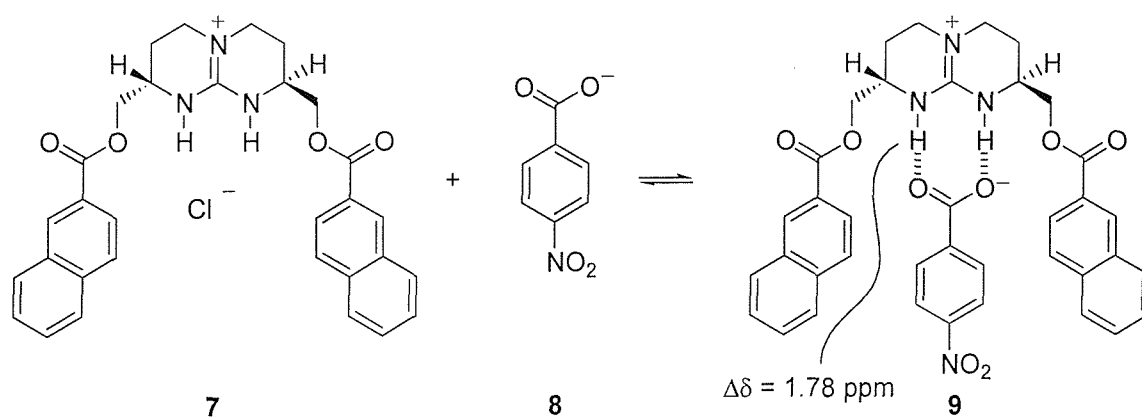


Figure 1.5: Lehn and Mendoza's chiral receptor **7** containing a rigid bicyclic guanidine

Mendoza altered the design of receptor **7** to generate receptor **10** for amino acids.¹⁰ The new receptor still featured a guanidinium as the binding site for carboxylate, but in addition incorporated a crown ether to bind ammonium, whilst keeping an aromatic planar surface (the naphthalene ring) for selective π -stacking interactions with the side chains of aromatic

amino acids. The receptor possessed a chiral structure (*S,S*-isomer shown) to allow enantioselective recognition (figure 1.6). The affinity of **10** toward amino acids was determined by liquid-liquid single extraction experiments, in which an aqueous solution of L-Trp **11**, L-Phe, or L-Val was extracted into a CH₂Cl₂ solution of **10**.

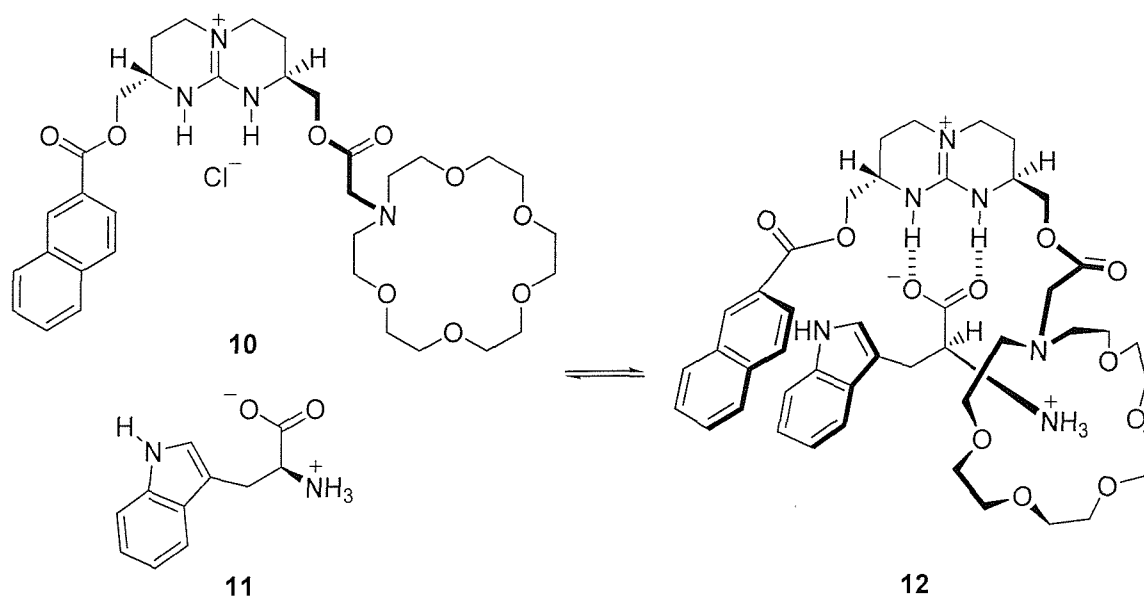


Figure 1.6: Mendoza's modified receptor **10** incorporating a crown ether moiety

The extraction efficiencies (*i.e.* the fraction of receptor molecules occupied by the substrate in the organic phase) as determined by NMR integration, were around 40% for L-Trp and L-Phe, but L-Val, without any aromatic side chain, was not detected. A competition experiment with a mixture of all three amino acids resulted in 100:97:6 Phe:Trp:Val ratios. Chiral recognition was confirmed by the observation in the NMR spectrum, that the corresponding *D*-enantiomers were not extracted. Reciprocally, use of (*R,R*)-**10** allowed the extraction of *D*-Phe or *D*-Trp, but not the *L*-enantiomers. A more precise account of the selectivity was achieved by HPLC analysis of diastomeric dipeptides, prepared from extracts of racemic samples of Phe or Trp and a suitable optically pure *L*-Leu derivative. The amount of *D*-isomer in the extracts was lower than 0.5% for *D*-Trp (determined as *L*-Leu-*D*-Trp) and 2% or less for *D*-Phe (as *L*-Leu-*D*-Phe). This high degree of chiral recognition can be explained by the three simultaneous non-covalent interactions of the substrate with the flexible and foldable receptor. ¹H-NMR data (upfield shifts for the naphthoyl protons) support the binding model illustrated in figure 1.6 for a 1:1 complex **12** of (*S,S*)-**10** with L-Trp **11**.

Schmidtchen has also used the rigid bicyclic guanidinium moiety to generate bisguanidinium **13** (figure 1.7), which was found to bind a range of dicarboxylate anions in methanol.¹¹ With monoanions (iodide and acetate) no change in chemical shift was observed at all. Dianions however, showed complexation induced shifts which could be cleanly fitted to a 1:1 host to guest stoichiometry. Though all dicarboxylates were bound by **13** in methanol, there were found to be peculiar quantitative differences. Despite its flexibility host **13** exhibits a preference for malonate (entry 3) over the shorter or longer analogs. Moreover, even the most rigid and extended guest (entry 7 in figure 1.7) is bound with considerable stability, indicating the adaptability of the host to the guest structure.

entry	substrate	K_a/M^{-1}
1		225
2		2540
3		16500
4		854
5		1240
6		833
7		633

Figure 1.7: Schmidtchen's bicyclic guanidinium receptor **13** for dicarboxylates

Diedrich has also constructed receptors for dicarboxylates.¹² His approach was to attach two phenylamidinium units to 1,1'-binaphthalene scaffolds (figure 1.8). The 1,1'-binaphthalene derivative (\pm)-**14** was found to be a highly efficient receptor for dicarboxylate guests, such as glutarate and isophthalate, even in competitive protic solvents such as methanol.

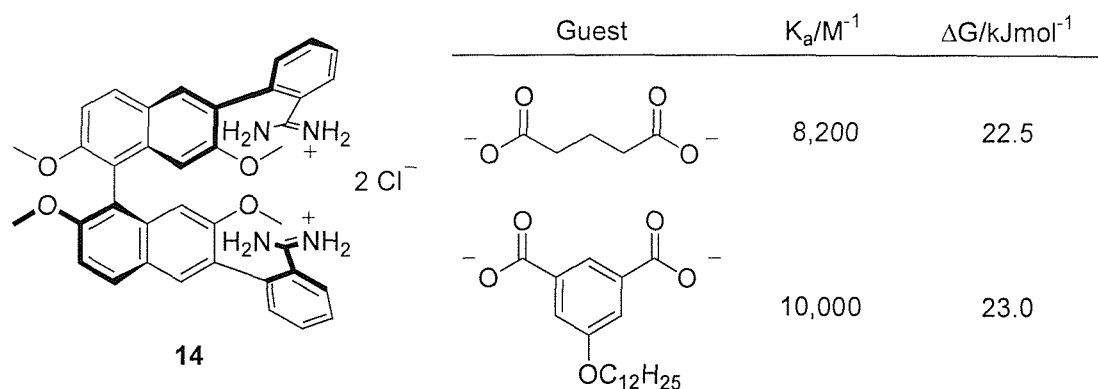


Figure 1.8: Diedrich's 1,1'-binaphthalene amidinium receptor **14** for dicarboxylates

A satisfactory fit of the titration data to the 1:1 host-guest complex model yielded association constants in the range 5000 – 10,000 M^{-1} (figure 1.8). A *van't Hoff* analysis of variable-temperature 1H -NMR titrations and isothermal microcalorimetry revealed that complexation in methanol is strongly entropically driven, with an unfavourable enthalpic change which partially compensates the entropic gain. These thermodynamic quantities were best explained by a particularly favourable solvation of the binding partners in the unbound state and the release of the methanol molecules, which solvate the free ions into the bulk solution upon complexation. Receptor (\pm)-**14** binds flexible glutarate and rigid isophthalate with similar association strength. The lack of response to guest preorganisation and poor guest selectivity is explained by the non-directionality of the coulombic charge-charge interactions in the complexes. Attempts to investigate the complexation of dicarboxylates by receptor (\pm)-**14** in water led to the precipitation of a solid. This precipitate was re-dissolved in DMSO- d_6 , and integration of the 1H NMR resonances confirmed that it consisted of the host-guest complex, with a 1:1 stoichiometry in each case.

Schmuck has also prepared some acyclic guanidinium receptors, which took the form of guanidinocarbonyl pyrroles such as **15** and **17** (figure 1.9).^{13, 14} Receptors **15** and **17** bound carboxylates by ion pairing in combination with multiple hydrogen-bonds. Guanidinium **15** incorporated a pyrrole NH to act as an additional hydrogen-bonding donor to carboxylate guests as shown in complex **16**. For selective binding of *N*-acetyl- α -amino acids, these primary interactions provided the necessary binding energy even in polar solvents, with additional interactions between the amino acid side chain and receptor being used to achieve selective recognition in **17**.

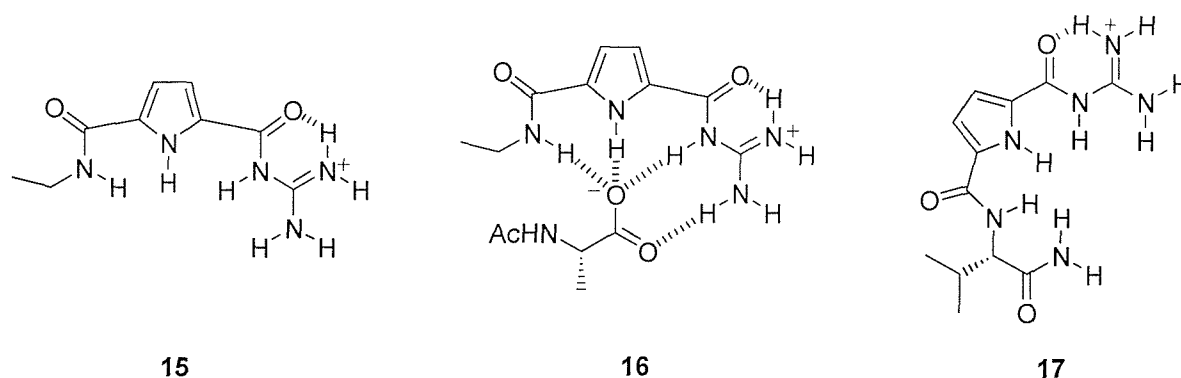


Figure 1.9: Schmuck's 2-(guanidinocarbonyl)pyrrole receptors **15** and **17**
(as picrate salts) for carboxylates

Receptor **15** was found to bind *N*-Ac- α -amino acid carboxylates in 40% H₂O/DMSO with association constants ranging from $K_a = 360$ to 1700 M^{-1} , depending on the structure of the amino acid side chain. Chiral receptor **17** bound carboxylates with association constants in the range $K_a = 350$ to 5275 M^{-1} in 40% water/DMSO. Receptor **17** was also able to enantioselectively bind amino acid carboxylates. The association constants for the enantiomers differed by a factor of 1.2 for phenylalanine and tryptophan and 1.6 for alanine. In the case of alanine and tryptophan, the L-enantiomer was bound better than the D-enantiomer, whereas with phenylalanine the D-enantiomer was preferred. These binding selectivities were rationalised by using molecular modeling calculations. It was found that with D-alanine there was an unfavourable steric repulsion between the methyl group of the amino acid and the isopropyl side chain of the receptor, which was not present in the complex with the L-enantiomer. In agreement with this, the association constant for the D-enantiomer was slightly lower than with the ethyl substituted receptor **15**, which lacks the sterically demanding isopropyl group. Accordingly, the association constant for **17** was larger relative to the binding by **15** due to an additional hydrogen-bond. With phenylalanine and tryptophan the aromatic system and the guanidiniocarbonyl pyrrole moiety of the receptor were found to be π -stacked. However, the side chains of amino acids which were bulkier than alanines methyl group, caused unfavourable steric interactions with the isopropyl group of the receptor and decreased the binding energy for both enantiomers relative to the binding of alanine. In the case of phenylalanine the association constants were again lower than with the ethyl substituted receptor **15** ($K_a = 1700\text{ M}^{-1}$). The steric repulsion was more severe in the complex with the L-enantiomer, whereas the D-enantiomer can adopt a complex conformation, which orientates the isopropyl group further away from

the *N*-acetyl group. In the complexes with tryptophan the association constants were slightly larger than with **15** ($K_a = 810 \text{ M}^{-1}$), probably because of the more extensive hydrophobic interactions or π -stacking, which is much better in the complex with the L-enantiomer.

Morán has synthesised planar receptor **18** (figure 1.10).¹⁵ This receptor includes a xanthone scaffold in addition to a guanidinium moiety and also incorporates a third hydrogen-bond from the xanthone NH to the carboxylate oxygens and possible π -stacking interactions with the diisopropylbenzoate residue.

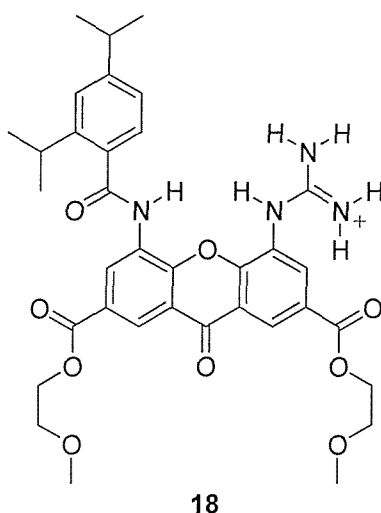
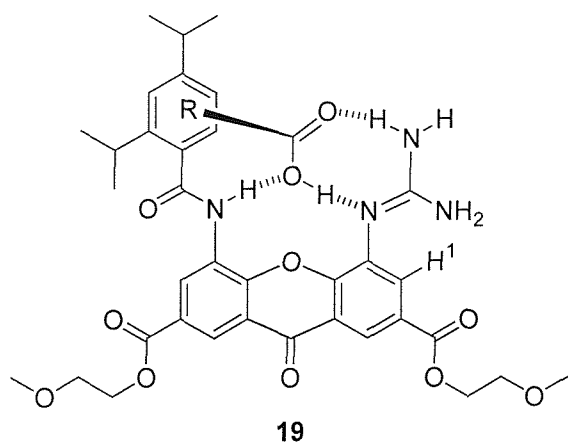


Figure 1.10: Morán's xanthone based receptor **18**

Addition of tetramethylammonium methanesulfonate to a solution of receptor **18** led to a large shift of the methanesulfonate signal in the ^1H NMR spectrum. Attempts to titrate tetramethylammonium acetate in CDCl_3 with receptor **18** using ^1H NMR spectroscopy did not afford the expected pattern for movement of the acetate methyl group. At the initial stages of the titration, shielding was observed (from 2.08 ppm to 1.55 ppm) but at a later stage a downfield shift took place (from 1.55 ppm to 1.85 ppm). Attempts to titrate other carboxylates in DMSO with the same receptor gave downfield shifts instead of the expected shielding of the carboxylate α -groups. These results were in agreement with a proton transfer from the guanidinium to the carboxylate. No complex was formed in DMSO between the neutral species, as the final chemical shifts of all guests corresponded well to those of the carboxylic acids in DMSO. A further clue pointing to the acidity of guanidinium **18** was that the neutral guanidine **19** (figure 1.11) could be obtained by washing the ethyl acetate solution with aqueous sodium hydrogencarbonate. Even though

no complex formation was expected for conventional carboxylic acids in DMSO, CPK models showed that in fact the free receptor of **19** may well be a good binder of acids. As is the case with Hamilton's amidopyridine receptors (section 1.3.2), the basicity of the nitrogen atoms were found to strongly favour association with the acidic carboxylic acid hydrogen. In a less competitive solvent such as CDCl₃, association takes place with decanoic acid giving an association constant of $6 \times 10^4 \text{ M}^{-1}$ (figure 1.11). In this case, the expected shielding of the methylene group does take place (from 2.26 to 1.55 ppm). The association constants of several acids of increasing pK_a were measured by means of a competitive scale to see if a hydrogen-bond arose when the acidity of the guest matched that of the guanidine. More than a thousand fold increase was observed on passing from decanoic acid (pK_a = 4.9) to monochloroacetic acid (pK_a = 2.9). To rule out the possibility that proton transfer might be interfering with the K_a measurement, a study of the UV spectra of receptor **19** was undertaken. To reduce complex formation, which could complicate data interpretation, DMSO was used as the solvent. Because a solvent with a high dielectric constant would favour proton transfer between neutral compounds, it was thought that if no such transfer was observed in DMSO, it would not be expected to occur in CDCl₃ either. While acetic and decanoic acid gave no change in the UV spectrum of receptor **19**, dichloroacetic acid led to the protonated guanidine. Addition of 1.5 equivalents of monochloroacetic acid afforded a spectrum which was similar to that of the protonated species but not superimposable. Larger amounts of monochloroacetic acid (5 equivalents) did not further change the spectrum. Morán attributed this to complex formation. When receptor **19** was titrated with monochloroacetic acid in DMSO, a K_a of $1.8 \times 10^4 \text{ M}^{-1}$ was measured. Strong deshielding was observed for proton H1 ($\Delta\delta = 0.53 \text{ ppm}$) *ortho* to the guanidine group. When saturation was reached, the addition of either dichloro or trichloroacetic acid further shifts proton H1, in agreement with final guanidinium protonation. It was concluded that monochloroacetic acid associates with receptor **19** in a very competitive solvent such as DMSO and that, under these conditions, small differences in the pK_a of the acid may yield large changes in the association constants.



Guest	K_a/M^{-1}
Dichloroacetic acid	1.4×10^9
Monochloroacetic acid	6.5×10^7
Decanoic acid	6.0×10^4

Figure 1.11: K_a values of various acids with guanidine **19** in $CDCl_3$

Davies has described the synthesis of steroidal based guanidinium receptors which are based on a cholic acid scaffold **20** (figure 1.12).¹⁷ The secondary hydroxy groups in cholic acid **20** were modified to generate receptors of type **21**. Groups A-C were spaced so as to allow co-operative effects on the substrate with minimum interference from intramolecular interactions. In order to achieve carboxylate extraction, one of the groups A-C was chosen to form a specific, electroneutral complex with the anionic centre. Thus, a guanidinium unit was chosen (figure 1.12). Solutions of **22** and **23** were able to extract carboxylic acids from neutral or basic aqueous solutions, presumably through exchange of chloride for carboxylate. In the case of *N*-Ac- α -amino acids the 1H NMR spectra of the complexed substrates were enantiomer dependent, allowing the determination of enantioselectivities, as well as extraction efficiencies, by simple integration. The results are shown in table 1.1.

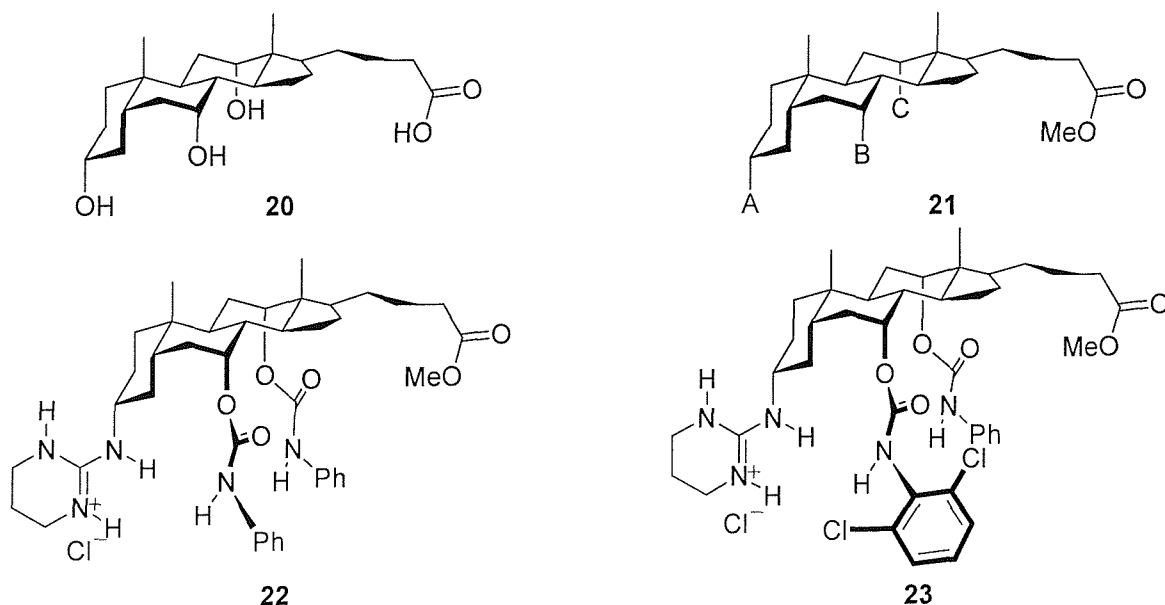


Figure 1.12: Davies' steroidal guanidinium receptors **22** and **23** for carboxylates in chloroform

Substrate	Receptor 22		Receptor 23	
	Extraction efficiency (mol%)	Enantio-selectivity (L:D)	Extraction efficiency (mol%)	Enantio-selectivity (L:D)
<i>N</i> -Ac-alanine	52	7:1	76	6:1
<i>N</i> -Ac-phenylalanine	87	7:1	93	9:1
<i>N</i> -Ac-tryptophan	83	7:1	92	6:1
<i>N</i> -Ac-valine	71	7:1	89	9:1
<i>N</i> -Ac- <i>tert</i> -leucine	†	†	82	5:2
<i>N</i> -Ac-methionine	†	†	93	9:1
<i>N</i> -Ac-proline	†	†	74	4:1
<i>N</i> -Ac-asparagine	0	†	0	†

Table 1.1: Extraction efficiencies of guanidiniums **22** and **23** towards various amino acid derivatives († not tried)

The extraction efficiencies were moderate to good for substrates with non-polar side-chains, although neither receptor was effective with the polar asparagine derivative. Receptor **22** proved remarkably consistent in its ability to differentiate between enantiomers, irrespective of side-chain bulk. Receptor **23** showed generally higher extraction abilities, possibly due to the greater acidity of the dichlorophenylcarbamoyl NH, and was more sensitive to side-chain structure. Perhaps surprisingly, the substrate with the most sterically hindered asymmetric center (*N*-Ac-*tert*-leucine) gave the lowest selectivity. ¹H NMR spectroscopy and molecular modeling both suggested plausible models for the binding geometries. A Monte Carlo Molecular Mechanics search on the complex between **23** and *N*-Ac-L-valinate yielded the configuration in which the carboxylate accepts hydrogen-bonds from the 7-carbamoyl and two guanidinium NH groups, while the acetyl oxygen was bound to the 12-carbamoyl NH. In support of this structure, it was found that upon complexation the receptor carbamate and 2 of the 3 guanidinium NH signals in the ¹H NMR spectrum moved downfield, while a weak intermolecular n.O.e was observed from the α -CH in *N*-Ac-L-valinate to the *ortho* protons in the phenyl groups of receptor **23**.

Anslyn has synthesised trisguanidinium **24**, which was found to be a chemosensor (synthetic sensor coupled with a signaling element) for citrate **25** in beverages.¹⁸ Trisguanidinium **24** was used to detect a specific compound in a multicomponent aqueous solution, in a manner similar to that of antibody-based biosensors in immunoassays. Receptor **24** was selective for the recognition of citrate in water over di- and monocarboxylates, phosphates, sugars, and simple salts, binding citrate better than simple dicarboxylic acids and monocarboxylic acids by factors of approximately 35 and 700 respectively. The receptor consists of three guanidinium groups for hydrogen-bonding and charge pairing with citrate. The steric gearing imparted by the ethyl groups on the 2-, 4-, and 6-positions ensures that the guanidinium moieties are preorganised on the same face of the benzene ring. This conformation yields several hydrogen-bonds and three sets of ionic interactions in the host-guest complex (figure 1.13), leading to good binding in water with a measured K_a of $6.8 \times 10^3 \text{ M}^{-1}$.

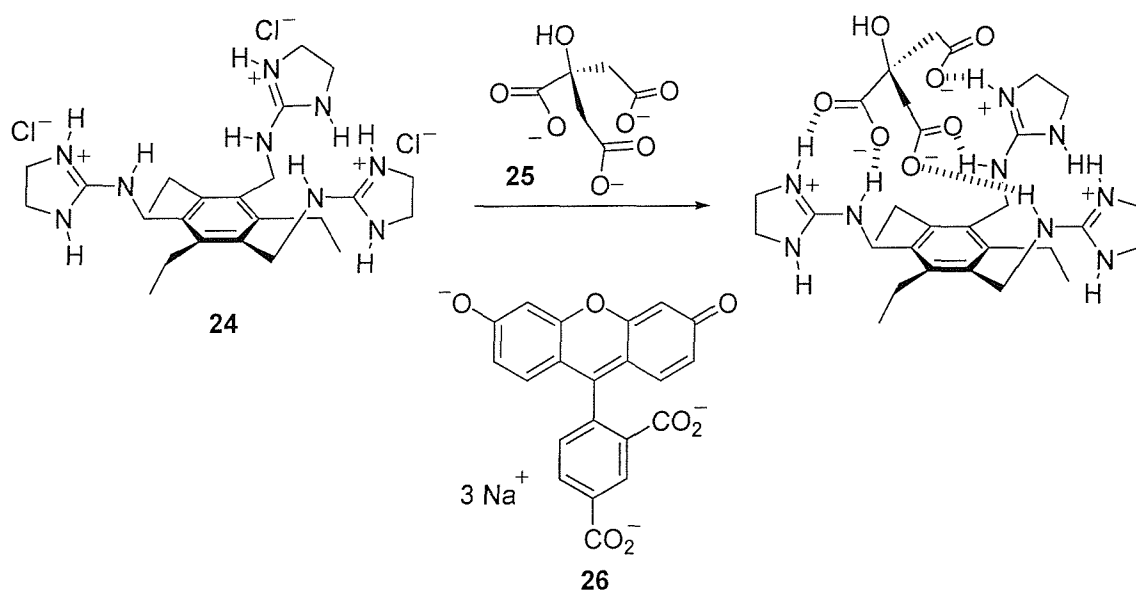


Figure 1.13: Chemosensor **24** for citrate in beverages

Anslyn's assay for citrate employed an ensemble of 5-carboxy-fluorescein **26** (a fluorescent probe) and **24**. The binding between **24** and **26** was observed to lower the pK_a of the phenol moiety of **26** due to the positively charged microenvironment presented by **24**. This shift in pK_a caused the phenol moiety to be in a higher state of protonation when **26** was free in solution. The absorbance or fluorescence of **26** is known to decrease with higher protonation of the phenol, hence, it was found that upon introduction of citrate to a mixture of **24** and **26** the absorbance and fluorescence of **26** decreased. Determining the

concentration of citrate in a large range of beverages was achieved by simply adding between 2 and 50 μL of the beverage to the sensing ensemble, determining the absorbance or fluorescence, and reading the amount of citrate off the calibration curves.

Kelly has described the first example of a molecular Vernier **27**,¹⁹ where three molecules of dicarboxylate **28** were found to combine with two molecules of a trisguanidinium **29** to give a pentamer of predetermined dimension (figure 1.14). In the Vernier mechanism, two complementary components having different unit lengths undergo side-by-side linear aggregation. Growth continues until the tips of the adjacent aggregates come into register, like the lines of a Vernier, whereupon growth ceases. Generation of **27** was achieved simply by mixing solutions of **28** and **29**. Vernier **27** spontaneously precipitated from the solution in >95% yield and in analytically pure form.

Particularly noteworthy was the finding that the Vernier was invariably produced in near quantitative yield regardless of the stoichiometry of the two components. Vernier formation was found to proceed until all of the limiting component was consumed, as determined by the amount of the insoluble Vernier produced and by NMR assay of the supernatant.

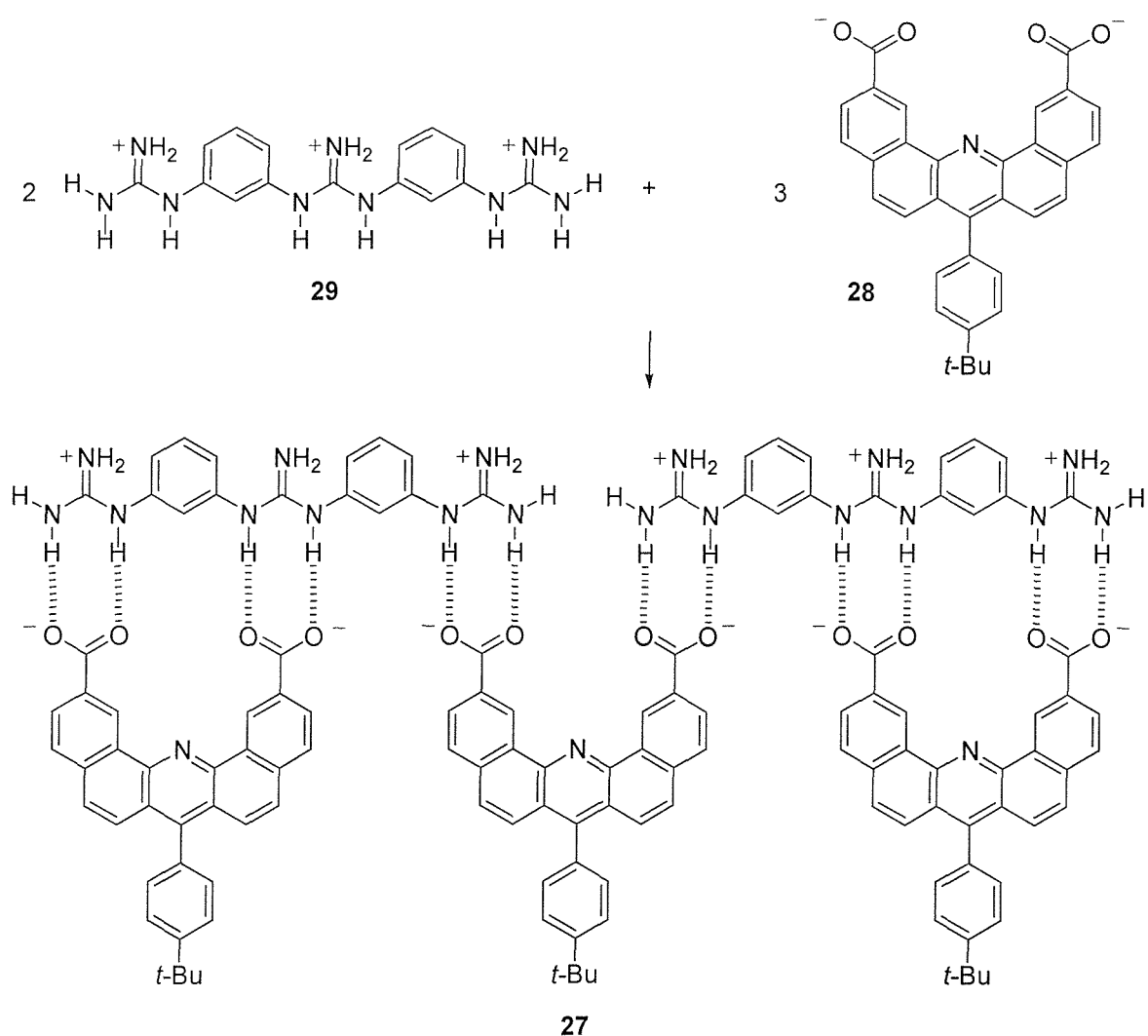


Figure 1.14: Kelly's molecular Vernier 27

1.3.2 Amidopyridine Receptors for Carboxylic Acids

The feature of the amidopyridine structural motif that has been utilised in a number of carboxylic acid receptors is its ability to form two complementary hydrogen-bonds from the carboxylic acid hydrogen to the pyridine nitrogen and the carboxylic acid carbonyl to the amide hydrogen as shown by complex **30** (figure 1.15). Hamilton was the first to use this motif to bind carboxylic acid derivatives when he incorporated two amidopyridine units in macrocycle **31** to bind diethyl malonic acid with an association constant of $7,300 \text{ M}^{-1}$ ($\Delta G = 22.0 \text{ kJ mol}^{-1}$) in CDCl_3 .⁸

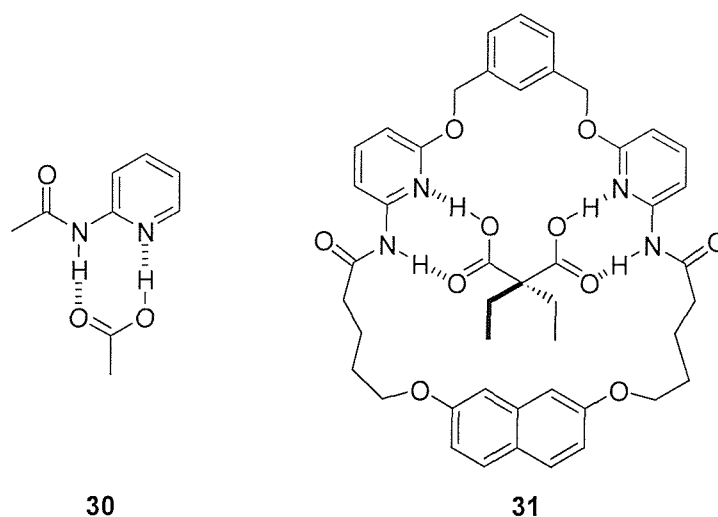


Figure 1.15: Hamilton's diethyl malonic acid receptor **31**

Helmchen has extended the two fold parallel hydrogen-bonds shown in **30** by incorporating an additional hydrogen-bond to the carbonyl oxygen *syn* lone pair in molecular clefts of type **32** (figure 1.16).²⁰ A series of sterically similar, yet electronically different hosts were prepared and the interaction of R¹ and R² examined. The capacity of the hosts synthesised to discriminate between enantiotopic nuclei was tested by monitoring their ability to induce chemical shift changes of enantiotopic protons.

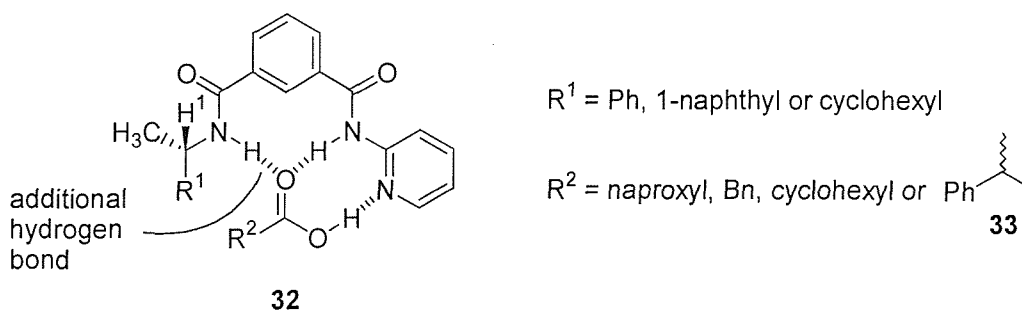


Figure 1.16: Helmchen's receptor **32** for carboxylic acids

One equivalent of the carboxylic acid was added to the host in CDCl₃. When R¹ = Ph or 1-naphthyl, carboxylic acid guests containing aromatic ring systems such as naproxen, phenylacetic acid and hydratropic acid **33** were found to cause the chemical shift of H1 to alter in the range $\Delta\delta = 0.279$ - 0.283 ppm. That host **32** did not induce measurable changes of H1 in any of the substrates when R¹ = cyclohexyl indicated π - π stacking interactions were occurring. Receptor **32** was also found to bind the *S*-enantiomer of hydratropic acid **33** ($K_a =$

1,100 M⁻¹) with a stronger association constant than that observed for the *R*-enantiomer ($K_a = 700 \text{ M}^{-1}$).

Kilburn has synthesised a novel receptor **34** which was found to bind the monopotassium salts of various dicarboxylic acids in chloroform solution.²¹ A combination of hydrogen-bonding interactions and an electrostatic association between the carboxylate anion and a crown ether bound potassium cation were used. The binding mode proposed in figure 1.17 was supported by considering the various extraction experiments, intermolecular n.O.e experiments and FAB mass spectrometry data.

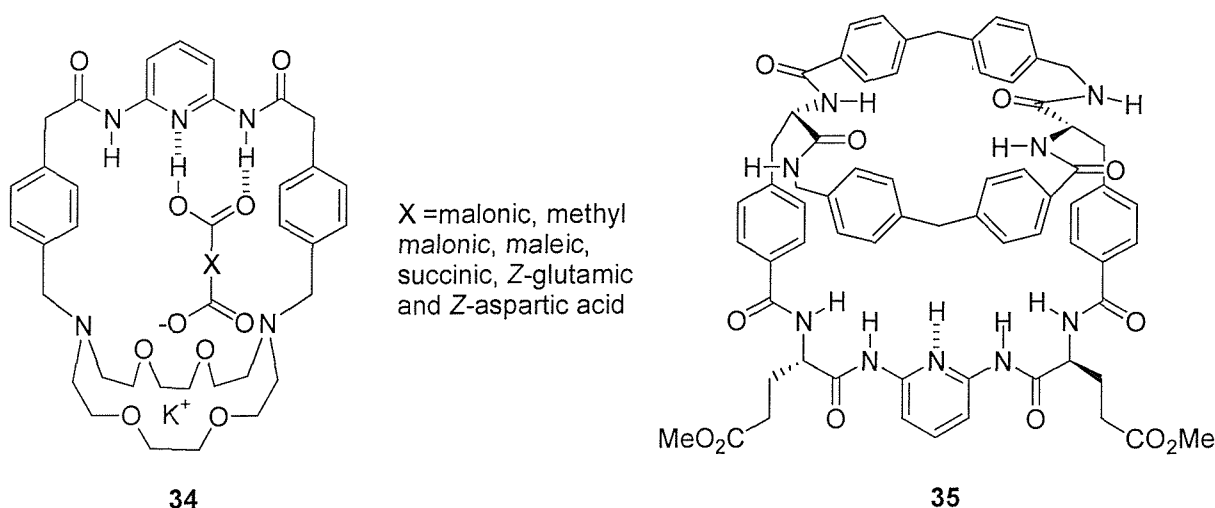


Figure 1.17: Kilburn's macrocyclic receptor **34** for monocarboxylate salts of diacids and macrobicyclic receptor **35** for dipeptides

A variety of monopotassium salts of diacids were extracted to varying extents (between 3 and 65%) in both solid-liquid and liquid-liquid extraction experiments. Shifts of the amide NH signals in the ¹H NMR spectra provided good evidence for hydrogen-bonding between the acid and diamidopyridine unit. The complex formed between macrocycle **34** and methylmalonic acid gave good intermolecular n.O.e signals for both the methyl doublet and the α -proton of the substrate to the aromatic protons of the benzene rings forming the side wall of the cavity. Samples of chloroform solutions of the complex containing the monopotassium salts of methylmalonic acid and maleic acid, and phenyl phosphinate were also studied by FAB mass spectrometry. In each case a peak corresponding to macrocycle + potassium ($M + K$)⁺, was observed in the positive ion FAB spectrum. The negative ion FAB

spectra, however, gave peaks corresponding to macrocycle + anion (carboxylate) complexes, $(M + A)^-$ with a daughter ion $(M-H)^-$, while under the same experimental conditions, the free macrocycle did not give any signal. In addition, the monopotassium salt of fumaric acid (which does not bind to the receptor according to the extraction experiments) gave no signal, confirming that adduct ion formation was not occurring in the ionisation of these samples. It was thought that upon fast atom bombardment, the complex can lose the potassium cation but the resultant bimolecular species, held together by the interaction of the carboxylic acid with the amidopyridine, remains intact. This, along with the extraction and NMR experiments, provided strong evidence for the proposed binding mode.

Kilburn has also synthesised a number of peptide receptors such as macrobicycle **35**,²² which feature a specific binding site for peptides with a free acid terminus (figure 1.17). The macrobicycle contains a diamidopyridine unit at the base of a bowl-shaped cavity and also incorporates peptide and aromatic ring functionality to form the walls and rim of the bowl. The macrocycle was found to bind a range of substrates, but was found to be a particularly strong and selective receptor for the peptide sequence Cbz-L-Ala-L-Ala-OH with a very high association constant of $33,000 \text{ M}^{-1}$ ($\Delta G = 25.3 \text{ kJ mol}^{-1}$).

Kilburn has also recently synthesised receptor **36** for peptides with a carboxylic acid terminus.²³ Solid-phase synthesis was employed to construct tweezer receptor **36** (figure 1.18), which was designed to bind to the carboxy terminus of peptides in organic media. A diamidopyridyl binding site was used to provide the primary binding interaction for the carboxylic acid. The tweezer arms have the potential to form both hydrophobic and β -sheet-like hydrogen-bonding interactions with the back bone of the peptide substrate. Unfortunately, tweezer receptor **36** was insoluble in neat CDCl_3 and CD_3CN , thus preventing NMR studies on the formation of a complex with DNS-L-Glu(O^tBu)-L-Ser(O^tBu)-L-Val-OH (a consensus peptide sequence from screening an inverted peptide library against a single tweezer receptor). However, a $500 \mu\text{M}$ solution of **36** in $\text{DMSO}:\text{CHCl}_3$ (2:98) could be prepared and complexation studies were carried out on this solution. The intensity of the fluorescence emission maximum for the dansyl group of the peptide guest decreased as successive aliquots of tweezer receptor **36** were added, with the drop in intensity exhibiting typical saturation. The data from this experiment showed a good fit for the presumed 1:1 binding and allowed an estimation of the association constant as 2.6

$\times 10^5 \text{ M}^{-1}$. It was concluded that, as anticipated, the incorporation of a specific binding site for the carboxylic acid terminus of peptide guests into a tweezer structure provided a considerably higher affinity than with a non-specific head group.

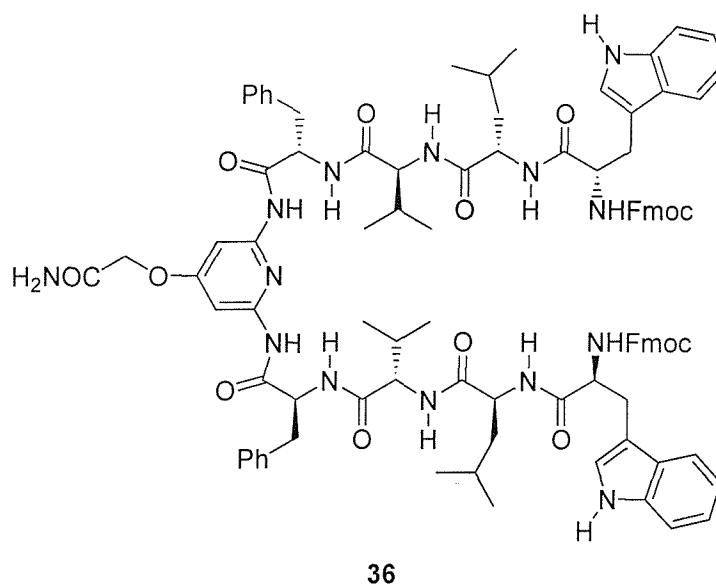


Figure 1.18: Kilburn's tweezer receptor **36** for *N*-terminal carboxylic acid peptides

As mentioned earlier Hamilton has used two amidopyridine units in macrocycle **31** to bind diethyl malonic acid using four hydrogen-bonds (figure 1.15).⁸ A wider separation of the two hydrogen-bonding regions was found to minimise carboxylic acid – carboxylic acid interactions and was found to change the binding specificity to longer dicarboxylates (figure 1.19). The association constant for macrocycle **31** with diethyl malonic acid was $7,300 \text{ M}^{-1}$ and for diamide **37** with adipic acid, in excess of $1 \times 10^5 \text{ M}^{-1}$. The lower association constant for macrocycle **31** with diethyl malonic acid reflects the unfavorable planar conformation required for binding into the macrocycle cavity. A solid-liquid extraction experiment found that a 1:1:1 mixture of diglycolic, benzene-1,4-diacetic and adipic acids in a CDCl_3 solution of diamide **37** resulted in the selective extraction of adipic acid into the solution.

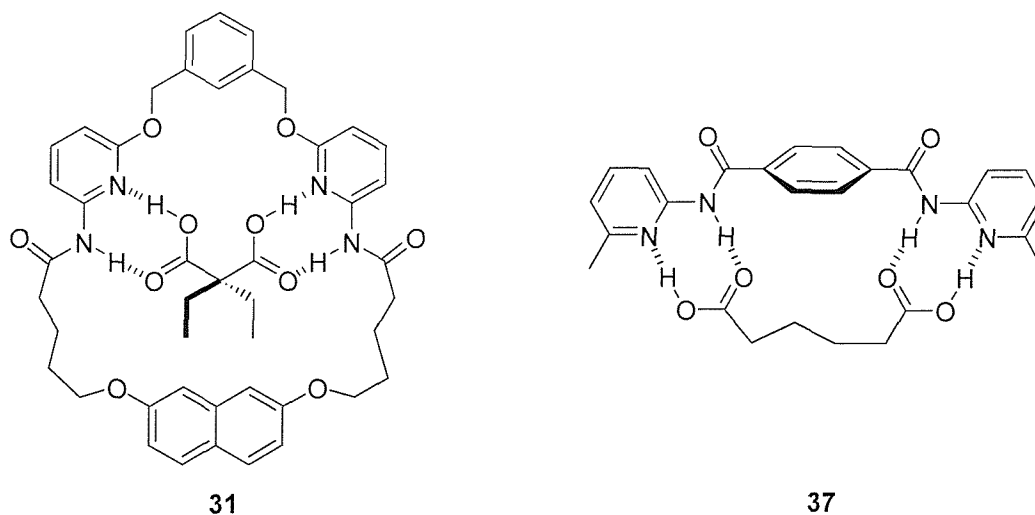


Figure 1.19: Hamilton's diacid receptors 31 and 37

Using a similar approach Diederich has synthesised helicopodand **38** (figure 1.20), incorporating two pyridinecarboxamides as the dicarboxylic acid binding site.²⁴

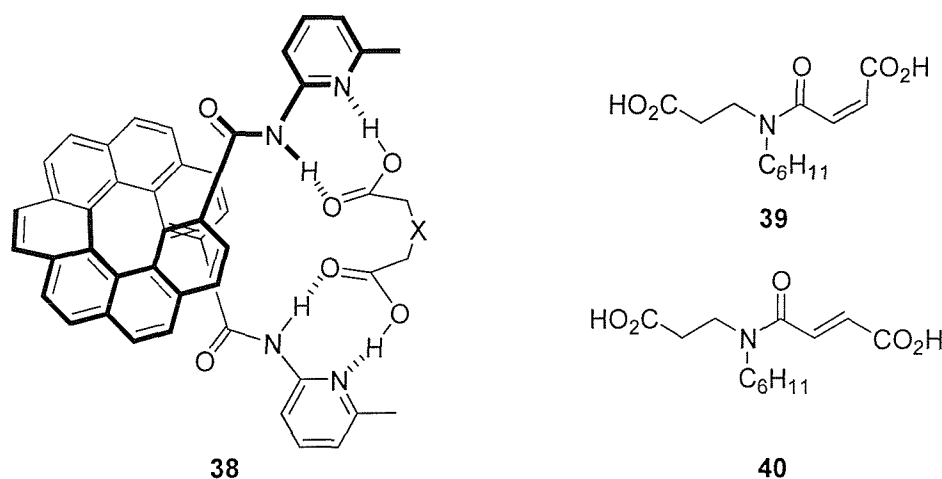


Figure 1.20: Diederich's helicopodand receptor 38 for diacids

In the productive 'in-in' conformation, **38** forms stable 1:1 complexes with α,ω -dicarboxylic acids. Diastereoselectivity of complexation was measured to be $\Delta\Delta G = 1.4 \text{ kcal mol}^{-1}$ for **39** and **40**, which differ only in the configuration at their double bond. Modeling suggested only the *E* derivative **39** possessed the correct geometry for a ditopic four-fold hydrogen-bonding interaction between its two carboxylic acid residues and the two CONH(py) groups in **38**. Diederich also prepared optically active molecular cleft **41**, which incorporated a spirobi[fluorene] spacer and two naphthyridinecarboxamide moieties as hydrogen-bonding sites (figure 1.21).²⁵

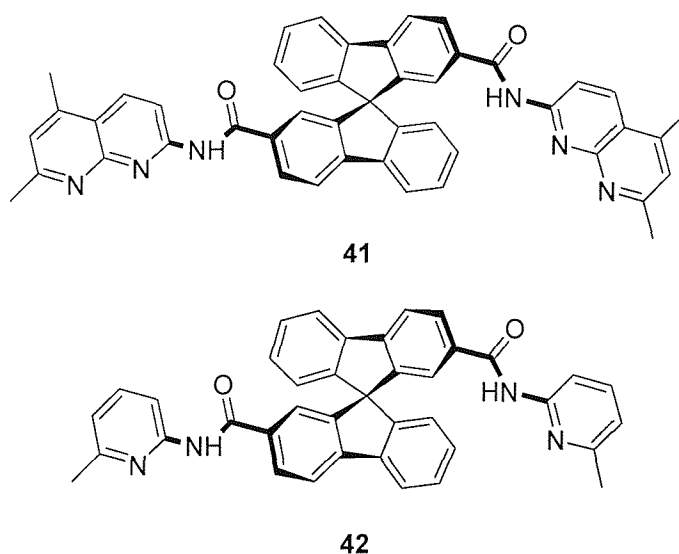


Figure 1.21: Diederich's spirobi[fluorene] based receptors **41** and **42**

Solution binding studies in CDCl_3 showed **41** was able to complex optically active dicarboxylic acids with a diastereoselectivity of complexation ($\Delta\Delta G$) between 0.5 and 1.6 kcal mol^{-1} . By covalently binding a closely related structure to silica gel a chiral stationary phase was generated. HPLC separations of racemic diacids in different solvents suggested that the attractive interactions between solute and immobilised chiral selector were a combination of hydrogen-bonding, which prevails in apolar eluants, and aromatic π - π stacking, which dominates in polar eluants. Changing the hydrogen-bonding sites from naphthyridinecarboxamide in **41** to pyridinecarboxamide in **42** did not significantly alter the free energy and enantioselectivity of complexation. This initially surprising observation was rationalised with two compensating effects. Naphthyridine *N*-atoms are weaker hydrogen-bond acceptors than pyridine *N*-atoms as the pK_a value is 1.84 lower for naphthyridine. On the other hand binding to **41** should be strengthened as a result of a more favourable DAA/AD (*i.e.* donor-acceptor-acceptor/acceptor-donor) hydrogen-bonding pattern. This differs to the DA/AD hydrogen-bonding pattern in **42**, and should thus enable the formation of a bifurcated hydrogen-bond between the naphthyridine donor site and the carboxylic acid protons.

1.3.3 Urea and Thiourea Receptors for Carboxylates

Ureas and thioureas have been shown to provide a strong binding site for carboxylates through two hydrogen-bonds from the urea/thiourea N-H hydrogens to the carboxylate

oxygen, as shown in complexes **43/44** (figure 1.22). Wilcox was the first to utilise ureas and thioureas such as **45** and **46** in carboxylate binding.²⁶ Urea **45** was found to bind benzoate with an association constant of $2.7 \times 10^4 \text{ M}^{-1}$ in CDCl_3 . Large shifts of the N-H protons were also observed, indicating strong hydrogen-bonding between the urea hydrogens and carboxylate oxygens.

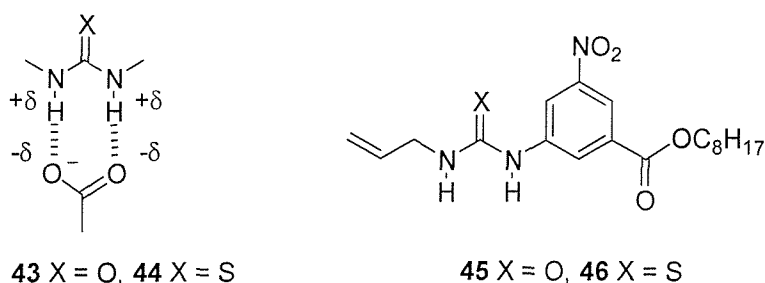


Figure 1.22: Wilcox's urea/thiourea carboxylate receptors **45** and **46**

Further work by Hamilton led to the use of the urea and thiourea in polar solvents such as DMSO.²⁷ Addition of tetramethylammonium acetate to a DMSO- d_6 solution of 1,3-dimethylurea gave large downfield shifts of the urea NH resonance (>1 ppm), which was consistent with the formation of a bidentate hydrogen-bonded complex as in **43** and gave an association constant of 45 M^{-1} . Further gains in the binding energy were achieved by increasing the acidity of the hydrogen-bonding donor sites by replacing the urea for a thiourea. Thiourea ($\text{p}K_a = 21.0$) is more acidic than urea ($\text{p}K_a = 26.9$), and therefore 1,3-dimethylthiourea complex **44** gave nearly a ten fold increase in stability over **43** with an association constant of 340 M^{-1} . As mentioned in section 1.3.1 Hamilton has synthesised guanidinium **5**, he found that the additional stabilisation of the complementary charges led to exceptionally strong binding between guanidinium **5** and acetate, giving an association constant of $12 \times 10^3 \text{ M}^{-1}$ in DMSO- d_6 (figure 1.4). A simple modification of amidopyridine **48** (previously synthesised by Hamilton, see section 1.3.2) involved replacing both the amidopyridine units as hydrogen-bonding donors with ureas/thioureas as shown in **49** and **50**. This had the advantages of creating four favourable secondary hydrogen-bonding interactions (as opposed to four unfavourable secondary interactions in **48**) and of increasing the strength of the primary interaction through the use of charged hydrogen-bonding acceptors (the carboxylate anion). Compounds **49** and **50** were found to effectively bind the bis-tetrabutylammonium salt of glutaric acid in DMSO- d_6 with association constants of $6.4 \times 10^2 \text{ M}^{-1}$ and $1.0 \times 10^4 \text{ M}^{-1}$ respectively. Hamilton had shown that by manipulating both the location and charges of hydrogen binding sites, synthetic receptors

can be converted from those that function only in nonpolar solvents to those that strongly bind in highly competitive solvents.

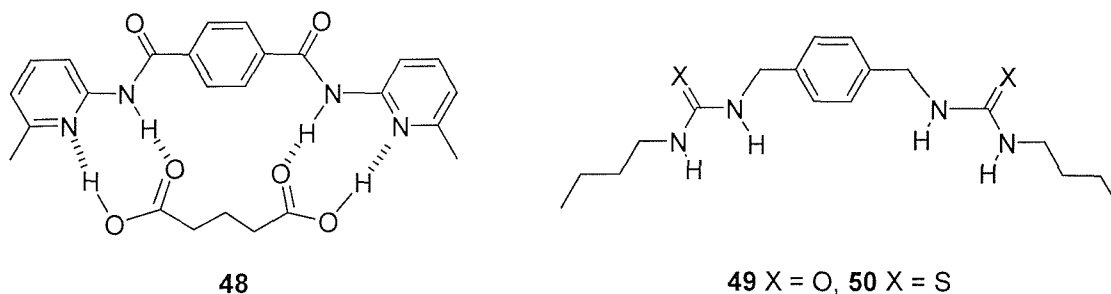


Figure 1.23: Replacement of amidopyridine groups with ureas increases complex stability

Umezawa has also used the urea and thiourea moieties to bind carboxylates.²⁸ Urea **51** and thiourea **52** were prepared, and their ability to bind acetate examined (Figure 1.24). The association constant for **51** with acetate was measured to be 43 M^{-1} and 470 M^{-1} for **52** with acetate in DMSO-d_6 . Job plot analysis clearly indicated a 1:1 complex stoichiometry as shown in complex **53**, and large changes in chemical shifts were observed for the thiourea N-H protons. Umezawa also found the thiourea to offer certain advantages over the urea moiety. Urea **51** was insoluble in solvents of low polarity such as CDCl_3 , whereas thiourea **52** was well solvated in CDCl_3 and showed no evidence of self-association. In contrast, a urea structurally related to **51**, with 1-heptyldecyl groups replacing the butyl groups, was found to self associate in CHCl_3 with a dimerisation constant of 130 M^{-1} .

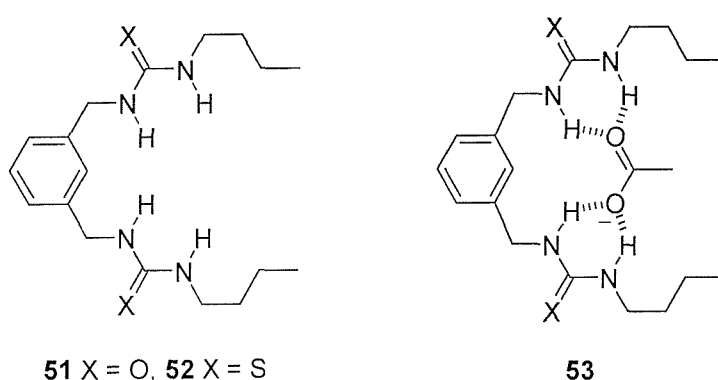
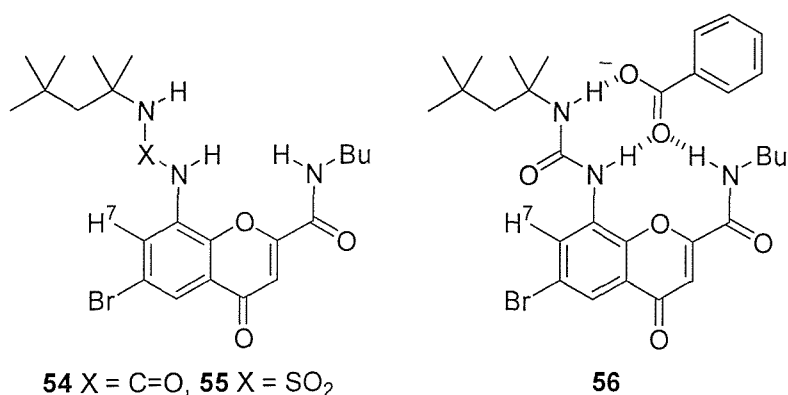


Figure 1.24: Tetradentate binding of acetate by a bisurea/bisthiourea **51/52**

Morán has made a urea and sulfuryl based receptor that is able to bind carboxylate through the use of both the carboxylate *syn* and *anti* lone pairs (Figure 1.25).²⁹ The association constant of urea receptor **54** with benzoate in DMSO was surprisingly small ($K_a = 20 \text{ M}^{-1}$)

compared with other known urea receptors ($K_a = 45 \text{ M}^{-1}$ for simple dimethylurea and acetate). CPK models revealed some steric interference between the benzoate aromatic ring in complex **56** and the receptor butyl substituent. Moreover, the urea function had to be twisted with respect to the chromenone ring due to the hindrance between the urea carbonyl and the chromenone H-7. This made the cleft wider and prevented the formation of any linear hydrogen-bonds. To overcome this drawback the sulfuryl amide **55** was prepared. The tetrahedral geometry of the sulfur atoms allowed H-7 to be placed between the two sulfuryl oxygens, leaving the NH bond in the chromenone plane. The association constant of this receptor with benzoate in DMSO was 330 M^{-1} and therefore higher than for urea **54**. The improved geometry combined with the higher acidity of the sulfuryl amide hydrogens accounted for its superior binding properties. The high chloroform solubility of sulfuryl amide **55** allowed titration in this solvent and the association constant with benzoate was over $1 \times 10^5 \text{ M}^{-1}$ and could not be accurately determined.



*Figure 1.25: Morán's chromenone based receptors **54** and **55** for carboxylates*

Receptor **57** combined two chromenone fragments with a urea function and was able to form four linear hydrogen-bonds with a carboxylate guest to form complex **59** (Figure 1.26). The association constant with benzoate in DMSO was $1.5 \times 10^4 \text{ M}^{-1}$ and therefore higher than with receptors **54** and **55**. Similarly, to prevent the twisted geometry of the urea receptors, the symmetric sulfuryl amide **58** was prepared. From a competitive titration in DMSO with symmetric urea **57**, it was possible to evaluate the association constant for **58** with benzoate to be at least ten times higher and therefore over $1 \times 10^5 \text{ M}^{-1}$.

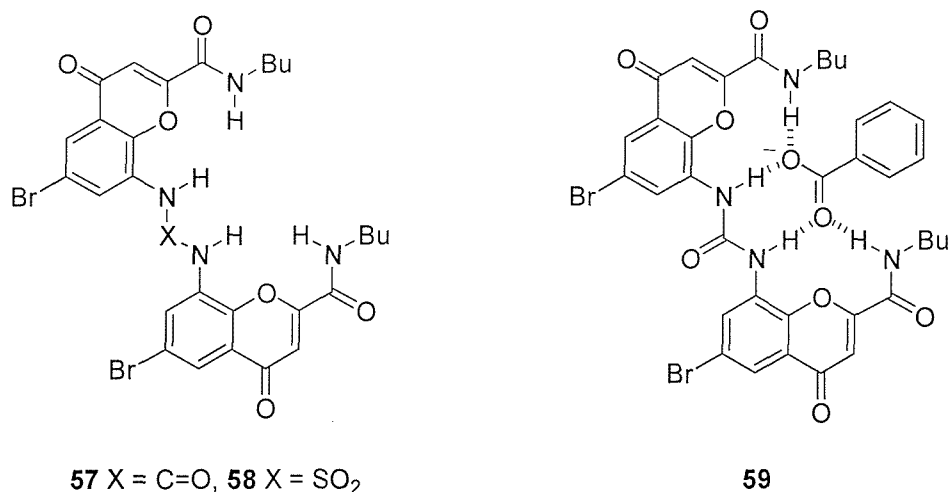


Figure 1.26: Morán's tetradentate chromenone based receptors **57** and **58** for carboxylates

Kilburn has synthesised a bowl shaped receptor **60** for amino acid derivatives (Figure 1.27), which incorporated a thiourea as the carboxylate binding site, and amide functionality to provide further hydrogen-bonding interactions with suitable guests.³⁰

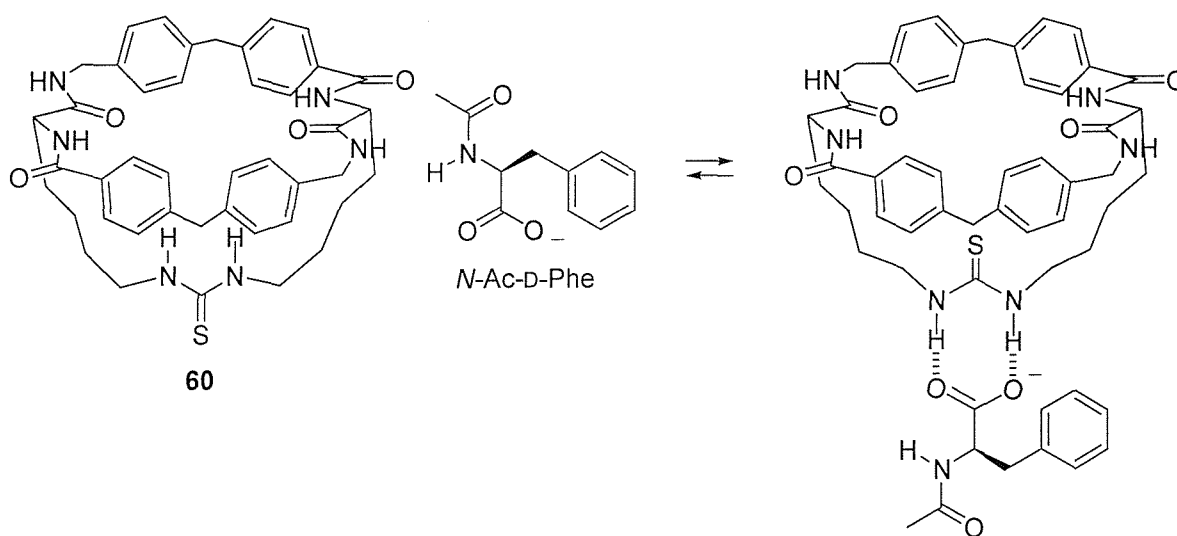


Figure 1.27: N-Ac-D-Phe is bound to the external face of macrocycle **60**

Binding studies showed little selectivity for the various substrates investigated. However, detailed NMR studies revealed that D-amino acid substrates bound predominantly on the outside of the macrobicycle cavity by a strong carboxylate-thiourea interaction (Figure 1.27). L-Amino acid substrates bound predominantly on the inside of the cavity, also establishing a strong carboxylate-thiourea interaction, but with the acetyl amide in a *cis* amide configuration (Figure 1.28). Molecular modeling studies suggested that the energetic

penalty associated with adopting a *cis* amide configuration in the host-guest complex was compensated by intermolecular hydrogen-bonds between the *cis* amide and macrocycle amide functionality.

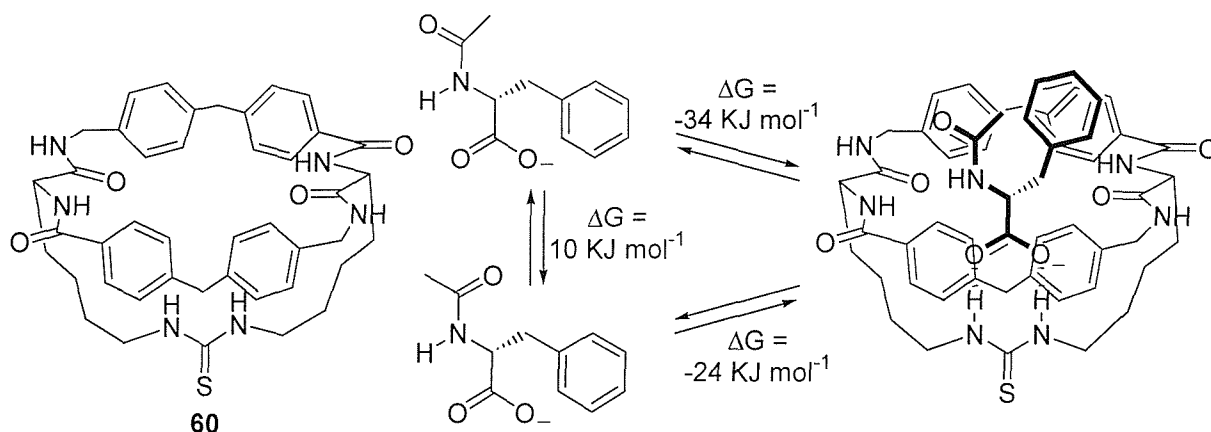


Figure 1.28: *N*-Ac-*L*-Phe is bound within the cavity of macrocycle **60**

The neutral anion receptors reported to date have used hydrogen-bonding³¹ and/or ion dipole interactions.³² Smith has improved upon the anion binding ability of neutral receptors by developing systems that incorporate internal Lewis acid co-ordination in order to achieve higher affinity carboxylate binding than observed for conventional ureas (Figure 1.29).³³ They helped to strengthen the hydrogen-bonding interaction by co-operative polarisation of the urea group, which could be accomplished by co-ordinating the urea carbonyl to a Lewis acid.

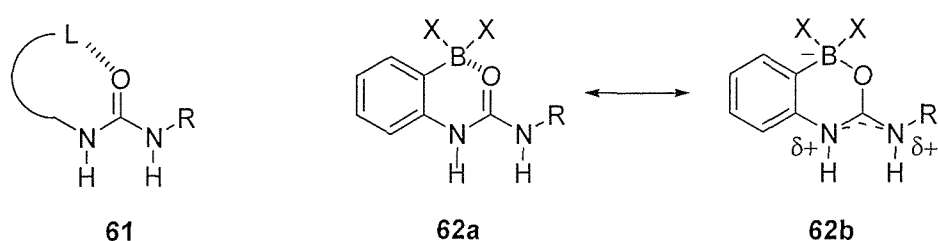
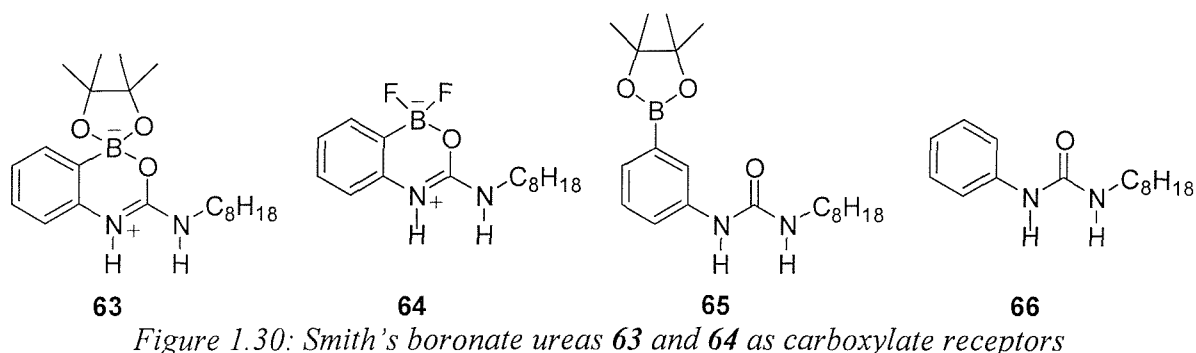


Figure 1.29: Smith's Lewis acid-urea conjugate **62**

One example of conjugate **61** is **62**, which can be represented by two limiting forms, **62a** and **62b**. There is literature precedent that suggests that **62b** would be the major resonance contributor.³⁴ Binding studies with tetrabutylammonium acetate and receptors **63** and **64** were carried out. Association constants were measured by ¹H NMR titration experiments in

DMSO-d₆ (table 1.2). The results were compared with compounds **65** and **66**. In each case 1:1 binding was verified by Job Plot analysis.



Host	K_a/M^{-1}	$\Delta G/kJ\ mol^{-1}$	$\Delta\delta_{max}/ppm$
66	3.7×10^2	14.5	2.14
65	3.9×10^2	14.6	2.16
63	7×10^3	21.7	3.75
64	6×10^4	27.0	3.96

Table 1.2. Association constants with acetate in DMSO

There was no major difference between **65** and **66** as the electronegativity of the boron is similar to hydrogen. Boronate ureas **63** and **64** gave higher association constants, due to an improved host hydrogen-bonding donation effect and the generation of a strong host molecular dipole. The greater binding ability of **64** reflected the structural change to a more withdrawing boron difluoride, which increased both effects. The strategic use of Lewis acids was an important discovery, which was further underlined by the fact that **64** was a better acetate binder than the guanidinium cation ($K_a = 1.2 \times 10^4$ in DMSO, see section 1.3.1).

Hong has extended Smiths approach by developing thiouronium based receptors **67** and **68** (Figure 1.31).³⁵ As has already been pointed out, the polarisation of a urea group by intramolecular co-ordination with a Lewis acidic boronate increased acetate binding affinities by over $12\ kJ\ mol^{-1}$ because of a larger host dipole moment. Hong reasoned that the thiouronium group, generated by *S*-alkylation of the thiourea group, would possess a larger dipole moment than the thiourea and therefore enhance the acidity of the thiourea NH residues. It should therefore function as a better carboxylate binder than the thiourea group.

Thiouroniums **67** and **68** were synthesised and association constants with benzoate determined by ^1H NMR titrations in DMSO-d_6 .

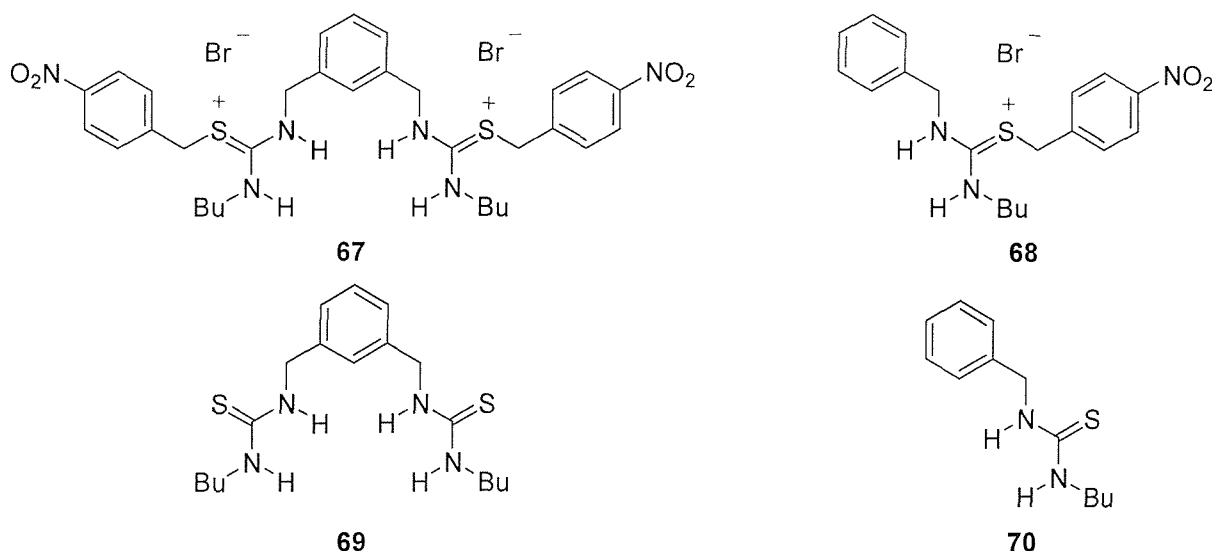


Figure 1.31: Hong's thiouronium receptors **67** and **68** for benzoate

Thiouronium receptors **67** and **68** were found to bind benzoate through hydrogen-bonding and electrostatic interactions such as those in complex **71** (Figure 1.32). Evidence for the formation of thiouronium complex **71** was supported by ^1H NMR titration spectra. In the ^1H NMR spectrum the aromatic region of receptor **67** was broad, which indicated that the bithiouronium salt was asymmetric and slightly distorted in substrate-free conditions as the two bromides could act as a substrate. That these signals were sharpened with increasing benzoate concentration illustrated that the receptor-substrate complex structure was symmetrical as depicted in **71**. In comparison to thioureas, thiouronium groups were stronger binders for carboxylates. For example, monothiourenium receptor **68** binds acetate more strongly in DMSO-d_6 ($K_a = 800 \text{ M}^{-1}$) than the corresponding monothiourea **70** ($K_a = 340 \text{ M}^{-1}$) and a bithiourea **69** ($K_a = 470 \text{ M}^{-1}$). Thiouroniums did, however, show poorer binding affinity than guanidinium based receptors, despite their apparent structural similarities. This implied that the cationic power of the thiouronium group was weaker than that of guanidinium, which can be explained by considering the larger sulfur dispersing the positive charge more than the smaller nitrogen.

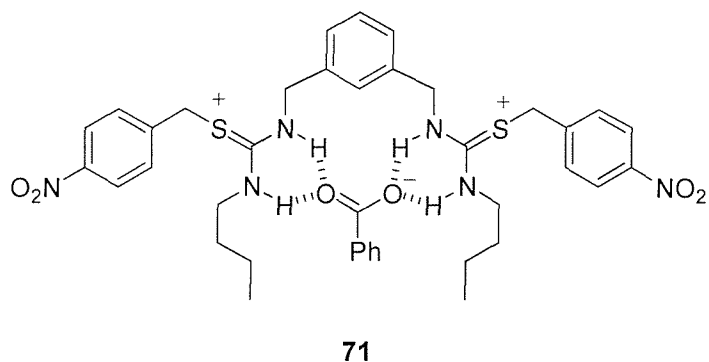


Figure 1.32: Tetradentate binding of benzoate by bistiourenium 67

1.3.4 Polyaza and Crown Ether Receptors for Carboxylates

Kimura was the first to use polyaza compounds as receptors for carboxylates. It was found that pentamines **72-74** and hexamine **75** (as their polyammonium salts) functioned as carboxylate receptors (Figure 1.33).³⁶

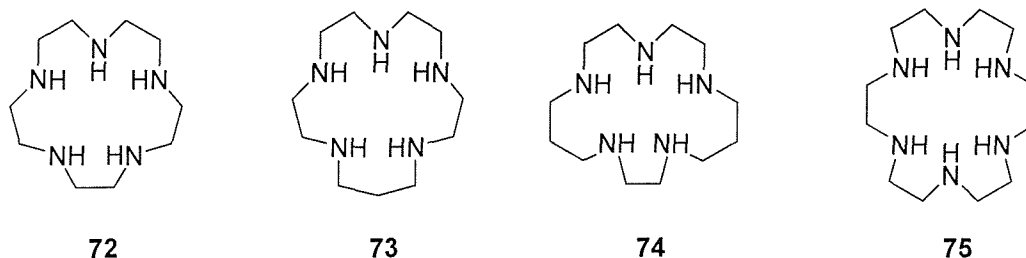


Figure 1.33: Kimura's polyaza receptors **72-75** for carboxylates

Guest	K_a/M^{-1}			
	72	73	74	75
Citrate	55	250	100	24
Succinate	†	120	92	18
Malonate	†	66	25	33
Malate	†	50	26	15
Maleate	†	76	†	29
Fumarate	†	†	†	†

Table 1.3: Association constants for **72-75** with a range of carboxylates in water († negligible binding)

The receptors were found to be selective for specific polycarboxylates such as succinate, maleate, malonate and citrate (table 1.3). No association was observed for the monocarboxylates acetate or lactate nor the dicarboxylates fumarate, glutarate or aspartate. Thus, receptors **72-75** only recognised the dicarboxylates exhibiting a suitable geometry and electronic arrangement. At pH ~ 7 all of the macrocycles could accommodate three protons in their cavities, causing the macrocyclic conformation to be fixed. Electrophoretic and polarographic results were consistent with 1:1 association of the triprotonated polyamine cations with di- or tricarboxylic (in the case of citrate) anions. By comparing association constants for **72-75** with a range of carboxylates the effect of the macrocycle ring size could be probed. The smallest 15-membered ring cation **72** was the poorest anion acceptor, which was thought to be due to steric hindrance marring the hydrogen-bonding sites for the ion-pair formation. The 16- and 17-membered macrocycles **73** and **74** were found to bind to dicarboxylates with similar orders of magnitude. The tricarboxylic citrate anions bound to receptors **72-75** more tightly than any of the dicarboxylate anions, indicating that electrostatic interactions were fundamental to the ion-pair complexation.

Lehn has synthesised polyaza macrocycles **76**, **77** and **78** (Figure 1.34), which as their polyammonium salts were found to bind a range of carboxylate anions.³⁷ All three fully protonated compounds **76-6H⁺**, **77-8H⁺** and **78-6H⁺** formed strong complexes with both inorganic and organic polyanions in aqueous solution. Complexation of monoanions was not detected. Since the pK_a 's of **76-6H⁺**, **77-8H⁺** and **78-6H⁺** are close to or above 7, binding occurs in the neutral pH range. Electrostatic interactions were found to play a major role in both the strength and selectivity of anion binding. Thus, for a given receptor molecule, the anions most strongly complexed were usually the smallest and most highly charged ones, i.e. those of highest charge density as can be seen from the binding sequence oxalate > malonate > succinate > and maleate > fumarate (table 1.4). Large polyanions such as citrate and 1,3,5-benzenetricarboxylate formed very strong complexes with the large and highly charged **77-8H⁺**.

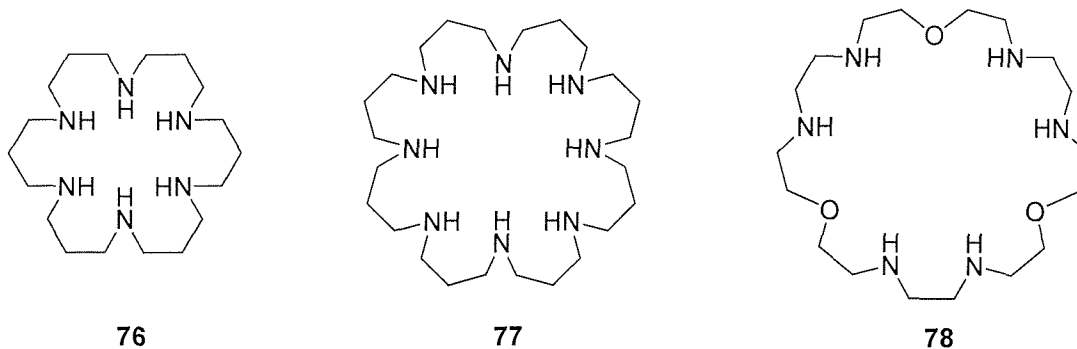


Figure 1.34: Lehn's polyaza macrocycles 76-78

Carboxylate	K_a/M^{-1}		
	76-6H ⁺	77-8H ⁺	78-6H ⁺
Oxalate	6.3×10^3	6.3×10^3	50×10^3
Malonate	2.0×10^3	5.0×10^3	6.3×10^3
Succinate	2.5×10^2	7.9×10^3	6.3×10^2
Tartrate	3.2×10^2	†	7.9×10^2
Maleate	5.0×10^3	12.5×10^3	10.0×10^3
Fumarate	1.6×10^2	7.9×10^2	4.0×10^2
Citrate	50×10^3	40×10^6	630×10^3
1,3,5-benzene-tricarboxylate	3.2×10^3	1.3×10^6	6.3×10^3

Table 1.4: Association constants for 76-6H⁺, 77-8H⁺ and 78-6H⁺ with a range of dicarboxylates († not tried)

Lehn has also incorporated polyfunctional substrate binding features in the design of ditopic co-receptor molecules for dianionic substrates (Figure 1.35). The fully protonated forms of hexaaza macrocycles **79-81** were found to complex dicarboxylate substrates **82** in water. The complexation selectivity was strikingly structurally dependent, shifting from $m = 2$ or 3 to $m = 5$ or 6 on going from **79-6H⁺** to **80-6H⁺**. This corresponded to the same increase in chain length, by three methylene groups, both for the most strongly bound dicarboxylates and for the (CH₂)_n bridges separating the triammonium binding units in **79-6H⁺** and in **80-6H⁺** (table 1.5). The smaller receptor **81-6H⁺** bound the smaller carboxylates more tightly than the longer ones. The observation of selectivity as a function of chain length revealed a

dominant structural factor in dicarboxylate binding. Electrostatic interactions, which favour binding of anions of high charge density, were found to dominate both the strength and the selectivity of complexation. The more stable complexes corresponded to the best fit between substrate length and site separation or the receptor, as shown by **83** and were supported by molecular modeling. Substrates that were either too short or too long formed less stable complexes.

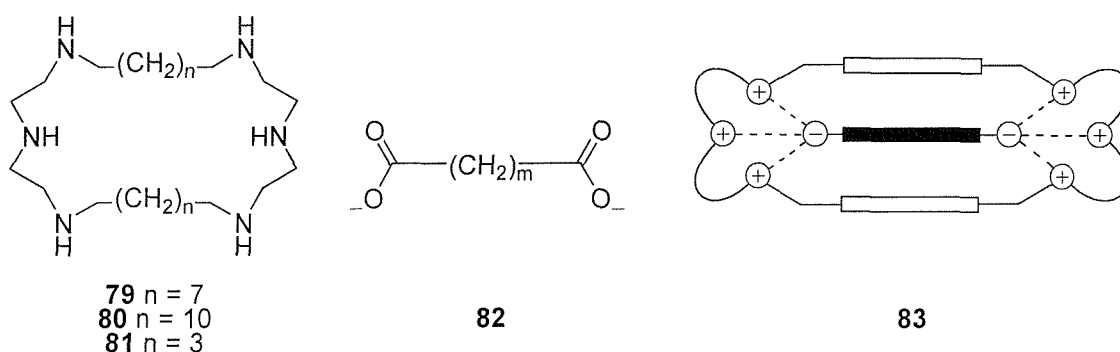


Figure 1.35: Ditopic polyammonium macrocycles **79-81**

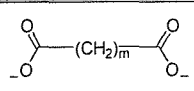
	K_a/M^{-1}		
	79-6H⁺	80-6H⁺	81-6H⁺
Malonate ($m = 1$)	45	57	27
Succinate ($m = 2$)	74	23	11
Glutarate ($m = 3$)	81	27	10
Pimilate ($m = 5$)	22	81	-
Suberate ($m = 6$)	-	70	-

Table 1.5: Association constants of **79-81** with a range of dicarboxylates in water

Lehn has further extended the aza crown series to generate **84** (Figure 1.36).³⁹ In the presence of increasing amounts of **84-6H⁺**, the ¹H NMR signals of various dianionic substrates were found to undergo marked upfield shifts, indicating that complexation occurred. Analysis of the data showed that the complexes formed had 1:1 stoichiometry and allowed their stability constants to be calculated (table 1.6). Receptor **84** formed stable complexes with dicarboxylates in weakly acidic aqueous solution. The shielding effect observed indicated that inclusion of the substrate into the cavity of the receptor molecule probably took place, yielding complexes such as **85**. The complexes exhibited structural selectivity. In the dicarboxylate series (**82**, Figure 1.35) adipate ($n = 4$) is bound more

strongly than either the shorter or the longer species. Thus, receptor **84** performs linear recognition of the substrate whose length probably corresponds best to the size of the intramolecular cavity. The stronger binding of fumarate as compared to maleate shows that structural effects dominate over purely electrostatic interactions, which should favour maleate, the substrate of higher charge density. The very strong binding of the terephthalate anion is remarkable. It indicates significant structural complementarity between the receptor and the substrate and results from both electrostatic and hydrophobic effects. The complex formed takes the form of cryptate structure **85**. The exact nature of this species was ascertained by determination of the crystal structure of a compound containing **84**-6H⁺ and three terephthalate dianions. One anion was located inside the molecular cavity while the other two are outside.

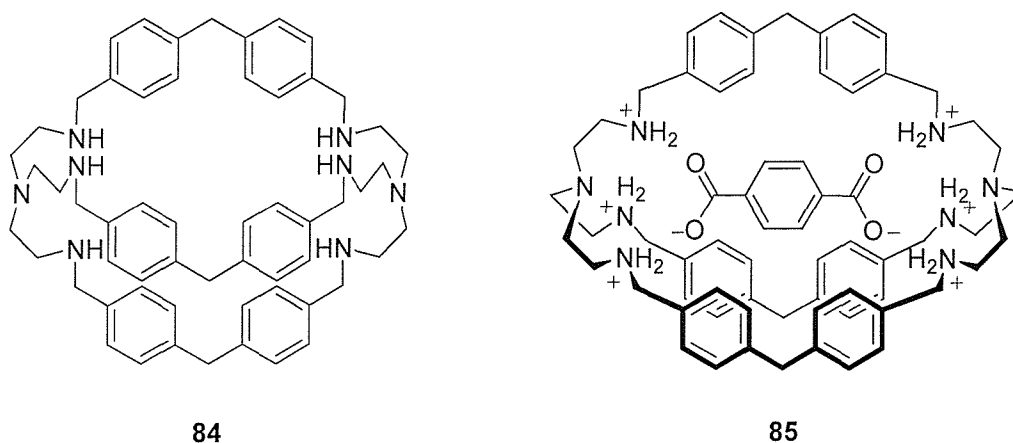


Figure 1.36: Lehn's cryptate receptor **84** for terephthalate

Substrate ${}^{-}\text{O}_2\text{C}-(\text{CH}_2)_n-\text{CO}_2{}^{-}$	K_a/M^{-1}
n = 2	1,400
n = 3	2,300
n = 4	2,600
n = 5	2,100
n = 6	1,900
n = 7	1,400
n = 8	1,500
Fumarate	4,100
Maleate	2,400
Terephthalate	25,000

Table 1.6: Association constants for cryptate **84** and range of dicarboxylates in water

Kilburn has synthesised a novel macrocycle **86**, featuring a crown ether ring, amide functionality and a rigid biaryl unit as a receptor for small peptide guests (Figure 1.37).⁴⁰ FAB mass spectrometry was used to probe the host-guest complex. It was found that in the absence of any guest, no signal corresponding to macrocycle **86** was observed, however, in the presence of the potassium carboxylate salts of *N*-Ac-glycine or *N*-Ac- β -alanine, peaks corresponding to macrocycle **86** were observed. In addition, in the case of the potassium carboxylate salt of *N*-Ac- β -alanine, peaks corresponding to [macrocycle + carboxylate anion + K^+]⁻ and to [macrocycle + carboxylate anion]⁻ (e.g. complex **87**) were observed. Under identical conditions, in the presence of the potassium carboxylate salts of *N*-^tBoc-glycine and *N*-^tBoc- β -alanine, no peaks corresponding to the macrocycle, or complexes of it, could be detected. Taken together this suggests that the *N*-acetyl substrates are bound within the macrocycle while the bulkier *N*-^tBoc substrates are not.

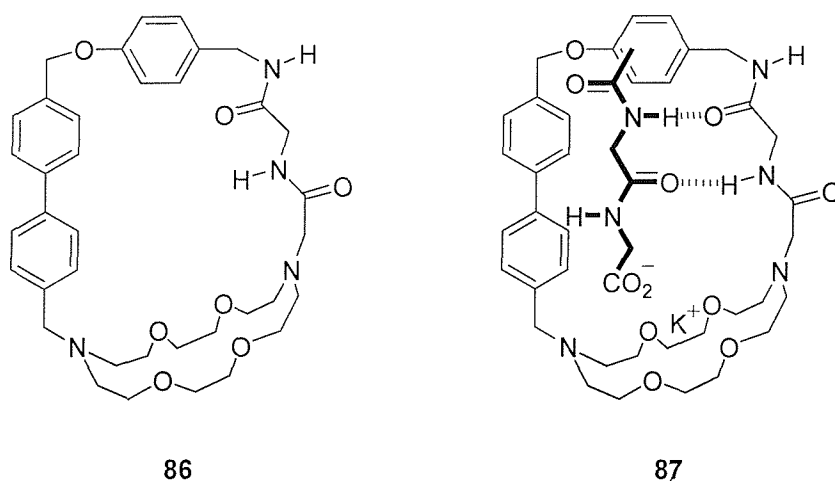


Figure 1.37: Kilburn's peptide receptor **86**

1.3.5 Miscellaneous Receptors for Carboxylates

Loeb has used calix[4]arene units, functionalised at the 1,3-positions of the upper rim with amido groups, to act as neutral, hydrogen-bonding receptors for acetate, benzoate, nicotinate, oxalate, isophthalate, terephthalate and fumarate (Figure 1.38).⁴¹ Binding strength and selectivity was tunable by varying the electron withdrawing ability of the terminal substituent (by replacing CH₂Cl for CHCl₂ or CCl₃). The carboxylate complexation properties of receptor **88** were investigated using ¹H NMR spectroscopy.

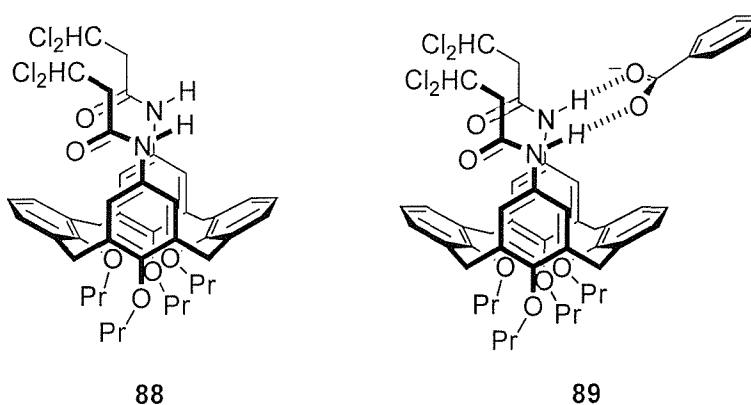


Figure 1.38: Loeb's calix[4]arene receptor **88** for benzoate.

The anion-receptor stoichiometry was confirmed to be 1:1 by a Job plot. Benzoate anion was found to bind in a bidentate fashion to the two amide protons present on the upper rim of calix[4]arene **88** as shown in complex **89** (Figure 1.38). In order for this to occur, the calix[4]arene must exist in the pinched cone conformation in which the rings bearing the

amide groups are essentially parallel. This is clearly demonstrated by observed changes in the ^1H NMR spectrum upon anion binding. The ^1H NMR spectrum of **88** exhibits a singlet for the four aromatic protons on the amido substituted rings and an unresolved multiplet for the six protons on the unsubstituted rings. Addition of benzoate ion results in an upfield shift of the substituted ring protons and a downfield shift and resolution of the protons on the unsubstituted ring. Association constants for various other mono-carboxylate anions with receptor **88** were obtained and these results demonstrated that receptor **88** was not only selective for carboxylate anions but had a particular affinity for benzoate anion.

Examination of CPK models suggested a more open conformation might provide a suitable geometric fit for some dicarboxylates. The binding of receptor **88** with oxalate anion showed 1:1 complexation. The changes evident in the aromatic region of the spectrum of **88** were opposite to those demonstrated with the benzoate anion. This suggested that the calix[4]arene exists in a pinched cone conformation in which the unsubstituted rings are parallel. This allows accommodation of the dianion and still maintains a 1:1 stoichiometry. In contrast, the larger dicarboxylate anions (isophthalate, terephthalate, fumarate) were found by Job plots to bind with an anion-receptor ratio of 1:2. ^1H NMR spectra showed the same trends observed for benzoate and suggested that the calix[4]arene receptors can be assembled around the anion with a similar co-ordination mode for each carboxylate group.

Anslyn has generated a bicyclic cyclophane **90**, which incorporated six convergent amide hydrogens into the centre of a binding pocket (Figure 1.39).⁴² Due to the geometry imposed by the cyclophane, a host-guest complex with acetate would involve hydrogen-bonding to π -electrons in preference to lone pair electrons. X-ray quality crystals of **90** were grown and as expected, the cavity was lined by six hydrogens all orientated toward the centre. Crystals of acetate complex **91** were grown from a $\text{H}_2\text{O}/\text{EtOH}/\text{CH}_2\text{Cl}_2$ solution in the presence of excess ammonium acetate. The acetate was found to be bound within the cavity to form a 1:1 complex. The anion is bound by four hydrogen-bonds from the amides of the acyl pyridine hydrogens. The association constant was measured to be 770 M^{-1} in 1:3 $\text{CDCl}_2/\text{CD}_3\text{CN}$ and the stoichiometry of the solution state complex was determined to be 1:1.

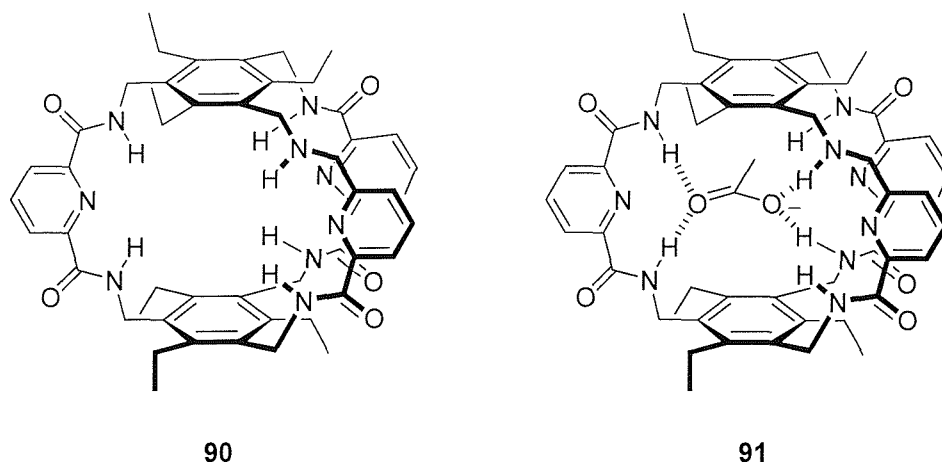


Figure 1.39: Anslyn's cyclophane receptor **90** for acetate

Sessler has reported the synthesis of sapphyrin-sapphyrin dimer **94** which was found to act as an effective receptor for dicarboxylate anions, unlike the control monomer **92**. Two protonated sapphyrins served as the key carboxylate binding sites while a flexible diaminopropane spacer served as the macrocycle to macrocycle linking chain as shown in **93** (Figure 1.40).⁴³ Initial screening studies involved mixing sapphyrin dimer **94** with several representative dicarboxylate anions such as oxalate or nitroterephthalates in methanol and subjecting the mixtures to high resolution FAB mass spectrometry. More definitive proof of binding came from transport experiments, where a standard U-tube experiment was used. It was found that at neutral pH dimer **94** acted as an efficient carrier for a range of dicarboxylates. Quantitative assessments of dicarboxylate binding efficiencies in methanol were made using ^1H NMR titrations. Both the transport and NMR titration experiments showed **94** to be a strong and selective receptor for dicarboxylate anions. Little affinity for monocarboxylates such as trifluoroacetate ($K_a < 20 \text{ M}^{-1}$) was observed, while dicarboxylates such as nitroterephthalate was found to be tightly bound giving an association constant of $9,100 \text{ M}^{-1}$.

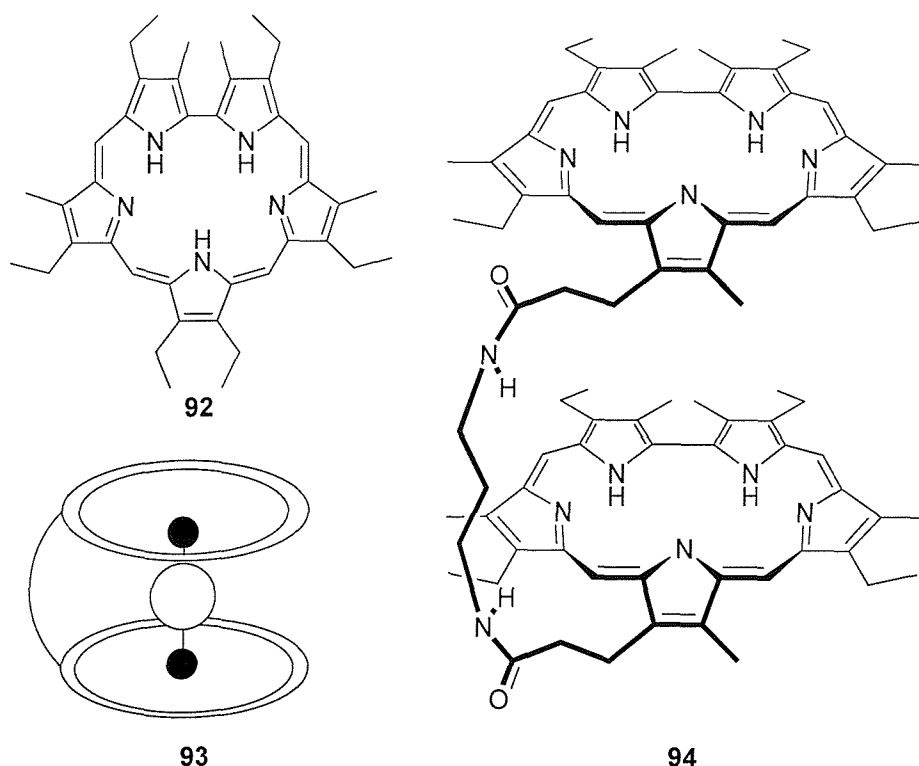


Figure 1.40: Sessler's saphyrin dimer receptor **94** for dicarboxylates

Sessler has extended dimer **94** to generate chiral saphyrin dimers **95-97** incorporating more rigid chiral spacers (Figure 1.41).⁴⁴ In methanol, the strength of *N*-Cbz-aspartate and *N*-Cbz-glutamate complexation was low ($K_a < 200 \text{ M}^{-1}$). It was found that open chain receptors **95** and **96** bind glutamate and aspartate with high affinity with association constants ranging from 3.9×10^4 to $3.2 \times 10^5 \text{ M}^{-1}$ and show selectivity for glutamate over aspartate. The enantioselectivity of the binaphthalene containing receptor **96** is higher than that of the diaminocyclohexane derived dimer **95**. Cyclic dimer **97** on the other hand, displays a lower affinity for aspartate/glutamate, but shows excellent chiral discrimination for D-Glu which is bound with four times the association constant than for the corresponding *L* enantiomer (table 1.7). Sessler suggests the increased selectivity observed for cyclic dimer **97** and glutamate probably reflects the fact that for a cyclic, more preorganised system the importance of a good size and shape match (between the receptor and stereogenic substrate) is emphasised.

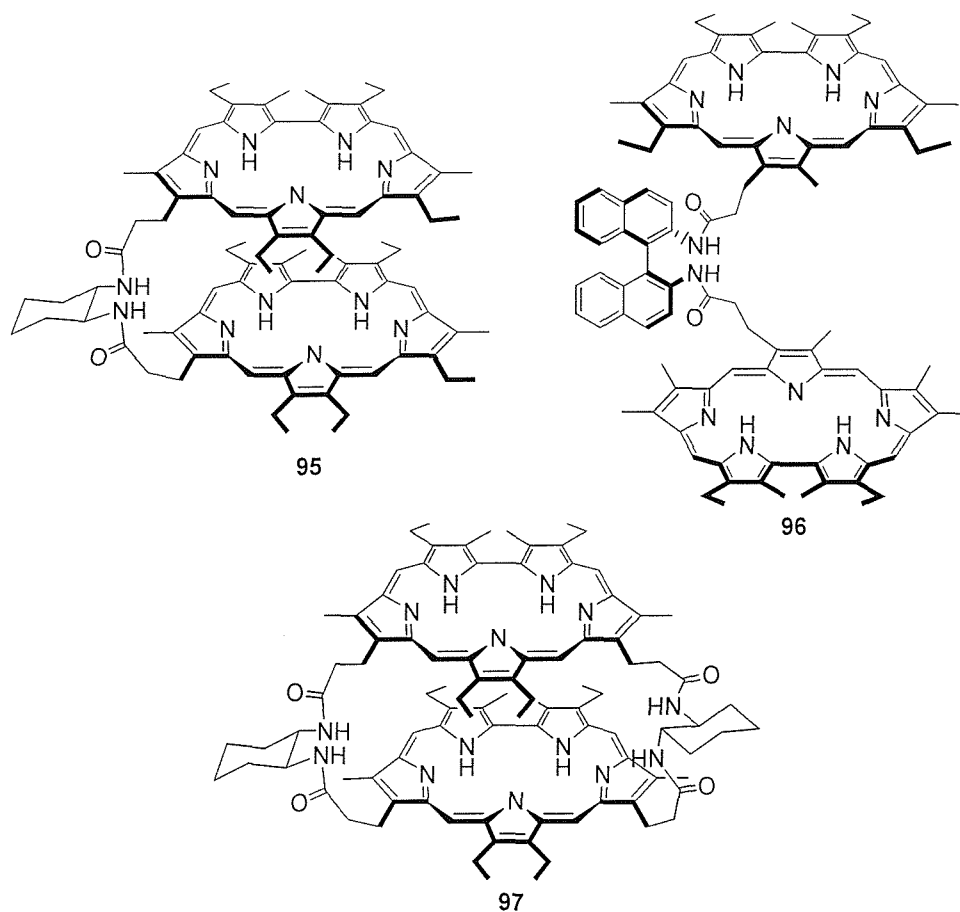


Figure 1.41: Chiral sapphyrin receptors **95-97** for dicarboxylates

Receptor	Substrate	K_a/M^{-1}
95	<i>N</i> -Cbz-L-Asp	45,000
95	<i>N</i> -Cbz-D-Asp	38,900
95	<i>N</i> -Cbz-L-Glu	112,700
95	<i>N</i> -Cbz-D-Glu	119,900
96	<i>N</i> -Cbz-L-Asp	20,600
96	<i>N</i> -Cbz-D-Asp	43,500
96	<i>N</i> -Cbz-L-Glu	324,500
96	<i>N</i> -Cbz-D-Glu	217,100
97	<i>N</i> -Cbz-L-Asp	16,700
97	<i>N</i> -Cbz-D-Asp	9,700
97	<i>N</i> -Cbz-L-Glu	3,800
97	<i>N</i> -Cbz-D-Glu	16,200

Table 1.7: Association constants for *N*-Cbz-aspartate/*N*-Cbz-glutamate

1.4 Aims of the Project

The preceding review has highlighted the important areas where progress has been made in the selective binding of carboxylate and carboxylic acid derivatives. One important point to note when comparing the ability of synthetic receptors to selectively bind substrates is that macrocyclic structures tend to be significantly more selective than non-cyclic receptors. The aim of this project was to construct a series of thiourea based receptors and examine their ability to selectively bind amino acid carboxylates. One of the problems we sought to address was that of the lower degree of selectivity found in acyclic receptors. Chapters two and three discuss the synthesis of thiourea based tweezer receptors and their ability to selectively bind a range of monocarboxylate amino acid derivatives. Attention is also given to the level of conformational control (preorganisation) present in the receptor. Having probed the properties of tweezer based receptors, chapter four goes on to describe the synthesis of a novel bithiourea based macrocycle and examines its behaviour with the *N*-Boc protected dicarboxylate salts of glutamate and aspartate.

Chapter Two

Synthesis of Pyrrolidine Based Bisthiourea Tweezers

2.1 Literature Precedent and Receptor Design

The Kilburn group has recently synthesised receptors for peptides with a carboxylic terminus.⁴⁵ Solid-phase synthesis was employed to construct receptor **98** (figure 2.1), which was designed to bind to the carboxy terminus of peptides in aqueous media. A guanidinium binding site was used to provide the primary binding interaction for the carboxylate. The tweezer arms have the potential to form both hydrophobic and β -sheet like hydrogen-bonding interactions with the backbone of the peptide substrate.

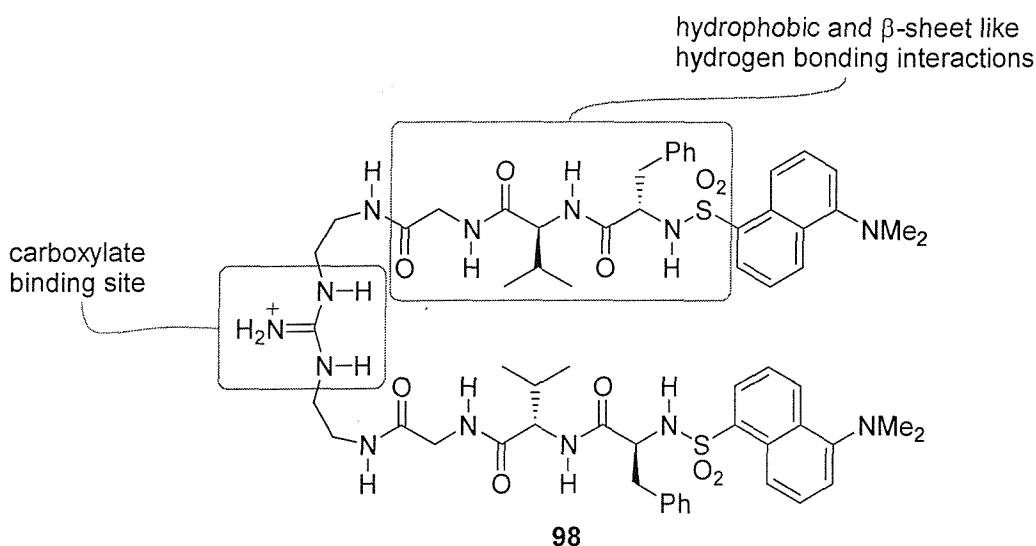


Figure 2.1: Dansyl-labelled guanidinium based tweezer receptor **98**

A 1000-member biased library of tripeptides, attached to TentaGel resin *via* the amino terminus, was screened against tweezer **98** in water. The tweezer receptor was found to bind to approximately 3% of the library members and following sequencing of 20 beads, showed 95% selectivity for valine at the carboxy terminus of the tripeptides and 40% selectivity for Glu(O^tBu) at the amino terminus. Binding of one of the peptides selected from the screening experiments, Cbz-Glu(O^tBu)-Ser(O^tBu)-Val-OH was measured to have an association constant of $4 \times 10^5 \text{ M}^{-1}$. It was also possible to screen a library of receptors for the binding of specific tripeptide sequences. However, problems were encountered with the direct screening of resin bound receptor library **99**, as the binding strength of the guanidine

appeared to have been reduced by the presence of the electron withdrawing sulfonamide linker (figure 2.2).

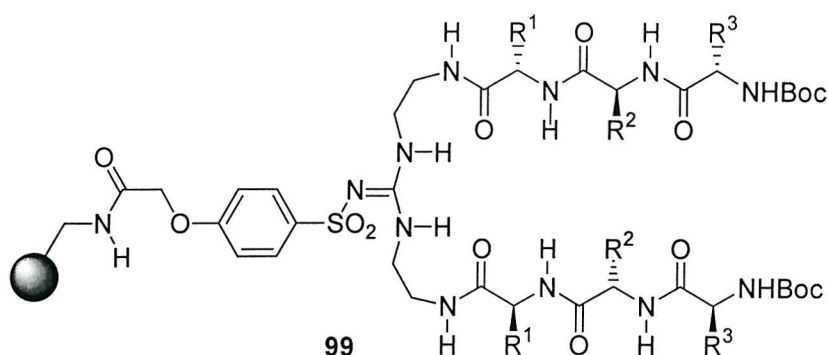


Figure 2.2: Resin bound library of tweezer receptors

It was also thought that the linker might create an unfavorable steric hindrance preventing the binding site orientating into the ideal conformation for binding. Thus, it was necessary to find an alternative which allows anchorage of the tweezer receptors to the solid support without influencing the binding properties.

Hamilton has developed a family of receptors **100** for carboxylates (figure 2.3) in which four amide N-H groups are positioned to bind to acetate anion *via* multiple hydrogen-bonding interactions.⁴⁶ The association constant was measured to be around $3 \times 10^2 \text{ M}^{-1}$ in CD_3CN . A far higher association constant was measured for the serine based receptor **101**, which was found to complex acetate with an association constant of $2.7 \times 10^5 \text{ M}^{-1}$ in CD_3CN . The higher association constant was due to the hydroxyl hydrogens forming two hydrogen-bonds with the acetate oxygens, causing the cyclohexyl amide protons to not be involved in binding.

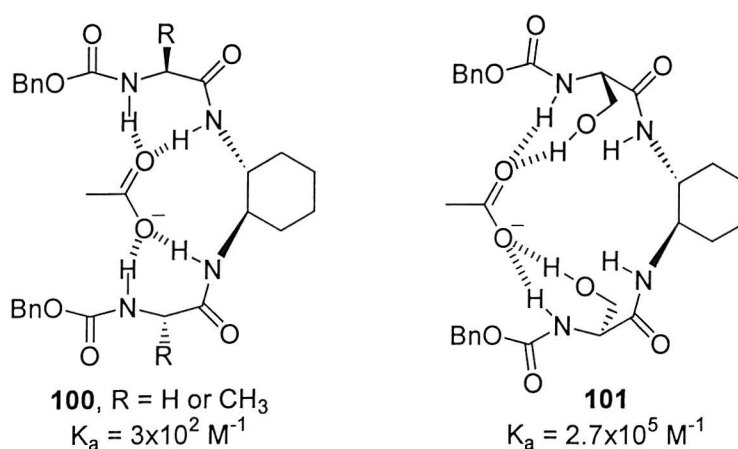


Figure 2.3: Hamilton's tetradentate acetate receptors

Inspired by Hamilton's work it was proposed to prepare tweezers such as bistiourea **102** or bisguanidinium **103** using conventional solution phase chemistry. It was anticipated that carboxylates would be bound by four hydrogen-bonds as shown in figure 2.4.

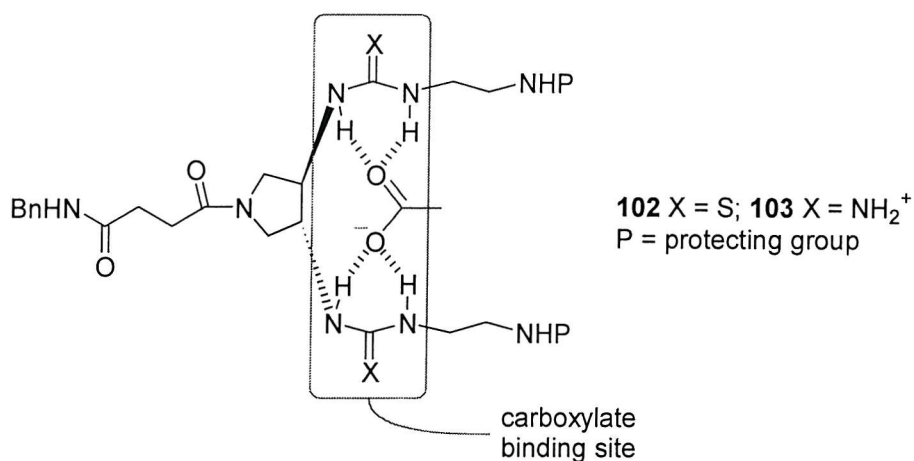


Figure 2.4: Bistiourea/bisguanidinium tweezer receptors

Once the solution phase chemistry and binding properties of bistiourea **102** or bisguanidinium **103** had been investigated a solid phase combinatorial approach to synthesise receptors such as tweezer **104** (figure 2.5) would be applied.

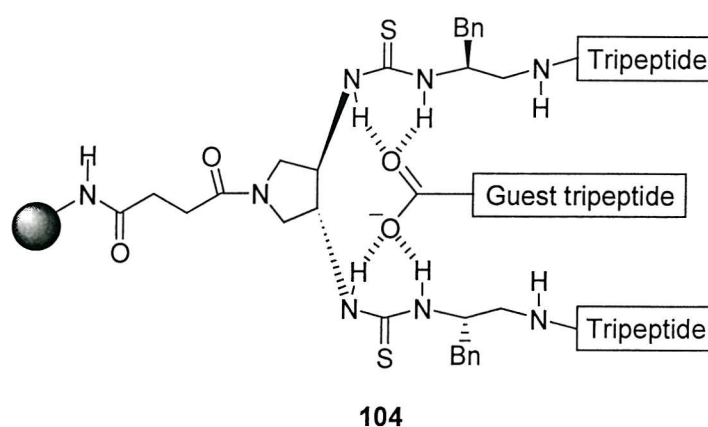
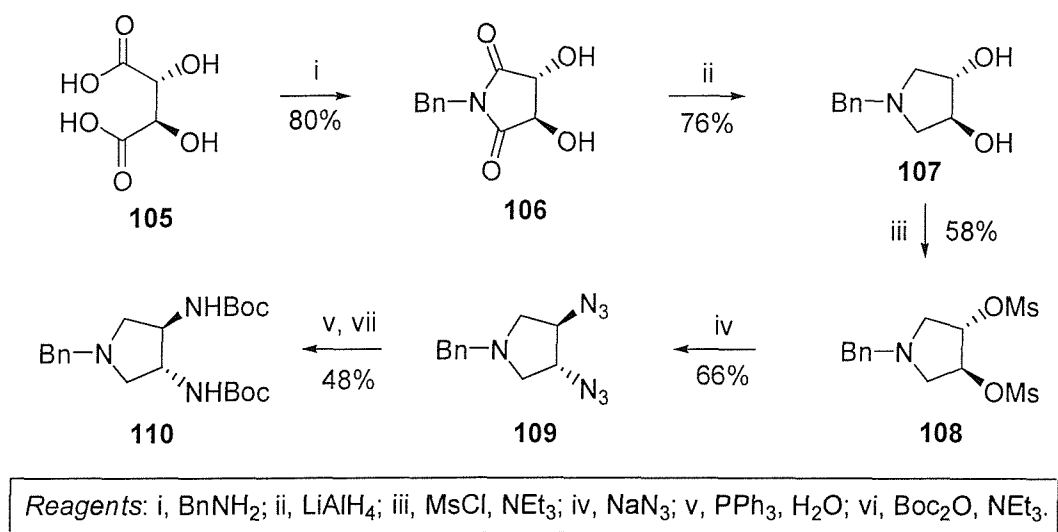


Figure 2.5: Resin bound bistiourea tweezer library

The 3,4-bis substituted pyrrolidine moiety in **102** and **103** provides a linkage that could serve as a spacer between the binding site and the resin, thereby avoiding the problems encountered with the direct screening of resin bound receptors. In addition, the 3,4-bis substituted pyrrolidine moiety also allows the sequential coupling of amino acids to the amino ethyl thioureas, enabling peptide arms to be added to the structure, giving rise to tweezers such as **104**.

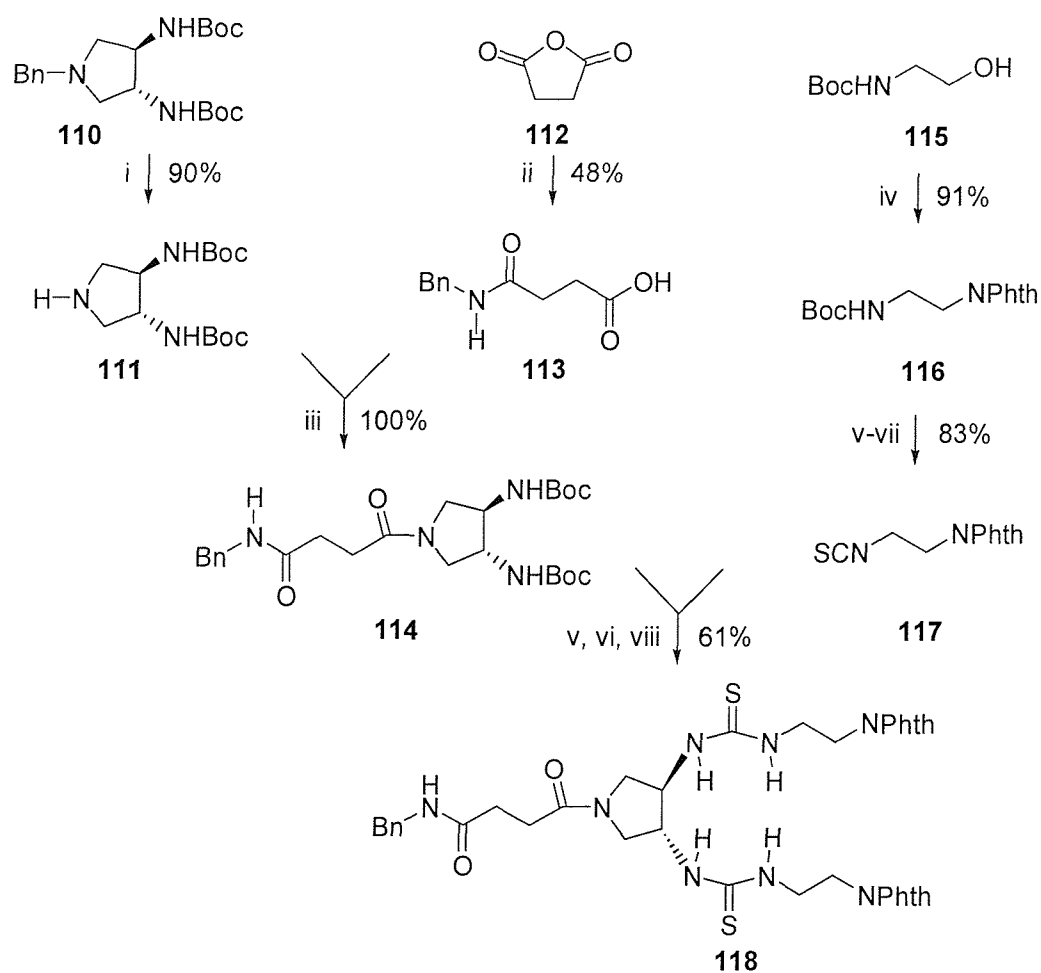
2.2 Synthesis of Bisthioureas 118 and 123

Key intermediate pyrrolidine **110** is the compound from which all of the bisthiourea receptors are derived. The synthesis of pyrrolidine **110** is based on a procedure developed by Nagel,⁴⁷ which starts from commercially available L-tartaric acid **105** (scheme 2.1).



Scheme 2.1: Synthesis of key intermediate pyrrolidine **110**

L-Tartaric acid **105** is condensed with benzylamine giving imide **106** in an excellent yield of 80%, imide **106** was subsequently reduced with lithium aluminium hydride to produce diol **107** in a very good 76% yield. Diol **107** was mesylated using mesyl chloride to produce dimesylate **108** in 58%, which upon reaction with sodium azide gave diazide **109** in a good 66% yield. The diazide was then reduced using the Staudinger protocol,⁴⁸ employing triphenylphosphine followed by an aqueous hydrolysis of the aminophosphorane. The resultant diamine was protected *in situ* with Boc carbonate furnishing diBoc pyrrolidine **110** in a yield of 48% over two steps. With pyrrolidine **110** in hand the synthesis of glycine derived bisthiourea **118** could be completed (scheme 2.2).



Reagents: i, H₂, Pd/C; ii, benzylamine; iii, EDC, HOBT, DMAP, pyridine; iv, phthalimide, PPh₃, DEAD; v, TFA; vi, NEt₃; vii, SCl₂, K₂CO₃; viii, add **117**.

Scheme 2.2: Synthesis of glycine derived bithiourea 118

Acid **113** was chosen to block the amine function in pyrrolidine **111** as the corresponding amide, and would also serve as a model for attachment to the solid phase. To this end succinic anhydride **112** was condensed with benzylamine to produce acid **113** in 48% yield. The benzyl group in pyrrolidine **110** was removed using hydrogen on palladium to furnish amine **111** in an excellent 90% yield. Amine **111** was condensed with acid **113** using water soluble carbodiimide (EDC), HOBT, DMAP and pyridine to generate amide **114** quantitatively. Thioisocyanate **117** was made using a modification of Burgess' oligourea synthesis.⁴⁹ Alcohol **115** was subjected to the Mitsunobu conditions⁵⁰ employing DEAD, triphenylphosphine and phthalimide providing differentially protected diamine **116** in an excellent yield of 91%. The Boc protecting groups of diamine **116** were selectively deprotected using TFA followed by triethylamine to liberate the corresponding free amine, which was then reacted with thiophosgene under basic conditions to give thioisocyanate **117** in 83% yield. To complete the synthesis of bithiourea **118**, Boc protected diamine **114** was

doubly deprotected using TFA followed by triethylamine to generate the corresponding free diamine which was reacted with thioisocyanate **117** forming bithiourea **118** exclusively in a very good 61% yield. To further encourage enantioselective binding, the design of the receptor was modified to include two additional chiral centres (figure 2.6), which was achieved by adding benzyl substituents adjacent to the thioureas. Consequently the synthesis of the receptor was altered to introduce the benzyl moiety *via* a phenylalanine derived thioisocyanate **122**.

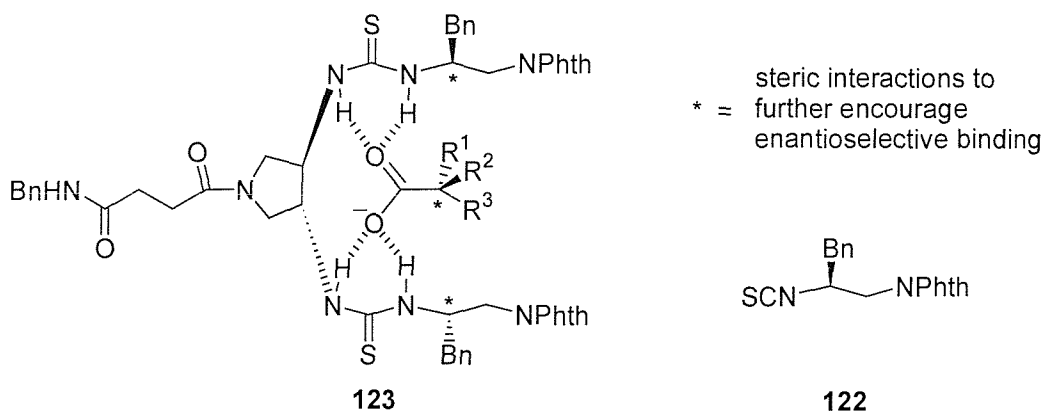
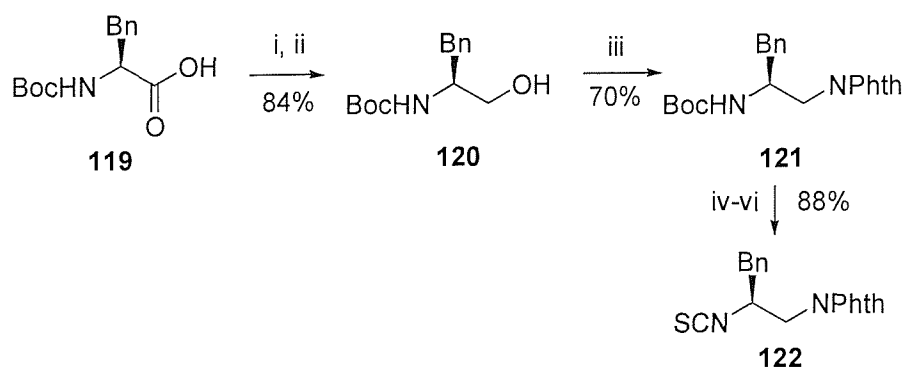


Figure 2.6: Modified receptor **123** incorporating phenylalanine derived moiety **122**

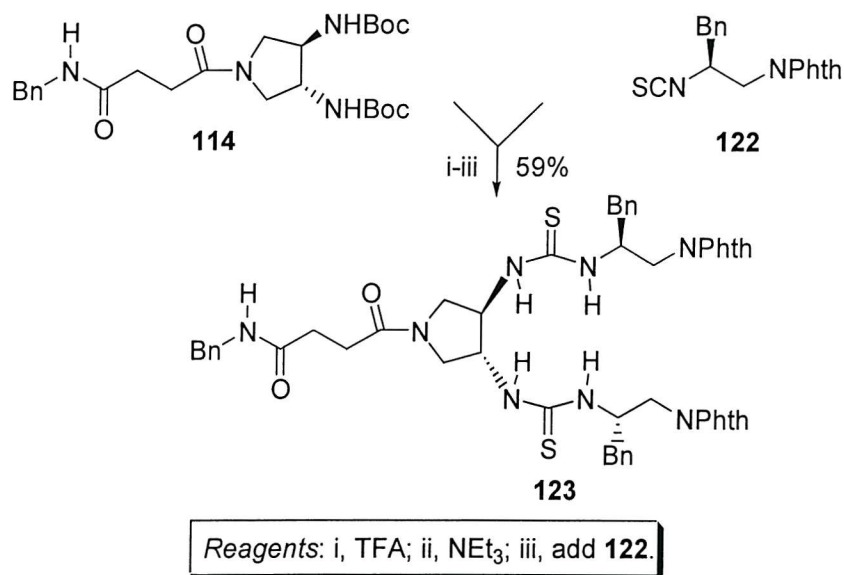
Initially *N*-Boc-L-Phe **119** was reduced to alcohol **120** *via* a mixed anhydride using ethylchloroformate followed by an *in situ* reduction with sodium borohydride providing alcohol **120** in 84% yield (scheme 2.3). Alcohol **120** was converted to phthalimide **121** using Mitsunobu conditions⁵⁰ with phthalimide in 70% yield. Boc protected amine **121** was reacted with TFA followed by triethylamine to liberate the corresponding free amine which was then reacted with thiophosgene under basic conditions to give thioisocyanate **122** in an excellent yield of 88%.



Reagents: i, ClCO_2Et , NMO; ii, NaBH_4 ; iii, phthalimide, PPh_3 , DEAD; iv, TFA; v, NEt_3 ; vi, SCCl_2 , K_2CO_3 .

Scheme 2.3: Synthesis of thioisocyanate **122**

The final step in the synthesis of bistiourea **123** was to treat Boc protected amine **114** with TFA (scheme 2.4), the corresponding TFA salt was deprotonated using triethylamine to afford the free amine. The amine was combined with thioisocyanate **122** to produce bistiourea **123** in a good yield of 59%.



Scheme 2.4: Synthesis of phenylalanine derived bistiourea **123**

2.3 Binding and Dimerisation Properties of Bistioureas **118** and **123**

The ¹H NMR spectra of all bistioureas synthesised showed unusual behaviour. The ¹H NMR spectrum of bistiourea **118** is shown below (figure 2.7).

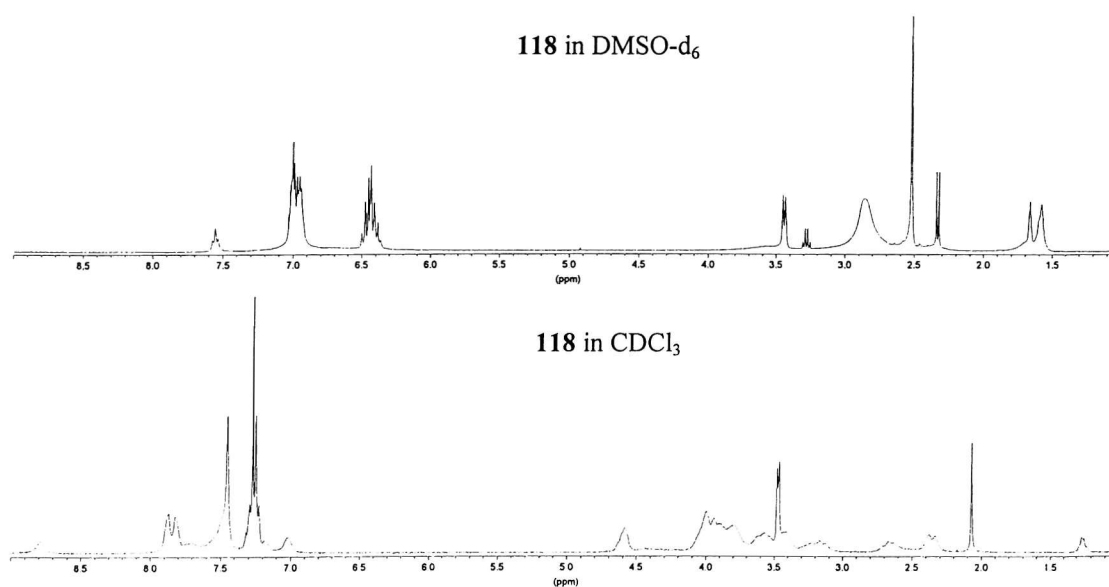


Figure 2.7: ¹H NMR spectrum of bistiourea **118**

In CDCl_3 the ^1H NMR spectrum of **118** contained broad signals, whereas the observed ^1H NMR in DMSO-d_6 gave mostly well resolved signals. Changing the solvent to DMSO-d_6 might be expected to sharpen the signals because the more polar solvent should break up any aggregates formed. By comparison to bithiourea **118** the ^1H NMR of **123** in CDCl_3 contains mostly well resolved peaks which broaden and shift considerably when the solvent is changed to DMSO-d_6 (figure 2.8).

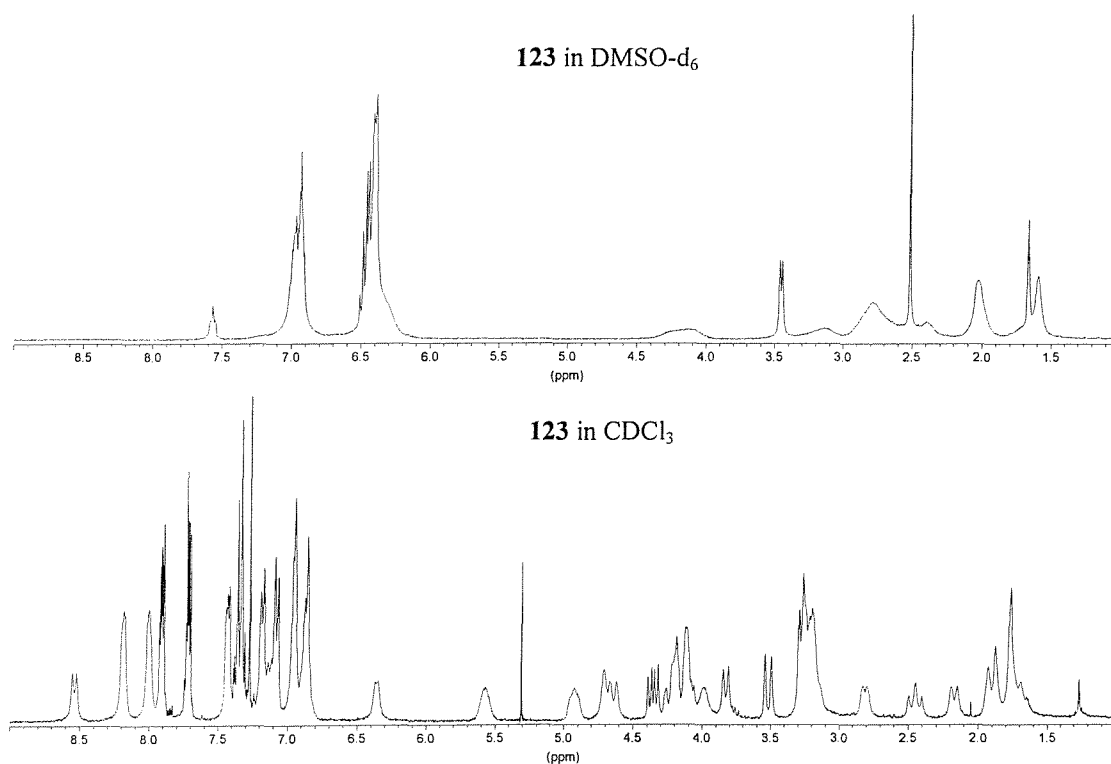


Figure 2.8: ^1H NMR spectrum of bithiourea **123**

A variable temperature ^1H NMR experiment was conducted with compound **123** in DMSO-d_6 , which resulted in some increase in the resolution of the signals at higher temperatures. The most information was gained by examination of the ^{13}C NMR spectrum of **123** in CDCl_3 (figure 2.9), which showed 36 signals including six carbonyl, seventeen aromatic and thirteen alkyl signals.

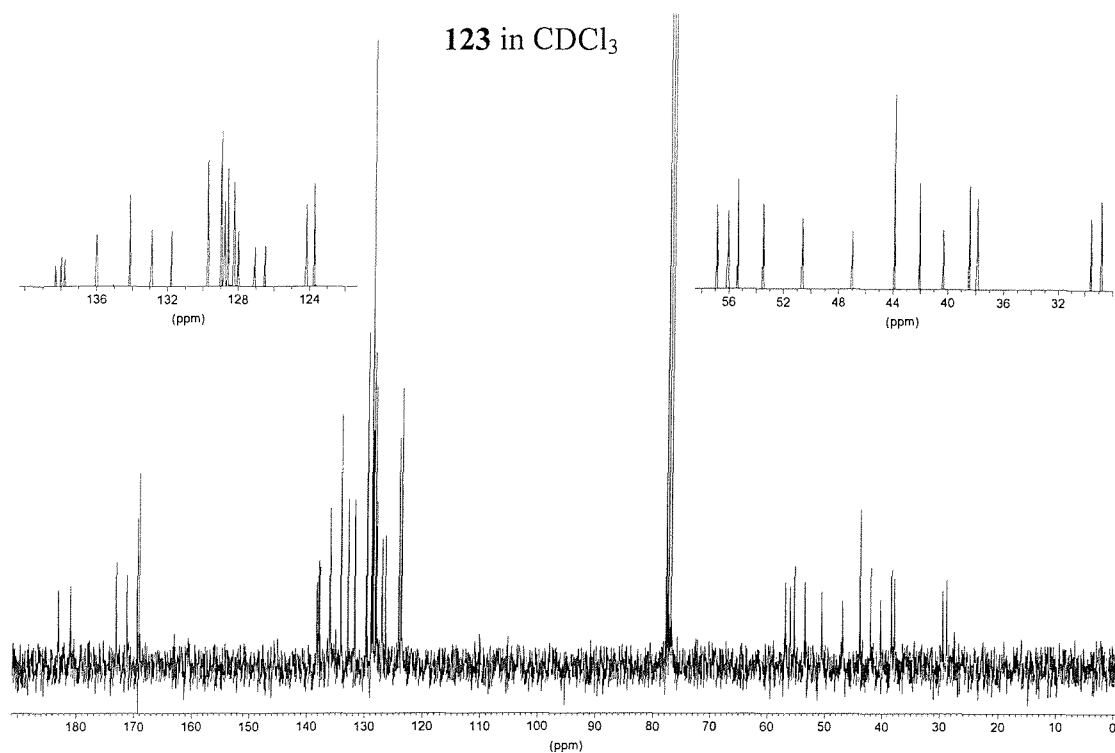


Figure 2.9: ¹³C NMR spectrum of bithiourea 123

The expected number of peaks for carbonyl carbons is four but six were observed, for the aromatic region eleven are expected but seventeen were seen and for the alkyl region ten are expected but thirteen are seen. This anomaly can be explained if it is assumed that each tweezer arm of bithiourea **123** is different in a magnetic field. It is most likely that each tweezer arm would be different in the ¹³C NMR spectrum if intermolecular hydrogen-bonded dimerisation was occurring (figure 2.10).

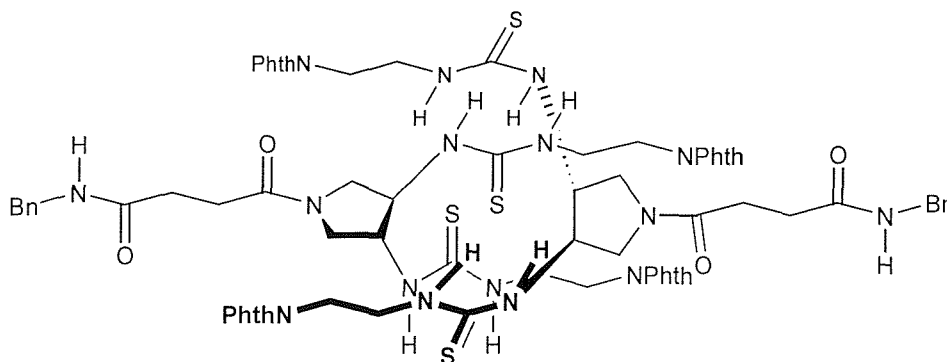


Figure 2.10: Bithiourea hydrogen-bonded dimer

All of these spectra can be explained by looking at the exchange rate between the dimer and monomer form in each solvent. In the case of bithiourea **118** the peaks in the ^1H NMR spectrum are broad in CDCl_3 and well resolved in DMSO-d_6 , this can be explained by assuming that there is a slow or intermediate exchange (on the NMR timescale) between the dimer and the monomer form of **118** in CDCl_3 . However, in DMSO the dimer does not appear to be formed to any great extent and therefore the spectrum for the monomer is seen. The observation is the reverse for bithiourea **123** where we see a well resolved ^1H NMR in CDCl_3 and a broad spectrum in DMSO-d_6 . This would be expected if bithiourea **123** was tightly locked into the dimer form in CDCl_3 and so the ^1H NMR for predominately the dimer structure is observed. In DMSO-d_6 the dimer is broken down to the extent that exchange between the monomer and dimer can take place. This exchange occurs on an NMR timescale and therefore we see the spectrum for both the dimer and the monomer in a similar manner to the spectrum observed for bithiourea **118** in CDCl_3 .

The formation of hydrogen-bonded bithiourea dimers has also been reported by Tobe⁵¹ who showed that the *m*-xylene bithiourea **124** formed an orthogonal dimer structure both in solution and the solid state through specific intermolecular hydrogen-bonding between the thiourea groups (figure 2.11). It seems probable that the pyrrolidine based bithioureas **118** and **123** may also dimerise in this manner which is supported by the NMR evidence discussed above.

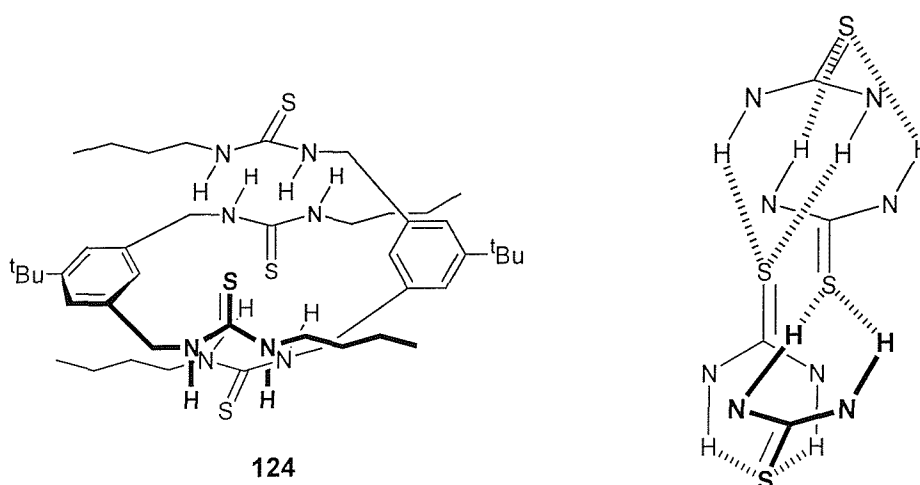


Figure 2.11: *Xylene bithiourea 124 hydrogen-bonded dimer*

Although the pyrrolidine based bithioureas **118** and **123** appeared to dimerise we wished to examine their ability to complex carboxylate salts. The broad ^1H NMR spectra observed for bithiourea **118** and **123** meant that the established method for determining association

constants by ^1H NMR titration experiments could not be used. However, using an extraction procedure identical to that used by Kilburn and Pernia³⁰ the association constant between tetrabutylammonium benzoate and dibenzyl thiourea could be measured. In CDCl_3 the association constant for benzoate and dibenzyl thiourea was measured to be $33.5 \times 10^3 \text{ M}^{-1}$. The expected association constant between bithioureas **118** and **123** and *N*-Ac-Phe carboxylate would be of a similar order of magnitude. However, the binding studies carried out (table 2.1) indicated that bithioureas **118** and **123** did not strongly complex to tetrabutyl ammonium carboxylates, presumably due to the dimerisation effect. The fact that the association constant for bithiourea **123** was considerably lower than that of bithiourea **118** is consistent with the formation of a more tightly bound dimer, which was also seen in the NMR experiments of neat host.

Host	K_a/M^{-1}	
	<i>N</i> -Ac-L-Phe	<i>N</i> -Ac-D-Phe
118	790	670
123	80	80

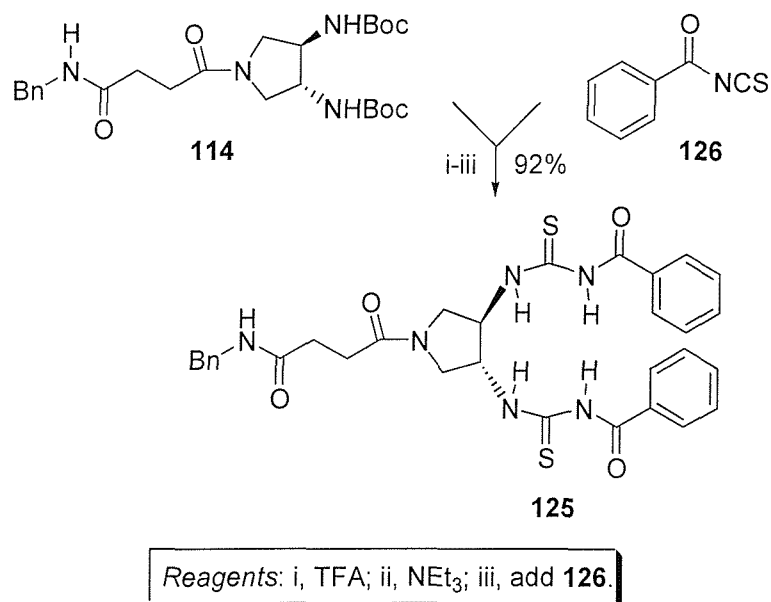
Table 2.1: Association constants for bithioureas **118** and **123** with *N*-Ac-Phe in chloroform

A number of experiments were conducted where host and guest were mixed in stoichiometric ratios and ^1H NMR spectra obtained. It was anticipated that the addition of one or more equivalents of guest would force the dimers formed to break apart. However, there were very little changes observed in the ^1H NMR spectra of host with guest compared to that of host alone and therefore it was concluded that the guest molecules had not disrupted the dimer and that very little binding had occurred.

The occurrence of dimerisation can only be conclusively proven by obtaining a single crystal X-ray structure of the bithioureas, thus far this has not been possible with the bithioureas synthesised to date. A single crystal of bithiourea **123** was obtained but was found to be a glass so no diffraction pattern was obtained.

In an effort to further probe the properties of the bithioureapyrrolidine moiety, benzoyl thiourea **125** was synthesised. Boc protected amine **114** was treated with TFA (scheme 2.5)

to give the corresponding TFA salt, which was deprotonated using triethylamine. The resultant free diamine was reacted with benzoylthioisocyanate **126** to afford benzoyl thiourea **125** in an excellent 92% yield.



Scheme 2.5: Synthesis of benzoyl thiourea **125**

The NMR spectrum of benzoyl thiourea **125** (figure 2.12) shows very well resolved signals, which were all assignable at room temperature in both the ¹H and ¹³C NMR spectra.

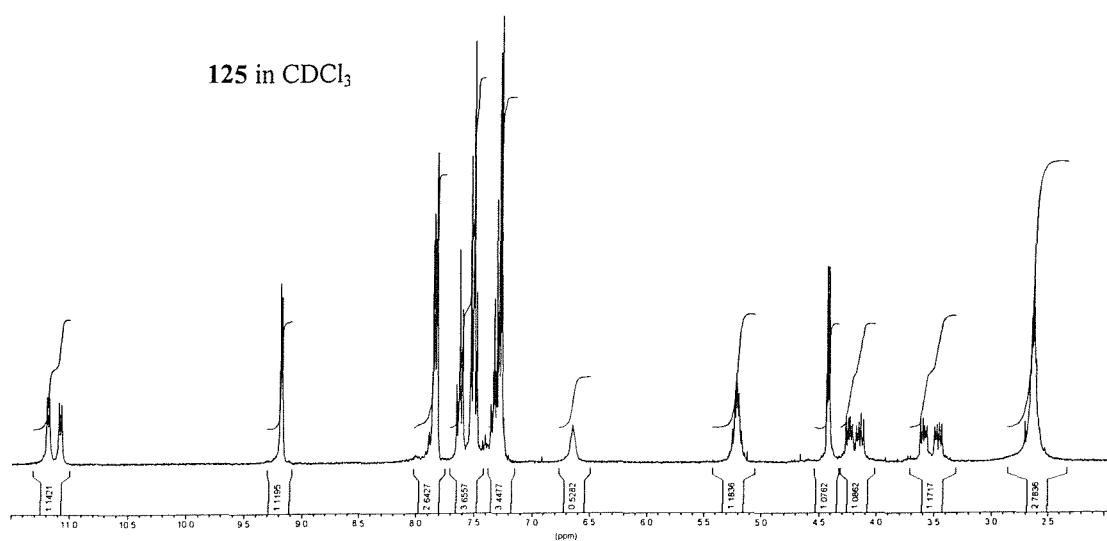
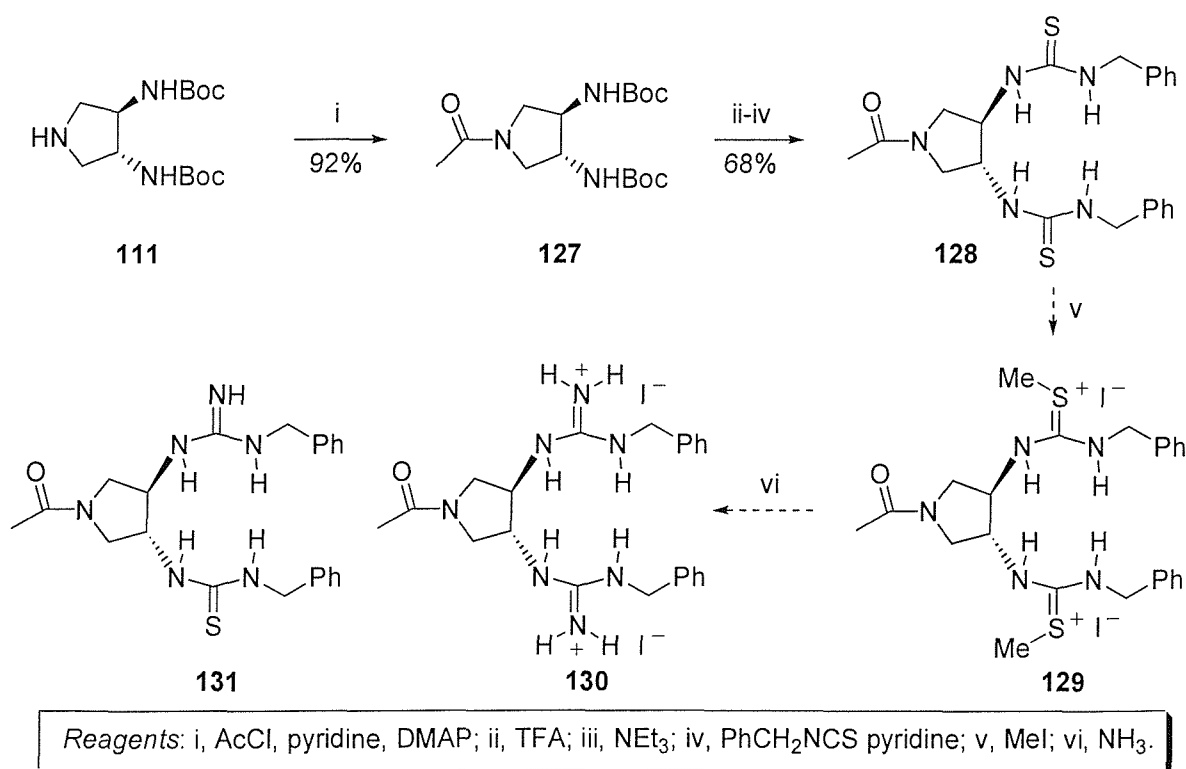


Figure 2.12: ¹H NMR spectrum of benzoyl thiourea **125**

Upon addition of *N*-Ac-Phe no change was seen in the ^1H NMR spectrum, a dilution experiment was performed on benzoyl thiourea **125** and again no change was observed. The failure of **125** to bind to *N*-Ac-Phe can be attributed to the increased stability of the dimer. The electron withdrawing benzoyl group serves to increase the acidity of the thiourea hydrogens thereby increasing the attraction between host molecules. In conclusion, the result of the bistiourea moiety aggregating is that the receptors are not able to bind amino acid carboxylate derivatives effectively.

2.4 Synthesis of Bisguanidiniums

The cause of the aggregation seen for the bistioureas was the hydrogen-bonding donor and acceptor sites. One way to eliminate the dimerisation problem would be to convert the thioureas to the corresponding guanidinium derivatives. These compounds would not form the hydrogen-bonded structure shown in figure 2.10 as the guanidinium carboxylate binding site only contains hydrogen-bonding acceptor sites.

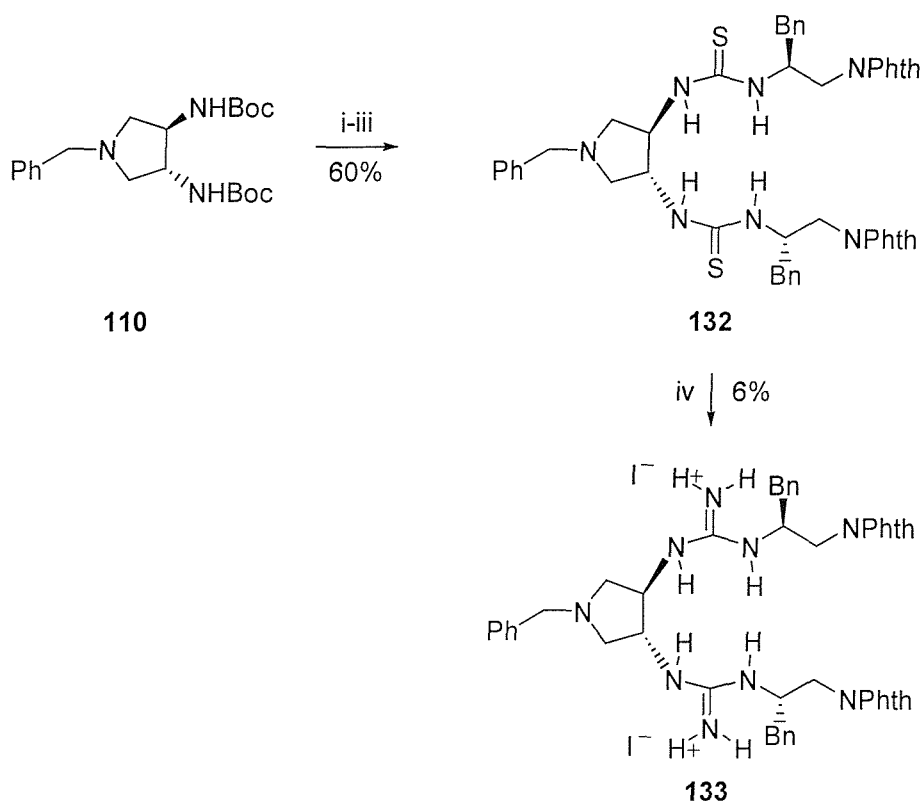


Scheme 2.6: Attempted synthesis of bisguanidinium **130**

To this end pyrrolidine **111** was treated with acetyl chloride, pyridine and catalytic DMAP to afford amide **127** in 92% yield (scheme 2.6). Boc protected diamine **127** was treated with TFA followed by triethylamine liberating the corresponding amine, which was then

condensed with benzylthioisocyanate furnishing bithiourea **128** in 68% yield. The method chosen for converting the thiourea to a guanidinium functionality was to first transform bithiourea **128** to bithiuronium iodide **129** followed by reaction with ammonia to produce the corresponding bisguanidinium iodide **130** and methanethiol. All attempts to form the bisguanidinium derivative **130** using the thiuronium methodology produced the monoguanidine **131**, with the second thiourea remaining unchanged.

In order that further attempts to synthesise bisguanidinium derivatives could be made bithiourea **132** was synthesised. Diboc **110** was deprotected using TFA and the corresponding ditrifluoroacetate deprotonated using triethylamine giving the corresponding free amine, which was coupled with two equivalents of thioisocyanate **122** to provide bithiourea **132** in a good 60% yield. Bisguanidinium **133** was successfully synthesised by treating bithiourea **132** with mercuric oxide and ammonia in a sealed tube which formed bisguanidinium in a disappointing 6% yield.



Reagents: i, TFA; ii, NEt₃; iii, add **122**; iv, HgO, NH₃, sealed tube

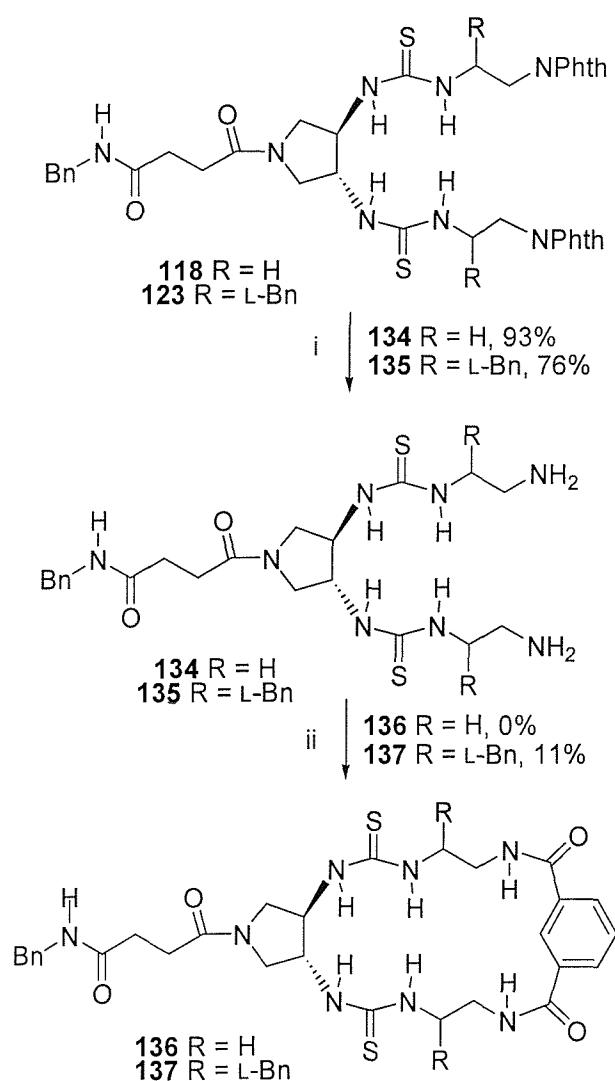
Scheme 2.7: Synthesis of bisguanidinium **133**

Only 3 mg was isolated and although a peak corresponding to $[M+H]^+$ was detected in the low resolution mass spectrum, no other characterisation could be obtained. In view of the

fact that the synthesis of bisguanidiniums such as **130** and **133** was found to be synthetically problematic it was decided to abandon this aspect of the project.

2.5 Attempted Catenation of Bisthioureas **118** and **123**

The fact that the bisthioureas were bound together by intermolecular hydrogen-bonds means that after deprotection of the corresponding diamine, the bound dimer could be capped with a suitable acid chloride generating novel catenanes. In order to determine whether bisthioureas **118** or **123** could be catenated the phthaloyl groups were removed using hydrazine hydrate furnishing diamine **134** in 93% and diamine **135** in 76% yield respectively (scheme 2.8).



Reagents: i, $\text{N}_2\text{H}_4 \cdot \text{H}_2\text{O}$; ii, isophthaloyldichloride, NEt_3 .

Scheme 2.8: Attempted catenane synthesis

It was found that diamine **134** was insoluble in CH₂Cl₂ and so the cyclisation was carried out in dry DMF. When diamine **134** was treated with isophthaloyldichloride in DMF and triethylamine none of the cyclised product **136** was isolated. Attention was then turned to the corresponding L-Bn derivative **135** which was found to be soluble in CH₂Cl₂. When diamine **135** was treated with isophthaloyldichloride in CH₂Cl₂ and triethylamine macrocycle **137** was obtained in 11% yield based on diphthalimide **123**. The material isolated after purification gave peaks in the low-resolution mass spectrum corresponding to [M+H]⁺, [M+Na]⁺ and [2M+Na]⁺. The peak at [2M+Na]⁺ could possibly correspond to catenane or macrocycle dimer however, due to the lack of a peak at [2M+H]⁺ it is more likely to correspond to macrocycle dimer. The ¹H NMR of **137** showed broad peaks at room temperature. However, when the spectra was acquired at elevated temperatures the peaks started to sharpen. Upon addition of one equivalent of *N*-Ac-L-Phe no changes were observed in the ¹H NMR spectrum.

2.6 Conclusions

A series of novel bithiourea pyrrolidines were successfully synthesised and their binding properties investigated. The bithioureas were found to form tightly bound dimers and were consequently unsuitable for the complexation of carboxylate salts, which is perhaps surprising given that thiourea **52** (chapter 1, section 1.3.3) was able to bind carboxylates. Attempts were made at utilising the dimerisation phenomenon to synthesise catenanes but this was unsuccessful. The synthesis of the corresponding bisguanidinium derivatives was carried out and was found to be problematic, which led to the abandonment of this part of the project.

Chapter Three

Synthesis of Dipyridyl Based Thiourea Tweezers

3.1 Receptor Design

Chapter two discussed the properties of bithiourea pyrrolidines such as **118** and **123**, which were found to self-associate. The self-association of the host molecules meant that the bithiourea pyrrolidines were not able to act as a carboxylate receptors. Considering this problem of self-association we sought to construct a new host scaffold which would be preformed (preorganised)⁵² into the correct conformation to bind to carboxylates.

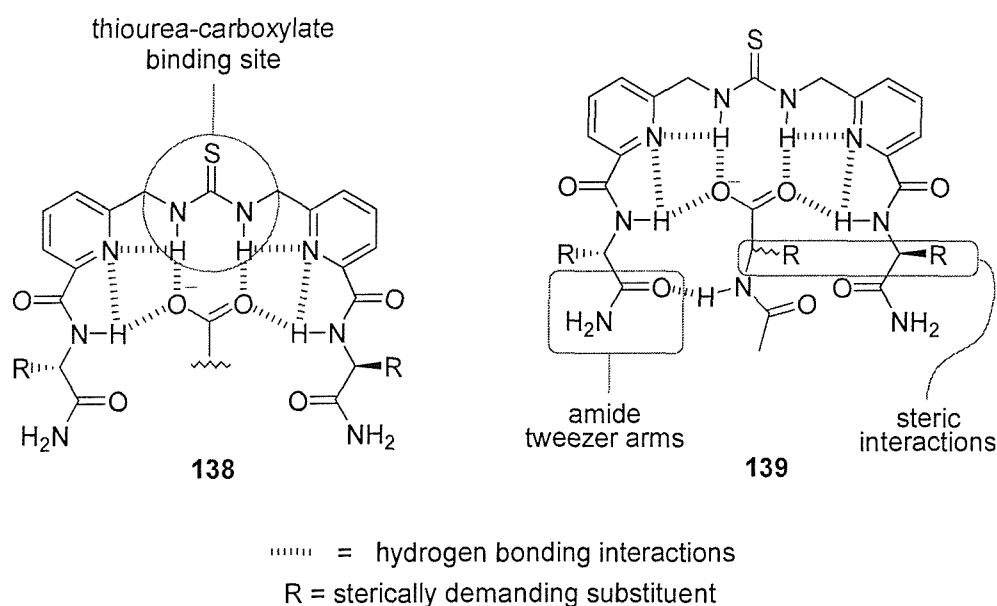


Figure 3.1: Design concept of tweezer receptor for enantioselective binding of carboxylates

The thiourea moiety was chosen to provide the primary interaction with the carboxylate guest (figure 3.1). In addition, tweezer receptor **138** was designed to preorganise into a U-shaped cleft *via* intramolecular hydrogen-bonds from the pyridine nitrogen to the thiourea and amide hydrogens. The thiourea and amide hydrogens were also intended to act as hydrogen-bonding donors to the *syn* and *anti* lone pairs of the carboxylate guest oxygens. To encourage chiral recognition between the tweezer receptor and carboxylate guest sterically demanding chiral groups were incorporated on the tweezer arms to interact with the amino acid side chain as shown in complex **139**. Amide groups were also included on the tweezer arms to form hydrogen-bonds to the guest *N*-acetyl group.

The 2,6-pyridyl derivative was found to prefer conformation A, which is stabilised by attractive electrostatic interactions between the amide protons and the pyridine nitrogen atom. In conformations B and C, there are unfavourable electrostatic interactions between the pyridine nitrogen and the carbonyl oxygen atoms. In contrast however, the lowest energy arrangement for the isophthaloyl derivative is conformation B. Moreover, intramolecular n.O.e contacts were detected for the isophthaloyl amide protons in **142** (figure 3.4) but were not detected for the pyridyl amide protons. These conformational preferences would lead to an open conformation for **142** and a folded conformation for **143**. Further confirmation of these findings was obtained from the observation that **143** bound two quinone molecules in the two cavities generated by its folded conformation, whereas **143** fails to bind quinone due to its open conformation.

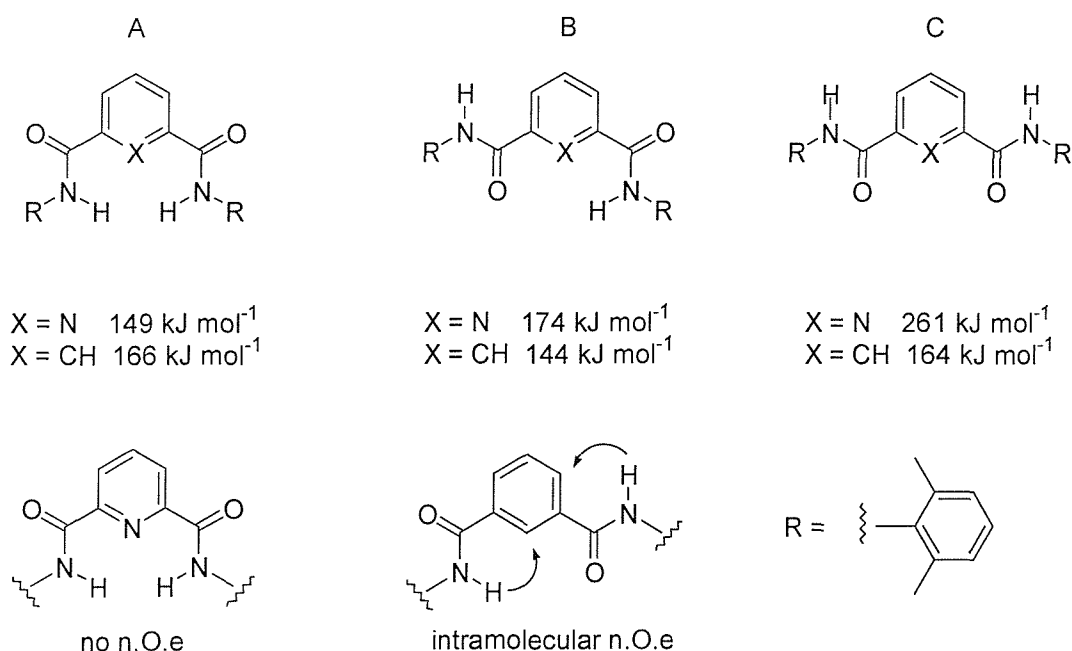


Figure 3.4: Conformational preferences of the individual subunits of **142** and **143**

With the above discussion in mind, there were two fundamental questions which were sought to be answered regarding tweezer receptor **138**. Firstly, was the receptor preorganised into a U-shaped cleft by intramolecular hydrogen-bonds, and secondly, how enantioselectively could receptor **138** bind a range of amino acid carboxylates?

To determine if receptor **138** was preorganised, pyridyl thiourea **144** and benzo thiourea **145** (figure 3.5) were to be prepared and a binding study with a simple carboxylate such as phenyl acetic carboxylate **146** carried out.

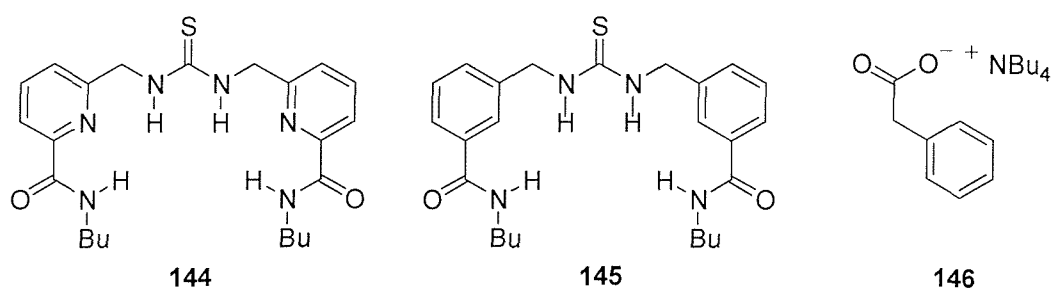
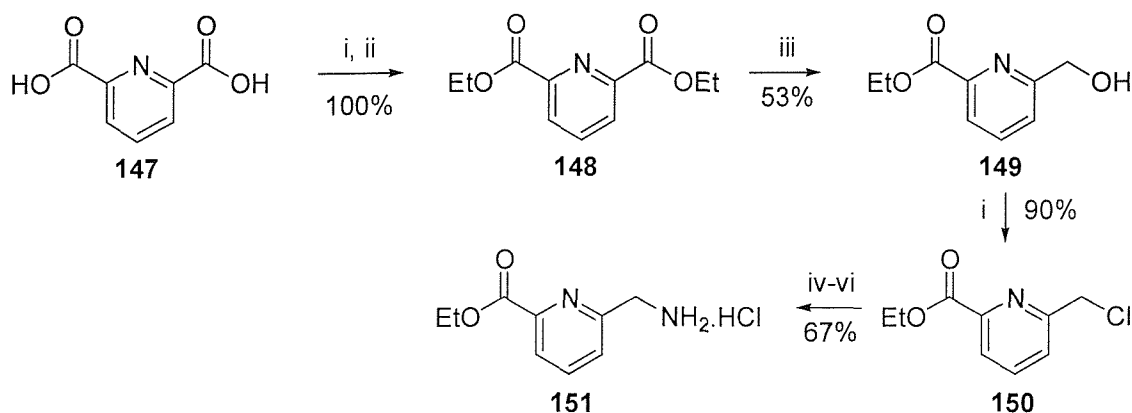


Figure 3.5: Experiment to determine degree of preorganisation

It was thought that pyridyl thiourea **144** might give a higher association constant than benzo thiourea **145** if **144** was preorganised into a U-shaped cleft, providing there was indeed four hydrogen-bonds between the thiourea and amide hydrogens to the pyridyl nitrogen as shown in **138**. It was assumed that there would be a smaller entropy loss upon binding if the tweezer arms were in the correct conformation for complexation before the binding event took place. A smaller entropy loss should lead to a higher overall association constant due to the additional energy gained as a result of preorganisation.

3.2 Synthesis of Amino Hydrochloride **151**

The synthesis of amino hydrochloride **151** (scheme 3.1) was accomplished by using the procedures of Fife⁵⁴ and Scrimin and Tonellato.⁵⁵ Pyridine-2,6-dicarboxylic acid **147** was first transformed into the corresponding diacid chloride using thionyl chloride, then the diacid chloride was esterified using ethanol to produce diethyl ester **148** in quantitative yield.



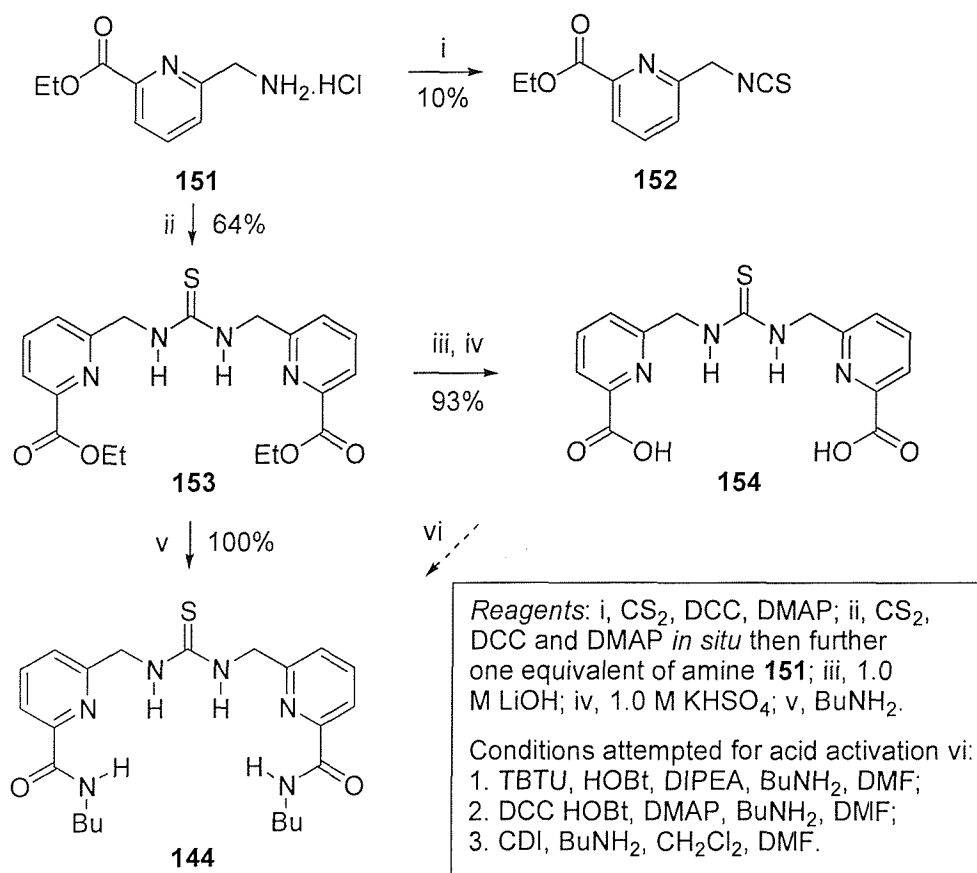
Reagents: i, SOCl₂; ii, EtOH; iii, NaBH₄; iv, potassium phthalimide; v, hydrazine hydrate; vi, HCl (g).

*Scheme 3.1: Synthesis of amino hydrochloride **151***

Diethylester **148** was then selectively reduced using sodium borohydride to give alcohol **149** in 53% yield. Treatment of alcohol **149** with thionyl chloride yielded chloride **150** in an excellent 90% yield. Chloride **150** was condensed with potassium phthalimide to afford the corresponding phthalimide, which was treated with hydrazine hydrate then gaseous hydrogen chloride to furnish amino hydrochloride **151** in an overall yield of 67%.

3.3 Synthesis of Achiral Pyridyl Tweezer **144**

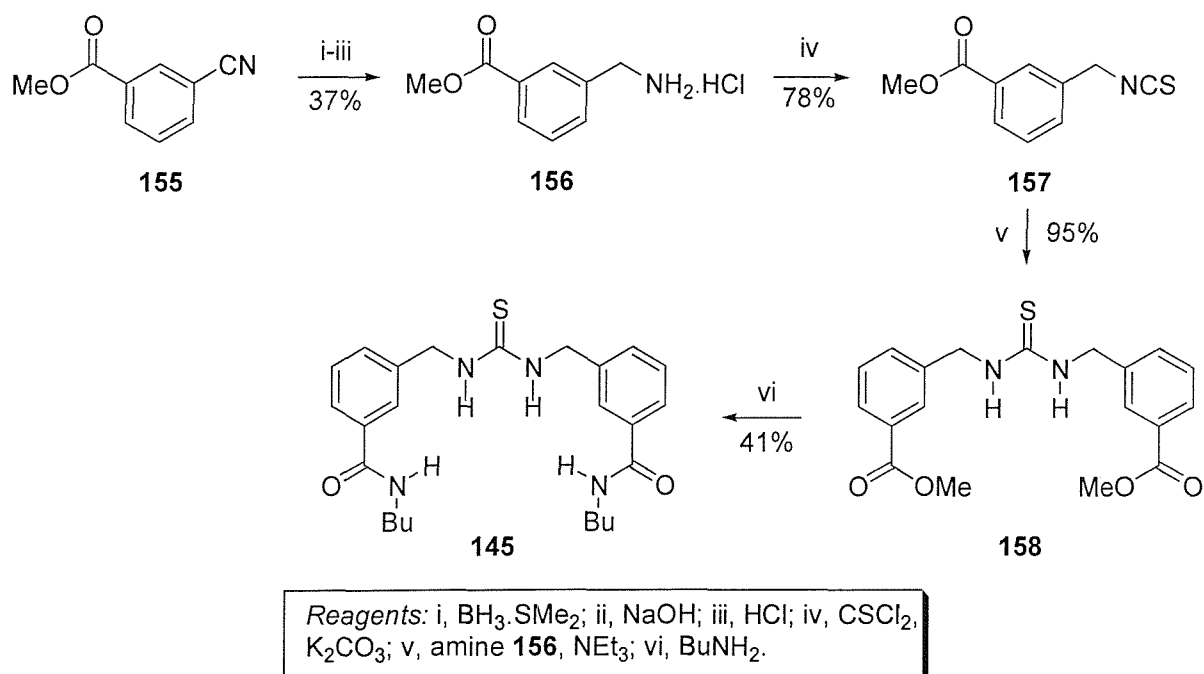
When amino hydrochloride **151** was treated with carbondisulfide, DCC and DMAP using the method of Anslyn,⁵⁶ thioisocyanate **152** was isolated in a poor yield of 10% (scheme 3.2). The low yield was attributed to the fact that thioisocyanate **152** was unstable on acidic silica. These instability problems were solved by not isolating the thioisocyanate. Thus, amino hydrochloride **151** was treated with carbon disulfide, DCC and DMAP at 0°C and after removal of the excess carbon disulfide, reaction with a further one equivalent of amino hydrochloride with DMAP gave thiourea **153** in a good yield of 64%.



Scheme 3.2: Synthesis of Achiral Pyridyl Tweezer **144**

The final step of the synthesis of achiral pyridyl tweezer **144** was to convert diester thiourea **153** to diamido thiourea **144**. It was hoped to achieve this by conversion of diester **153** to diacid **154** followed by coupling of the diacid with two equivalents of butylamine using conventional peptide coupling conditions. Diester **153** was hydrolysed using lithium hydroxide to provide diacid **154** in an excellent 93% yield. Unfortunately, all attempts to couple butylamine with diacid **154** using conventional techniques failed. However, when diester **153** was refluxed in neat butylamine, diamido thiourea **144** was formed quantitatively.

3.4 Synthesis of Achiral Benzo Tweezer 145



Scheme 3.3: Synthesis of achiral benzo tweezer **145**

The synthesis of benzo tweezer **145** starts with the reduction of the cyano group of cyanide **155** using borane dimethylsulfide complex, which after basic work up followed by precipitation of the corresponding amine with gaseous hydrogen chloride furnished amine hydrogen chloride **156** in 37% yield. Treatment of **156** with potassium carbonate and thiophosgene gave thioisocyanate **157** in a good yield of 78%. Coupling of **157** with the free amine of **156** then furnished diester **158** in an excellent yield of 95%. The synthesis of

achiral benzo thiourea **145** was completed by treating diester **158** with refluxing butylamine to give dibenzo thiourea **145** in 41% yield.

3.5 Binding Studies of Achiral Pyridyl Tweezer **144** and Achiral Benzo Tweezer **145**

With both pyridyl tweezer **144** and benzo tweezer **145** in hand the corresponding association constants for these systems with phenylacetic carboxylate **146** were measured using the procedure outlined in chapter five, section 5.5. Benzo thiourea **145** bound **146** with an association constant of 740 M^{-1} , whereas pyridyl thiourea **144** bound **146** with an association constant of 420 M^{-1} in 10% DMSO- d_6 /CDCl $_3$ (figure 3.6).

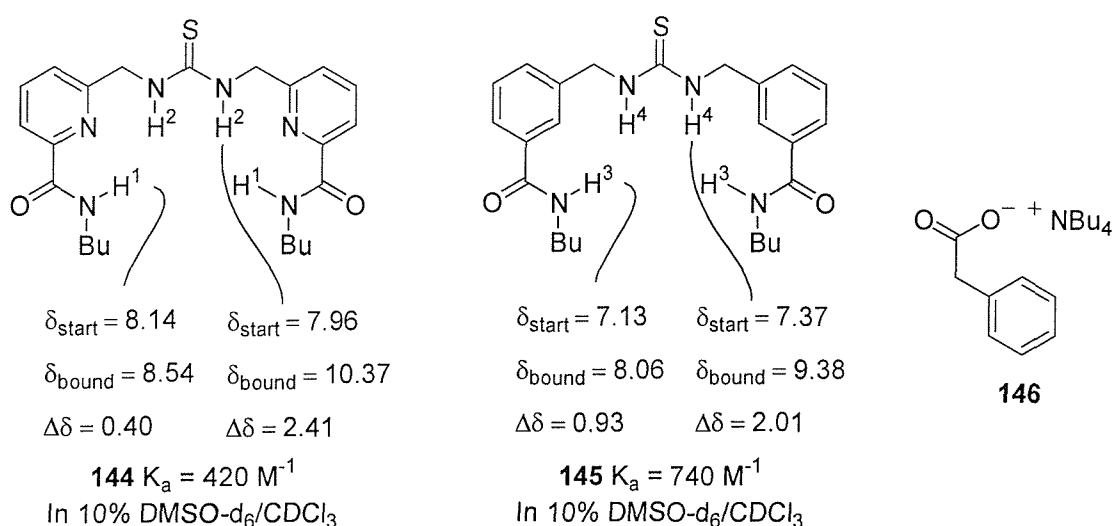


Figure 3.6: Binding study of thioureas **144** and **145** with phenyl acetic carboxylate **146**

Although the association constant for **145** was marginally larger than that for **144**, evidence for preorganisation of **144** was gained by examination of the starting chemical shifts of the amide hydrogens H1 and H3. Amide hydrogen H1 had a starting chemical shift of 8.14 ppm, whereas amide hydrogen H3 had a starting chemical shift of 7.13 ppm. Thus, H1 showed a chemical shift 1.01 ppm further downfield than H3, indicating the possibility of hydrogen-bonds between the pyridyl nitrogens and amide hydrogens. Likewise the thiourea hydrogens (H2) in **144** were found to be 0.59 ppm further downfield in **144** than H4 in **145**, again indicating hydrogen-bonding interactions. The free host chemical shifts for Hunter's pyridyl cyclic dimer **141** and cyclic tetramer **143** were also significantly more downfield than the corresponding free host chemical shifts for benzo cyclic dimer **140** and cyclic

tetramer **142** (figure 3.2 and 3.3).⁵² The stronger association constant observed for benzo thiourea **145** over pyridyl thiourea **144** is consistent with recent work by Crabtree⁵⁷ who found the nitrogen lone pair in pyridyl amide **159** electrostatically repels negatively charged anions (e.g. carboxylates) more than the C-H in benzo amide **160** (figure 3.7). This resulted in the association constant for pyridyl amide **159** being lower than benzo amide **160**.

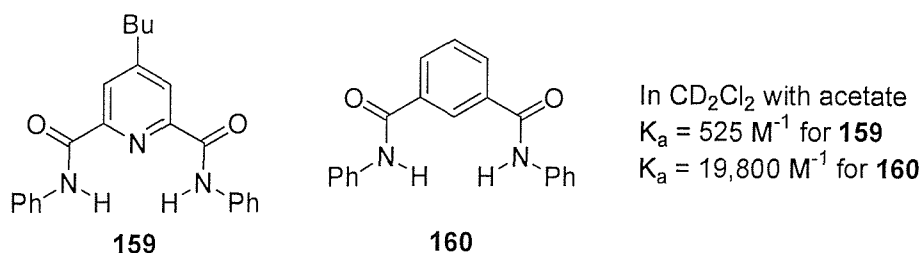


Figure 3.7: Crabtree's anion receptors

A crystal structure of tweezer **144** (figure 3.8) showed that it formed a dimer in the solid state. The amide of one side of tweezer **144** had been pushed out of the plane of the pyridine ring to form a dimer *via* intermolecular hydrogen-bonds from the thiourea hydrogens and one amide hydrogen to the amide oxygen lone pairs. However, the side not involved in dimer formation was found to be in the correct conformation with hydrogen-bonds from the amide hydrogen to the pyridyl nitrogen and the thiourea hydrogen to the pyridyl nitrogen. A simple solution dilution experiment of tweezer **144** was carried out (from 4 mM to 40 mM), by obtaining the two ¹H NMR spectra at these concentrations. There was no change in the positions of any of the signals in the spectra, which indicated that tweezer **144** did not dimerise in solution to any significant extent.

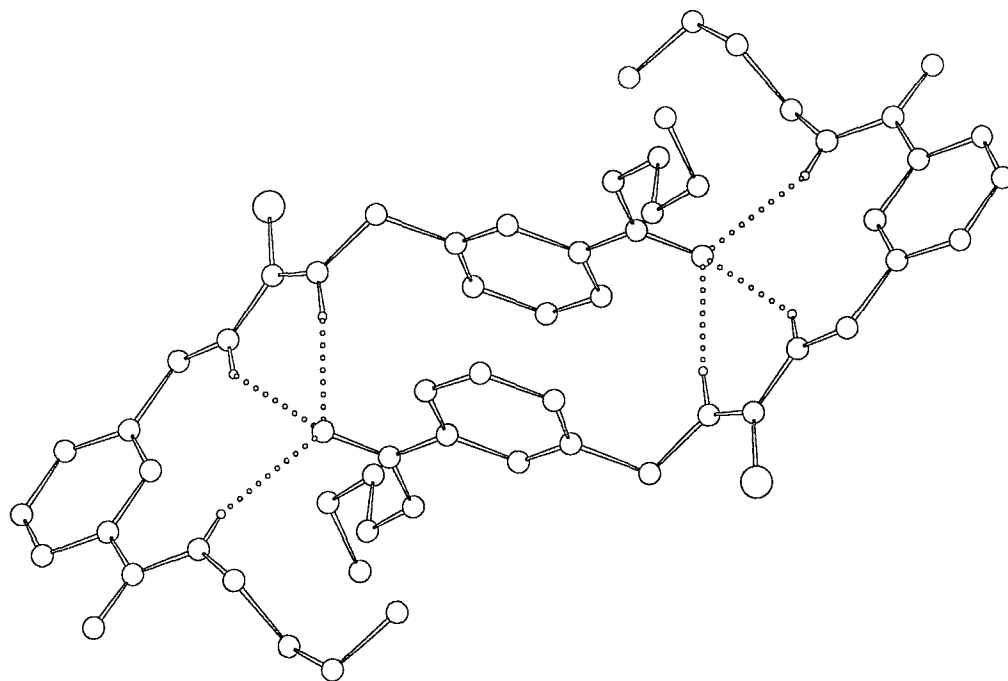


Figure 3.8: Crystal structure of tweezer **144**

Molecular modeling studies on the conformational properties of the methyl derivative of tweezer **144** (*i.e.* the butyl group was replaced by a methyl group) were carried out (figure 3.9). The molecular modeling package used was MacroModel V5.0⁵⁸ along with its implementation of the OPLS*⁵⁹ forcefield. Solvent was included in all the calculations through the use of the GB/SA continuum model for chloroform.⁶⁰ Initially the free receptor was examined. The structure was subjected to a minimisation process (using the Polak-Ribiek method), which served to change bond lengths and angles to those which are reasonable. After the first minimisation the structure was subjected to a simulated annealing process, where the temperature was set to 600 K and the system cooled over the course of 1 ns to 0 K. In addition to the above parameters, the SHAKE algorithm⁶¹ was applied to all bonds and the timestep was set to 1.5 fs. The process of allowing slow cooling should allow the tweezer to explore a number of conformations. After the simulated anneal, the structure should be near or at the global energy minimum. The process of minimisation and simulated annealing was repeated several times to generate a series of structures, all of which gave a representation of the structure at its global energy minimum. The free tweezer (figure 3.9) was found to not adopt a U-shape but instead one of the tweezer arms twisted, such that the amide groups were pointing in opposite directions. In a separate experiment acetate was docked with the tweezer by eye and the thiourea hydrogen – carboxylate oxygen bond

distances set to a typical hydrogen-bonding distance of 1.8 ± 0.2 Å. After repeating the minimisation/simulated annealing process ten times as described above, two additional hydrogen-bonds were formed from the amide hydrogens to the *syn* lone pairs of the carboxylate oxygens. This observation is in agreement with the large changes in chemical shift of both the thiourea and amide hydrogens of tweezer **144** which occurred upon addition of carboxylate guest during the ^1H NMR titration binding studies.

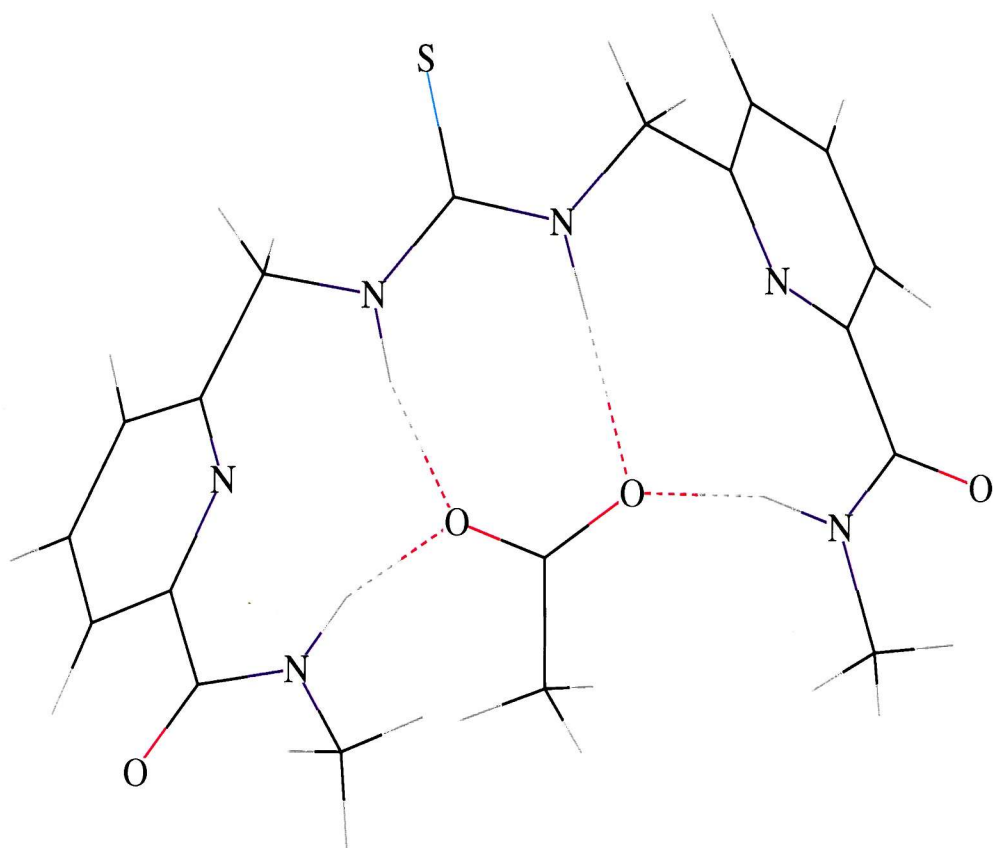
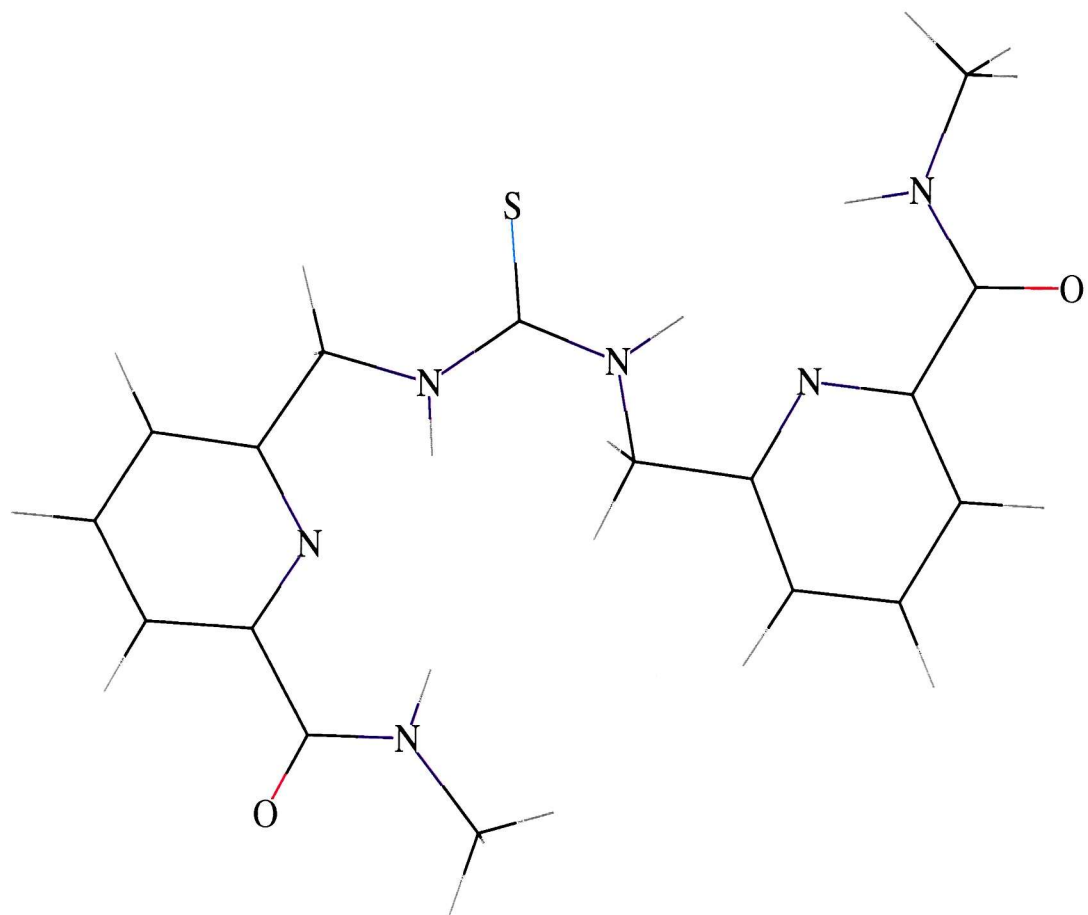


Figure 3.9: Molecular modeling studies on the methyl derivative of tweezer 144

As a result of the experiments undertaken *vide supra*, it was concluded that tweezer **144** and **145** successfully bound phenylacetic carboxylate *via* hydrogen-bonds from the thiourea and amide hydrogens to the carboxylate oxygen lone pairs. Although the association constant for benzo thiourea **145** was marginally higher than that for the corresponding pyridyl thiourea **144** the chemical shifts for both the thiourea and amide hydrogens in **144** were significantly more downfield than in benzo thiourea **145**. The higher free host chemical shift values for **144** suggested hydrogen-bond formation between the thiourea/amide hydrogens and pyridyl nitrogens and therefore a degree of preorganisation. Thus, we could neither verify nor reject the preorganised conformation hypothesis for pyridyl tweezer **138**, so an alternative approach was sought.

Since the difference in relative association constants between the pyridine and benzo series could not be used as a measure of the level of preorganisation present in the pyridyl series, we decided to prepare both pyridyl- and benzo- chiral tweezers **161** and **162** (figure 3.10).

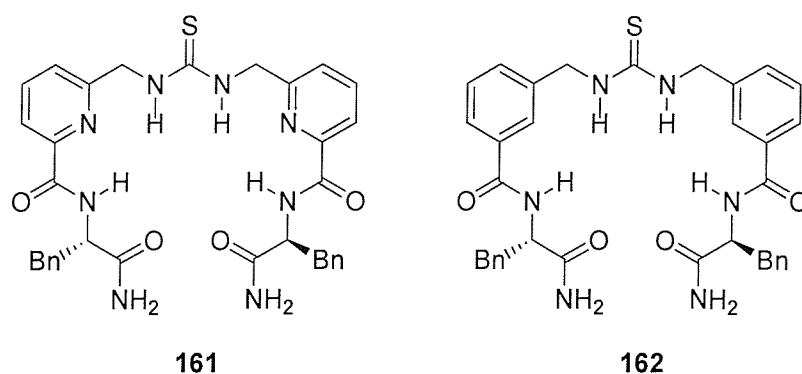
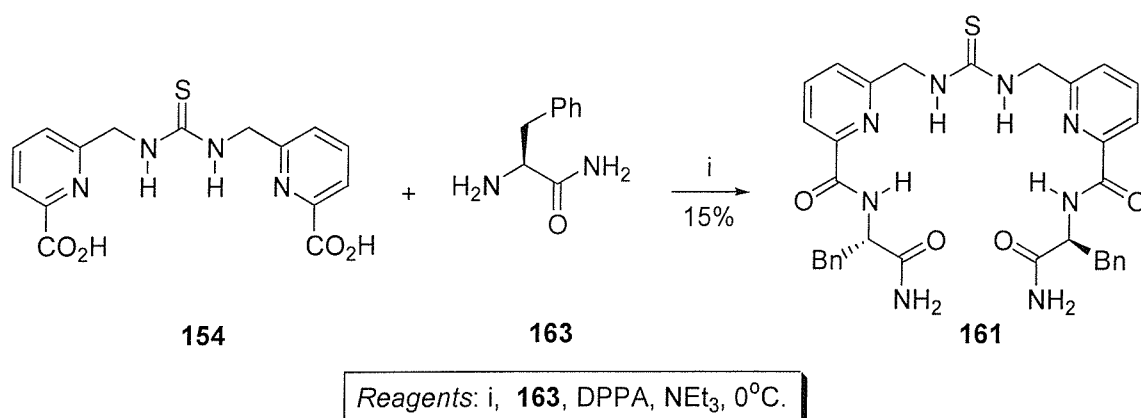


Figure 3.10: Tweezers **161** and **162** for comparison of enantioselectivities ($\Delta\Delta G$) as a measure of preorganisation

Comparison of the difference in enantioselectivities ($\Delta\Delta G$) between chiral pyridyl tweezer **161** and chiral benzo tweezer **162** for the enantiomers of a given carboxylate substrate should show if pyridyl tweezer **161** is preorganised into a U-shaped cleft. If the difference in free energies ($\Delta\Delta G$) between the enantiomers of a carboxylate guest is larger for pyridyl tweezer **161** than benzo tweezer **162** then we could conclude that this difference is due to the increased level of preorganisation in **161**.

3.6 Synthesis of Chiral Pyridyl Tweezer 161

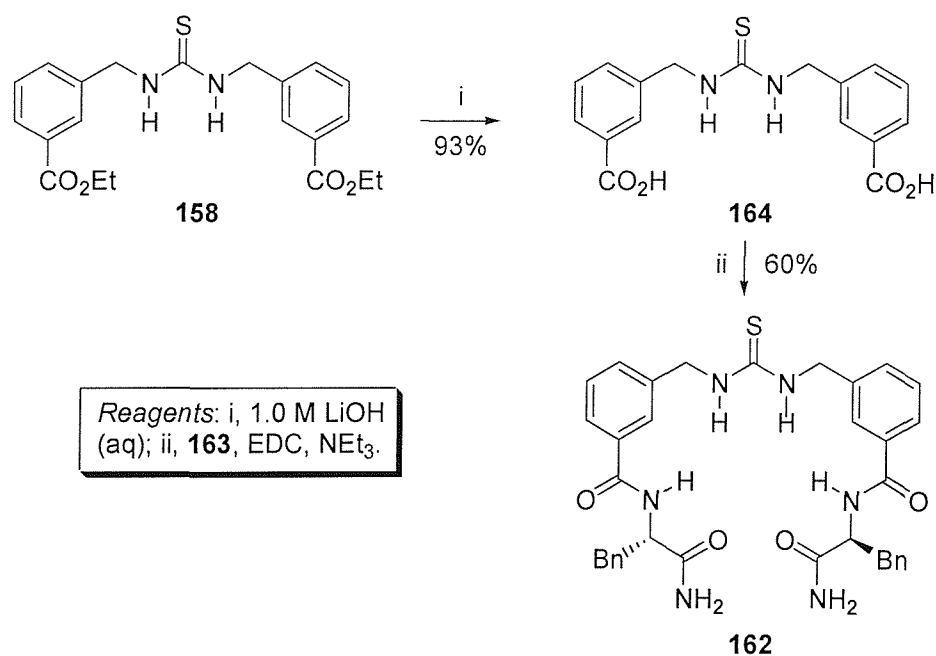
The problems encountered when trying to couple butylamine with diacid **154** to form pyridyl amide **144** (section 3.3) were also met when trying to couple chiral amine **163** with diacid **154**. Unsuccessful conditions attempted for the activation of diacid **154** included TBTU, DCC and CDI. When the azide activating reagent DPPA⁶² was used along with triethylamine, pyridyl tweezer **161** was produced in a disappointing 15% yield (scheme 3.4). Although the reaction was not high yielding, sufficient quantities of material (>100 mg) was obtained allowing the binding properties to be investigated.



Scheme 3.4: Synthesis of chiral pyridyl tweezer **161**

3.7 Synthesis of Chiral Benzo Tweezer 162

Diester **158** was hydrolysed using aqueous lithium hydroxide giving diacid **164** in an excellent yield of 93% (scheme 3.5). Diacid **164** was successfully coupled amine **163** using water soluble carbodiimide (EDC) and triethylamine to give benzo tweezer **162** in a gratifying yield of 60%.



Scheme 3.5: Synthesis of chiral benzo tweezer 162

3.8 Binding Properties of Chiral Pyridyl Tweezer **161** – Optimisation of Enantioselectivity

In order to investigate the ability of chiral tweezer **161** to enantioselectively bind substrates, a range of amino acids were chosen with differing side chain functionality. Phenylalanine and alanine were picked to see the effect of side chain steric bulk upon binding. Amino acids with similar side chain hydrogen-bonding functionality such as asparagine and glutamine were selected to probe the effect of side chain length whilst tryptophan was chosen to probe the effect of the steric bulk of the hydrogen-bond donor on binding selectivity. Initial attempts at obtaining association constants by conventional ¹H NMR titration experiments were unsuccessful due to an unexpected signal broadening effect. The peaks in the proton spectra broadened upon addition of successive aliquots of guest. A separate experiment showed that when one equivalent of guest was added to the host and a ¹H NMR immediately obtained, the peaks were very broad. After leaving the system to equilibrate overnight the peaks sharpened. Thus, to avoid the problem the host-guest solution was allowed to equilibrate for 12 hours after each aliquot of guest was added.

Guest	K_a/M^{-1}	$\Delta G/kJ mol^{-1}$	$\Delta\Delta G/kJ mol^{-1}$
<i>N</i> -Ac-L-Ala 165	3,450	20.3	0.8
<i>N</i> -Ac-D-Ala 166	2,520	19.5	
<i>N</i> -Ac-L-Phe 167	4,770	21.1	1.1
<i>N</i> -Ac-D-Phe 168	2,990	20.0	
<i>N</i> -Ac-L-Asn 169	1,690	18.5	1.8
<i>N</i> -Ac-D-Asn 170	800	16.7	
<i>N</i> -Ac-L-Gln 171	9,000	22.7	1.7
<i>N</i> -Ac-D-Gln 172	4,520	21.0	
<i>N</i> -Boc-L-Gln 173	1,190	17.7	1.0
<i>N</i> -Boc-D-Gln 174	810	16.7	
<i>N</i> -Ac-L-Ser 175	380	14.8	0.6
<i>N</i> -Ac-D-Ser 176	480	15.4	
<i>N</i> -Ac-L-Trp 177	12,400	23.5	0.5
<i>N</i> -Ac-D-Trp 178	14,800	24.0	
<i>N</i> -Boc-L-Trp 179	3,140	20.1	0.9
<i>N</i> -Boc-D-Trp 180	2,225	19.2	
<i>R</i> -Nap 181	26,200	25.4	0.2
<i>S</i> -Nap 182	28,300	25.6	

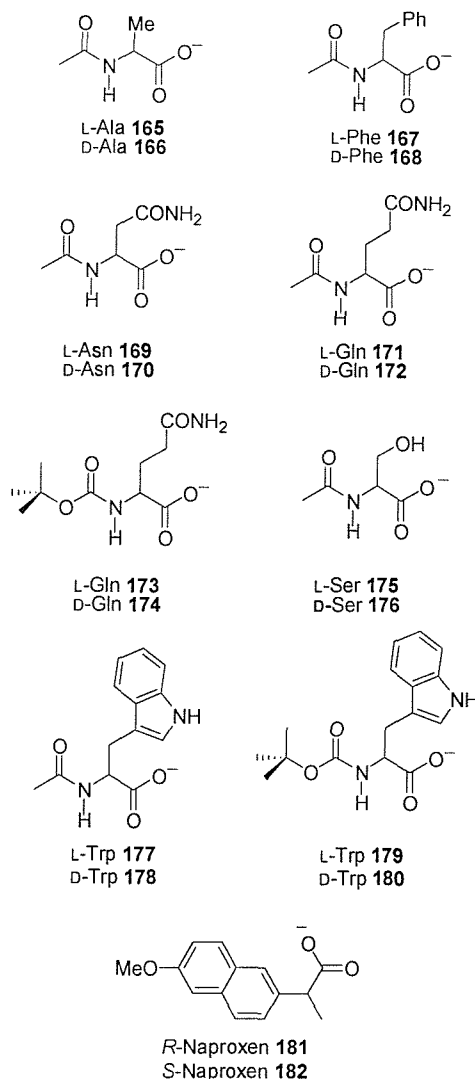


Table 3.1: Screening of a range of guests against pyridyl tweezer **161** in $CDCl_3$ (experimental error in association constants was 10%)

It was found that tweezer **161** was moderately enantioselective for the L forms of all guests except tryptophan and serine, where D was found to bind more selectively (table 3.1). *N*-Ac-L-Gln **171** and *N*-Ac-L-Asn **169** were bound twice as strongly as the D enantiomers **172** and **170** respectively as evidenced by the association constants measuring twice as large. In contrast, *N*-Ac-L-Ala and *N*-Ac-L-Phe were not bound as selectively, which is presumably a consequence of the lack of side chain hydrogen-bonding functionality in phenylalanine and alanine. The association constants for both *N*-Ac-L-Trp and *N*-Ac-D-Trp were significantly larger than those for the other amino acids, although the enantioselectivity was found to be smaller than for the other amino acids.

A further study was undertaken using *N*-Boc-Gln **173/174** and *N*-Boc-Trp **179/180** to ascertain whether the increased steric bulk of the Boc group would enhance the level of enantioselectivity. For *N*-Boc-Gln **173/174** the association constants were both found to be lower than in the *N*-acetyl case as was the level of enantioselectivity. The association constants for *N*-Boc-Trp **179/180** were similarly lower than the *N*-acetyl case although the enantioselectivity was higher for *N*-Boc-Trp ($\Delta\Delta G = 0.9 \text{ kJ mol}^{-1}$ for *N*-Boc-Trp **179/180** and $\Delta\Delta G = 0.5 \text{ kJ mol}^{-1}$ for *N*-Ac-Trp **177/178**).

Table 3.2 shows the overall change of the thiourea (H1), amide (H2) and *N*-terminal amide (H3) chemical shifts for tweezer **161** upon addition of the guests, shown at 100% saturation in CDCl₃. The signal for thiourea H1 was observed to change between 1.62 and 2.13 ppm, whereas the amide signal H2 changed between 0.29 and 0.66 ppm. The fact that the thiourea shifts were significantly larger than the amide shifts is consistent with the notion that the thiourea-carboxylate interaction is the predominant one. The large shifts of *N*-terminal amide H3 of between 0.30 and 0.86 ppm provide good evidence that hydrogen-bonds between either the *N*-acetyl group or amino acid side chain are being formed. The shifts in H3 also support the notion that tweezer **161** is bound in the conformation shown by complex **139** (section 3.1, figure 3.1).

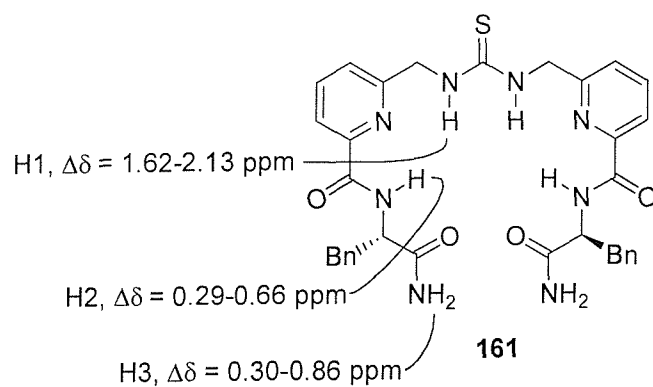


Figure 3.11: Chemical shifts of protons H1-H3 during binding studies in CDCl_3

Guest	Thiourea (H1)	Amide (H2)	N-term amide (H3)
<i>N</i> -Ac-L-Ala 165	1.84	0.50	0.75
<i>N</i> -Ac-D-Ala 166	1.68	0.46	0.77
<i>N</i> -Ac-L-Phe 167	1.90	0.42	0.74
<i>N</i> -Ac-D-Phe 168	1.95	0.47	0.73
<i>N</i> -Ac-L-Asn 169	1.67	0.39	0.37
<i>N</i> -Ac-D-Asn 170	1.66	0.29	0.32
<i>N</i> -Ac-L-Gln 171	1.62	0.58	0.55
<i>N</i> -Ac-D-Gln 172	1.70	0.62	0.56
<i>N</i> -Boc-L-Gln 173	2.00	0.48	0.62
<i>N</i> -Boc-D-Gln 174	1.97	0.46	0.60
<i>N</i> -Ac-L-Ser 175	2.07	0.46	0.33
<i>N</i> -Ac-D-Ser 176	2.13	0.60	0.30
<i>N</i> -Ac-L-Trp 177	1.80	0.43	0.86
<i>N</i> -Ac-D-Trp 178	1.80	0.45	0.49
<i>N</i> -Boc-L-Trp 179	1.91	0.53	0.50
<i>N</i> -Boc-D-Trp 180	1.94	0.62	0.51
<i>R</i> -Nap 181	1.84	0.66	0.80
<i>S</i> -Nap 182	1.88	0.60	0.79

Table 3.2: Overall change of thiourea (H1), amide (H2) and N-terminal amide (H3) chemical shifts (in ppm) for **161** in CDCl_3

3.9 Binding Properties of Chiral Thioureas **161** and **162** – Investigation of the Preorganisation Hypothesis

To establish if pyridyl tweezer **161** was preorganised, binding studies for both benzo tweezer **162** and pyridyl tweezer **161** were carried out. In order to maximise possible hydrogen-bonding interactions an apolar hydrophobic solvent such as chloroform was the solvent of choice. However, benzo tweezer **162** was not soluble in chloroform so 10% DMSO- d_6 in $CDCl_3$ was used. Both pyridyl tweezer **161** and benzo tweezer **162** were found to be selective for *N*-Ac-L-Phe **167** (table 3.3) as shown by the fact that the association constants were all measured to be larger for *N*-Ac-L-Phe **167** than *N*-Ac-D-Phe **168**. For benzo tweezer **162** the association constant was measured to be 2330 M^{-1} and 1840 M^{-1} for **167** and **168** respectively, the difference in free energies of binding ($\Delta\Delta G$) was found to be 0.5 kJ mol^{-1} . For pyridyl tweezer **161** the association constant was measured to be 680 and 530 M^{-1} for **167** and **168** respectively, the difference in free energies of binding was found to be 0.6 kJ mol^{-1} . Although pyridyl tweezer **161** was 0.1 kJ mol^{-1} more enantioselective than benzo tweezer **162** the level of accuracy present in the experiment (estimated to be at 10%) means that the difference is not meaningful. To further maximise hydrogen-bonding interactions in the host-guest complex and to increase the level of enantioselectivity observed, *N*-Ac-Phe **167/168** were changed for asparagine derivatives **169/170**, which contain additional hydrogen-bonding functionality. It was envisaged that the equivalent experiment with asparagine giving more pronounced differences, as pyridyl tweezer **161** was found to bind asparagine more enantioselectively than phenylalanine in $CDCl_3$ (section 3.8) and should therefore be more enantioselective in 10% DMSO/ $CDCl_3$. *N*-Ac-Asp was indeed found to show more pronounced enantioselectivity for pyridyl tweezer **161** ($\Delta\Delta G = 1.5\text{ kJ mol}^{-1}$) than for benzo tweezer **162** ($\Delta\Delta G = 0.4\text{ kJ mol}^{-1}$), suggesting that the presence of the pyridyl nitrogen might preorganise the receptor to a degree.

Host	Guest	K_a / M^{-1}	ΔG / $kJmol^{-1}$	$\Delta\Delta G$ / $kJmol^{-1}$
161	<i>N</i> -Ac-L-Phe 167	680	16.3	0.6
	<i>N</i> -Ac-D-Phe 168	530	15.7	
162	<i>N</i> -Ac-L-Phe 167	2330	19.3	0.5
	<i>N</i> -Ac-D-Phe 168	1840	18.8	
161	<i>N</i> -Ac-L-Asn 169	710 [†]	16.4	1.5
	<i>N</i> -Ac-D-Asn 170	1320 [†]	17.9	
162	<i>N</i> -Ac-L-Asn 169	3160 [†]	20.1	0.4
	<i>N</i> -Ac-D-Asn 170	3770 [†]	20.5	

Table 3.3: Binding studies with tweezer **161** and **162** in 10% DMSO-*d*₆/CDCl₃ († these are preliminary results for which the error is estimated to be 25%)

3.10 Design Concept of Second Generation Tweezer Receptor **183**

Having synthesised and investigated the properties of pyridyl tweezer **161** the design of a receptor for a specific compound was undertaken. The specific compound to which selective binding was desired was Naproxen **184**. Naproxen has been used as a drug for the treatment of rheumatoid arthritis⁶³ and is produced in large quantities as the racemic mixture. This mixture is then separated into the optically pure compounds prior to use.⁶⁴ If a selective receptor for Naproxen could be developed it might be possible to use the receptor to separate a racemic Naproxen mixture into the respective *R* and *S* enantiomers. The development of synthetic receptors for single substrates is an extremely challenging goal in itself, and relies on controlling intermolecular interactions to direct binding events.

Naproxen represents an even greater challenge as there is little polar functionality to which the host-guest chemist can take advantage of when trying to incorporate complementary functionalities into the host molecule. The approach we took was to use the thiourea moiety in **183** (figure 3.12) to provide the primary interaction with the naproxenate carboxylate oxygens. In addition, electron deficient *p*-nitrobenzene groups were included on the tweezer arms to encourage π - π stacking interactions with the electron rich naphthalene ring. To achieve chiral recognition, sterically demanding benzyl groups were incorporated on the tweezer arms to interact with the Naproxen methyl group.

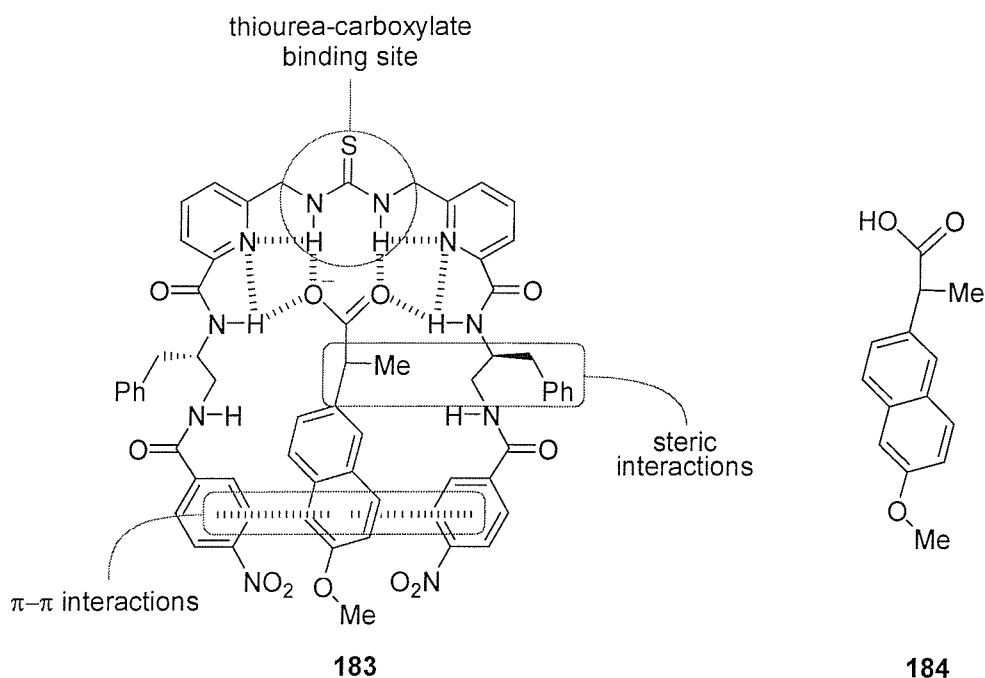
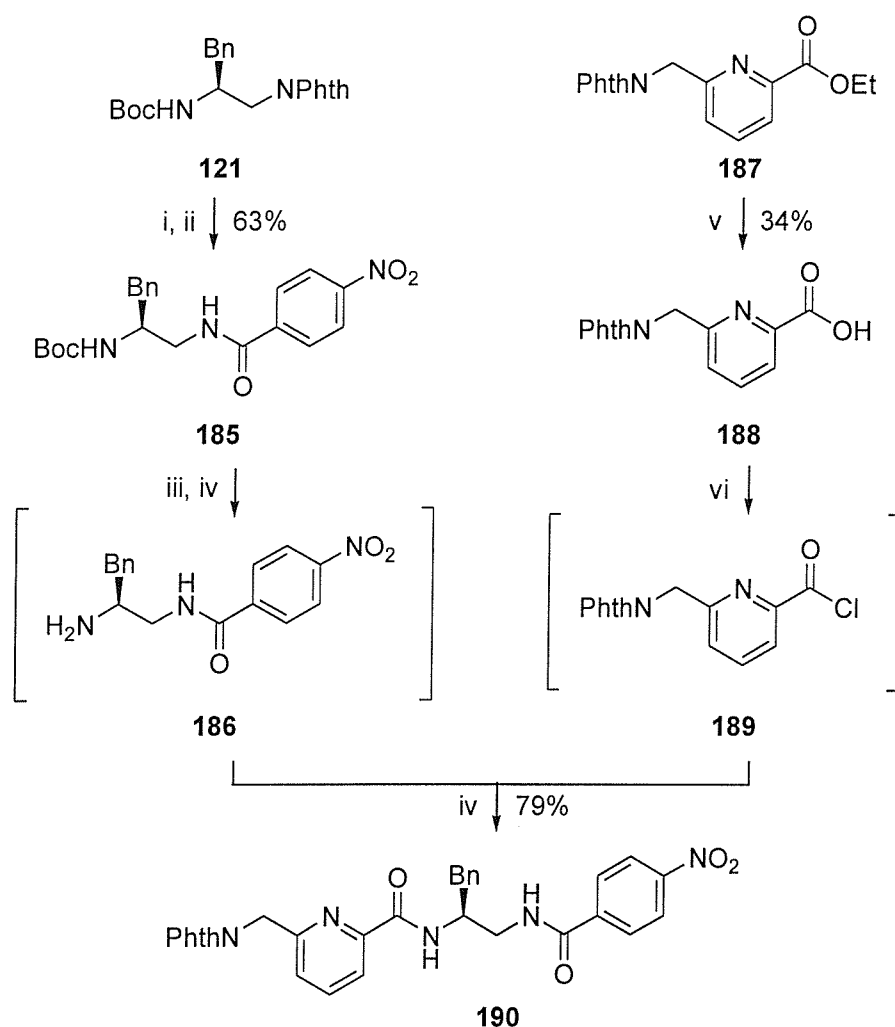


Figure 3.12: Second Generation Tweezer Receptor **183** for Naproxen **184**

3.11 Synthesis of Second Generation Tweezer Receptor **183**

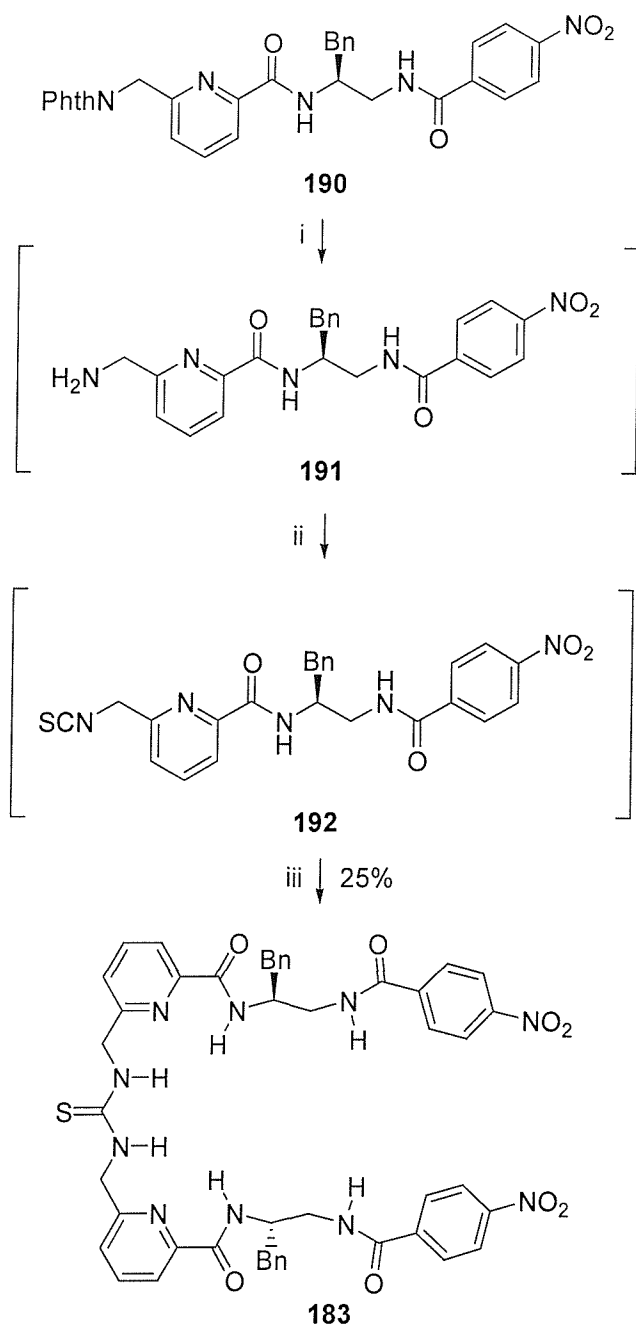
Phthalimide **121** was deprotected using hydrazine hydrate to produce the corresponding amine which was reacted with *p*-nitrobenzoyl chloride, DMAP and triethylamine giving amide **185** in 63% yield (scheme 3.6). Removal of the Boc group of amide **185** using TFA, followed by treatment of the resultant TFA salt with DMAP furnished amine **186**. Attempts to deprotect ester **187** (an intermediate in synthesis of amine **151**, section 3.3) *via* conventional basic hydrolysis using both aqueous sodium hydroxide at varying concentrations and lithium hydroxide at varying concentrations all failed and led to hydrolysis of the phthalimido imide. Acidic hydrolysis using a mixture of formic and concentrated sulfuric acid also failed. However, ester **187** was successfully deprotected using sodium iodide and trimethylsilyl chloride following the procedure of Olah⁶⁵ to give acid **188** in 34% yield. Acid **188** was converted to acid chloride **189** using thionyl chloride. Amine **186** was then condensed with acid chloride **189** in the presence of DMAP to give amide **190** in an excellent yield of 79%.



Reagents: i, $N_2H_4 \cdot H_2O$; ii, *p*-nitrobenzoyl chloride, NEt_3 , DMAP; iii, TFA; iv, DMAP; v, NaI, $TMSCl$; vi, $SOCl_2$.

Scheme 3.6: Synthesis of phthalimide precursor 190

Phthalimide **190** was deprotected using hydrazine hydrate to produce the corresponding amine **191** (scheme 3.7). Without isolation, amine **191** was reacted with carbon disulphide, DCC in the presence of DMAP to give thioisocyanate **192**. This was then coupled *in situ* with a further equivalent of amine **191** to provide thiourea **183** in an overall yield of 25%.



Reagents: i, $\text{N}_2\text{H}_4 \cdot \text{H}_2\text{O}$; ii, CS_2 , DCC, DMAP;
 iii, add second equivalent of amine **191**, DMAP.

Scheme 3.7: Synthesis of second generation tweezer **183**

3.12 Binding Properties of Tweezer Receptor **183**

Having successfully synthesised tweezer **183**, it was possible to perform binding studies in CDCl₃ (table 3.4). The association constant for *R*-Naproxen **181** was measured to be 1570 M⁻¹ and 1870 M⁻¹ for *S*-Naproxen **182**, which showed a selectivity of 5:6 in favour of *S*-Naproxen. In comparison to the first generation receptor **161** this was an improvement in the binding selectivity of 0.1 (*i.e.* there was a selectivity of 10:11 in favour of *S*-Naproxen with tweezer **161**). As the results of the binding study with Naproxen showed the receptor to be only slightly enantioselective for *S*-Naproxen a further study was undertaken. The substrate chosen was *N*-Boc-Trp **179/180** due to its electron rich indole side chain. We anticipated that the electron rich side chain might π -stack with the *p*-nitrobenzamide groups of tweezer **183**. Tweezer **183** was showed a selectivity of 2:1 in favour of the D enantiomer.

Guest	K _a / M ⁻¹	ΔG / kJmol ⁻¹	$\Delta\Delta G$ / kJmol ⁻¹
<i>R</i> -Nap 181	1570	18.4	0.4
<i>S</i> -Nap 182	1870	18.8	
<i>N</i> -Boc-L-Trp 179	1925	18.7	1.7
<i>N</i> -Boc-D-Trp 180	3785	20.4	

Table 3.4: Binding studies with second generation tweezer **183** in CDCl₃

Further examination of the ¹H NMR spectra from the binding studies of substrates **179-182** with tweezer **183** revealed that shifts of both amide hydrogens H1 and H2 occurred (table 3.5). The fact that H2 shifted considerably provides good evidence that there are interactions between the naproxen naphthalene ring and the tryptophan side chain with the *p*-nitrobenzoate moiety in tweezer **183**. It was also found that shifts of ~ 0.2 ppm were seen for the pyridyl triplet (H3).

Guest	Amide (H1)	Amide (H2)	Pyridyl Triplet (H3)
<i>R</i> -Nap 181	0.51	1.17	0.22
<i>S</i> -Nap 182	0.37	1.21	0.21
L-Trp 179	0.48	1.10	0.23
D-Trp 180	0.38	1.10	0.24

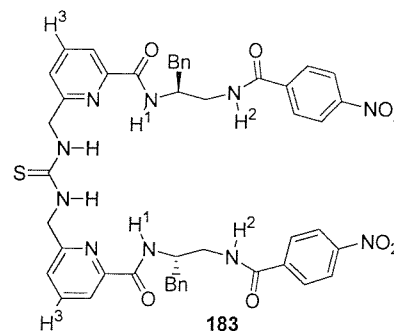


Table 3.5: Limiting chemical shifts for second generation tweezer **183** in $CDCl_3$

Evidence for π -stacking interactions was gained by examining the shifts of the aromatic hydrogens of the *p*-nitrobenzene group during the binding study (figure 3.13). The hydrogen further downfield (assigned as H1 due to the presence of the nitro group) shifted 0.14 ppm after addition of two equivalents of *S*-naproxen and the hydrogen ortho to the amide (H2) shifted 0.22 ppm downfield. Similar shifts were observed during the tryptophan binding study with tweezer **183**, where H1 shifted 0.10 ppm and H2 shifted 0.22 ppm after addition of two equivalents of L-Trp **179**.

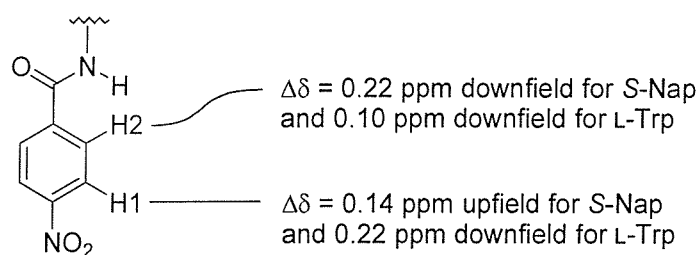


Figure 3.13: Evidence for π -stacking between host and guest

3.13 Conclusions

A series of novel thiourea tweezer receptors were successfully synthesised and their binding properties investigated. *N*-Ac-Asn was indeed found to show more pronounced enantioselectivity for pyridyl tweezer **161** than for benzo tweezer **162**, suggesting that the presence of the pyridyl nitrogen might preorganise the receptor to a degree. It was also concluded that these tweezers form well defined complexes with a range of carboxylates. Both the thiourea and amide hydrogens were involved in forming hydrogen-bonds to the carboxylate *syn* and *anti* lone pairs and the additional functionality in **161/162** served to

form additional hydrogen-bonds to the guests (figure 3.11). In the case of the second generation tweezer **183**, evidence in support of π -stacking interactions was observed. All these observations are consistent with the proposed mode of binding outlined in section 3.1. Chiral receptors **161** and **183** bound a range of chiral carboxylates with enantioselectivities of 2:1, which is lower than those typically observed for macrocyclic structures (>5:1). It is therefore possible to conclude that the inherent preorganisation of macrocycles cannot be rivaled by conformationally unrestricted tweezers of the type discussed in this chapter.

Chapter Four

Synthesis of a Novel Bisthiourea Macrocycle

4.1 Receptor Design

A method for the detection of glutamic acid in biological systems is of considerable interest to biologists. If a fluorescent tag was attached to an enantioselective glutamate receptor, it might be possible to extend the host-guest system into a test for glutamate in biological media. It is for this reason that in addition to the tweezer receptor chemistry an enantioselective receptor for glutamate has been developed. Bisthiourea **193** is designed to bind to *N*-Boc-glutamate through the eight hydrogen-bonds shown in complex **194** (figure 4.1).

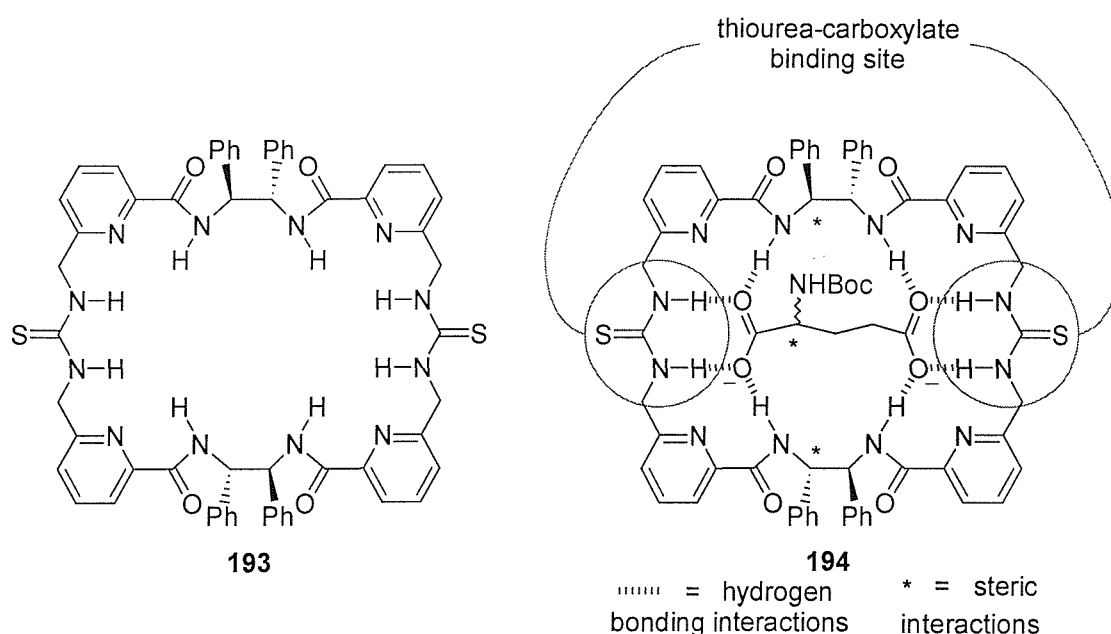


Figure 4.1: Design concept of macrocyclic receptor for glutamate

CPK modeling of the complex formed between **193** and glutarate (figure 4.2) showed a tight fit between host and guest. When glutarate was replaced with glutamate, the chiral centres in the host and guest were aligned, creating steric interactions which should favour high levels of enantioselective binding.

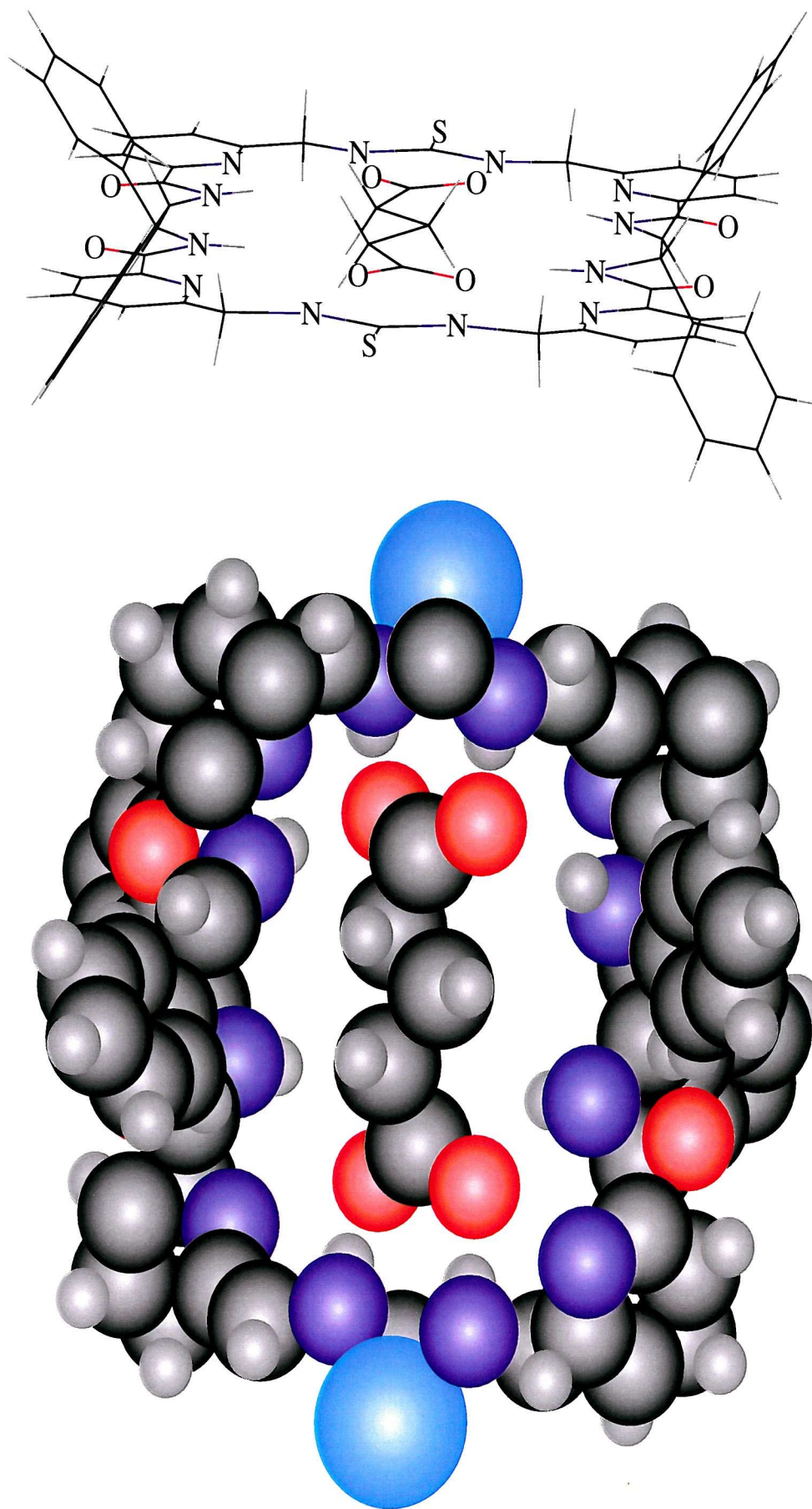
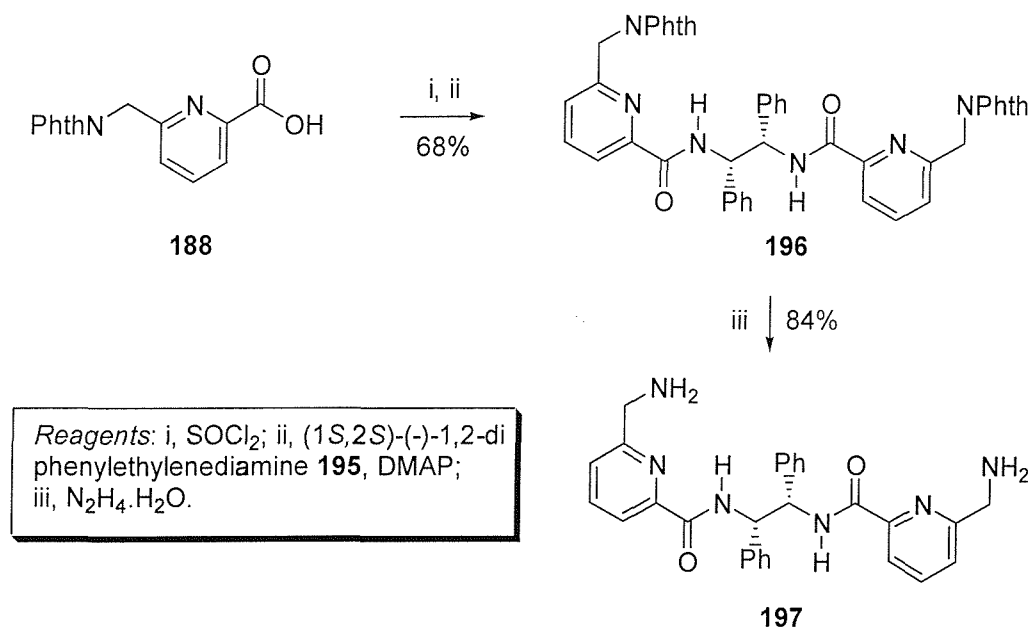


Figure 4.2: CPK modeling of complex formed between 193 and glutarate

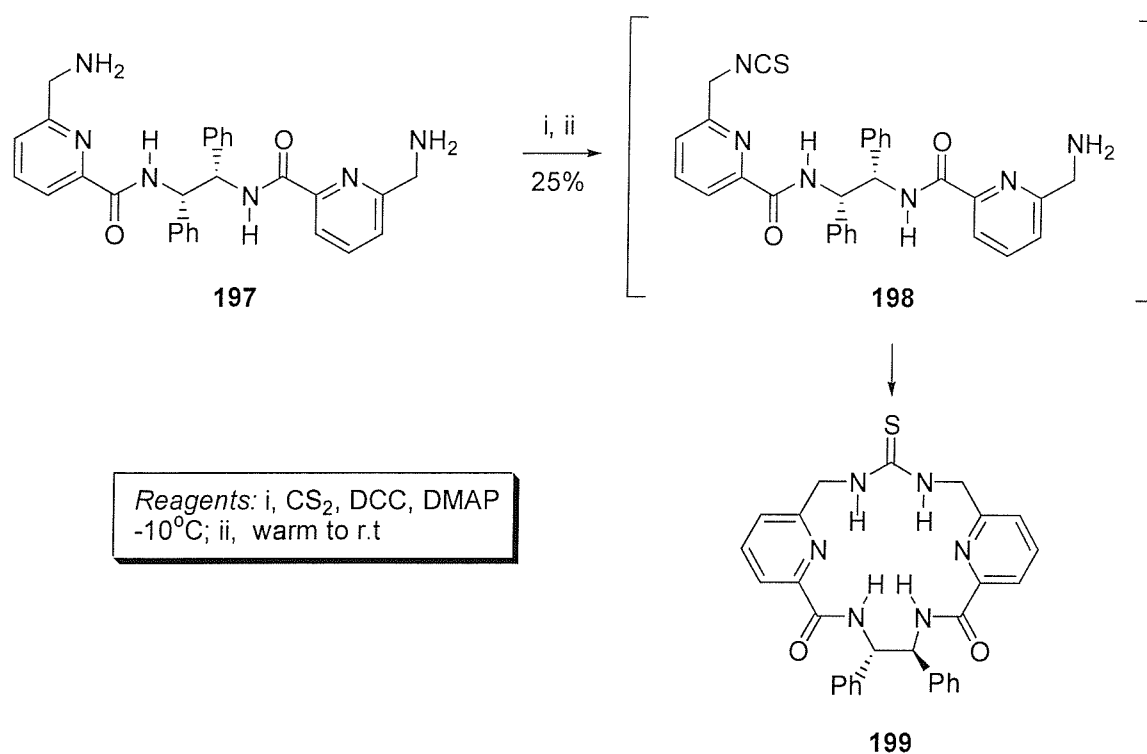
4.2 Synthesis of Bisthiourea 193

Acid **188** was reacted with thionyl chloride to give the corresponding acid chloride, which was subsequently reacted with diamine **195** in the presence of DMAP providing diamide **196** in a good 68% yield (scheme 4.1). Diphtalimide **196** was deprotected using hydrazine hydrate to furnish diamine **197** in an excellent 84% yield.



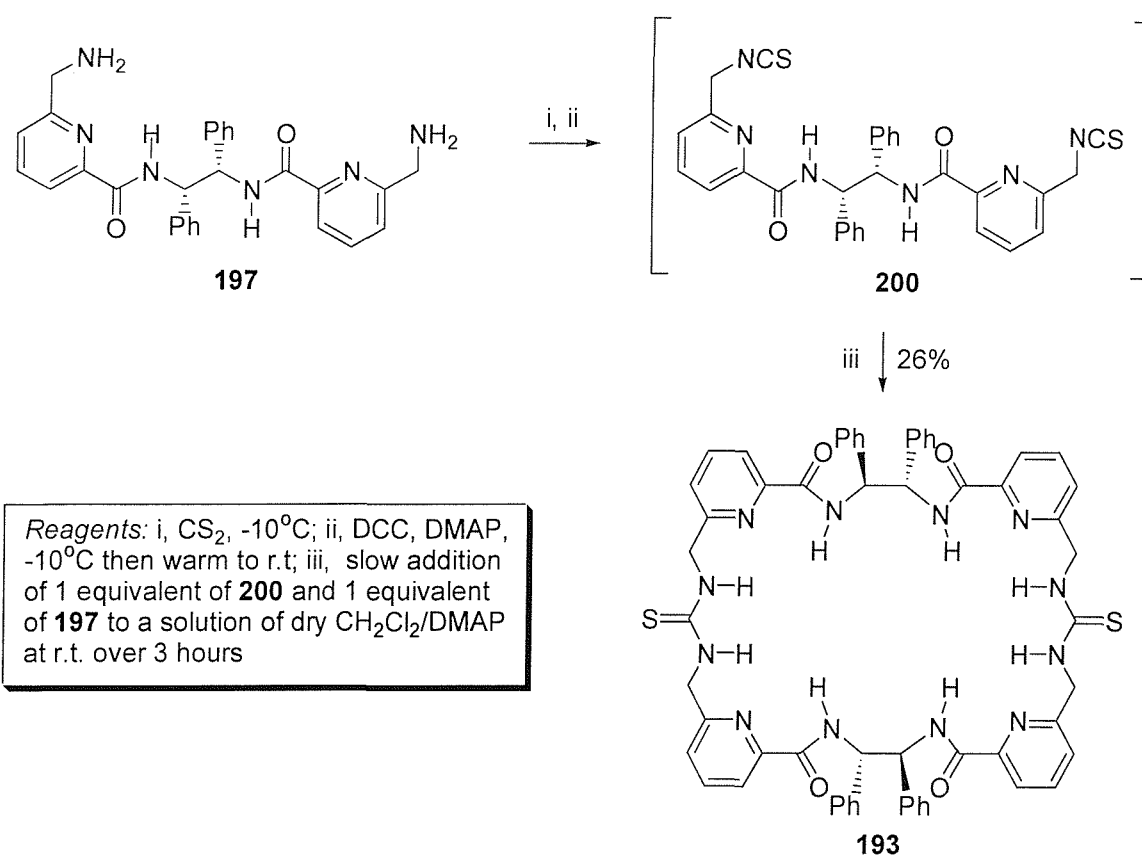
Scheme 4.1: Synthesis of diamine **197**

With diamine **197** in hand attempts to form bisthioisocyanate **200** were made. The first attempt at making bisthiourea **193** using DCC, carbon disulfide and DMAP gave monothiourea **199** in 25% (scheme 4.2). The excess carbon disulfide present after the intended reaction to the diisothiocyanate was not removed from the reaction mixture before adding the second equivalent of diamine **197**. In addition, conditions such as the temperature and reaction time meant that the conditions were not suitable for diisothiocyanate formation and led to intramolecular trapping of the monoisothiocyanate **198** with the second amine giving monothiourea **199**.



Scheme 4.2: Intramolecular trapping of monothioisocyanate 198

After changing the conditions by lowering the temperature to -10°C , extending the reaction time between carbon disulfide and diamine **197** before adding DCC and by using slow addition/high dilution techniques, formation of bithioisocyanate was detected by TLC. After one equivalent of amine **197** and equivalent of bithioisocyanate **200** were added to a solution of CH_2Cl_2 and catalytic DMAP *via* syringe pump over three hours, bithiourea **193** was formed in a satisfactory yield of 26% (scheme 4.3). This methodology gave access to enough material (>50 mg) to allow the binding properties to be studied.



Scheme 4.3: Synthesis of bistiourea 193

4.3 Binding Properties of Bistiourea 193

Bistiourea **193** was found to be soluble in chloroform however, the peaks in the proton spectra were found to be broad at room temperature and when heated to 40°C. The spectrum was well resolved in DMSO-d₆, showing some broad peaks at room temperature which resolved into assignable multiplets when heated to 90°C (figure 4.3). To probe the affect of the chain length between the two carboxylate groups and how it influences the binding properties of macrocycle **193**, binding studies with both *N*-Boc-glutamate and *N*-Boc-aspartate were undertaken (table 4.1).

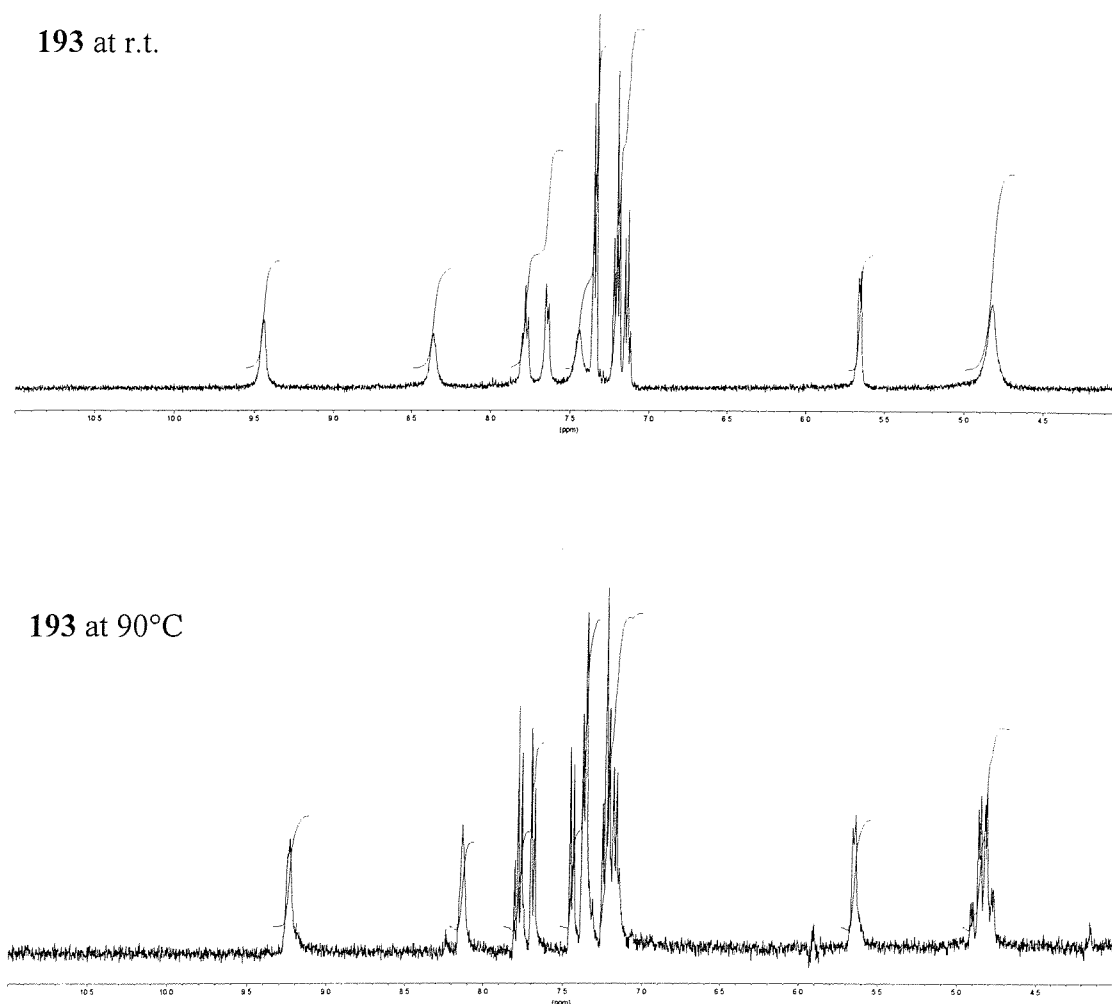


Figure 4.3: ^1H NMR spectra in DMSO-d_6

4.3.1 Binding in DMSO-d_6

Association constants in DMSO-d_6 were obtained by ^1H NMR titration experiments. It was found that macrocycle **193** bound *N*-Boc-L-Glutamate **201** with an association constant of 5890 M^{-1} and *N*-Boc-D-Glutamate **202** with an association constant of 930 M^{-1} in DMSO-d_6 , with the titration curves corresponding to an association stoichiometry of 1:1. The difference in association constants between **201** and **202** with macrocycle **193** represents an L:D enantioselectivity of 6:1 ($\Delta\Delta\Delta G = 4.7 \text{ kJ mol}^{-1}$). Changes in the thiourea/amide hydrogens of macrocycle **193** with *N*-Boc-Glutamate **201/202** are shown in figure 4.4. Large shifts were observed for both *N*-Boc-Glutamate enantiomers with the thiourea protons H1 shifting $\sim 1.3 \text{ ppm}$ and the amide protons shifting 0.65 ppm .

Guest	K_a/M^{-1}	$\Delta\Delta G/kJ\ mol^{-1}$
<i>N</i> -Boc-L-Glu 201	5,890	21.7
<i>N</i> -Boc-D-Glu 202	930	17.0

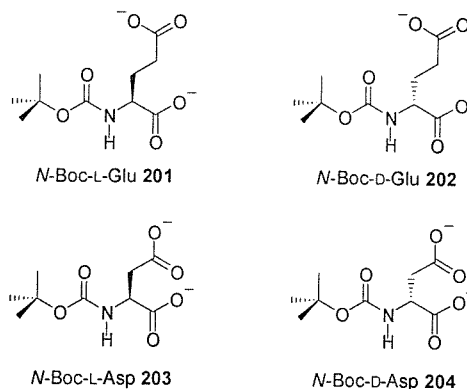


Table 4.1: Association constants for glutamate with macrocycle **193** in $DMSO-d_6$

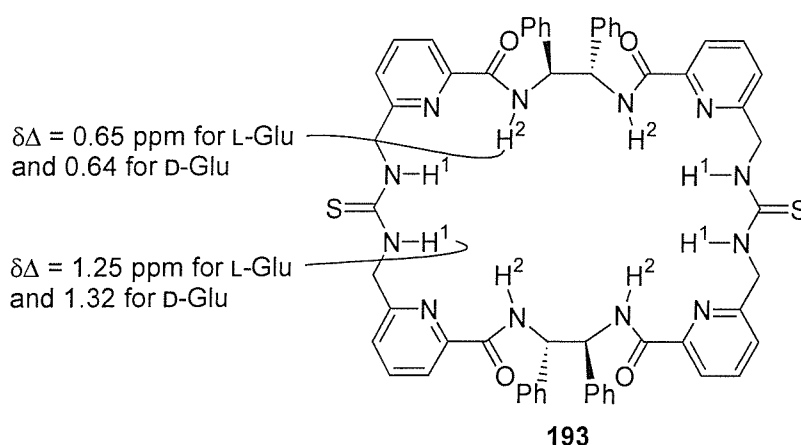
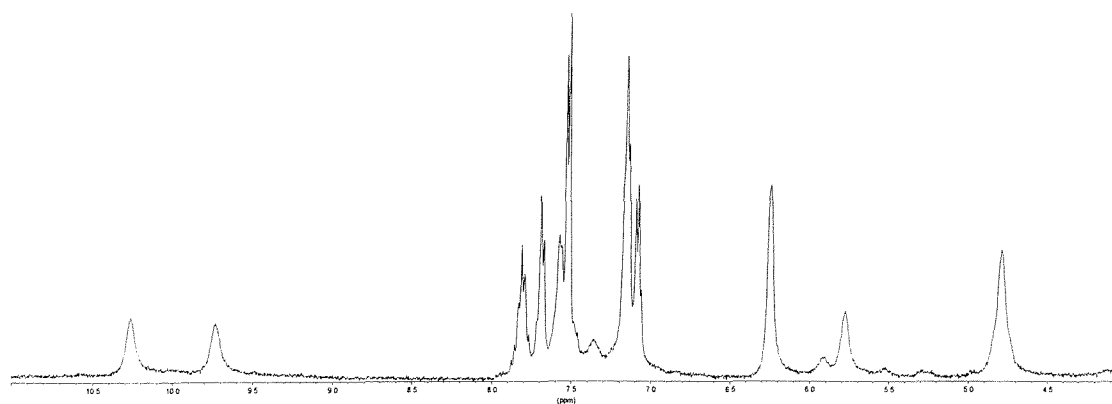


Figure 4.4: Changes in the thiourea/amide hydrogens of macrocycle **193** with *N*-Boc-Glutamate **201/202**

Addition of the aspartate enantiomers **203** or **204** caused the thiourea and amide peaks in the 1H NMR spectra of **193** to broaden and decrease in intensity upon addition of successive aliquots of guest. In addition, a new set of broad signals were found to appear, which became well resolved after the addition of four equivalents of guest (figure 4.5). It was therefore concluded that macrocycle **193** exhibited changeable binding kinetics, showing slow chemical exchange for aspartate compared to glutamate. The binding of the aspartate enantiomers was relatively slow on the NMR timescale so that we observed one set of peaks for the unbound macrocycle (which decreased in intensity) on addition of guest, and a new set of peaks for the bound host-guest complex, which increased in intensity on addition of guest. It was therefore not possible to measure an association constant by monitoring the change in the peak positions of the thiourea/amide protons. In principle, one could measure

the integrals to obtain an association constant, but in practice, the peaks were too broad, presumably because of the chemical exchange on an intermediate timescale. To further probe the binding of the aspartate enantiomers ^1H NMR spectra were recorded of 1:1 mixtures of both enantiomers of aspartate **203/204** and macrocycle **193** at higher temperatures (figure 4.6). At 90°C , the neat macrocycle gave a well-resolved spectrum. Spectra of the 1:1 mixtures of aspartate **203/204** and macrocycle **193** were also well resolved as a single set of peaks at 90°C . The thiourea signal H1 had shifted 0.24 ppm and the amide signal H2 had shifted 0.11 ppm downfield relative to neat macrocycle **193**, suggesting that at the elevated temperatures the kinetics of binding were now fast on the NMR timescale. This means that a ^1H NMR titration of aspartate with macrocycle **193** could be carried out at 90°C , although due to time constraints this has not yet been done.



*Figure 4.5: ^1H NMR spectrum of macrocycle **193** after the addition of four equivalents of *N*-Boc-*L*-Asp **203***

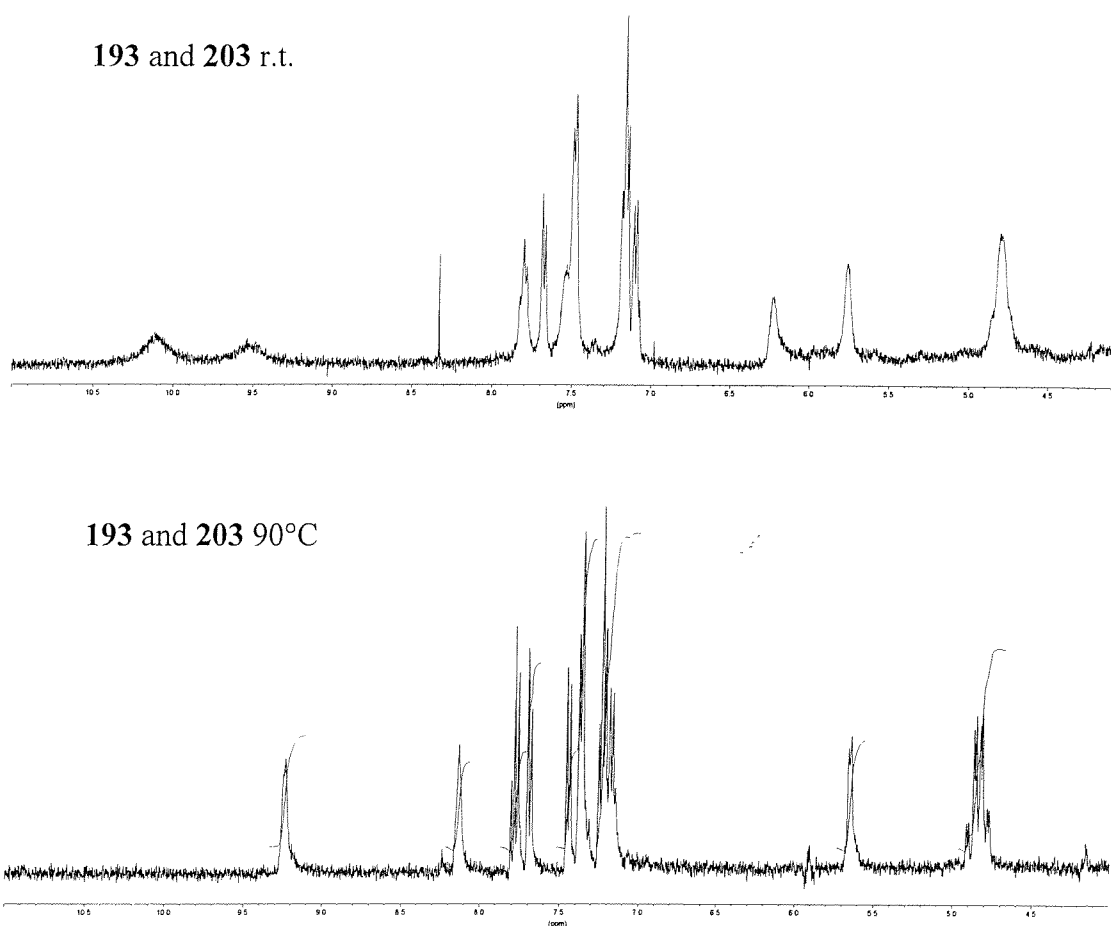


Figure 4.6: ^1H NMR spectra of a 1:1 mixture of macrocycle **193** with *N*-Boc-*L*-Asp **203** at r.t. and 90°C

4.3.2 Binding in Chloroform

In chloroform, the ^1H NMR spectrum for macrocycle **193** was broad, however at -40°C the spectrum was found to resolve into sharp signals (figure 4.7). The spectrum was far more complex than that observed in DMSO-d_6 , with many more signals than would be expected based on the apparent symmetry of the host.

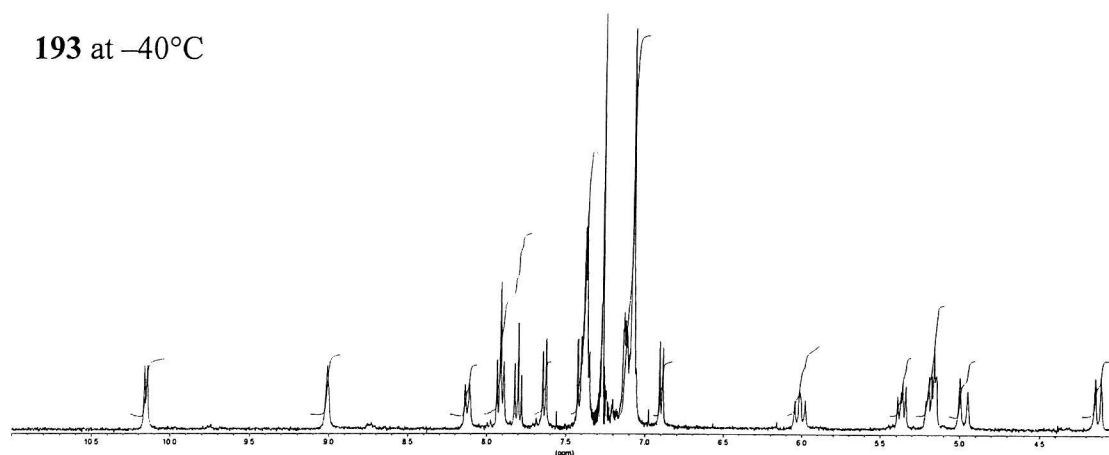
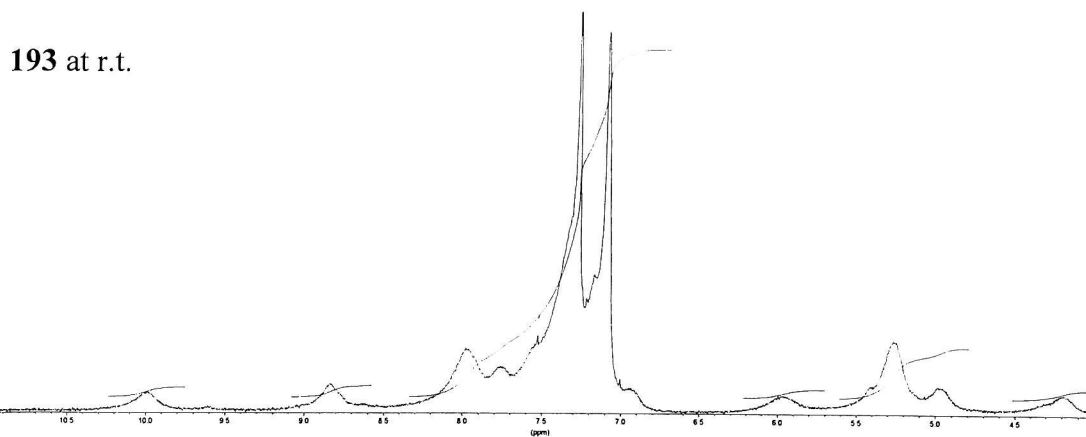


Figure 4.7: ^1H NMR spectra in CDCl_3

Molecular modeling of the neat macrocycle in chloroform using the OPLS* forcefield and the same procedure outlined in chapter 3 is shown in figure 4.8. It was found that the neat macrocycle formed an asymmetric conformation, with an intramolecular hydrogen-bond from one of the thioureas to one of the amide carbonyls being observed.

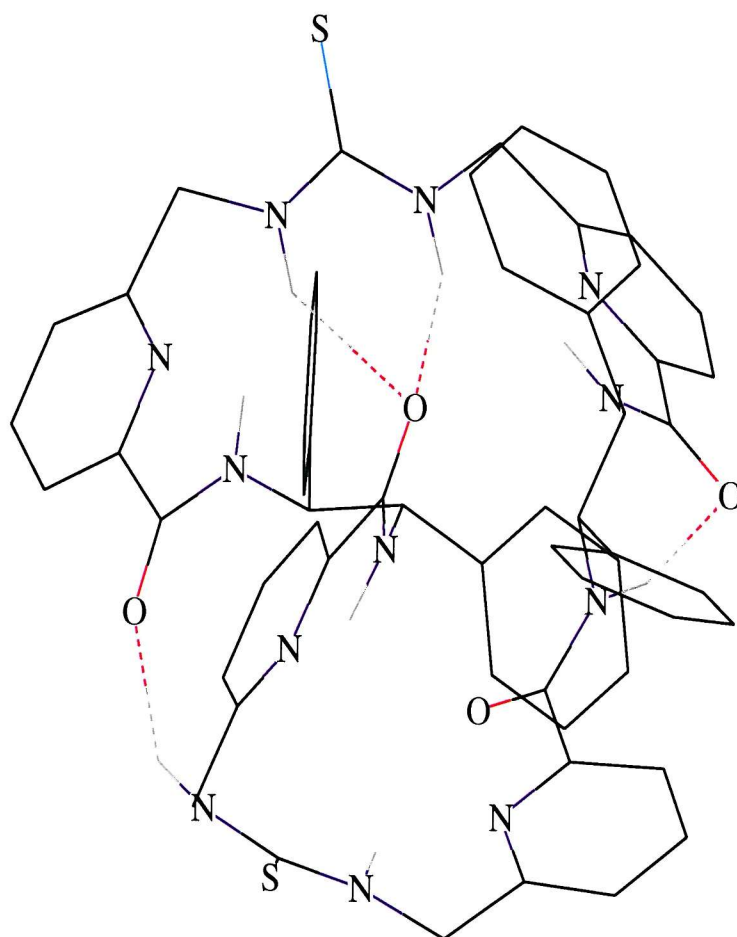
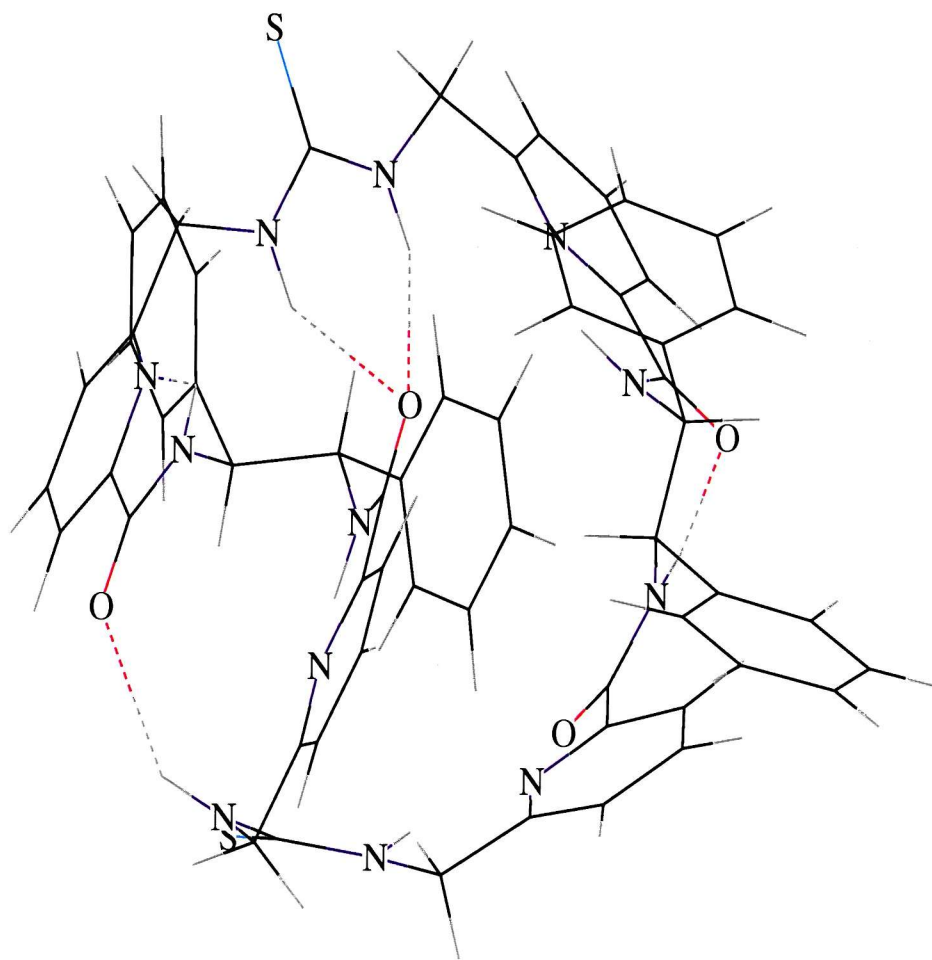


Figure 4.8: Molecular modeling of neat macrocycle **193** in CDCl_3

This was consistent with the crystal structure obtained of tweezer **144**, which was found to form a dimer *via* hydrogen-bonds from the thiourea hydrogens of one molecule of **144** to the carbonyl of another molecule of **144** (section 3.5, figure 3.8). This is consistent with the asymmetry found in the ^1H NMR spectrum at -40°C and thus, it appears that macrocycle **193** is locked into a twisted conformation at -40°C as is shown schematically in figure 4.9. DMSO is a more polar solvent than chloroform and therefore breaks up the intramolecular hydrogen-bonds giving rise to a well resolved spectrum, which is entirely consistent with a symmetrical conformer. At room temperature in CDCl_3 , the ^1H spectrum is broad, suggesting that the macrocycle is in slow chemical exchange between a twisted conformation found at -40°C and a symmetric conformation found in DMSO-d_6 .

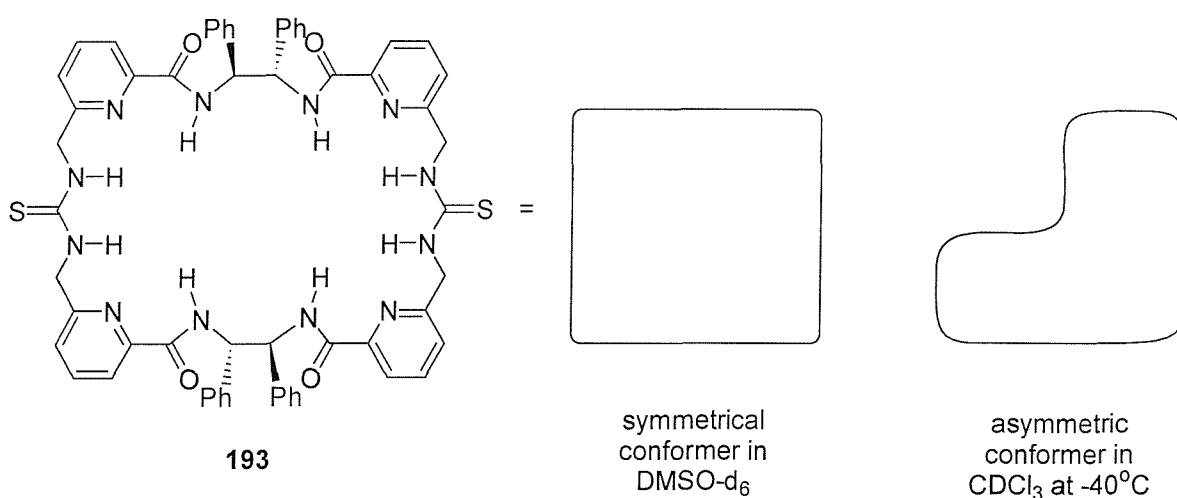


Figure 4.9: Schematic diagram of probable conformers of macrocycle **193** in CDCl_3

^1H NMR spectra of the 1:1 mixtures of substrates **201-204** with macrocycle **193** were obtained. The peaks observed in the ^1H NMR spectra of both the aspartate enantiomers **203** and **204** did not appear to show any change compared to the parent macrocycle **193** both at room temperature and at -40°C , which indicated that the aspartate-macrocycle interaction was too weak to break up the intramolecular hydrogen-bonds present in macrocycle **193**.

^1H NMR spectra of 1:1 mixtures of *N*-Boc-glutamate **201/202** with macrocycle **193** were also obtained. Changes in the spectra were observed at room temperature, however the spectra were still very broad, which meant binding constants could not be determined by ^1H NMR titrations.

Attempts were made at obtaining association constants for substrates **201-204** with macrocycle **193** in chloroform using UV spectroscopic titrations. It was found that very small changes in the absorbance occurred upon addition of increasing amounts of guest (~0.08). However, plots of the small changes in absorbance from the UV titration data, did show saturation type behaviour for substrates **201-204**. In chloroform the spectra for all 1:1 mixtures of glutamate **201/202** and aspartate **203/204** with macrocycle **193** were broad at room temperature with little or no change from that of the parent macrocycle being seen. The 1:1 mixtures of guests **201-204** with macrocycle **193** in chloroform were all cooled down to -40°C and ^1H NMR spectra obtained and all of the mixtures were found to resolve into well resolved signals. It was therefore concluded that there was very weak or no binding in chloroform and the small changes in the absorbance during the UV titration were due to weak cation- π interactions between the tetrabutylammonium cation and the phenyl aromatic rings. Cation- π interactions have been reported by Dougherty,⁷⁰ Kubik and Goddard.⁷¹

4.4 Conclusions and Outlook

The synthesis of novel macrocycle **193** has been accomplished and its ability to bind *N*-Boc-glutamate and *N*-Boc-aspartate examined. Macrocycle **193** was found to form alternative conformers in DMSO and chloroform. In DMSO, a symmetric conformation was observed and twisted conformation was seen at -40°C in chloroform. Macrocycle **193** was also found to enantioselectively bind to *N*-Boc-L-glutamate over *N*-Boc-D-glutamate, with an L:D enantioselectivity of 6:1 in DMSO- d_6 .

In view of the fact that high levels of enantioselective binding of *N*-Boc-glutamate with macrocycle **193** was observed in DMSO- d_6 , a second generation macrocycle could now be synthesised. If the thioureas were substituted for guanidiniums, selective binding in water might be possible. One could also envisage changing the diamine spacer from diphenylethylenediamine **195** to dicyclohexylamine, which is conformationally more restricted and may lock the macrocycle into a more planar conformation.

Chapter Five

Experimental

5.1 General Experimental and Instrumentation

5.1.1 General Experimental

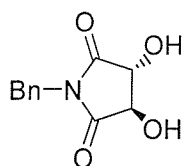
Reactions which required a dry atmosphere were conducted in flame dried glassware under an atmosphere of nitrogen. Reactions were carried out in solvents of commercial grade and where necessary were distilled prior to use (for solvent distilling procedures see Purification of Laboratory Chemical by Perrin and Armarego). THF was distilled under nitrogen from benzophenone and sodium and CH_2Cl_2 was distilled from calcium hydride, as was petroleum ether where the fraction boiling between 40 and 60°C was used. TLC was done on foil backed sheets coated with silica gel (0.25 mm) which contained the fluorescent indicator UV_{254} . Flash column chromatography was performed on Sorbsil C60, 40-60 mesh silica.

5.1.2 Instrumentation

^1H NMR spectra were obtained at 300 MHz on Brüker AC300 and Brüker AM 300 spectrometers, at 360 MHz on a Brüker AM360 spectrometer and at 400 MHz on a Brüker DPX400 spectrometer. ^{13}C NMR spectra were obtained at 75.5 MHz on Brüker AC300 and Brüker AM 300 spectrometers and at 100 MHz on a Brüker DPX400 spectrometer. Spectra were referenced with respect to the residual solvent peak for the deuterated solvent. Infrared spectra were obtained on Perkin-Elmer 1600 series and Golden Gate FT-IR machines. Spectra were obtained either from KBr disks or as neat films supported on sodium chloride plates on the Perkin-Elmer machine and as solids on the Golden Gate machine. All melting points were measured in open capillary tubes using a Gallenkamp Electrothermal Melting Point Apparatus and are uncorrected. Optical rotations were measured on an Optical Activity AA-100 polarimeter using the solvent stated, the concentration given is in g/100 mL. Electrospray mass spectra were obtained on a Micromass platform with a quadrupole mass analyser. FAB spectra were obtained on a VG Analytical 70-250-SE normal geometry double focusing mass spectrometer. High resolution accurate mass measurements were carried out at 10,000 resolution using mixtures of polyethylene glycols and/or polyethylene glycol methyl ethers as mass calibrants for FAB.

5.2 Experimental for Chapter Two

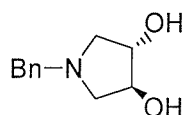
(3*R*,4*R*)-1-benzyl-3,4-dihydroxy-2,5-pyrrolidindione **106**⁴⁷



106

This procedure was modified from that of Nagel.⁴⁷ L-Tartaric acid (100 g, 0.67 mol) and benzylamine (80 mL, 0.73 mol) were dissolved in xylene (600 mL) and placed in a 2 L round bottomed flask equipped with a Dean-Stark apparatus (it is important that the reaction vessel be considerably larger than the volume of solvent, as the reaction mixture is prone to bumping). The reaction mixture was refluxed for 8 hours, after 24 mL of water was collected. The resultant solid was filtered off, washed with acetone and recrystallised from hot ethanol yielding a white solid (118 g, 0.53 mol, 80%): m.p. 195-197°C (lit. 196-198°C);⁴⁷ $R_f = 0.43$ (10% methanol/ CH_2Cl_2); I.R. (Nujol): $\nu_{\text{max}} = 3285$ (w), 2940 (s), 2905 (s), 2855 (s), 1710 (s), 1455 (m) cm^{-1} ; $^1\text{H NMR}$ (300 MHz, DMSO-d_6) δ 7.36–7.24 (5H, m, ArH), 6.31 (2H, d, $J = 2$ Hz, OH), 4.59 (1H, d, $J = 15$ Hz, $\text{CH}_A\text{H}_B\text{Ph}$), 4.52 (1H, d, $J = 15$ Hz, $\text{CH}_A\text{H}_B\text{Ph}$), 4.40 (2H, d, $J = 2$ Hz, $\text{CH}(\text{OH})$); $^{13}\text{C NMR}$ (75.5 MHz, DMSO-d_6) δ 174.5, 135.9, 128.5, 127.4, 74.4, 74.3. All data agrees with that reported by Nagel.⁴⁷

(3*S*,4*S*)-1-benzyl-3,4-pyrrolidindiol **107**⁴⁷

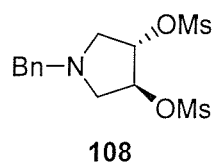


107

This procedure was modified from that of Nagel.⁴⁷ (3*R*,4*R*)-1-benzyl-3,4-dihydroxy-2,5-pyrrolidindione **106** (13.8 g, 66 mmol) was added to a suspension of lithium aluminium hydride (5.0 g, 130 mmol) in THF (130 mL) at 0°C. The reaction mixture was stirred at r.t. for 1 hour then heated at reflux overnight. After allowing to cool to r.t. ether (300 mL), water (5 mL), sodium hydroxide (20%, 5 mL) and water (15 mL) were sequentially added

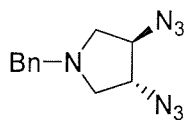
to give a white precipitate. The precipitate was filtered and washed extensively with CH₂Cl₂ (10 x 100 mL). The filtrate was dried (MgSO₄) and concentrated *in vacuo* yielding a brown residue which solidified on standing (9.6 g, 50 mmol, 76%): R_f = 0.23 (10% methanol/CH₂Cl₂); m.p 85-87°C (lit. 100°C);⁴⁷ ¹H NMR (300 MHz, DMSO-d₆) δ 7.35-7.15 (5H, m, ArH), 4.99 (2H, bs, OH), 3.87 (2H, m, CHOH), 3.64 (1H, d, *J* = 13 Hz, CH_AH_BPh), 3.54 (1H, d, *J* = 13 Hz, CH_AH_BPh), 2.81 (2H, dd, *J* = 10, 5 Hz, CH_AH_BCHOH), 2.3 (2H, dd, *J* = 10, 5 Hz, CH_AH_BCHOH). All data agrees with that reported by Nagel.⁴⁷

(3*S*,4*S*)-1-benzyl-3,4-bis(methylsulfonyloxy)pyrrolidine 108⁴⁷



This procedure was modified from that of Nagel.⁴⁷ Methanesulfonylchloride (8.2 mL, 106 mmol) was added to a mixture of (3*S*,4*S*)-1-benzyl-3,4-pyrrolidindiol **107** (10.2 g, 53 mmol), triethylamine (14.7 ml, 106 mmol) and CH₂Cl₂ (50 ml) at 0°C. After stirring at r.t. overnight the reaction mixture was washed with water (2 x 15 mL), stirred vigorously for 1 minute with 1.0 M HCl (250 mL), and the aqueous layer treated with sodium hydroxide (15%, 100 mL). The oil formed was extracted with CH₂Cl₂ (3 x 100 mL), dried (MgSO₄) and concentrated *in vacuo* yielding an oil which solidified upon trituration with cold petroleum ether (10.7 g, 58%, 31 mmol): R_f = 0.36 (50% ethyl acetate/petroleum ether); m.p. 56-58°C (lit 56°C);⁴⁷ ¹H NMR (300 MHz, DMSO-d₆) δ 7.38-7.28 (5H, m, ArH), 5.15 (2H, t, *J* = 4 Hz, CHOMs), 3.64 (2H, s, NCH₂Ar), 3.26 (6H, s, CH₃SO₃), 3.05 (2H, dd, *J* = 11, 4 Hz, CH_AH_BCHOMs), 2.65 (2H, dd, *J* = 11, 4 Hz, CH_AH_BCHOMs); ¹³C NMR (75.5 MHz, DMSO-d₆), δ 137.7, 128.7, 128.4, 127.3, 82.9, 58.3, 57.3, 37.4. All data agrees with that reported by Nagel.⁴⁷

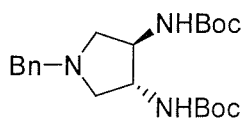
(3*R*,4*R*)-1-benzyl-3,4-bis(azido)pyrrolidine 109⁴⁷



109

This procedure was modified from that of Nagel.⁴⁷ Sodium azide (10.7 g, 164 mmol) was added to a mixture of (3*R*,4*R*)-1-benzyl-3,4-bis(methylsulfonyloxy) pyrrolidine **108** (8.7 g, 25 mmol), water (6 mL) and DMF (60 mL) at 0°C. The reaction mixture was heated to 95°C with stirring for 3 days. After allowing to cool to r.t. the reaction mixture was poured into water (100 mL) and the product extracted with ether (3 x 50 mL). The combined organic extracts were dried (MgSO₄) and the solvent removed *in vacuo*, the crude product was purified by flash column chromatography (SiO₂) eluting in 5% ethyl acetate/petroleum ether to give a colourless oil (4.03 g, 17.0 mmol, 66%): R_f = 0.78 (50% ethyl acetate/petroleum ether); I.R. (NaCl): ν_{\max} = 3335 (w), 3030 (w), 2925 (w), 2800 (m), 2360 (m), 2100 (s), 1675 (m), 1495 (m), 1455 (m) cm⁻¹; ¹H NMR (300 MHz, CDCl₃) δ 7.26-7.15 (5H, m, ArH), 3.79 (2H, d, *J* = 6.5 Hz, CHN₃), 3.65 (1H, d, *J* = 13 Hz, CH_AH_BPh), 3.57 (1H, d, *J* = 13 Hz, CH_AH_BPh), 2.92 (2H, dd, *J* = 10, 6.5 Hz, CH_AH_BCHN₃), 2.54 (2H, dd, *J* = 10, 6.5 Hz, CH_AH_BCHN₃); ¹³C NMR (75.5 MHz, CDCl₃), δ 137.8, 128.7, 128.7, 127.5, 65.9, 59.5, 57.8. All data agrees with that reported by Nagel.⁴⁷

(3*R*,4*R*)-1-benzyl-3,4-bis(*N*-*tert*-butylcarbonate)pyrrolidine 110⁶⁷

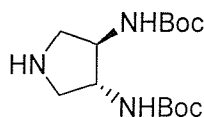


110

This procedure was modified from that of Still.⁶⁷ Triphenylphosphine (10.4 g, 40 mmol) was added to a solution of (3*R*,4*R*)-1-benzyl-3,4-bis(azido)pyrrolidine **109** (4.0 g, 16 mmol) in toluene (200 mL). After stirring at r.t. for 1 hour and an additional 3 hours heating at reflux, water (0.95 mL, 53 mmol) in THF (26 mL) was added and the mixture heated at reflux overnight. The solvent was removed *in vacuo* and CH₂Cl₂ (40 mL) added along with di-*tert*-butyldicarbonate (7.2 g, 33 mmol) and triethylamine (4.6 mL, 33 mmol) and stirred

for 12 hours. The resulting solution was concentrated *in vacuo* yielding a pale pink solid which was purified by flash column chromatography (SiO₂) eluting in CH₂Cl₂ then 80% ethyl acetate/petroleum ether yielding a white solid (3.01 g, 8.0 mmol, 48%): R_f = 0.61 (10% methanol/CH₂Cl₂); m.p 139-141 °C; ¹H NMR (300 MHz, CD₃OD) δ 7.36-7.26 (5H, m, ArH), 3.90 (2H, br m, CHNHBoc), 3.63 (2H, d, *J* = 12 Hz, NCH₂Ph), 2.89 (2H, dd, *J* = 9.5, 6.5 Hz, CH_AH_BCHNHBoc), 2.43 (2H, dd, *J* = 9.5, 6.5 Hz, CH_AH_BCHNHBoc); 1.40 (18H, s, C(CH₃)₃); ¹³C NMR (75.5 MHz, CD₃OD), δ 158.0, 139.0, 133.7, 133.1, 128.3, 80.2, 61.1, 59.8, 57.3, 28.6. All data agrees with that reported by Still.⁶⁷

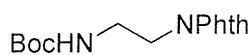
(3*R*,4*R*) 3,4-bis(*N*-*tert*-butylcarbonate)pyrrolidine 111⁶⁷



111

This procedure was modified from that of Still.⁶⁷ Activated palladium on charcoal (20 mg, 10% by weight) was added to a degassed solution of (3*R*,4*R*)-3,4-bis(*N*-*tert*-butylcarbonate)pyrrolidine **110** (200 mg, 0.51 mmol) and ammonium formate (48 mg, 0.80 mmol) in methanol (10 mL). After heating at reflux for 2 hours the solution was cooled to r.t. and filtered through a pad of celite. The filtrate was concentrated *in vacuo* and the resultant solid dissolved in CH₂Cl₂ (5 mL), the insoluble material was filtered off yielding a white solid (138 mg, 0.46 mmol, 90%): R_f = 0.54 (10% methanol/CH₂Cl₂); ¹H NMR (300 MHz, CDCl₃) δ 5.00 (2H, br s, NHBoc), 3.81 (2H, br s, CHNHBoc), 3.33 (2H, dd, *J* = 11, 6 Hz, CH_AH_BCHNHBoc), 2.75 (2H, dd, *J* = 11, 6 Hz, CH_AH_BCHNHBoc), 2.01 (1H, s, CH₂NH), 1.45 (18H, s, C(CH₃)₃); ¹³C NMR (75.5 MHz, CDCl₃), δ 156.00, 79.84, 58.15, 51.96, 28.51. All data agrees with that reported by Still.⁶⁷

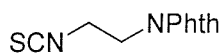
***N*-tert-butoxycarbonyl-*N*-phthaloyl-1,2-diaminoethane 116⁴⁹**



116

This procedure was modified from that of Burgess.⁴⁹ Diethyl azodicarboxylate (0.96 mL, 6.20 mmol) was added over 10 minutes to an ice-cold mixture of *N*-Boc-glycinol (1.00 g, 6.20 mmol), triphenylphosphine (1.95 g, 7.44 mmol), and phthalimide (1.00 g, 6.82 mmol) in THF (30 mL). The reaction mixture was stirred for 3 hours after which the THF was removed *in vacuo* and the resultant residue purified *via* flash column chromatography (SiO₂) eluting in 20% ethyl acetate/petroleum ether affording a white powder (4.00 g, 13.80 mmol, 91%): R_f = 0.65 (80% ethyl acetate/petroleum ether); m.p. 134-136°C (lit. 136-138°C);⁴⁹ ¹H NMR (300 MHz, CDCl₃) δ 7.86-7.83 (2H, m, Ar), 7.73-7.70 (2H, m, Ar), 4.92 (1H, br s, NH), 3.83 (2H, t, *J* = 6 Hz, CH₂NPhth), 3.43 (2H, apparent q, *J* = 6 Hz, BocNHCH₂), 1.33 (9H, s, C(CH₃)₃); ¹³C NMR (75.5 MHz, CDCl₃) δ 168.6, 156.1, 134.1, 132.2, 123.4, 79.6, 39.7, 38.2, 28.4. All data agrees with that reported by Burgess.⁴⁹

2-(2-isothiocyanatoethyl)-2,3-dihydro-1-*H*-1,3-isoindol-1-one 117

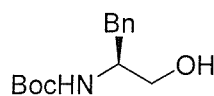


117

This procedure was modified from that of Anslyn.⁶⁸ A 50% mixture of TFA in CH₂Cl₂ (5 mL) was added to an ice cold solution of *N*-tert-butoxycarbonyl-*N*-phthaloyl-1,2-diaminoethane **116** (1.37 g, 4.73 mmol) in CH₂Cl₂ (25 mL). After stirring at r.t. for 2 hours the solvent was removed *in vacuo* and the resultant oil triturated with ether to provide a white solid. Triethylamine (0.73 mL, 5.20 mmol) was added to a suspension of the white solid in CH₂Cl₂ (5 mL) and the mixture stirred for 4 hours. The solvent was removed *in vacuo* and the resultant oil dissolved in CHCl₃ (10 mL) which was added dropwise to a solution of thiophosgene (0.79 mL, 10.41 mmol) in CHCl₃ (10 mL) along with K₂CO₃ (1.44 g, 10.41 mmol) in water (10 mL). Once the addition was complete the mixture was stirred at r.t. for 1 hour and heated at reflux for 12 hours. The mixture was allowed to cool to r.t. and the organic layer washed with 2.0 M HCl (3 x 15 mL), dried (MgSO₄) and the solvent

removed *in vacuo* yielding a yellow solid which was purified *via* flash column chromatography (SiO₂) eluting in 10% ethyl acetate/petroleum ether to afford a yellow solid (0.92 g, 3.96 mmol, 83%) which could be further purified by crystallisation from ethyl acetate/petroleum ether: R_f = 0.53 (50% ethyl acetate /petroleum ether); m.p. 92-93°C; I.R. (thin film in CH₂Cl₂) ν_{max} = 2210 (w), 2094 (m), 1778 (m), 1716 (s), 1430 (w), 1395 (s), 1388 (w) cm⁻¹; ¹H NMR (300 MHz, CDCl₃) δ 7.90-7.87 (2H, m, Ar), 7.77-7.74 (2H, m, Ar), 3.98 (2H, t, *J* = 6 Hz, CH₂), 3.84 (2H, t, *J* = 6 Hz, CH₂); ¹³C NMR (75.5 MHz, CDCl₃) δ 167.9, 134.5, 131.9, 123.8, 43.5, 37.4.

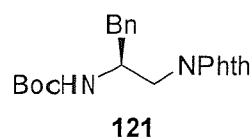
***N*-tert-butyl-[(1*S*)-1-benzyl-2-hydroxyethyl]carbamate 120⁴⁹**



120

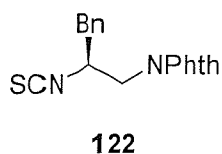
This procedure was modified from that of Burgess.⁴⁹ 4-Methylmorpholine (4.17 mL, 37.90 mmol) was added to a stirred solution of *N*-Boc-L-Phe (10.0 g, 37.90 mmol) in THF (200 mL) at -10°C along with ethylchloroformate (3.62 mL, 37.90 mmol). After 10 minutes NaBH₄ (4.30 g, 0.11 mol) was added in one portion after which methanol (380 mL) was added dropwise at 0°C. The mixture was stirred for 10 minutes, neutralised with 1.0 M HCl (76 mL) and the organic solvents removed *in vacuo*. The aqueous phase was extracted with ethyl acetate (3 x 250 mL) and the organic phase washed consecutively with 1.0 M HCl (150 mL), water (400 mL), 5% sodium bicarbonate (200 mL) and water (2 x 400 mL), dried (Na₂SO₄) and the solvent removed *in vacuo* yielding a white solid which was purified by recrystallisation from ether/petroleum ether (8.01 g, 31.78 mmol, 84%): m.p. 90-91°C (lit. 90-91°C);⁴⁹ I.R. (KBr disc) ν_{max} = 3438 (w), 1703 (m), 1502 (m), 1368 (w), 1167 (w), 1031 (w), 929 (w) cm⁻¹; ¹H NMR (300 MHz, CDCl₃) δ 7.32-7.21 (5H, m, Ar), 4.83 (1H, s, *NH*), 3.88 (1H, m, CHCH₂OH), 3.67 (1H, dd, *J* = 11, 4 Hz, PhCH_AH_B), 3.56 (1H, dd, *J* = 11, 6 Hz, PhCH_AH_B), 2.85 (2H, d, *J* = 7 Hz, CH₂OH), 2.40 (1H, s, OH), 1.43 (9H, s, C(CH₃)₃); ¹³C NMR (75.5 MHz, CDCl₃), δ 156.3, 138.0, 129.5, 128.7, 126.7, 79.9, 64.4, 53.9, 37.6, 28.9; *m/z* (ES⁺) 252.2 (M+H)⁺. All data agrees with that reported by Burgess.⁴⁹

(S)-N-tert-butoxycarbonyl-3-phenyl-N-phthaloyl-1,2-diaminopropane 121⁴⁹



This procedure was modified from that of Burgess.⁴⁹ Diethyl azodicarboxylate (0.98 mL, 6.20 mmol) was added over 10 minutes to an ice-cold mixture of *N*-tert-butyl-[(1*S*)-1-benzyl-2-hydroxyethyl]carbamate **120** (1.00 g, 6.20 mmol), triphenylphosphine (1.95 g, 7.44 mmol), and phthalimide (1.00 g, 6.82 mmol) in THF (30 mL). The reaction mixture was stirred for 3 hours after which the THF was removed *in vacuo* and the resultant residue purified by flash chromatography (SiO₂) eluting in 20% ethyl acetate/petroleum ether to afford a white powder (2.26 g, 5.94 mmol, 70%) which could be further purified by recrystallisation from ethyl acetate/petroleum ether: R_f = 0.74 (80% ethyl acetate/petroleum ether); m.p. 155-157°C (lit. 155-157°C);⁴⁹ I.R. (KBr disc) ν_{max} = 2359 (w), 1775 (w), 1719 (m), 1504 (w), 1398 (w), 1170 (w) cm⁻¹; ¹H NMR (300 MHz, CDCl₃) δ 7.83 (2H, dd, *J* = 5, 3 Hz, Ar), 7.69 (2H, dd, *J* = 5, 3 Hz, Ar), 7.34-7.21 (5H, m, Ar), 4.67 (1H, d, *J* = 8 Hz, NH), 4.32 (1H, br s, NHCH), 3.79-3.65 (2H, m, CH₂), 2.96-2.83 (2H, m, CH₂), 1.22 (9H, s, C(CH₃)₃); ¹³C NMR (75.5 MHz, CDCl₃) δ 168.6, 155.6, 137.0, 134.0, 132.2, 129.4, 128.8, 126.9, 123.4, 79.5, 50.4, 41.9, 39.2, 28.2. All data agrees with that reported by Burgess.⁴⁹

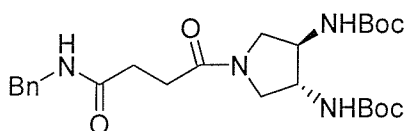
2-[(2*S*)-2-isothiocyanato-3-phenylpropyl]-2,3-dihydro-1*H*-1,3-isoindol-1-one 122



This procedure was modified from that of Anslyn.⁶⁸ A 50% mixture of TFA in CH₂Cl₂ (5 mL) was added to an ice cold solution of (S)-*N*-tert-butoxy carbonyl-3-phenyl-*N*-phthaloyl-1,2-diaminopropane **121** (2.26 g, 5.59 mmol) in CH₂Cl₂ (25 mL). After stirring at r.t. for 2 hours the solvent was removed *in vacuo* and the resultant oil triturated with ether providing a white solid. Triethylamine (0.6 mL, 6.14 mmol) was added to a suspension of the white solid in CHCl₃ (15 mL) and the mixture stirred for 30 minutes. The solvent was removed *in vacuo* and the resultant oil dissolved in CHCl₃ (10 mL) which was added dropwise to a

mixture of thiophosgene (0.94 mL, 12.30 mmol) in CHCl₃ (15 mL) with K₂CO₃ (1.70 g, 12.30 mmol) in water (15 mL). Once the addition was complete the mixture was stirred at r.t. for 1 hour and heated at reflux for 12 hours. After allowing to cool to r.t. the organic layer was washed with 2.0 M HCl (3 x 15 mL), dried (MgSO₄) and the solvent removed *in vacuo* yielding a yellow solid which was purified flash column chromatography (SiO₂) eluting in 10% ethyl acetate/petroleum ether yielding a yellow solid (1.59g, 4.93 mmol, 88%) which could be further purified by crystallisation from ethyl acetate/petroleum ether: R_f = 0.54 (40% ethyl acetate/petroleum ether) m.p. 104-105°C; [α]_D = 42.2° (c = 1, CH₂Cl₂); I.R. (thin film in CH₂Cl₂) ν_{max} = 2096 (m), 1775 (m), 1721 (s), 1498 (w), 1470 (w), 1396 (s), 1368 (m) cm⁻¹; ¹H NMR (300 MHz, CDCl₃) δ 7.92-7.86 (2H, m, Ar), 7.79-7.74 (2H, m, Ar), 7.37-7.24 (5H, m, Ar), 4.41 (1H, m, SCNCHBn), 4.01 (1H, dd, *J* = 9, 5 Hz, CH_AH_BPh), 3.81 (1H, dd, *J* = 9, 5 Hz, CH_AH_BPh) 3.07-2.94 (2H, m, CHCH₂NPhth); ¹³C NMR (75.5 MHz, CDCl₃) δ 168.0, 135.8, 134.5, 131.9, 129.4, 129.0, 127.5, 123.8, 57.98, 41.9, 40.3.

***N*-1-benzyl-4-{(3*R*,4*S*)-3,4-di[*N*-*tert*-butylcarbonate]tetrahydro-1*H*-1-pyrrolyl}-4-oxobutanamide 114**

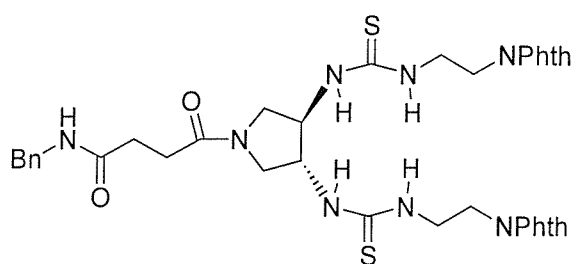


114

EDC (188 mg, 0.98 mmol) was added to a solution of 4-(benzylamino)-4-oxobutanoic acid (170 mg, 0.82 mmol) in dry CH₂Cl₂ (25 mL) along with HOBT (132 mg, 0.98 mmol), DMAP (20 mg) and (3*R*,4*R*) 3,4-bis(*N*-*tert*-butylcarbonate)pyrrolidine **111** (322 mg, 0.82 mmol). After stirring for 72 hours the solution was washed with 1.0 M HCl (3 x 25 mL) and 1.0 M NaOH (3 x 25 mL). The organic layer was dried (MgSO₄) and concentrated *in vacuo* providing a white solid which was crystallised from ethyl acetate/petroleum ether to give a white solid (365 mg, 0.74 mmol, 100%): m.p. 97-99°C; I.R. (KBr disc) ν_{max} = 3439 (w), 3318 (w), 2981 (w), 1705 (s), 1638 (s), 1512 (s), 1454 (m), 1393 (w), 1368 (m) cm⁻¹; ¹H NMR (300 MHz, DMSO-*d*₆) δ 8.36 (1H, t, *J* = 6 Hz, BnNH), 7.33-7.22 (5H, m, ArH), 7.18 (1H, d, *J* = 7 Hz, NHBoc), 7.14 (1H, d, *J* = 7 Hz, NHBoc), 4.25 (2H, d, *J* = 6 Hz, PhCH₂N),

3.88 (2H, m, CHNHBoc), 3.73 (1H, dd, $J = 10, 7$ Hz, CH_AH_B CHNHBoc), 3.52 (1H, dd, $J = 12, 7$ Hz, CH_AH_B CHNHBoc), 3.21 (1H, dd, $J = 10, 6$ Hz, CH_AH_B CHNHBoc), 3.06 (1H, dd, $J = 12, 6$ Hz, CH_AH_B CHNHBoc), 2.41 (4H, m, COCH₂CH₂CO), 1.38 (18H, s, C(CH₃)₃); ¹³C NMR (75.5 MHz, DMSO-d₆) δ 171.5 (C=O), 170.1 (C=O), 155.2 (^tBuOC=O), 139.7 (quartAr), 128.3 (Ar), 127.2 (Ar), 126.7 (Ar), 78.1 (C(CH₃)₃), 49.2 (CNHBoc), 48.7 (CH₂NCO), 42.1 (PhCH₂), 30.0 (COCH₂), 28.8 (COCH₂), 28.2 (C(CH₃)₃); m/z (ES⁺) 491.5 (M+H)⁺; Anal. Calcd. for C₂₁H₃₈N₄O₆: C, 61.21; H, 7.81; N, 11.42. Found; C, 60.84; H, 7.79; N, 11.24.

N*-1-benzyl-4-{(3*R*,4*S*)-3,4-di[({2-(*N*-phthaloyl)ethyl}amino)carbothioyl]amino}tetrahydro-1*H*-1-pyrrolyl}-4-oxobutanamide **118*

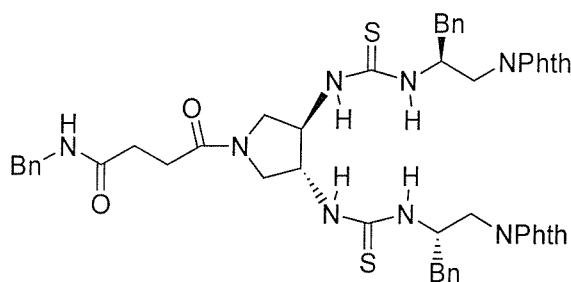


118

A 50% solution of TFA in CH₂Cl₂ (10 mL) was added dropwise to a solution of *N*-1-benzyl-4-{(3*R*,4*S*)-3,4-di[*tert*-butylcarbonate]tetrahydro-1*H*-1-pyrrolyl}-4-oxobutanamide **114** (1.04 mg, 2.13 mmol) in CH₂Cl₂ (20 mL) and the mixture stirred for 2 hours. The solvent was removed *in vacuo* and the resultant oil triturated from ether yielding a white solid (1.05 g, 2.03 mmol, 95%) which was used in the next step without further purification. The white solid (475 mg, 0.91 mmol) was suspended in CH₂Cl₂ (5 mL). Triethylamine (0.77 mL, 5.49 mmol) was added and the mixture stirred for 3 hours. 2-(2-*isothio* cyanatoethyl)-2,3-dihydro-1-*H*-1,3-*iso*indole-dione **117** (425.0 mg, 1.83 mmol) was added in one portion and the mixture stirred at r.t. overnight. The organic solution was washed with 2.0 M HCl (2 x 10 mL), dried (MgSO₄) and the solvent removed *in vacuo* yielding a pale brown solid which was purified by flash column chromatography (SiO₂) eluting in CH₂Cl₂-10% methanol/CH₂Cl₂ to provide a white solid (441 mg, 0.63 mmol, 61% based on TFA salt **114**) which could be further purified by crystallisation from ethanol/water: $R_f = 0.46$ (10% methanol/CH₂Cl₂); I.R. (KBr disc) $\nu_{max} = 3303$ (br s), 3066 (m), 2974 (m), 2932 (m), 2359 (w), 2341 (m), 1691 (s), 1653 (s), 1540 (s), 1454 (s), 1392 (m), 1366 (s), 1251 (s),

1166 (s) cm^{-1} ; ^1H NMR δ (1H, t, $J = 5.5\text{H}$, NH), 7.88-7.80 (12H, br m), 7.35-7.22 (5H, br m), 4.6-4.2 (4H, br m), 3.9-3.5 (12H, br m), 3.1-3.2 (2H, br m), 2.5-2.6 (2H, br m); ^{13}C NMR (75.5 MHz, CD_3OD) δ 171.5, 170.4, 168.0, 139.7, 138.0, 134.3, 131.8, 128.3, 127.2, 126.7, 122.9, 57.2, 55.6, 50.1, 48.6, 42.1, 37.4, 37.3, 30.0, 29.1; m/z (ES^+) 695.5 ($\text{M}+\text{H}$) $^+$; Anal. Calcd. for $\text{C}_{31}\text{H}_{50}\text{N}_8\text{O}_6\text{S}_2$: C, 53.58; H, 7.25; N, 16.12. Found: C, 51.70; H, 7.19; N, 15.74.

N*-1-benzyl-4-[(3*S*, 4*R*)-3-[(2*R*)-2-(phthaloyl)-3-phenylpropyl]amino]carbothiol amino]-4-[(2*S*)-2-(phthaloyl)-3-phenylpropyl]amino] tetrahydro-1*H*-1-pyrrolyl}-4-oxobutanamide **123*

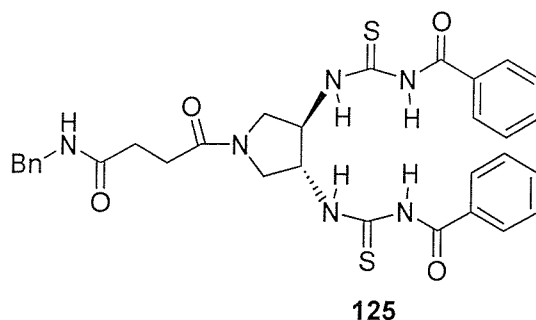


123

A 50% solution of TFA in CH_2Cl_2 (5 mL) was added to an ice cold solution of *N*-1-benzyl-4-[(3*R*,4*S*)-3,4-di[*tert*-butylcarbonate]tetrahydro-1*H*-1-pyrrolyl]-4-oxobutanamide **114** (0.64 g, 1.30 mmol) in CH_2Cl_2 (15 mL) and the mixture stirred for 3 hours. The solvent was removed *in vacuo* and the resultant oil triturated from ether giving a white solid which was suspended in CHCl_3 (15 mL) and triethylamine (1.09 mL, 7.80 mmol) added. After stirring at r.t. for 1 hour 2-[(2*S*)-2-*isothiocyano*-3-phenylpropyl]-2,3-dihydro-1*H*-1,3-*iso*indole-1,3-dione **122** (0.88 g, 2.73 mmol) was added and the mixture stirred at r.t. for 30 minutes and heated at reflux for 12 hours. After allowing to cool to r.t. the organic layer was washed with 2.0 M HCl (4 x 20 mL), dried (MgSO_4) and the solvent removed *in vacuo* yielding a pale yellow solid which was purified by flash column chromatography (SiO_2) eluting in 0.5% methanol/ CH_2Cl_2 giving a white solid (1.13 g, 1.21 mmol, 59%) which could be further purified by crystallisation from hot CHCl_3 : $R_f = 0.62$ (10% methanol/ CH_2Cl_2); m.p. 143-144°C; $[\alpha]_D = +86.6^\circ$ ($c = 1$, CH_2Cl_2); I.R. (KBr disc) $\nu_{\text{max}} = 3409$ (m), 3319 (m), 3219 (w), 3068 (w), 3033 (w), 2944 (w), 1774 (m), 1713 (s), 1665 (m), 1625 (s), 1561 (s), 1544 (m), 1522 (m), 1498 (m), 1467 (m), 1430 (m), 1393 (s) cm^{-1} ; The

peaks in the ^1H NMR spectrum are all very broad due to aggregation outlined in chapter two and are therefore not included, the spectra are shown in figure 2.8. ^{13}C NMR (75.5 MHz, DMSO- d_6) δ 171.5 (C=O), 170.4 (C=O), 168.0 (C=O), 139.8 (Ar), 137.9 (Ar), 134.3 (Ar), 131.8 (Ar), 129.1 (Ar), 128.3 (Ar), 127.3 (Ar), 126.8 (Ar), 126.2 (Ar), 123.1 (Ar), 55.4, 53.7, 52.2, 48.8, 42.1, 41.1, 38.1, 30.0, 29.4; m/z (ES $^+$) 936.4 (M+H) $^+$.

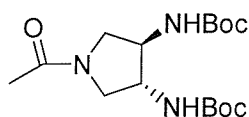
***N*-benzyl-4-((3*R*,4*S*)-3,4-di{[(benzoylamino)carbothioyl]amino}tetrahydro-1*H*-1-pyrrolyl)-4-oxobutanamide 125**



A 20% solution of TFA in CH_2Cl_2 (7 mL) was added to an ice cold solution of *N*1-benzyl-4-((3*R*,4*S*)-3,4-di[*tert*-butylcarbonate]tetrahydro-1*H*-1-pyrrolyl)-4-oxobutanamide **114** (300 mg, 0.61 mmol) in CH_2Cl_2 (3 mL) and the mixture allowed to warm to r.t. then stirred for 2 hours. The solvent was removed *in vacuo* and the resultant oil triturated from ether (5 mL) giving a white solid, which was suspended in CH_2Cl_2 (5 mL) and triethylamine (0.51 mL, 3.66 mmol) added. After stirring at r.t. for 10 minutes benzoylthioisocyanate (163 μL , 1.22 mmol) was added and the mixture stirred for 12 hours. The solution was washed with 2.0 M HCl (3 \times 10 mL), dried (MgSO_4) and the solvent removed *in vacuo* to provide a yellow solid which was purified by recrystallisation from chloroform/petroleum ether to furnish a yellow solid (346 mg, 0.67 mmol, 92%): R_f = 0.55 (10% methanol/ CH_2Cl_2); m.p. = 116-115 $^\circ\text{C}$; $[\alpha]_D^{25} = +29.5^\circ$ ($c = 1$, CH_2Cl_2); ^1H NMR (300 MHz, CDCl_3) δ 11.19 (1H, d, $J = 6.5$ Hz, C=SNHC=O), 11.09 (1H, d, $J = 6.5$ Hz, C=SNHC=O), 9.18 (2H, d, $J = 4.0$ Hz, CHNHC=S), 7.86-7.82 (4H, m, Ar), 7.66-7.26 (11H, m, Ar), 6.65 (1H, br s, BnNHC=O), 5.20 (2H, m, NCH $_2$ CH(NH)), 4.43 (2H, d, $J = 6$ Hz, PhCH $_2$ NH), 4.26 (1H, dd, $J = 11, 6.5$ Hz, NCH $_A$ CH $_B$ CHNH), 4.13 (1H, dd, $J = 13, 7$ Hz, NCH $_A$ CH $_B$ CHNH), 3.60 (1H, dd, $J = 11, 6.5$ Hz, NCH $_A$ CH $_B$ CHNH), 3.45 (1H, dd, $J = 13, 7$ Hz, NCH $_A$ CH $_B$ CHNH), 2.63 (4H, m, COCH $_2$ CH $_2$ CO); ^{13}C NMR (75.5 MHz, CDCl_3), δ 181.3 (C=S), 172.3 (C=O), 171.3 (C=O),

167.1 (C=O), 138.5 (Ar), 133.9 (Ar), 131.6 (Ar), 129.3 (Ar), 128.8 (Ar), 127.9 (Ar), 127.7 (Ar), 127.6 (Ar), 59.1, 57.1, 49.5, 48.6, 43.8, 31.1, 29.8; m/z (ES⁺) 518.1 (M+H)⁺.

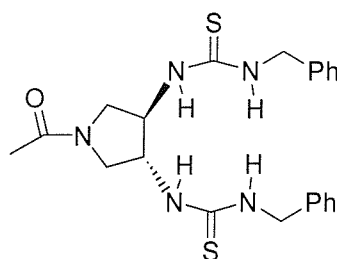
(3R,4R)-1-acetyl-3,4-bis(*N*-*tert*-butylcarbonate)pyrrolidine 127



127

Acetyl chloride (198 μ L, 2.79 mmol) was added to a mixture of (3R,4R) 3,4-bis(*tert*-butylcarbonate) pyrrolidine **111** (0.70 g, 2.32 mmol), pyridine (263 μ L, 3.25 mmol) and DMAP (50 mg) in CH₂Cl₂ (20 mL). After stirring for 24 hours the mixture was washed with 1.0 M HCl (3 x 50 mL), dried (MgSO₄) and the solvent removed *in vacuo* yielding a white solid which was purified by crystallisation from ethyl acetate/petroleum ether providing a white solid (732 mg, 2.13 mmol, 92%): m.p. 92-93°C; [α]_D = + 27.8° (c = 2, CH₂Cl₂); I.R. (KBr disc) ν_{\max} = 3430 (w), 3324 (br w), 2982 (m), 1707 (s), 1641 (s), 1510 (s), 1456 (m), 1393 (m), 1368 (w), 1166 (s) cm⁻¹; ¹H NMR (300 MHz, DMSO-d₆) δ 7.15 (2H, t, J = 9 Hz, NHBoc), 3.92-3.83 (2H, m, CHNHBoc), 3.71 (1H, dd, J = 10, 6 Hz, CH_AH_BCH NHBoc), 3.51 (1H, dd, J = 12, 6 Hz, CH_AH_BCHNHBoc), 3.19 (1H, dd, J = 10, 6 Hz, CH_AH_BCHNHBoc), 3.05 (1H, dd, J = 12, 6 Hz, CH_AH_BCHNHBoc), 1.88 (3H, s, CH₃CO), 1.39 (18H, s, (CH₃)₃CO); ¹³C NMR (75.5 MHz, DMSO-d₆) δ 168.4 (C=O), 155.22 (C=O), 78.1 (C(CH₃)₃), 54.5, 53.0, 50.1, 48.5, 28.2 (C(CH₃)₃), 21.9 (CH₃CO); m/z (ES⁺) 344.5 (M+H)⁺.

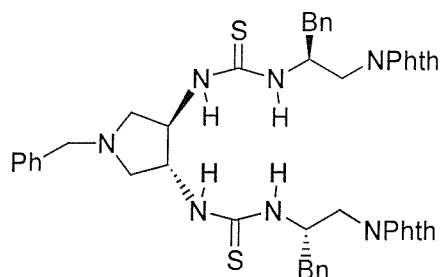
(3*R*,4*R*)-1-acetyl-3,4-bis(phenylmethylthiourea)pyrrolidine 128



128

A 50% solution of TFA in CH₂Cl₂ (7 mL) was added dropwise to an ice cold mixture of (3*R*,4*R*)-1-acetyl-3,4-bis(*tert*-butylcarbonate)pyrrolidine **127** (0.35 g, 1.02 mmol) in CH₂Cl₂ (10 mL) and the solution stirred for 12 hours. The solvent was removed *in vacuo* and the resultant pale yellow oil triturated from ether yielding a yellow solid which was suspended in CH₂Cl₂ (10 mL) and triethylamine (0.84 mL, 6.00 mmol) added. After stirring at r.t. for 15 minutes the suspension had disappeared and benzylthioisocyanate (292 μL, 2.20 mol) was added and the mixture stirred at r.t. for 12 hours and heated at reflux for 1 hour. The CH₂Cl₂ layer was washed with 2.0 M HCl (20 mL) and the insoluble material filtered off and combined with the CH₂Cl₂ layer. Methanol (5 mL) was added and the solution dried (MgSO₄) yielding a white solid which was purified by flash column chromatography (SiO₂) eluting in 3% methanol/CH₂Cl₂ furnishing a white solid (0.29 g, 0.66 mmol, 68%): R_f = 0.49 (10% methanol/CH₂Cl₂); m.p. 104-106°C; [α]_D = +21.4° (c = 2, 10% methanol/CH₂Cl₂); I. R. (neat) ν_{max} = 3310 (w), 3160 (w), 2360 (w), 1625 (s), 1550 (m), 1525 (m), 1450 (m), 1245 (m) cm⁻¹; ¹H NMR (300 MHz, DMSO-d₆) δ 7.91 (4H, br m, NHC=S), 7.35-7.22 (10, br m, ArH), 4.9-4.4 (6H, br m), 3.9-3.6 (2H, br m), 3.4-3.1 (2H, br m), 1.92 (3H, s, CH₃C=O); ¹³C NMR (75.5 MHz, DMSO-d₆) δ 182.7 (C=S), 168.6 (C=O), 139.0 (quart Ar), 128.4 (Ar), 127.5 (Ar), 127.0 (Ar), 57.5, 56.2, 50.2, 48.7, 47.3, 22.0 (CH₃CO); *m/z* (ES⁺) 442.4 (M+H)⁺; HRMS (FAB): found 442.1735. C₂₂H₂₈N₅OS₂ requires 442.1735.

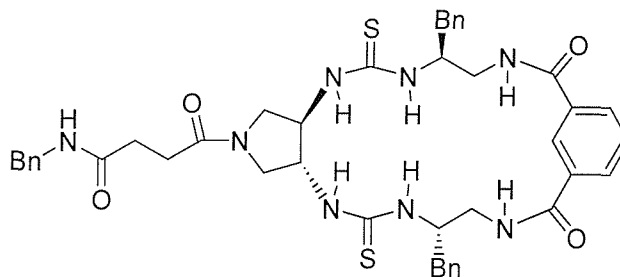
N*-1-{(2*R*)-2-[(3*S*,4*R*)-4-[(1*S*)-2-(phthalimido)-1-(phenylmethyl)ethyl]amino}carbothioyl)amino]-1-(phenylmethyl)tetrahydro-1*H*-3-pyrrolyl]amino}carbothioyl amino]-3-phenyl propyl}phthalimide **132*



132

A 50% solution of TFA in CH₂Cl₂ (5 mL) was added to an ice cold solution of (3*R*,4*R*)-1-benzyl-3,4-bis(*tert*-butylcarbonate)pyrrolidine **110** (200 mg, 0.51 mmol) in CH₂Cl₂ (5 mL), after allowing to warm to r.t. the mixture was stirred for 3 hours. The solvent was removed *in vacuo* and the resultant oil triturated from ether giving a white solid which was suspended in CHCl₃ (5 mL) and triethylamine (0.43 mL, 3.12 mmol) added. After stirring at r.t. for 10 minutes 2-[(2*S*)-2-isothiocyanato-3-phenylpropyl]-2,3-dihydro-1*H*-1,3-isoindole-dione **122** (260 mg, 1.12 mmol) was added and the mixture stirred at r.t. for 10 minutes and heated at reflux for 48 hours. After allowing to cool to r.t. the solvent was removed *in vacuo* yielding a yellow solid which was purified by flash column chromatography (SiO₂) eluting in 0.5% methanol/CH₂Cl₂ giving a pale yellow solid which could be further purified by crystallisation from ethyl acetate/petroleum ether (258 mg, 0.31 mmol, 60%): R_f = 0.67 (10% methanol/CH₂Cl₂); m.p. 123-124°C; [α]_D = + 78.4° (c = 1, CH₂Cl₂); I.R. (KBr disc) ν_{max} = 3408 (br s), 1773 (w), 1713 (s), 1615 (w), 1557 (w), 1497 (w), 1433 (m), 1397 (s) cm⁻¹; ¹H NMR (300 MHz, DMSO-d₆), δ 7.9 - 7.6 (8H, br m, Ar, NHC=S), 7.5-7.1 (15H, br m, Ar), 5.1-4.9 (2H, br m), 4.3-4.0 (2H, br m), 3.8-3.4 (6H, br m), 3.0-2.7 (6H, br m), 2.4-2.1 (2H, br m); ¹³C NMR (75.5 MHz, DMSO-d₆), δ 167.9 (C=O), 138.6 (Ar), 137.9 (Ar), 134.4 (Ar), 134.3 (Ar), 131.7 (Ar), 129.1 (Ar), 128.7 (Ar), 128.2 (Ar), 127.0 (Ar), 126.2 (Ar), 123.0 (Ar), 59.0, 58.1, 55.0, 53.7; *m/z* (ES⁺) 836.7 (M+H)⁺.

N*-1-phenylmethyl-4-[(5*R*,9*R*,13*R*,17*S*)-2,20-dioxo-5,17-di(phenylmethyl)-7,15-dithioxo-3,6,8, 11,14,16,19-heptaazatricyclo[19.3.1.0^{9,13}]pentacosa-1(25),21,23-trien-11-yl]-4-oxobutanamide **137*



137

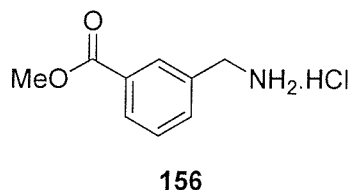
Hydrazine hydrate (26 μ L, 0.53 mmol) was added to a solution of *N*-1-benzyl-4-[(3*S*, 4*R*)-3-[[[(2*R*)-2-(phthaloyl)-3-phenylpropyl]amino]carbothiol) amino]-4-[[[(2*S*)-2-(phthaloyl)-3-phenylpropyl] amino]carbothiyl]amino] tetrahydro-1*H*-1-pyrrolyl]-4-oxobutanamide **123** (250 mg, 0.27 mmol) in ethanol (4 mL) and the mixture refluxed for 74 hours. The solvent was removed *in vacuo* and the resultant white solid suspended in 2.0 M HCl (2 mL). The reaction mixture was stirred at 60°C for 10 minutes and r.t. for 30 minutes, after which the resultant white solid was filtered off and the solvent removed from the filtrate giving a white solid (209 mg). 1.0 M NaOH (30 mL) was added to the white solid, and was subsequently extracted with CH₂Cl₂ (4 x 25 mL), the combined extracts were dried (MgSO₄) and the solvent removed *in vacuo* furnishing a white solid (137 mg, 76%). The white solid was used in the next step without further purification. *Isophthaloyldichloride* (34 mg, 0.17 mmol) was added to a solution of triethylamine (59 μ L, 0.42 mmol) and the white solid (94 mg, 0.14 mmol) in CH₂Cl₂ (1.5 mL) and the mixture stirred for 30 minutes. The organic layer was washed with 1.0 M HCl (3 x 5 mL), dried (MgSO₄) and the solvent removed *in vacuo* providing a pale yellow solid which was purified by flash column chromatography (SiO₂) eluting in 5% methanol/CH₂Cl₂ yielding a white solid (15.8 mg, 20 μ mol, 11%, based on starting diphthalimide **123**): R_f = 0.41 (10% methanol/CH₂Cl₂); m.p. 126-128°C; $[\alpha]_D^{25} = +69.2^\circ$ ($c = 1$, 10% methanol/CH₂Cl₂); I.R. (neat) $\nu_{\max} = 3245$ (br m), 2355 (w), 1635 (s), 1530 (s), 1445 (m), 1260 (s), 1080 (s) cm⁻¹; ¹H NMR (360 MHz, DMSO-*d*₆, acquired at 100°C), δ 8.25 (1H, br s), 8.13-8.01 (3H, br m, NHCO), 7.99 (2H, dd, $J = 8, 1.5$ Hz, ArH), 7.97 (1H, d, $J = 2$ Hz, ArH), 7.82-7.72 (4H, m, NHCS), 7.64 (1H, t, $J = 8$ Hz, ArH), 7.45-7.30 (15H, m, ArH), 5.02-4.93 (2H, m), 4.75-4.59 (2H, br m), 4.40



(2H, d, $J = 6$ Hz), 4.00 (1H, m), 3.89 (1H, m), 3.71 (1H, dd, $J = 5, 3.5$ Hz), 3.69 (1H, dd, $J = 5, 3.5$ Hz), 3.56-3.48 (2H, m), 3.49-3.20 (3H, br m), 3.00 (1H, d, $J = 7$ Hz), 2.96 (1H, d, $J = 7$ Hz), 2.68-2.53 (6H, m); m/z (ES⁺) 805.8 (M+H)⁺.

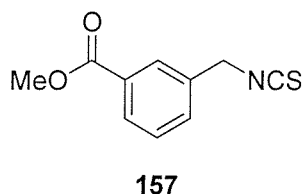
5.3 Experimental for Chapter Three

Methyl-3-(ammoniomethyl)benzoate chloride 156



1.0 M Boranedimethylsulphide complex in THF (22.2 mL, 44.4 mmol) was added to an oxygen free stirred solution of methyl-3-(cyano)benzoate (4.77 g, 29.6 mmol) in THF (150 mL). The reaction mixture was heated at reflux for 2 hours, stirred at r.t. for 12 hours and after cooling to 0°C 6.0 M HCl (15 mL, 88.8 mmol) was added. The resultant solution was heated at reflux for 1 hour and cooled to 0°C after which 3.0 M NaOH (50 mL, 148.0 mmol) added. The mixture was extracted with ether (3 x 100 mL), dried (MgSO₄) and gaseous HCl bubbled through the solution to precipitate a white solid (2.21 g, 9.30 mmol, 37%): m.p. 168-170°C; I.R. (neat) ν_{\max} = 3465 (m), 3140 (m), 2840, 1680 (s), 1610 (m), 1425 (m), 1295 (s), 1210 (s) cm⁻¹; ¹H NMR (300 MHz, DMSO-d₆) δ 8.70 (3H, br s, NH₃), 8.22 (1H, s, ArH), 8.06 (1H, d, *J* = 8 Hz, ArH), 7.92 (1H, d, *J* = 8 Hz, ArH), 7.68 (1H, t, *J* = 8 Hz, ArH), 4.20 (2H, d, *J* = 3 Hz, ArCH₂), 3.98 (3H, s, CH₃); ¹³C NMR (75.5 MHz, DMSO-d₆) δ 166.0 (C=O), 134.9 (Ar), 134.1 (Ar), 129.9 (Ar), 129.1 (Ar), 52.3, 41.8.

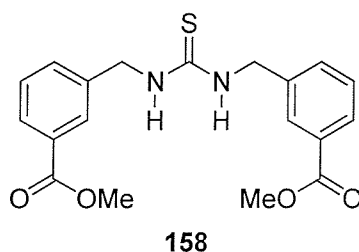
Methyl-3-(isothiocyanatomethyl)benzoate 157



This procedure was modified from that of Anslyn.⁶⁸ Potassium carbonate (0.69 g, 4.96 mmol) was added to a suspension of methyl-3-(ammoniomethyl) benzoate chloride **156** (1.00 g, 4.96 mmol) in water (15 mL). After the suspension had disappeared the mixture was added dropwise to a stirred mixture of potassium carbonate (1.37 g, 9.92 mmol) in water and thiophosgene (0.76 mL, 9.92 mmol) in CH₂Cl₂ (45 mL). The resultant mixture

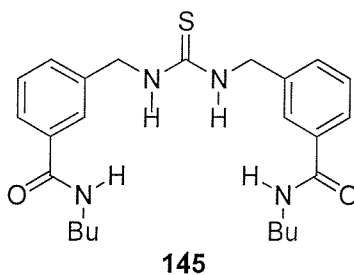
was stirred at r.t. for 1 hour and heated at reflux for 12 hours after which the layers were separated, the organic layer dried (MgSO₄) and the solvent removed *in vacuo* to produce an orange oil which was purified by flash column chromatography (SiO₂) eluting in 20% ethyl acetate/petroleum ether yielding a pale orange oil (0.72 g, 3.47 mmol, 78%): R_f = 0.30 (20% ethyl acetate/petroleum ether); I.R. (neat) ν_{\max} = 2170 (m), 2090 (m), 1710 (s), 1430 (m), 1350 (m), 1280 (m), 1200 (m), 1110 (m) cm⁻¹; ¹H NMR (300 MHz, DMSO-d₆) δ 8.85-7.99 (2H, m, ArH), 7.57-7.47 (2H, m, ArH), 4.79 (2H, s, ArCH₂), 3.95 (3H, s, CH₃).

Methyl-3-(((3-(methoxycarbonyl)benzyl)amino)carbothioyl)amino]methyl} benzoate 158



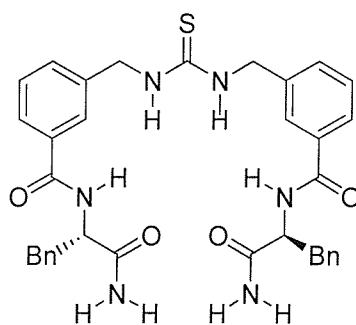
Methyl-3-(ammoniomethyl)benzoate chloride **156** (0.67 g, 3.31 mmol) was added to a stirred solution of methyl-3-(isothiocyanatomethyl)benzoate **157** (0.69 g, 3.31 mmol) and triethylamine (1.38 mL, 9.93 mmol) in CH₂Cl₂ (30 mL). The mixture was heated at reflux for 12 hours and after allowing to cool to r.t. washed with 2.0 M HCl (3 x 20 mL), dried (MgSO₄) and the solvent removed *in vacuo* yielding an orange viscous oil (1.17 g, 3.14 mmol, 95%): ¹H NMR (300 MHz, CDCl₃) δ 7.85-7.83 (4H, m, ArH), 7.46-7.44 (2H, m, ArH), 7.32 (2H, t, *J* = 8 Hz, ArH), 6.74 (2H, br s, NH), 4.70 (4H, d, *J* = 5 Hz, ArCH₂), 3.83 (6H, s, CH₃); ¹³C NMR (75.5 MHz, CDCl₃) δ 182.9 (C=S), 167.1 (C=O), 137.9 (Ar), 132.4 (Ar), 130.6 (Ar), 129.1 (Ar), 128.7 (Ar), 52.4, 48.2; *m/z* (ES⁺) 373.5 (M+H)⁺, 395.5 (M-Na)⁺.

N*-1-butyl-3-(((3-((butylamino)carbonyl)benzyl)amino)carbothioyl)amino) methyl)benzamide **145*



Ethyl-6-(((6-(ethoxycarbonyl)-2-pyridyl)methyl)amino)carbothioyl)amino) methyl)-2-pyridinecarboxylate **158** (50 mg, 0.13 mmol) was dissolved in butylamine (5 mL) and heated at reflux overnight. After allowing to cool to r.t. the excess butylamine was removed *in vacuo* yielding a white solid which was purified by crystallisation from ethyl acetate/methanol giving a white solid (25 mg, 55 μ mol, 41%); $R_f = 0.47$ (ethyl acetate); m.p. 88-90°C; I. R. (neat) $\nu_{\max} = 3285$ (m), 3225 (m), 3060 (m), 2960 (m), 2930 (m), 2865 (m), 1635 (s), 1585 (m), 1535 (s), 1435 (m), 1300 (s), 1205 (m), 1150 (m) cm^{-1} ; ^1H (300 MHz, CDCl_3) δ 7.54-7.51 (4H, m, ArH), 7.40 (2H, d, $J = 9$ Hz, ArH), 7.32 (2H, d, $J = 8$ Hz, ArH), 6.98 (2H, br m, NHC=O), 6.38 (2H, br m, S=CNH), 4.72 (4H, d, $J = 5$ Hz, S=CNHCH₂), 3.32 (4H, q, $J = 6$ Hz, O=CNHCH₂), 1.60-1.50 (4H, m, CH₂), 1.43-1.27 (4H, m, CH₃), 0.94 (6H, t, $J = 7$ Hz, CH₂CH₃); ^{13}C NMR (100 MHz, 10% DMSO-d₆/CDCl₃) δ 166.8 (C=O), 136.7 (Ar), 133.0 (Ar), 128.5 (Ar), 126.7 (Ar), 124.1 (Ar), 124.0 (Ar), 37.8, 29.4, 18.1, 11.5; m/z (ES)⁺ 456.4 (M+H)⁺.

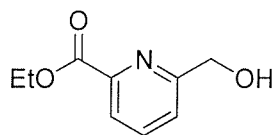
N*-1-[(1*S*)-2-amino-1-benzyl-2-oxoethyl]-3-[[[3-([(1*R*)-2-amino-1-benzyl-2-oxoethyl]amino)carbonyl]benzyl]amino]carbothioyl]amino]methyl]benzamide **162*



162

1.0 M LiOH (2.86 mL, 0.29 mmol) was added to a suspension of methyl-3-[[[3-(methoxycarbonyl)benzyl]amino]carbothioyl]amino]methyl]benzoate **158** (105 mg, 0.28 mmol) in 1,4-dioxane (3 mL) and the mixture stirred for 3 hours. The mixture was acidified to pH = 1 using 1.0 M HCl, the excess solvent was removed *in vacuo* yielding a white solid which was suspended in water (4 mL). The water was removed by filtration and the insoluble white solid washed with a further portion of water (2 mL). The solid was dried *in vacuo* over P₂O₅ yielding a white solid (86 mg, 0.25 mmol, 93%). EDC (63 mg, 0.33 mmol) was added to a stirred mixture of the solid intermediate (50 mg, 0.15 mmol), HOBt (45 mg, 0.33 mmol) and DMAP (40 mg, 0.33 mmol) in CH₂Cl₂ (3 mL). After 10 minutes, (2*S*)-2-amino-3-phenylpropanamide (98 mg, 0.60 mmol) was added and the mixture stirred for a further 15 hours. The solvent was removed *in vacuo* and the resultant white residue purified by flash column chromatography (SiO₂) eluting in 2% methanol/CH₂Cl₂ yielding a white solid (55 mg, 87 μmol, 60%): R_f = 0.38 (10% methanol/CH₂Cl₂); m.p. 145-147°C; [α]_D = -26.2° (c = 1, 10% methanol/CH₂Cl₂); I. R. (neat) ν_{max} = 2360 (w), 1640 (m), 1530 (m), 1265 (m), 1080 (br m) cm⁻¹; ¹H NMR (400 MHz, 10% DMSO-d₆/CDCl₃) δ 7.81 (2H, d, *J* = 7.5 Hz, Ar*H*), 7.69 (2H, s, Ar*H*), 7.57 (2H, d, *J* = 7.5 Hz, Ar*H*), 7.58 (2H, br s, NHC=S), 7.40 (2H, d, *J* = 7.5 Hz, Ar*H*) 7.29 (2H, t, *J* = 7.5 Hz, Ar*H*), 7.23-7.09 (12H, m, Ar*H*), 6.34 (4H, s, NH₂C=O), 4.81-4.79 (2H, m, CH(NH)CH₂), 4.73 (4H, d, *J* = 4.5 Hz, CH₂NH), 3.19 (2H, dd, *J* = 8.0, 5.5 Hz, CH_AH_BPh), 3.05 (2H, dd, *J* = 8.0, 5.5 Hz, CH_AH_BPh); ¹³C NMR (100 MHz, methanol-d₄) δ 176.6 (C=O), 170.2 (C=O), 139.0 (Ar), 135.9 (Ar), 132.2 (Ar), 130.7 (Ar), 130.0 (Ar), 129.8 (Ar), 128.1 (Ar), 127.8 (Ar), 127.5 (Ar), 56.6, 39.3; *m/z* (ES)⁺ 637.4 (M+H)⁺; HRMS (FAB): found 659.2417. C₃₅H₃₆N₆O₄NaS requires 659.2416.

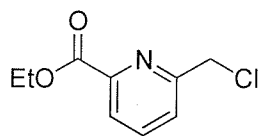
Hydroxymethylpyridine-2-carboxylic acid ethylester **149**⁵⁴



149

This procedure was modified from that of Fife.⁵⁴ 2,6-Pyridinedicarboxylic acid (100 g, 0.6 mol) was heated at reflux with thionyl chloride (350 mL) for 24 hours. After removal of the thionyl chloride *in vacuo* the remaining solid was suspended in dry CH₂Cl₂ (50 mL) and dry ethanol (500 mL) was slowly added dropwise and stirred overnight at r.t. The ethanol solution was made neutral by the dropwise addition of saturated aqueous sodium carbonate and water (around 50 mL). The solution was dried (MgSO₄), the insoluble material filtered off and the solvent removed *in vacuo* yielding a pale orange solid (132.3g, 99%) which was dissolved in dry ethanol (850 mL). Sodium borohydride (13.5g, 0.36 mol) was added and the mixture heated at reflux for 2 hours. After allowing to cool to r.t. the solution was concentrated *in vacuo* to a volume of 200 mL and water (200 mL) added. The solution was further concentrated *in vacuo* to a final volume of 200 mL, extracted with CHCl₃ (3 x 200 mL), dried (MgSO₄) and the solvent removed *in vacuo* furnishing a yellow solid which was purified by crystallisation from CHCl₃/petroleum ether yielding a pale yellow solid (57.6g, 0.32 mol, 53%): m.p. 95-97°C (lit. 95-97°C)⁵⁴; ¹H NMR (300 MHz, CDCl₃) δ 8.01 (1H, d, *J* = 8 Hz, pyrH), 7.83 (1H, t, *J* = 8 Hz, pyrH), 7.53 (1H, d, *J* = 8 Hz, pyrH), 4.86 (2H, s, ArCH₂), 4.45 (2H, q, *J* = 7 Hz, CH₂CH₃), 1.40 (3H, t, *J* = 7 Hz, CH₂CH₃); ¹³C NMR (75.5 MHz, CDCl₃) δ 165.3, 160.6, 147.5, 137.9, 124.1, 123.9, 64.8, 62.2, 14.5. All data agrees with that reported by Fife.⁵⁴

6-chloromethylpyridine-2-carboxylicacidethylester **150**⁵⁵

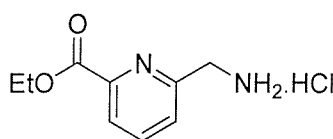


150

This procedure was modified from that of Scrimin and Tonellato.⁵⁵

Hydroxymethylpyridine-2-carboxylic acid ethylester **149** (8.01 g, 44.2 mmol) was dissolved in thionyl chloride (20 mL) at 0°C with stirring. After 1 hour, the excess thionyl chloride was removed *in vacuo* without heating. Toluene (20 mL) was added to the oily residue and cold 1.0 M NaHCO₃ added dropwise until the bubbling had subsided. The organic layer was dried (MgSO₄) and the solvent removed *in vacuo* producing a clear oil (7.91 g, 39.6 mmol, 90%): ¹H NMR (300 MHz, CDCl₃) δ 8.06 (1H, d, *J* = 8 Hz, pyr*H*), 7.89 (1H, t, *J* = 8 Hz, pyr*H*), 7.72 (1H, d, *J* = 8 Hz, pyr*H*), 4.86 (2H, s, ArCH₂), 4.48 (3H, q, *J* = 7 Hz, CH₂CH₃), 1.42 (2H, t, *J* = 7 Hz, CH₂CH₃); ¹³C NMR (75.5 MHz, CDCl₃) δ 164.8, 157.3, 147.8, 138.0, 126.0, 124.3, 62.0, 46.3, 14.3. All data agrees with that reported by Scrimin and Tonellato.⁵⁵

6-methylammoniumpyridine-2-carboxylic acid ethylester hydrochloride salt **151**⁵⁵



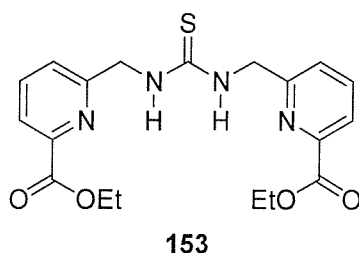
151

This procedure was modified from that of Scrimin and Tonellato.⁵⁵

6-Chloromethylpyridine-2-carboxylic acid ethylester **150** (2.03 g, 10.2 mmol) was dissolved in anhydrous DMF (2 mL) and slowly added to potassium phthalimide (1.91 g, 10.3 mmol) in anhydrous DMF (2 mL). After stirring for 2 hours at r.t. and overnight at 60°C the solvent was removed *in vacuo* and the resultant solid dissolved in CHCl₃ (30 mL) and washed with 0.2 M NaOH (3 x 30 mL), water (50 mL), dried (MgSO₄) and the solvent removed *in vacuo* yielding a white solid. The white solid was dissolved in ethanol (150 mL) and hydrazine hydrate (0.43 mL, 8.90 mmol) added and the mixture refluxed for 20 minutes until no starting material remained. The solvent was reduced to a volume of 50 mL *in vacuo* and

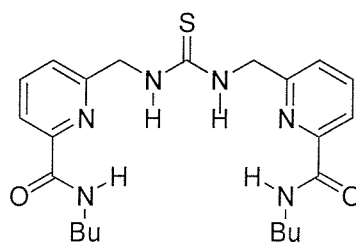
ether (125 mL) added. The resultant insoluble white solid was filtered off and gaseous HCl passed through the filtrate, after which the resultant precipitate was filtered off furnishing a white residue (2.09 g, 7.0 mmol, 67%): ^1H NMR (300 MHz, 5% DMSO- d_6 /CDCl $_3$) δ 8.19 (3H, br s, NH_3), 7.50 (1H, d, $J = 8$ Hz, pyrH), 7.40 (1H, t, $J = 8$ Hz, pyrH), 7.20 (1H, d, $J = 8$ Hz, pyrH), 3.85 (2H, q, $J = 7$ Hz, CH_2CH_3), 3.70 (2H, q, $J = 6$ Hz, CH_2NH_3), 0.84 (3H, t, $J = 7$ Hz, CH_2CH_3); ^{13}C NMR (75.5 MHz, DMSO- d_6) δ 164.6, 154.4, 147.4, 138.7, 126.6, 124.5, 61.6, 43.1, 14.4. All data agrees with that reported by Scrimin and Tonellato.⁵⁵

Ethyl-6-(((6-(ethoxycarbonyl)-2-pyridyl)methyl)amino)carbothioyl)amino methyl)-2-pyridinecarboxylate **153**



DMAP (0.57 mg, 4.70 mmol) was added to a suspension of 6-methylammoniumpyridine-2-carboxylic acid ethylester hydrochloride salt **151** (0.41 mg, 1.88 mmol), DCC (0.19 mg, 0.94 mmol) and carbon disulfide (0.40 mL, 6.58 mmol) in dry CHCl $_3$ (10 mL) at -10°C . The solution was stirred at r.t. for 1 hour and heated at reflux overnight. The solvent was removed *in vacuo* and the resultant orange oil purified by flash column chromatography (SiO $_2$) eluting in 70% ethyl acetate/petroleum ether furnishing a yellow solid which could be further purified by crystallisation from ethyl acetate/petroleum ether (0.25 mg, 0.63 mmol, 64%): $R_f = 0.44$ (ethyl acetate); m.p. = $103\text{-}104^\circ\text{C}$; I.R. (neat) $\nu_{\text{max}} = 3545$ (w), 3300 (w), 1705 (m), 1530 (m), 1290 (s), 1240 (s), 1170 (m), 1020 (m) cm^{-1} ; ^1H NMR (300 MHz, CDCl $_3$) δ 8.56 (2H, br s, NH), 8.02 (2H, d, $J = 8$ Hz, pyrH), 7.83 (2H, t, $J = 8$ Hz, pyrH), 7.50 (2H, d, $J = 8$ Hz, pyrH), 5.02 (4H, s, CH_2), 4.49 (4H, q, $J = 7$ Hz, CH_2), 1.45 (6H, t, $J = 7$ Hz, CH_3); ^{13}C NMR (75.5 MHz, CDCl $_3$) δ 183.3 (C=S), 165.1 (C=O), 157.4 (Ar), 147.2 (Ar), 138.0 (Ar), 125.7 (Ar), 124.0 (Ar), 62.2, 49.5, 14.4; m/z (ES $^+$) 403.0 (M+H) $^+$, 424.9 (M+Na) $^+$.

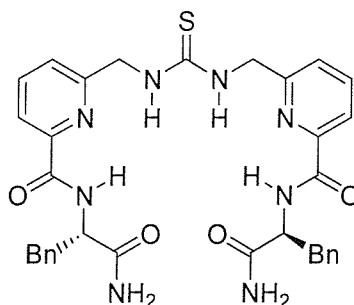
***N*-2-butyl-6-([6-((butylamino)carbonyl)-2-pyridyl)methyl]amino)carbothioyl
amino)methyl]-2-pyridinecarboxamide 144**



144

Ethyl-6-([6-((ethoxycarbonyl)-2-pyridyl)methyl]amino)carbothioyl amino)methyl]-2-pyridinecarboxylate **153** (26 mg, 65 μ mol) was dissolved in butylamine (4 mL) and the solution heated at reflux overnight. The excess butylamine was removed *in vacuo* and the resultant yellow solid recrystallised from hot ethyl acetate/petroleum ether yielding a white solid (32 mg, 65 μ mol, 100%): $R_f = 0.31$ (ethyl acetate); m.p. = 95-96°C; I.R. (neat) $\nu_{\max} = 3360$ (m), 3300 (m), 2950 (m), 2860 (m), 2360 (w), 1670 (m), 1640 (m), 1570 (m), 1570 (m), 1530, (s), 1445 (s), 1360 (s), 1315 (m), 1260 (m), 1210 (m) cm^{-1} ; ^1H NMR (300 MHz, CDCl_3) δ 8.29 (2H, br s, NH), 8.02 (2H, br s, NH), 7.96 (2H, d, $J = 8$ Hz, pyrH), 7.77 (2H, t, $J = 8$ Hz, pyrH), 7.48 (2H, d, $J = 8$ Hz, pyrH), 4.98 (4H, s, ArCH_2), 3.29-3.23 (4H, m, NCH_2), 1.49-1.39 (4H, m, CH_2CH_2), 1.28-1.15 (4H, m, CH_2CH_2), 0.80 (6H, t, $J = 7$ Hz, CH_3); ^{13}C NMR (75.5 MHz, CDCl_3) δ 164.1 (C=O), 155.9 (Ar), 155.9 (Ar), 149.0 (Ar), 138.8 (Ar), 125.2 (Ar), 121.3 (Ar), 49.5 (alkyl), 39.6 (alkyl), 31.8 (alkyl), 20.3 (alkyl), 13.8 (alkyl); m/z (ES^+) 457.4 ($\text{M}+\text{H}^+$), 479.5 ($\text{M}+\text{Na}^+$); HRMS (FAB): found 457.2386. $\text{C}_{23}\text{H}_{33}\text{N}_6\text{O}_2\text{S}$ requires 457.2386.

N*-2-[(1*S*)-2-amino-1-benzyl-2-oxoethyl]-6-({[6-({[(1*R*)-2-amino-1-benzyl-2-oxoethyl]amino} carbonyl)-2-pyridyl]methyl}amino)carbothioyl]amino)methyl)-2-pyridinecarboxamide **161*

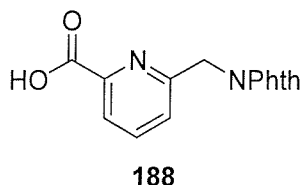


161

DPPA usage in this procedure was modified from the method of Mochel.⁶⁹ 1.0 M LiOH (20.1 mL 20.1 mmol) was added to ethyl-6-({[6-(ethoxycarbonyl)-2-pyridyl]methyl} amino)carbothioyl} amino)methyl)-2-pyridinecarboxylate **153** (0.81 g, 2.01 mmol) in 1,4-dioxane (23 mL) and the mixture stirred for 1 hour. 1.0 M KHSO₄ (20.1 mL, 20.1 mmol) was added and the water removed *in vacuo* and by azeotroping with acetonitrile (20 mL). Methanol (5 mL) was added to the resultant solid and the insoluble material filtered off, the excess methanol was removed *in vacuo* and methanol (3 mL) added to the resultant solid, the insoluble material was again filtered off yielding a pale yellow solid (0.65 mg, 1.88 mmol, 93%). DPPA (416 μL, 1.92 mmol) followed by triethylamine (534 μL, 3.83 mmol) was added to a stirred mixture of the above solid (302 mg, 0.87 mmol) and (2*S*)-2-amino-3-phenylpropanamide (314 mg, 1.92 mmol) in DMF (0.5 mL) at 0°C. The mixture was stirred at 0°C for 2 hours and at r.t. for 2 days after which the solvent was removed *in vacuo* yielding an oil which was suspended in CH₂Cl₂ (15 mL), washed with water (15 mL), dried (MgSO₄) and the solvent removed *in vacuo* yielding an oil which was purified by flash column chromatography (SiO₂) eluting in 1% methanol/CH₂Cl₂ yielding a white solid (83.5 mg, 0.13 μmol, 15%): $R_f = 0.43$ (10% methanol/CH₂Cl₂); m.p. = 126-128°C; $[\alpha]_D = -36.0^\circ$ (c = 1, CH₂Cl₂); I.R. (neat) $\nu_{max} = 2395$ (br m), 2360 (w), 1660 (s), 1650 (s), 1515 (s), 1410 (m), 1260 (m) cm⁻¹; ¹H NMR (300 MHz, CDCl₃) δ 8.80 (2H, d, $J = 8$ Hz, C=ONHCH), 8.00 (2H, br s, C=SNH), 7.91 (2H, d, $J = 8$ Hz, pyr*H*), 7.74 (2H, t, $J = 8$ Hz, pyr*H*), 7.43 (2H, d, $J = 8$ Hz, Ar*H*), 7.23-7.01 (10H, m, Ar*H*), 6.47 (2H, br s, CHCONH), 6.34 (2H, br s, CHCONH), 5.05-4.92 (4H, m, C=SNHCH₂), 4.90-4.85 (2H, m, C=ONHCH), 3.17 (2H, dd, $J = 14, 7$ Hz, CH_AH_BPh), 3.12 (2H, dd, $J = 14, 7$ Hz, CH_AH_BPh); ¹³C NMR (75.5 MHz,

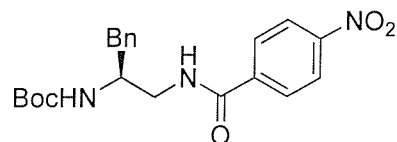
CDCl₃) δ 175.69 (C=O), 165.8 (C=O), 158.6 (Ar), 149.6 (Ar), 139.3 (Ar), 138.0 (Ar), 130.4 (Ar), 129.4 (Ar), 127.8 (Ar), 125.9 (Ar), 121.5 (Ar), 55.6, 39.4; m/z (ES⁺) 639.6 (M+H)⁺, 661.6 (M+Na)⁺, 677.5 (M+K)⁺; HRMS (FAB): found 661.2321. C₃₃H₃₄N₈O₄NaS requires 661.2321.

6-[(1,3-dioxo-2,3-dihydro-1*H*-2-isoindolyl)methyl]-2-pyridinecarboxylic acid **188**



This procedure is modified from that of Olah.⁶⁵ Chlorotrimethylsilane (16.6 mL, 0.13 mmol) was added to a solution of ethyl-6-[(1,3-dioxo-2,3-dihydro-1*H*-2-isoindolyl)methyl]-2-pyridinecarboxylate **187** {intermediate in **151** synthesis} (10.1 g, 32.7 mmol) and sodium iodide (19.6 g, 0.13 mmol) in acetonitrile (50 mL) at 0°C. The reaction was allowed to warm to r.t. and then heated under reflux for 4 days. After allowing to cool to r.t. water (200 mL) was added after which the reaction mixture was taken up into CH₂Cl₂ (100 mL) and washed successively with water (100 mL) and aqueous sodium thiosulphate (150 mL) to remove inorganic salts and residual iodine. The organic phase was extracted with saturated sodium hydrogen carbonate (50 mL) and then the aqueous phase acidified to pH 3 using 2.0 M HCl. The acidic solution was extracted with 5% methanol/CH₂Cl₂ (3 x 150 mL), dried (MgSO₄) and the solvent removed *in vacuo* yielding a white solid (3.12 g, 11.0 mmol, 34%): R_f = 0.21 (10% methanol/CH₂Cl₂); m.p. = 219-221°C; I.R. (neat) ν_{\max} = 3360 (br w), 2360 (w), 1750 (s), 1705 (s), 1600 (m), 1420 (m), 1395 (s), 1370 (m), 1325 (m), 1270 (m), 1110 (s) cm⁻¹; ¹H NMR (400 MHz, 10% DMSO-d₆/CDCl₃) δ 7.96 (1H, d, J = 7.5 Hz, pyr*H*), 7.84-7.81 (2H, m, Phth*H*), 7.77 (1H, t, J = 7.5 Hz, pyr*H*), 7.75-7.71 (2H, m, Phth*H*), 7.33 (1H, d, J = 7.5 Hz, pyr*H*), 5.03 (2H, s, PhthNCH₂); ¹³C NMR (100 MHz, methanol-d₄) δ 167.5 (C=O), 165.7 (C=O), 155.5 (Ar), 147.6 (Ar), 137.8 (Ar), 134.0 (Ar), 131.5 (Ar), 123.7 (Ar), 123.2 (Ar), 123.1 (Ar), 42.5 (CH₂).

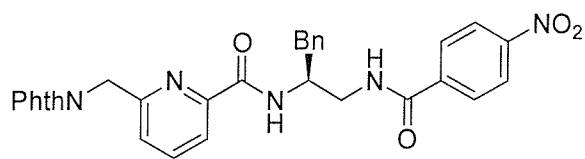
tert-butyl-*N*-{(1*S*)-1-benzyl-2-[(4-nitrobenzoyl)amino]ethyl}carbamate **185**



185

Hydrazine hydrate (90 μ L, 1.88 mmol) was added to a solution of (*S*)-*N*-*tert*-butoxycarbonyl-3-phenyl-*N*-phthaloyl-1,2-diaminopropane **121** in ethanol (25 mL) and the mixture heated at reflux for 6 hours. After cooling to r.t. the insoluble material was removed by filtration and the excess of solvent removed *in vacuo* providing a pale yellow solid which was suspended in dry CH_2Cl_2 (20 mL). 4-nitrobenzoyl chloride (523 mg, 2.82 mmol) then triethylamine (0.39 mL, 2.82 mmol) and DMAP (50 mg, 10% by weight) were added. After stirring at r.t. overnight the crude material was purified by flash column chromatography (SiO_2) eluting in 30% ethyl acetate/petroleum ether yielding a white residue. This residue was suspended in CH_2Cl_2 (5 mL) and the insoluble material filtered off, the filtrate was concentrated *in vacuo* to yield a white solid (312 mg, 0.80 mmol, 63%): $R_f = 0.5$ (30% ethyl acetate/petroleum ether); m.p. = 184-186°C; I.R. (neat) $\nu_{\text{max}} = 3350$ (m), 2360 (m), 1690 (s), 1644 (m), 1550 (m), 1524 (s), 1330 (m), 1265 (m), 1165 (m), 1055 (s), 1015 (s) cm^{-1} ; ^1H NMR (300 MHz, 10% $\text{CDCl}_3/\text{DMSO-d}_6$) δ 8.80 (1H, t, $J = 5$ Hz, NHCH), 8.32 (2H, d, $J = 9$ Hz, ArH), 8.07 (2H, d, $J = 9$ Hz, ArH), 7.31-7.16 (5H, m, ArH), 6.81 (1H, d, $J = 9$ Hz, NHCH_2), 3.93 (1H, m, CHCH_2), 3.38-3.33 (2H, m, CH_2), 2.80 (1H, dd, $J = 14, 5.5$ Hz, CHCH_AH_B), 2.70 (1H, dd, $J = 14, 5.5$ Hz, CHCH_AH_B), 1.29 (9H, s, $\text{C}(\text{CH}_3)$); ^{13}C NMR (100 MHz, DMSO-d_6) δ 163.2, 153.6, 147.2, 138.6, 137.2, 129.0, 127.4, 127.1, 126.3, 124.2, 121.7, 75.8, 49.7, 42.0, 36.1, 26.5; m/z (ES^+) 400.4 ($\text{M}+\text{H}$) $^+$.

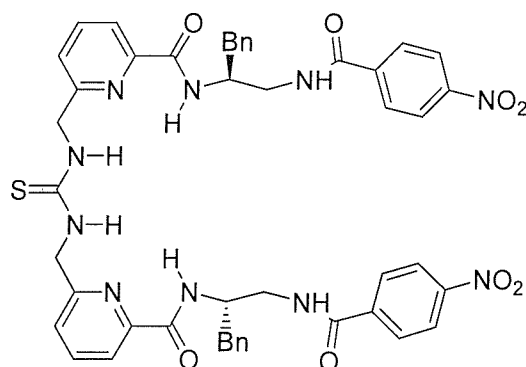
***N*-2-[(1*S*)-1-benzyl-2-[(4-nitrobenzoyl)amino]ethyl]-6-[(1,3-dioxo-2,3-dihydro-1*H*-2-isoindolyl)methyl]-2-pyridinecarboxamide 190**



190

A 50% mixture of TFA in CH₂Cl₂ (5 mL) was added to an ice cold solution of *tert*-butyl-*N*-[(1*S*)-1-benzyl-2-[(4-nitrobenzoyl)amino]ethyl] carbamate **185** (212 mg, 0.53 mmol) in CH₂Cl₂ (10 mL) and the mixture stirred for 12 hours. The solvent was removed *in vacuo* yielding a pale yellow oil which was triturated from ether (2 x 10 mL) giving a pale yellow oily residue (214 mg, 98%). DMAP (70 mg, 0.57 mmol) was added to the oily residue in dry DMF (5 mL) and the mixture stirred at r.t. for 1 hour. In parallel, 6-[(1,3-dioxo-2,3-dihydro-1*H*-2-isoindolyl)methyl]-2-pyridinecarboxylic acid **188** (192 mg, 0.68 mmol) was heated at reflux in thionyl chloride (2 mL) for 8 hours and stirred at r.t. overnight. The excess thionyl chloride was removed *in vacuo* yielding a white solid which was dissolved in dry DMF (5 mL) and added dropwise to the solution of amine in DMF. The mixture was stirred at r.t. for 2 days after which the solvent was removed *in vacuo*. The resultant brown residue was purified by filtering through a pad of silica eluting in neat ethyl acetate yielding a white solid (230 mg, 0.41 mmol, 79%): $R_f = 0.59$ (ethyl acetate); m.p = 174-176°C; $[\alpha]_D = -11.3^\circ$ (c = 1, CH₂Cl₂); I.R. (neat) $\nu_{\max} = 3350$ (w), 2360 (w), 1685 (s), 1644 (s), 1600 (w), 1550 (m) 1325 (s), 1165 (s), 1015 (s) cm⁻¹; ¹H NMR (400 MHz, CDCl₃) δ 8.17 (2H, d, $J = 8.5$ Hz, Ar*H*), 8.12 (1H, d, $J = 7.5$ Hz, NHCHCH₂), 7.96 (1H, d, $J = 7.5$ Hz, pyr*H*), 7.90-7.88 (3H, m, $J = 9$ Hz, Ar*H* and NHCH₂CH), 7.85-7.82 (2H, m, Ar*H*), 7.76 (1H, t, $J = 7.5$ Hz, pyr*H*), 7.73-7.69 (2H, m, Ar*H*), 7.40 (2H, d, $J = 7.5$ Hz, pyr*H*), 7.23-7.13 (5H, m, Ar*H*), 4.97 (2H, s, CH₂Phth), 4.37 (1H, m, NHCHCH₂), 3.65 (1H, m, NHCH_ACH_B), 3.39 (1H, m, NHCH_ACH_B), 2.80 (2H, m, CH₂Ph); ¹³C NMR (100 MHz, CDCl₃) δ 168.4, 166.1, 165.7, 154.7, 149.9, 149.0, 140.1, 139.0, 136.9, 134.9, 132.4, 129.5, 129.3, 128.7, 127.5, 125.3, 124.1, 121.6, 51.5, 47.3, 43.0, 39.3.

N*-2-{(1*R*)-1-benzyl-2-[(4-nitrobenzoyl)amino]ethyl}-6-[[[6-[[{(1*S*)-1-benzyl-2-[(4-nitrobenzoyl)amino]ethyl]amino)carbonyl]-2-pyridyl]methyl]amino]carbothioyl}amino)methyl]-2-pyridinecarboxamide **183*



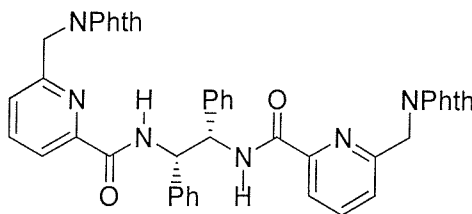
183

Hydrazine hydrate (17 μ L, 0.35 mmol) was added to a solution of *N*-2-{(1*S*)-1-benzyl-2-[(4-nitrobenzoyl)amino]ethyl}-6-[(1,3-dioxo-2,3-dihydro-1*H*-2-isoindolyl)methyl]-2-pyridinecarboxamide **190** (196 mg, 0.35 mmol) in ethanol (5 mL) and the mixture heated at reflux overnight. The insoluble material was filtered off and the solvent removed *in vacuo* from the filtrate yielding a yellow residue which was used in the next step without further purification. Carbon disulfide (74 μ L, 1.21 mmol) was added to a solution of the yellow residue (75 mg, 1.73 μ mol) in dry CH_2Cl_2 (2 mL) at -10°C . DCC (36 mg, 174 μ mol) along with DMAP (43 mg, 0.35 mmol) was added and the mixture stirred for 1 hour at -10°C . After allowing to warm to r.t. the excess solvent and carbon disulfide was removed *in vacuo*. The resultant orange oil was dissolved in dry CH_2Cl_2 (2 mL) and further yellow residue (75 mg, 1.73 μ mol) added. After stirring at r.t. for 5 days the solvent was removed *in vacuo* and the resultant brown residue purified by flash column chromatography (SiO_2) eluting in 10% methanol/ CH_2Cl_2 yielding a yellow residue (60 mg, 66 μ mol, 25% based on amine intermediate): $R_f = 0.59$ (ethyl acetate); $[\alpha]_D = +36.0^\circ$ ($c = 2$, CH_2Cl_2); I.R. (neat) $\nu_{\text{max}} = 3285$ (w), 1650 (m), 1595 (m), 1518 (s), 1340 (m), 1080 (m) cm^{-1} ; $^1\text{H NMR}$ (400 MHz, CDCl_3) δ 8.89 (2H, d, $J = 5$ Hz, NHCH), 8.44 (2H, br m, $\text{C}=\text{SNH}$), 8.11 (4H, d, $J = 8.5$ Hz, ArH), (2H, d, $J = 7.5$ Hz, pyrH), 7.89(2H, t, $J = 7.5$ Hz, pyrH), 7.83 (4H, d, $J = 8.5$ Hz, ArH), 7.73 (2H, br m, CH_2NHCO), 7.56 (2H, d, $J = 7.5$ Hz, pyrH), 7.33-7.22 (10H, m, ArH), 5.10 (2H, d, $J = 17$ Hz, $\text{CH}_A\text{CH}_B\text{NHC}=\text{S}$), 5.02 (2H, d, $J = 17$ Hz, $\text{CH}_A\text{CH}_B\text{NHC}=\text{S}$), 4.51 (2H, m, CH_BN), (1H, dd, $J = 14, 9.5$ Hz, $\text{CHCH}_A\text{CH}_B\text{NH}$), (1H, dd, $J = 14, 2.5$ Hz, $\text{CHCH}_A\text{CH}_B\text{NH}$), (1H, dd, $J = 14, 8$ Hz, $\text{CHCH}_A\text{CH}_B\text{Ph}$), (1H, dd, $J = 14, 8$ Hz,

CHCH_ACH_BPh); ¹³C NMR (100 MHz, CDCl₃) δ 182.3, 165.9, 162.6, 154.1, 148.1, 146.4, 137.7, 135.5, 127.4, 126.7, 125.6, 123.9, 122.3, 120.0, 51.0, 47.2, 42.7, 37.3; *m/z* (ES⁺) 910.4 (M+H)⁺.

5.4 Experimental for Chapter Four

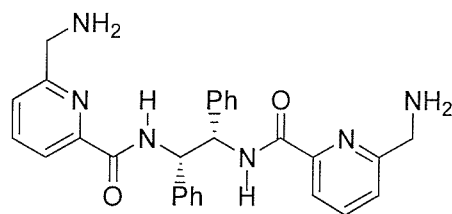
N-2-(1*S*,2*S*)-2-[(6-[(1,3-dioxo-2,3-dihydro-1*H*-2-isoindolyl)methyl]-2-pyridyl)carbonyl]amino]-1,2-diphenylethyl}-6-[(1,3-dioxo-2,3-dihydro-1*H*-2-isoindolyl)methyl]-2-pyridinecarboxamide **196**



196

6-[(1,3-dioxo-2,3-dihydro-1*H*-2-isoindolyl)methyl]-2-pyridinecarboxylic acid **188** (1.5 g, 5.3 mmol) was heated at reflux in thionyl chloride (20 mL) for 4 hours after which the excess thionyl chloride was removed *in vacuo* yielding a white solid which was dissolved in dry CH₂Cl₂ (10 mL). (1*S*,2*S*)-(-)-1,2-diphenylethylenediamine (0.57 g, 2.7 mmol) was added followed by DMAP (1.3 g, 10.6 mmol) and the mixture stirred at r.t. for 3 days. A silica pad of the crude material was made and the product purified by flash column chromatography (SiO₂) eluting in 35% ethyl acetate/petroleum ether furnishing a white solid (1.36 g, 1.84 mmol, 68%): R_f = 0.55 (ethyl acetate); m.p. 105-107°C; [α]_D = + 15.0° (c = 1, CH₂Cl₂); I.R. (neat) ν_{max} = 2365 (w), 1770 (w), 1710 (s), 1670 (m), 1510 (m), 1385 (s), 945 (s) cm⁻¹; ¹H NMR (300 MHz, CDCl₃) δ 8.79-8.71 (2H, m, CH(NH)Ph),* 7.97-7.90 (6H, m, pyr*H*, Phth*H*), 7.81-7.77 (4H, m, Phth*H*), 7.73 (2H, t, *J* = 8 Hz, pyr*H*), 7.32 (2H, d, *J* = 8 Hz, pyr*H*), 7.22 -7.02 (12H, m, Ar*H*), 5.39-5.32 (2H, m, CH(NH)Ph),* 5.07 (2H, d, *J* = 16 Hz, PhthNCH_A(H_B)pyr), 5.01 (2H, d, *J* = 16 Hz, PhthNCH_A(H_B)pyr); ¹³C NMR (75.5 MHz, CDCl₃) δ 168.1 (C=O), 164.1 (C=O), 154.2, 149.5, 138.7, 138.2, 134.2, 132.4, 128.5, 127.7, 123.7, 121.2, 59.2, 42.6; *m/z* (ES⁺) 741.5 (M+H)⁺, 763.4 (M+Na)⁺. [* system has been modeled using gNMR version 3.6 and was found to be consistent with a non-first order AA'BB' system]; HRMS (FAB): found 763.2281. C₄₄H₃₂N₆O₆Na requires 763.2281.

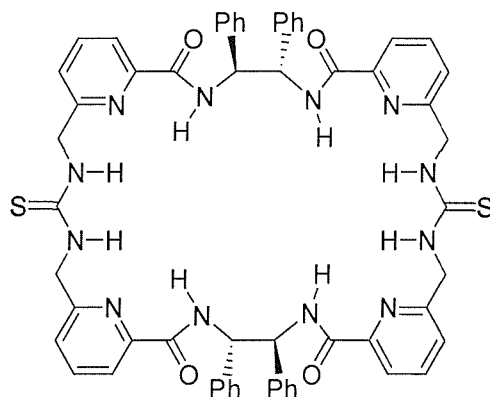
***N*-2-[(1*S*,2*S*)-2-([6-(aminomethyl)-2-pyridyl]carbonyl)amino]-1,2-diphenylethyl]-6-(aminomethyl)-2-pyridinecarboxamide 197**



197

Hydrazine monohydrate (80 μ L, 1.64 mmol) was added to a solution of *N*-2-(1*S*,2*S*)-2-[(6-[(1,3-dioxo-2,3-dihydro-1*H*-2-isoindolyl)methyl]-2-pyridyl]carbonyl)amino]-1,2-diphenylethyl]-6-[(1,3-dioxo-2,3-dihydro-1*H*-2-isoindolyl)methyl]-2-pyridine carboxamide **196** (0.61 g, 0.82 mmol) in ethanol (5 mL) and the mixture heated at reflux for 8 hours. After allowing to cool to r.t. the solvent was removed *in vacuo* yielding a white solid to which 2.0 M HCl (5 mL) was added. The solution was heated to reflux for 30 minutes, after which the insoluble material was filtered off and the aqueous filtrate basified to pH = 10 using 1.0 M NaOH. The precipitated amine was extracted with CH₂Cl₂ (5 x 15 mL) and the combined extracts dried (MgSO₄) after which the excess solvent was removed *in vacuo* yielding a white residue (330 mg, 0.69 mmol, 84%): m.p. 73-75°C; [α]_D = + 29.4° (c = 1, 10% methanol/CH₂Cl₂); I.R. (neat) ν_{\max} = 2360 (w), 1657 (w), 1590 (w), 1510 (m), 1445 (m), 995 (m) cm⁻¹; ¹H NMR (300 MHz, CDCl₃) δ 9.22 (2H, br m, NHC=O),* 8.00 (2H, d, *J* = 7.5 Hz, pyr*H*), 7.74 (2H, t, *J* = 7.5 Hz, pyr*H*), 7.33 (2H, d, *J* = 7.5 Hz, pyr*H*), 7.28-7.20 (12H, m, Ar*H*), 5.58-5.55 (2H, m, CH(NH)Ph),* 4.04 (2H, d, *J* = 15.5 Hz, CH_A(H_B)NH₂), 5.01 (2H, d, *J* = 15.5 Hz, CH_A(H_B)NH₂); ¹³C NMR (75.5 MHz, CDCl₃) δ 165.5 (C=O), 161.4 (C=O), 149.5 (Ar), 139.4 (Ar), 138.4 (Ar), 129.3 (Ar), 129.2 (Ar), 128.9 (Ar), 128.5 (Ar), 128.4 (Ar), 127.5 (Ar), 127.3 (Ar), 124.6 (Ar), 120.9 (Ar). 60.1, 48.0. [*system has been modeled using gNMR version 3.6 and was found to be consistent with a non-first order AA'BB' system].

(14*S*,15*S*,35*S*,36*S*)-14,15,35,36-tetraphenyl-4,25-dithioxo-3,5,13,16,24,26,34,37,43,44,45,46-dodecaazapentacyclo[37.31.1^{7,11}.1^{18,22}.1^{28,32}]hexatetraconta-1(43),7,9,11(46),18,20,22(45),28,30, 32,39,41-dodecaene-12,17,33,38-tetraone 193



193

Carbon disulfide (207 μL , 3.43 mmol) was added to a mixture of *N*-2-[(1*S*,2*S*)-2-({[6-(aminomethyl)-2-pyridyl]carbonyl}amino)-1,2-diphenylethyl]-6-(aminomethyl)-2-pyridinecarboxamide **197** (100 mg, 0.25 mmol) in dry CH_2Cl_2 (5 mL) at -10°C and the mixture stirred for 1 hour. DCC (101 mg, 0.49 mmol) was added and the mixture stirred for a further 45 minutes at -10°C then 30 minutes at r.t. The excess carbon disulfide and solvent was removed *in vacuo* yielding a white solid which was dissolved in dry CH_2Cl_2 (5 mL). This solution was added to dry CH_2Cl_2 (25 mL) containing DMAP (10 mg, 10% by weight) along with a further one equivalent of amine **197** (100 mg, 0.20 mmol) in dry CH_2Cl_2 (5 mL) under a slow stream of nitrogen over 3 hours *via* syringe pump addition. After stirring at r.t. overnight the excess solvent was removed *in vacuo* and the resultant yellow residue purified by flash column chromatography (SiO_2) eluting in 30% ethyl acetate/petroleum ether yielding a white residue (61 mg, 58 μmol , 26%): $R_f = 0.48$ (ethyl acetate); $[\alpha]_D = +146.0^\circ$ ($c = 1$, CH_2Cl_2); I.R. (neat) $\nu_{\text{max}} = 3310$ (br m), 2360 (w), 2330 (w), 1670 (m), 1525 (m), 1450 (w), 1360 (w), 1255 (w) cm^{-1} ; ^1H NMR (400 MHz, DMSO-d_6 , acquired at 90°C) δ 9.38 (4H, d, $J = 5.5$ Hz, NHC=O), 8.27 (4H, t, $J = 5.5$ Hz, NHC=S), 7.93 (4H, t, $J = 7.5$ Hz, pyrH), 7.84 (4H, d, $J = 7.5$ Hz, pyrH), 7.59 (4H, d, $J = 7.5$ Hz, pyrH), 7.48-7.26 (24H, m, pheH), 5.82-5.77 (2H, m, CHNHC=O), 5.03 (4H, dd, $J = 16, 5$ Hz, $\text{CH}_A\text{H}_B(\text{Ar})\text{NHC=S}$), 4.95 (4H, dd, $J = 16, 5$ Hz, $\text{CH}_A\text{H}_B(\text{Ar})\text{NHC=S}$); ^{13}C NMR (100 Hz, DMSO-d_6) δ 165.1 (C=O), 157.3 (Ar), 149.4 (Ar), 139.8 (quartAr), 138.7 (Ar), 128.5 (Ar), 128.0 (Ar), 127.6 (Ar), 124.8 (Ar), 120.8 (Ar), 60.2, 58.1, 49.2; m/z (ES^+) 1044.8 (M+H) $^+$, 1067.8 (M+Na) $^+$.

5.5 Experimental for binding studies

Obtaining association constants by ^1H NMR titration experiments involves titration of a solution of host with guest and recording a ^1H NMR spectrum after each addition. Protons in the host or guest may undergo a change in chemical shift upon complexation. Any protons involved in hydrogen-bonding usually undergo a more dramatic shift and are therefore commonly used to determine association constants. After the data from the titration experiment has been acquired, curve fitting software is employed to determine the association constant. Free host and free guest are in equilibrium with host-guest complex and as association and dissociation occur on a timescale faster than that of NMR, the observed chemical shift of any proton (δ_{obs}) involved in binding will be a weighted average of the fully bound (δ_{bound}) and the fully unbound (δ_{free}) chemical shifts. After an initial estimate for K_a and $\Delta\delta$, the theoretical δ_{obs} can be obtained for each data point. The theoretical values for the chemical shifts are compared with the experimentally observed ones and the sum of the difference between each point is determined using the following equation:

$$\text{Sum of differences} = \sum (\delta_{\text{obs}(\text{experimental})} - \delta_{\text{obs}(\text{theoretical})})$$

If the sum of the differences is positive (or negative), the K_a is increased (or decreased) and the value $\Delta\delta$ is recalculated and the whole calculation repeated until the values converge. The shape of the binding curve is wholly dependent on K_a , $[\text{H}]_{\text{total}}$ and $[\text{G}]_{\text{total}}$. At higher K_a 's or higher concentrations, the observed binding curve will be steeper. A more detailed explanation of the theoretical basis to the above discussion has been published by Wilcox.⁶⁶

Method Used for Obtaining Binding Constants

All ^1H NMR titration experiments were conducted on either a Bruker AM 300 or Bruker DPX 400 spectrometer at 298 K. All CDCl_3 was passed over a pad of basic alumina prior to use and collected over molecular sieves (4Å). Guest stock solutions were typically made up such that 10 μL of that solution contained 0.1 equivalents of guest with respect to host. The hydrogens monitored during binding studies were the thiourea or amide protons in the host molecule unless otherwise stated. For a greater degree of accuracy, association constants

quoted in the results and discussion chapters are taken as are the average of all the association constants obtained from each proton monitored in the host molecule (where data from the experiment allowed more than one proton to be followed). The software used to determine the binding constants was kindly provided by C.A. Hunter, where a 1:1 binding mode was assumed. All data obtained corresponded well with the theoretical model for 1:1 binding stoichiometry.

Binding data for phenylacetic carboxylate 146 with pyridylthiourea 144:

Proton observed:	thiourea
Solvent:	10% DMSO-d ₆ /CDCl ₃
Starting volume of host solution	500 μL
Concentration of host solution:	7.88 mM
Concentration of guest solution:	81.57 mM
Association constant:	420 ± 42 M ⁻¹

Volume added/μL	Chemical Shift/ppm
0	7.69
10	8.31
20	8.62
30	8.89
40	9.14
50	9.33
60	9.50
100	9.72
120	9.86
160	10.00
200	10.01

Binding data for phenylacetic carboxylate 146 with benzothiourea 145:

Proton observed:	thiourea
Solvent:	10% DMSO-d ₆ /CDCl ₃
Starting volume of host solution	500 μL
Concentration of host solution:	7.04 mM
Concentration of guest solution:	70.97 mM
Association constant:	740 ± 74 M ⁻¹

Volume added/μL	Chemical Shift/ppm
0	7.37
10	7.67
20	7.96
30	8.21
40	8.42
50	8.61
60	8.74
80	8.92
100	9.03
120	9.09
160	9.16
200	9.18

Binding data for N-Ac-L-Phe derivative 167 with dipyridylthiourea 161

Proton observed:	thiourea
Solvent:	10% DMSO-d ₆ /CDCl ₃
Starting volume of host solution	600 μL
Concentration of host solution:	5.92 mM
Concentration of guest solution:	35.66 mM
Association constant:	680 ± 68 M ⁻¹

Volume added/μL	Chemical Shift/ppm
0	7.937
10	8.036
20	8.159
30	8.304
75	8.859
100	9.020
150	8.220
200	9.376
250	8.453

Binding data for N-Ac-D-Phe derivative 168 with dipyridylthiourea 161

Proton observed:	thiourea
Solvent:	10% DMSO-d ₆ /CDCl ₃
Starting volume of host solution	600 μL
Concentration of host solution:	5.92 mM
Concentration of guest solution:	35.66 mM
Association constant:	530 ± 53 M ⁻¹

Volume added/μL	Chemical Shift/ppm
0	7.937
10	8.036
20	8.161
30	8.317
75	8.852
100	9.008
150	9.237
200	9.417
250	9.469

Binding data for N-Ac-L-Phe derivative 167 with dibenzothiourea 162

Proton observed:	thiourea
Solvent:	10% DMSO-d ₆ /CDCl ₃
Starting volume of host solution	600 μL
Concentration of host solution:	3.94 mM
Concentration of guest solution:	23.63 mM
Association constant:	2330 ± 233 M ⁻¹

Volume added/μL	Chemical Shift/ppm
0	7.369
10	7.485
20	7.605
30	7.715
40	7.819
65	8.006
100	8.272
150	8.432
200	8.477
250	8.521

Binding data for N-Ac-D-Phe derivative 168 with dibenzothiourea 162

Proton observed:	thiourea
Solvent:	10% DMSO-d ₆ /CDCl ₃
Starting volume of host solution	600 μL
Concentration of host solution:	3.94 mM
Concentration of guest solution:	23.63 mM
Association constant:	1840 ± 184 M ⁻¹

Volume added/μL	Chemical Shift/ppm
0	7.369
10	7.495
20	7.629
65	8.114
100	8.374
150	8.538
200	8.621
250	8.671

Binding data for N-Ac-L-Ala 165 with dipyridylthiourea 161

Proton observed:	amide
Solvent:	CDCl ₃
Starting volume of host solution	600 μL
Concentration of host solution:	3.91 mM
Concentration of guest solution:	23.47 mM
Association constant:	3,450 ± 345 M ⁻¹

Volume added/μL	Chemical Shift/ppm
0	8.822
20	8.919
30	8.958
40	9.004
50	9.070
60	9.119
80	9.182
100	9.187
125	9.234
150	9.260

Binding data for N-Ac-D-Ala 166 with dipyridylthiourea 161

Proton observed:	amide
Solvent:	CDCl ₃
Starting volume of host solution	600 μL
Concentration of host solution:	3.91 mM
Concentration of guest solution:	23.47 mM
Association constant:	2,520 ± 252 M ⁻¹

Volume added/μL	Chemical Shift/ppm
0	8.822
20	8.923
40	8.993
50	9.047
60	9.045
80	9.146
100	9.152
125	9.197
150	9.217

Binding data for N-Ac-L-Phe 167 with dipyridylthiourea 161

Proton observed:	amide
Solvent:	CDCl ₃
Starting volume of host solution	600 μL
Concentration of host solution:	5.48 mM
Concentration of guest solution:	32.87 mM
Association constant:	5570 ± 557 M ⁻¹

Volume added/μL	Chemical Shift/ppm
0	8.805
10	8.837
20	8.858
30	8.918
40	8.957
50	8.991
75	9.091
100	9.144
150	9.191
200	9.204
250	9.211

Binding data for N-Ac-L-Phe 167 with dipyridylthiourea 161

Proton observed:	thiourea
Solvent:	CDCl ₃
Starting volume of host solution	600 μL
Concentration of host solution:	5.48 mM
Concentration of guest solution:	32.87 mM
Association constant:	2940 ± 294 M ⁻¹

Volume added/μL	Chemical Shift/ppm
0	7.75
10	7.90
30	8.28
40	8.46
100	9.21
150	9.45
200	9.53
250	9.56

Binding data for N-Ac-L-Phe 167 with dipyridylthiourea 161

Proton observed:	<i>N</i> -terminal amide
Solvent:	CDCl ₃
Starting volume of host solution	600 μL
Concentration of host solution:	5.48 mM
Concentration of guest solution:	32.87 mM
Association constant:	5600 ± 560 M ⁻¹

Volume added/μL	Chemical Shift/ppm
0	6.117
10	6.061
20	6.037
30	5.933
40	5.866
50	5.794
75	5.610
100	5.513
150	5.431
200	5.402
250	5.390

Binding data for N-Ac-D-Phe 168 with dipyridylthiourea 161

Proton observed:	amide
Solvent:	CDCl ₃
Starting volume of host solution	600 μ L
Concentration of host solution:	5.48 mM
Concentration of guest solution:	32.87 mM
Association constant:	3070 \pm 307 M ⁻¹

Volume added/ μ L	Chemical Shift/ppm
0	8.807
10	8.838
20	8.878
30	8.918
40	8.963
50	9.008
100	9.170
150	9.229
200	9.246
250	9.253

Binding data for N-Ac-D-Phe 168 with dipyridylthiourea 161

Proton observed:	thiourea
Solvent:	CDCl ₃
Starting volume of host solution	600 μL
Concentration of host solution:	5.48 mM
Concentration of guest solution:	32.87 mM
Association constant:	3520 ± 352 M ⁻¹

Volume added/μL	Chemical Shift/ppm
0	7.770
10	7.894
20	8.063
30	8.242
40	8.443
50	8.622
75	8.710
100	9.290
200	9.600
250	9.640

Binding data for N-Ac-D-Phe 168 with dipyridylthiourea 161

Proton observed:	<i>N</i> -terminal amide
Solvent:	CDCl ₃
Starting volume of host solution	600 μL
Concentration of host solution:	5.48 mM
Concentration of guest solution:	32.87 mM
Association constant:	2390 ± 239 M ⁻¹

Volume added/μL	Chemical Shift/ppm
0	6.120
10	6.062
20	6.008
30	5.950
40	5.886
50	5.821
100	5.570
150	5.472
200	5.445
250	5.432

Binding data for N-Ac-L-Asn 169 with dipyridylthiourea 161

Proton observed:	thiourea
Solvent:	CDCl ₃
Starting volume of host solution	600 μL
Concentration of host solution:	5.48 mM
Concentration of guest solution:	32.87 mM
Association constant:	2,000 ± 200 M ⁻¹

Volume added/μL	Chemical Shift/ppm
0	7.760
20	8.067
30	8.228
40	8.388
50	8.533
100	8.970
150	9.130
200	9.207
250	9.311
300	9.340

Binding data for N-Ac-L-Asn 169 with dipyridylthiourea 161

Proton observed:	amide
Solvent:	CDCl ₃
Starting volume of host solution	600 μL
Concentration of host solution:	5.48 mM
Concentration of guest solution:	32.87 mM
Association constant:	960 ± 96 M ⁻¹

Volume added/μL	Chemical Shift/ppm
0	8.805
20	8.868
30	8.900
40	8.932
50	8.961
100	9.050
150	9.095
200	9.113
250	9.141
300	9.148

Binding data for N-Ac-L-Asn 169 with dipyridylthiourea 161

Proton observed:	<i>N</i> -terminal amide
Solvent:	CDCl ₃
Starting volume of host solution	600 μL
Concentration of host solution:	5.48 mM
Concentration of guest solution:	32.87 mM
Association constant:	2100 ± 210 M ⁻¹

Volume added/μL	Chemical Shift/ppm
0	6.091
20	6.061
30	6.042
40	6.016
50	5.984
100	5.883
150	5.834
200	5.814
250	5.807
300	5.801

Binding data for N-Ac-D-Asn 170 with dipyridylthiourea 161

Proton observed:	thiourea
Solvent:	CDCl ₃
Starting volume of host solution	600 μL
Concentration of host solution:	5.48 mM
Concentration of guest solution:	32.87 mM
Association constant:	1060 ± 106 M ⁻¹

Volume added/μL	Chemical Shift/ppm
0	7.780
10	7.896
20	8.072
30	8.205
40	8.351
50	8.467
100	8.840
150	9.020
200	9.158
250	9.226
300	9.273

Binding data for N-Ac-D-Asn 170 with dipyridylthiourea 161

Proton observed:	amide
Solvent:	CDCl ₃
Starting volume of host solution	600 μL
Concentration of host solution:	5.48 mM
Concentration of guest solution:	32.87 mM
Association constant:	770 ± 77 M ⁻¹

Volume added/μL	Chemical Shift/ppm
0	8.803
10	8.824
20	8.848
30	8.871
40	8.894
50	8.913
100	8.975
150	9.014
200	9.039
250	9.050
300	9.058

Binding data for N-Ac-D-Asn 170 with dipyridylthiourea 161

Proton observed:	<i>N</i> -terminal amide
Solvent:	CDCl ₃
Starting volume of host solution	600 μL
Concentration of host solution:	5.48 mM
Concentration of guest solution:	32.87 mM
Association constant:	570 ± 57 M ⁻¹

Volume added/μL	Chemical Shift/ppm
0	6.177
10	6.096
30	6.101
40	6.087
50	6.070
100	5.997
150	5.953
200	5.928
250	5.918

Binding data for N-Ac-L-Gln 171 with dipyridylthiourea 161

Proton observed:	amide
Solvent:	CDCl ₃
Starting volume of host solution	600 μL
Concentration of host solution:	3.91 mM
Concentration of guest solution:	23.48 mM
Association constant:	9,000 ± 900 M ⁻¹

Volume added/μL	Chemical Shift/ppm
0	8.822
20	8.898
30	8.923
40	8.958
50	9.015
60	9.058
80	9.122
100	9.148
125	9.187
150	9.211

Binding data for N-Ac-D-Gln 172 with dipyridylthiourea 161

Proton observed:	amide
Solvent:	CDCl ₃
Starting volume of host solution	600 μL
Concentration of host solution:	3.91 mM
Concentration of guest solution:	23.48 mM
Association constant:	4,520 ± 452 M ⁻¹

Volume added/μL	Chemical Shift/ppm
0	8.822
20	8.912
30	8.938
40	8.978
50	9.031
60	9.069
80	9.135
100	9.172
125	9.224
150	9.245

Binding data for N-Boc-L-Gln 173 with dipyridylthiourea 161

Proton observed:	amide
Solvent:	CDCl ₃
Starting volume of host solution	600 μL
Concentration of host solution:	3.91 mM
Concentration of guest solution:	23.49 mM
Association constant:	1230 ± 123 M ⁻¹

Volume added/μL	Chemical Shift/ppm
0	8.819
10	8.852
20	8.884
30	8.912
40	8.955
50	8.964
75	9.055
100	9.104
125	9.162
150	9.189
175	9.210
200	9.222
250	9.234
300	9.246
350	9.246
450	9.250
550	9.250

Binding data for N-Boc-L-Gln 173 with dipyridylthiourea 161

Proton observed:	thiourea
Solvent:	CDCl ₃
Starting volume of host solution	600 μL
Concentration of host solution:	3.91 mM
Concentration of guest solution:	23.49 mM
Association constant:	1,150 ± M ⁻¹

Volume added/μL	Chemical Shift/ppm
0	7.789
10	7.950
20	8.093
30	9.210
40	8.388
50	8.402
75	8.770
100	8.975
125	9.172
150	9.320
175	9.403
200	9.435
250	9.497
300	9.543
350	9.562
450	9.591
550	9.606

Binding data for N-Boc-D-Gln 174 with dipyridylthiourea 161

Proton observed:	amide
Solvent:	CDCl ₃
Starting volume of host solution	600 μL
Concentration of host solution:	3.91 mM
Concentration of guest solution:	23.49 mM
Association constant:	850 ± 85 M ⁻¹

Volume added/μL	Chemical Shift/ppm
0	7.789
10	7.950
20	8.093
30	8.210
40	8.388
50	8.402
75	8.770
100	8.978
125	9.172
150	9.320
175	9.403
200	9.435
250	9.497
300	9.543
350	9.562
450	9.591
550	9.606

Binding data for N-Boc-D-Gln 174 with dipyridylthiourea 161

Proton observed:	thiourea
Solvent:	CDCl ₃
Starting volume of host solution	600 μL
Concentration of host solution:	3.91 mM
Concentration of guest solution:	23.49 mM
Association constant:	770 ± M ⁻¹

Volume added/μL	Chemical Shift/ppm
0	7.789
10	7.920
20	8.170
40	8.256
50	8.371
75	8.616
100	8.862
125	9.039
150	9.140
200	9.262
250	9.345
300	9.401
350	9.423
450	9.467

Binding data for N-Ac-L-Ser 175 with dipyridylthiourea 161

Proton observed:	amide
Solvent:	CDCl ₃
Starting volume of host solution	600 μL
Concentration of host solution:	3.91 mM
Concentration of guest solution:	23.49 mM
Association constant:	260 ± 26 M ⁻¹

Volume added/μL	Chemical Shift/ppm
0	8.800
10	8.837
20	8.859
30	8.883
40	8.906
75	8.976
100	9.016
125	9.049
150	9.077
250	9.148
300	9.164
400	9.209

Binding data for N-Ac-L-Ser 175 with thiourea 161

Proton observed:	thiourea
Solvent:	CDCl ₃
Starting volume of host solution	600 μ L
Concentration of host solution:	3.91 mM
Concentration of guest solution:	23.49 mM
Association constant:	$510 \pm 51 \text{ M}^{-1}$

Volume added/ μ L	Chemical Shift/ppm
0	7.795
10	7.944
20	8.054
30	8.180
40	8.291
75	8.604
100	8.779
125	8.913
150	9.017
200	9.118
250	9.270
300	9.322
400	9.455

Binding data for N-Ac-D-Ser 176 with thiourea 161

Proton observed:	thiourea
Solvent:	CDCl ₃
Starting volume of host solution	600 μL
Concentration of host solution:	3.91 mM
Concentration of guest solution:	23.49 mM
Association constant:	470 ± 47 M ⁻¹

Volume added/μL	Chemical Shift/ppm
0	7.795
10	7.945
20	8.059
30	8.174
40	8.289
50	8.385
75	8.614
100	8.777
125	8.916
250	9.255
300	9.356
400	9.477

Binding data for N-Ac-D-Ser 176 with thiourea 161

Proton observed:	amide
Solvent:	CDCl ₃
Starting volume of host solution	600 μL
Concentration of host solution:	3.91 mM
Concentration of guest solution:	23.49 mM
Association constant:	480 ± 48 M ⁻¹

Volume added/μL	Chemical Shift/ppm
0	8.800
10	8.834
20	8.857
30	8.878
40	8.902
50	8.924
75	8.974
100	9.015
125	9.049
150	9.077
200	9.122
250	9.144
300	9.177
400	9.216

Binding data for N-Ac-L-Trp 177 with dipyridylthiourea 161

Proton observed:	amide
Solvent:	CDCl ₃
Starting volume of host solution	600 μL
Concentration of host solution:	3.91 mM
Concentration of guest solution:	23.48 mM
Association constant:	12,400 ± 1,240 M ⁻¹

Volume added/μL	Chemical Shift/ppm
0	8.822
20	8.907
30	8.939
40	8.978
50	9.033
60	9.076
80	9.153
100	9.182
125	9.221
150	9.234

Binding data for N-Ac-D-Trp 178 with dipyridylthiourea 161

Proton observed:	amide
Solvent:	CDCl ₃
Starting volume of host solution	600 μL
Concentration of host solution:	3.91 mM
Concentration of guest solution:	23.48 mM
Association constant:	14,800 ± 1,480 M ⁻¹

Volume added/μL	Chemical Shift/ppm
0	8.822
20	8.899
30	8.927
40	8.975
50	9.022
60	9.068
80	9.144
100	9.183
125	9.229
150	9.248

Binding data for N-Boc-L-Trp 179 with dipyridylthiourea 161

Proton observed:	amide
Solvent:	CDCl ₃
Starting volume of host solution	600 μL
Concentration of host solution:	3.91 mM
Concentration of guest solution:	23.49 mM
Association constant:	3,100 ± 310 M ⁻¹

Volume added/μL	Chemical Shift/ppm
0	8.819
10	8.843
40	8.921
50	8.962
75	9.020
100	9.083
125	9.123
150	9.151
200	9.179
250	9.197
300	9.207
350	9.214
450	9.218

Binding data for N-Boc-L-Trp 179 with dipyridylthiourea 161

Proton observed:	thiourea
Solvent:	CDCl ₃
Starting volume of host solution	600 μL
Concentration of host solution:	3.91 mM
Concentration of guest solution:	23.49 mM
Association constant:	3,180 ± 318 M ⁻¹

Volume added/μL	Chemical Shift/ppm
0	7.770
10	7.930
40	8.364
50	8.535
75	8.906
100	9.213
125	9.365
150	9.444
200	9.505
250	9.558
300	9.579
350	9.593
450	9.622

Binding data for N-Boc-D-Trp 180 with dipyridylthiourea 161

Proton observed:	amide
Solvent:	CDCl ₃
Starting volume of host solution	600 μL
Concentration of host solution:	3.91 mM
Concentration of guest solution:	23.49 mM
Association constant:	1,690 ± M ⁻¹

Volume added/μL	Chemical Shift/ppm
0	8.817
10	8.860
20	8.902
40	8.984
50	9.043
75	9.146
100	9.239
125	9.288
150	9.318
175	9.339
200	9.352
250	9.367
300	9.358
350	9.391
450	9.394

Binding data for N-Boc-D-Trp 180 with thiourea 161

Proton observed:	thiourea
Solvent:	CDCl ₃
Starting volume of host solution	600 μL
Concentration of host solution:	3.91 mM
Concentration of guest solution:	23.49 mM
Association constant:	2,760 ± 276 M ⁻¹

Volume added/μL	Chemical Shift/ppm
0	7.770
10	8.000
20	8.170
40	8.420
50	8.584
75	8.917
100	9.206
125	9.310
150	9.431
175	9.470
200	9.505
250	9.563
300	9.593
350	9.610
450	9.633

Binding data for R-Naproxen 181 with dipyridylthiourea 161

Proton observed:	amide
Solvent:	CDCl ₃
Starting volume of host solution	600 μL
Concentration of host solution:	3.91 mM
Concentration of guest solution:	23.48 mM
Association constant:	26,200 ± 2,620 M ⁻¹

Volume added/μL	Chemical Shift/ppm
0	8.822
20	8.912
30	8.964
40	9.047
50	9.129
60	9.194
80	9.312
100	9.369
125	9.435
150	9.458

Binding data for S-Naproxen 182 with dipyridylthiourea 161

Proton observed:	amide
Solvent:	CDCl ₃
Starting volume of host solution	600 μL
Concentration of host solution:	3.91 mM
Concentration of guest solution:	2.348 mM
Association constant:	28,300 ± 2,830 M ⁻¹

Volume added/μL	Chemical Shift/ppm
0	8.822
20	8.914
30	8.973
40	9.057
50	9.135
60	9.199
80	9.299
100	9.373
125	9.411
150	9.435

Binding data for R-Naproxen 181 with second generation thiourea 183

Proton observed:	pyridyl triplet
Solvent:	CDCl ₃
Starting volume of host solution	600 μL
Concentration of host solution:	3.74 mM
Concentration of guest solution:	44.81 mM
Association constant:	1,570 ± 157 M ⁻¹

Volume added/μL	Chemical Shift/ppm
0	7.813
10	7.786
20	7.752
30	7.712
40	7.687
50	7.666
75	7.636
100	7.625
125	7.616
150	7.611
200	7.606

Binding data for S-Naproxen 182 with second generation thiourea 181

Proton observed:	pyridyl triplet
Solvent:	CDCl ₃
Starting volume of host solution	600 μL
Concentration of host solution:	3.74 mM
Concentration of guest solution:	44.82 mM
Association constant:	1,870 ± 187 M ⁻¹

Volume added/μL	Chemical Shift/ppm
0	7.813
10	7.788
20	7.747
30	7.712
50	7.665
75	7.640
100	7.628
125	7.620
150	7.617
200	7.610

Binding data for N-Boc-L-Trp 179 with second generation thiourea 183

Proton observed:	pyridyl triplet
Solvent:	CDCl ₃
Starting volume of host solution	600 μL
Concentration of host solution:	3.91 mM
Concentration of guest solution:	23.49 mM
Association constant:	1,925 ± 193 M ⁻¹

Volume added/μL	Chemical Shift/ppm
0	8.818
10	8.857
20	8.896
40	8.980
50	9.035
75	9.137
100	9.223
125	9.264
150	9.287
175	9.303
200	9.309
250	9.323
350	9.333
450	9.335

Binding data for N-Boc-D-Trp 180 with second generation thiourea 183

Proton observed:	pyridyl triplet
Solvent:	CDCl ₃
Starting volume of host solution	600 μL
Concentration of host solution:	3.91 mM
Concentration of guest solution:	23.49 mM
Association constant:	3,785 ± 379 M ⁻¹

Volume added/μL	Chemical Shift/ppm
0	7.770
10	7.930
20	8.070
40	8.364
50	8.535
75	8.906
100	9.213
125	9.365
150	9.444
175	9.484
200	9.505
250	9.558
300	9.579
350	9.593
450	9.622

Binding data for N-Boc-L-Glu 201 with macrocycle 193

Proton observed:	thiourea
Solvent:	DMSO-d ₆
Starting volume of host solution	800 μL
Concentration of host solution:	2.35 mM
Concentration of guest solution:	94.16 mM
Association constant:	7,140 ± 714 M ⁻¹

Volume added/μL	Chemical Shift/ppm
0	8.395
20	8.447
40	8.548
60	8.653
80	8.754
100	8.856
140	9.093
180	9.251
220	9.359
260	9.444
300	9.483
360	9.510
420	9.537
480	9.556
540	9.556
600	9.564

Binding data for N-Boc-L-Glu 201 with macrocycle 193

Proton observed:	amide
Solvent:	DMSO-d ₆
Starting volume of host solution	800 μL
Concentration of host solution:	2.35 mM
Concentration of guest solution:	94.16 mM
Association constant:	4,660 ± 466 M ⁻¹

Volume added/μL	Chemical Shift/ppm
0	9.471
20	9.496
40	9.555
60	9.603
80	9.656
100	9.713
140	9.803
180	9.886
220	9.946
260	9.989
300	10.011
360	10.033
420	10.048
480	10.050
540	10.058
600	10.068

Binding data for N-Boc-D-Glu 202 with macrocycle 193

Proton observed:	thiourea
Solvent:	DMSO-d ₆
Starting volume of host solution	800 μL
Concentration of host solution:	2.35 mM
Concentration of guest solution:	94.16 mM
Association constant:	1,300 ± 130 M ⁻¹

Volume added/μL	Chemical Shift/ppm
0	8.395
10	8.430
20	8.464
30	8.505
50	8.586
80	8.720
100	8.828
120	8.911
140	9.019
180	9.187
220	9.296
260	9.934
300	9.427
340	9.460
380	9.481
420	9.487

Binding data for N-Boc-D-Glu 202 with macrocycle 193

Proton observed:	amide
Solvent:	DMSO-d ₆
Starting volume of host solution	800 μL
Concentration of host solution:	2.35 mM
Concentration of guest solution:	94.16 mM
Association constant:	730 ± 73 M ⁻¹

Volume added/μL	Chemical Shift/ppm
0	9.471
10	9.487
20	9.502
30	9.521
50	9.557
80	9.618
100	9.660
120	9.703
140	9.746
180	9.807
220	9.865
260	9.895
300	9.926
340	9.942
380	9.949
420	9.956

5.6 X-Ray Data for Achiral Pyridyl Tweezer 144

Table 1. Crystal data and structure refinement for C₂₃H₃₂N₆O₂S.

Identification code	99KIL001	
Empirical formula	C ₂₃ H ₃₂ N ₆ O ₂ S	
Formula weight	456.61	
Temperature	150(2) K	
Wavelength	0.71073 Å	
Crystal system	Triclinic	
Space group	P-1	
Unit cell dimensions	a = 9.4566(3) Å	α = 89.975(2)°.
	b = 10.7149(4) Å	β = 79.123(2)°.
	c = 13.2326(4) Å	γ = 65.1932(12)°.
Volume	1190.56(7) Å ³	
Z	2	
Density (calculated)	1.274 Mg/m ³	
Absorption coefficient	0.168 mm ⁻¹	
F(000)	488	
Crystal size	0.20 x 0.05 x 0.05 mm ³	
Theta range for data collection	2.10 to 26.36°.	
Index ranges	-11 ≤ h ≤ 11, -13 ≤ k ≤ 13, -16 ≤ l ≤ 16	
Reflections collected	18090	
Independent reflections	4737 [R(int) = 0.0430]	
Completeness to theta = 26.36°	97.1 %	
Max. and min. transmission	0.9917 and 0.9672	
Refinement method	Full-matrix least-squares on F ²	
Data / restraints / parameters	4737 / 0 / 418	
Goodness-of-fit on F ²	1.081	
Final R indices [I > 2σ(I)]	R1 = 0.0429, wR2 = 0.0976	
R indices (all data)	R1 = 0.0529, wR2 = 0.1023	
Extinction coefficient	0.034(3)	
Largest diff. peak and hole	0.244 and -0.217 e.Å ⁻³	

Table 3. Bond lengths [Å] and angles [°] for C₂₃H₃₂N₆O₂S.

S(1)-C(12)	1.6833(18)	C(14)-N(5)-C(18)	117.67(15)
O(2)-C(19)	1.248(2)	C(19)-N(6)-C(20)	123.56(16)
N(5)-C(14)	1.337(2)	C(12)-N(4)-C(13)	125.59(16)
N(5)-C(18)	1.346(2)	C(10)-N(2)-C(6)	118.65(15)
O(1)-C(5)	1.233(2)	C(5)-N(1)-C(4)	123.72(16)
N(6)-C(19)	1.326(2)	C(12)-N(3)-C(11)	124.64(16)
N(6)-C(20)	1.461(2)	N(2)-C(6)-C(7)	122.72(17)
N(4)-C(12)	1.353(2)	N(2)-C(6)-C(5)	116.47(15)
N(4)-C(13)	1.447(2)	C(7)-C(6)-C(5)	120.80(16)
N(2)-C(10)	1.335(2)	C(6)-C(7)-C(8)	118.22(17)
N(2)-C(6)	1.349(2)	N(5)-C(18)-C(17)	123.95(16)
N(1)-C(5)	1.331(2)	N(5)-C(18)-C(19)	116.20(15)
N(1)-C(4)	1.454(2)	C(17)-C(18)-C(19)	119.85(16)
N(3)-C(12)	1.343(2)	N(5)-C(14)-C(15)	121.96(16)
N(3)-C(11)	1.449(2)	N(5)-C(14)-C(13)	116.33(16)
C(6)-C(7)	1.381(3)	C(15)-C(14)-C(13)	121.72(16)
C(6)-C(5)	1.511(3)	O(2)-C(19)-N(6)	123.91(16)
C(7)-C(8)	1.388(3)	O(2)-C(19)-C(18)	120.52(16)
C(18)-C(17)	1.380(3)	N(6)-C(19)-C(18)	115.57(15)
C(18)-C(19)	1.505(2)	N(3)-C(11)-C(10)	109.40(15)
C(14)-C(15)	1.399(3)	O(1)-C(5)-N(1)	124.41(17)
C(14)-C(13)	1.510(3)	O(1)-C(5)-C(6)	120.76(16)
C(11)-C(10)	1.515(2)	N(1)-C(5)-C(6)	114.83(15)
C(10)-C(9)	1.396(2)	N(2)-C(10)-C(9)	122.08(16)
C(17)-C(16)	1.391(3)	N(2)-C(10)-C(11)	116.95(15)
C(16)-C(15)	1.373(3)	C(9)-C(10)-C(11)	120.97(16)
C(20)-C(21)	1.518(3)	C(18)-C(17)-C(16)	117.86(17)
C(8)-C(9)	1.380(3)	N(3)-C(12)-N(4)	113.92(16)
C(21)-C(22)	1.525(3)	N(3)-C(12)-S(1)	122.57(13)
C(22)-C(23)	1.522(3)	N(4)-C(12)-S(1)	123.50(14)
C(3)-C(4)	1.518(3)	C(15)-C(16)-C(17)	119.00(18)
C(3)-C(2)	1.529(3)	N(4)-C(13)-C(14)	112.33(15)
C(2)-C(1)	1.510(3)	N(6)-C(20)-C(21)	112.00(15)
		C(16)-C(15)-C(14)	119.55(17)

C(9)-C(8)-C(7)	119.67(17)	C(4)-C(3)-C(2)	111.88(17)
C(20)-C(21)-C(22)	112.90(16)	N(1)-C(4)-C(3)	113.38(16)
C(8)-C(9)-C(10)	118.64(18)	C(1)-C(2)-C(3)	112.69(18)
C(23)-C(22)-C(21)	113.45(17)		

Symmetry transformations used to generate equivalent atoms:

References

1. J. M. Lehn, *Angew. Chem., Int. Ed. Engl.*, **1988**, *27*, 89.
2. J. M. Cram and D. J. Cram, *Science*, **1974**, *183*, 803.
3. C. J. Pederson, *J. Am. Chem. Soc.*, **1967**, *89*, 7017.
4. O. Kennard and J. Walker, *J. Chem. Soc.*, **1963**, 5513.
5. J. F. Riordan, K. D. McElvany and C. L. Borders, *Science*, **1977**, *195*, 884.
6. M. H. Freedman, A. L. Grossberg and D. Pressman, *J. Biol. Chem.*, **1968**, *195*, 884.
7. B. Dietrich, D. L. Fyles, T. M. Fyles and J-M. Lehn, *Helv. Chim. Acta*, **1979**, 280.
8. F. Garcia-Tellado, S. Goswami, S-K. Chang, S. Geib and A. D. Hamilton, *J. Am. Chem. Soc.*, **1990**, *112*, 7393.
9. A. Echavarren, A. Galán, J-M. Lehn, J. de Mendoza. *J. Am. Chem. Soc.*, **1989**, *111*, 4994.
10. A. Echavarren, A. Galán, J. de Mendoza. *J. Am. Chem. Soc.*, **1992**, *114*, 1511.
11. P. Schießl, F. P. Schmidtchen, *Tetrahedron Lett.*, **1993**, *34*, 2449.
12. L. Sebo, B. Schweizer and F. Diederich, *Helv. Chim. Acta*, **2000**, *83*, 80.
13. C. Schmuck, *Chem. Commun.*, **1999**, 843.
14. C. Schmuck, *Chem. Eur. J.*, **2000**, *6*, 709.
15. M. Martín, M. Almaraz, J. V. Hernández, A. Tejada, M. Cruz Caballero and J. R. Morán, *Heterocycles*, **1999**, *50*, 47.
16. B. J. Whitlock and H. W. Whitlock, *J. Am. Chem. Soc.*, **1990**, *112*, 3910.
17. L. J. Lawless and A. P. Davies, *Chem. Commun.*, **1999**, 9.
18. A. Metzger and E. V. Anslyn, *Angew. Chem., Int. Ed. Engl.*, **1998**, *37*, 649.
19. T. Ross Kelly, R. L. Xie, C. K. Weinreb and T. Bregant, *Tetrahedron Lett.*, **1998**, *39*, 3675.
20. A. Bilz, T. Stork and G. Helmchen, *Tetrahedron: Asymmetry*, **1997**, *8*, 3999.
21. S. Flack, J-L, Chaumette, G. J. Langley, M. Webster and J. D. Kilburn, *J. Chem. Soc., Chem. Commun.*, **1993**, 399.
22. P. D. Henley, C. P. Waymark, I. Gillies and J. D. Kilburn, *J. Chem. Soc., Perkin Trans. 1*, **2000**, 1021.
23. T. Fessmann and J. D. Kilburn, *Angew. Chem., Int. Ed. Engl.*, **1999**, *38*, 1993.
24. L. Owens, . Thilgen, C. Knobler and F. Diederich, *Helv. Chim. Acta*, **1993**, 2757.
25. J. Cuntze and F. Diederich, *Helv. Chim. Acta*, **1997**, 897.

26. P. J. Smith, M. V. Reddington and C. S. Wilcox, *Tetrahedron Lett.*, **1992**, *41*, 6085.
27. E. Fan, A. van Arman, S. Kincaid and A.D. Hamilton, *J. Am. Chem. Soc.*, **1993**, *115*, 369.
28. S. Nishizawa, P. Buhlmann, M. Iwao and Y. Umezawa, *Tetrahedron Lett.*, **1995**, *36*, 6483.
29. C. Raposo, M. Crego, L. Mussons, C. Caballero and R. R. Morán, *Tetrahedron Lett.*, **1994**, *35*, 3409.
30. (a) G.J. Pernia, J.D. Kilburn, M. Rowley, *J. Am. Chem. Soc.*, **1995**, 305. (b) G.J. Pernia, J.D. Kilburn, J.W. Essex, R.J. Mortishire-Smith, M. Rowley, *J. Am. Chem. Soc.*, **1996**, *118*, 10220.
31. (a) K. Jeong, J. W. Park and Y. L. Cho, *Tetrahedron Lett.*, **1996**, *37*, 2795 (b) S. Nishizawa, P. Buhlmann, M. Iwao and Y. Umezawa, *Tetrahedron Lett.*, **1995**, *36*, 6483. (c) H. Ishida, M. Suga, K. Donowaki and K. Ohkubo, *J. Org. Chem.*, **1995**, *60*, 5374. (d) A. M. Kelly-Rowley, V. M. Lynch and E. V. Anslym, *J. Am. Chem. Soc.*, **1995**, *117*, 3438. (e) J. Scheerder, M. Fochi, J.F.J. Engbersoen and D. N. Reinhoudt, *J. Org. Chem.*, **1994**, *59*, 7815 and references cited therein.
32. (a) P. B. Savage, S. K. Holmgren and S. H. Gellman, *J. Am. Chem. Soc.*, **1994**, *116*, 4069. (b) K. Worm. F. P. Schmidtchen, A. Schier, A. Schafer and M. Hesse, *Angew. Chem., Int. Ed. Engl.*, **1994**, *33*, 327.
33. J. T. Bien, M. J. Eschner, B. D. Smith, *J. Org. Chem.*, **1995**, *60*, 4525.
34. M. P. Groziak, A. D. Ganguly and P. D. Robinson, *J. Am. Chem. Soc.*, **1995**, *60*, 4525.
35. W.-S. Yeo, J.-I. Hong, *Tetrahedron Lett.*, **1998**, *39*, 8137-8140.
36. E. Kimura, A. Sakonaka, T. Yatsunami and M. Kodama, *J. Am. Chem. Soc.*, **1981**, *103*, 3041.
37. B. Dietrich, M. W. Hosseini, J. M. Lehn and R. B. Sessions, *J. Am. Chem. Soc.*, **1981**, *103*, 1282.
38. M. W. Hosseini and J. M. Lehn, *J. Am. Chem. Soc.*, **1982**, *104*, 3525.
39. J. M. Lehn, R. Méric, J-P. Vigeron, I. Bkouche-Waksman and C. Pascard, *J. Chem. Soc., Chem. Commun.*, **1991**, 62.
40. H. Patel, J. D. Kilburn, G. J. Langley, P. D. Edwards, T. Mitchell and R. Southgate, *Tetrahedron Lett.*, **1994**, *35*, 481.
41. B. R. Cameron and S. J. Loeb, *Chem. Commun.*, **1997**, 573.

42. A. P. Bisson, V. M. Lynch, M-K. C. Monahan and E. V. Anslyn, *Angew. Chem., Int. Ed. Engl.*, **1997**, *36*, 2341.
43. V. Král, A. Andrievsky and J. L. Sessler, *J. Am. Chem. Soc.*, **1995**, *117*, 2953.
44. V. Král, A. Andrievsky, V. Lynch and J. L. Sessler, *J. Am. Chem. Soc.*, **1997**, *119*, 9385.
45. M. Bonnat, J. D. Kilburn and M. Bradley, *Tetrahedron Lett.*, **1996**, *37*, 5409.
46. J. S. Albert and A. D. Hamilton, *Tetrahedron Lett.*, **1993**, *34*, 7363.
47. U. Nagel, E. Kinzel and J. Andrade, *Chem. Ber.*, **1986**, *119*, 3326.
48. Studinger and Meyer, *Helv. Chim. Acta*, **1919**, *2*, 635.
49. K. Burgess, J. Ibarzo and D. S. Linthicum, *J. Am. Chem. Soc.*, **1997**, *119*, 1556.
50. O. Mitsunobu, M. Wada and T. Sano, *J. Am. Chem. Soc.*, **1972**, *94*, 679.
51. Y. Tobe, S. Sasaki, K. Hiroshi and K. Naemura, *Tetrahedron Lett.*, **1997**, *38*, 4791.
52. D. J. Cram, *Angew. Chem., Int. Ed. Engl.*, **1988**, *27*, 1009.
53. C. A. Hunter and D. H. Purvis, *Angew. Chem., Int. Ed. Engl.*, **1992**, *31*, 792.
54. T. H. Fife and T.J. Przystas, *J. Am. Chem. Soc.*, **1982**, *104*, 2251.
55. P. Scrimin, U. Tonellato, D. Milani and R. Fornasier, *J. Chem. Soc., Perkin Trans. II*, **1986**, 233.
56. J. Smith, J. L. Liras, S. E. Schneider and E. V. Anslyn, *J. Org. Chem.*, **1996**, *61*, 8811.
57. K. Kavallieratos, C. M. Bertao and R. H. Crabtree, *J. Org. Chem.*, **1999**, *64*, 1675.
58. F. Mohamadi, N. G. J. Richards, W. C. Guida, R. Liskamp, M. Lipton, C. Caufield, G. Chang, T. Hendrickson and W. C. Still, *J. Comp. Chem.*, **1990**, *11*, 440.
59. W. L. Jorgensen and J. Tirado-Rives, **1988**, *110*, 1657.
60. W. C. Still, A. Tempczyk and R. C. Hawley, *J. Am. Chem. Soc.*, **1990**, *112*, 6127.
61. J. P. Ryckaert, G. Ciccotti and H. J. C. Berendsen, *J. Comput. Phys.*, **1977**, *23*, 327.
62. T. Shioiri, K. Ninomiya and S. Yamada, *J. Am. Chem. Soc.*, **1972**, *94*, 6203.
63. E. C. Huskisson and A. Greenwood, *European Journal of Rheumatology and Inflammation*, **1984**, *6*, 242.
64. A. Franck and C. Ruchardt, *Chem. Lett.*, **1984**, *8*, 1431.
65. G. A. Olah, S. C. Narang, B. Gupta and R. Malhotra, *J. Org. Chem.*, **1979**, *44*, 1247.
66. (i) C. S. Wilcox and M. D. Cowart, *Tetrahedron Lett.*, **1996**, *27*, 5563 (ii) C. S. Wilcox In *Frontiers in Supramolecular Organic Chemistry and Photochemistry*; H.-J. Schneider and H. Durr, Ed; VCH: Weinheim, **1991**; pp 123.
67. S. Soo Yoon and W. C. Still, *Tetrahedron*, **1995**, *51*, 567.

68. D. M. Kneeland, K. Ariga, V. M. Lynch, C-Y. Huang and E. V. Anslyn, *J. Am. Chem. Soc.*, **1993**, *115*, 10042.
69. D. F. Lawson and V. D. Mochel, *J. Am. Chem. Soc.*, **1972**, *94*, 6203.
70. J. C. Ma and D. A. Dougherty, *Chem. Rev.*, **1997**, *97*, 1303.
71. (a) S. Kubik and R. Goddard, *J. Org. Chem.*, **1999**, *64*, 9475. (b) S. Kubik, *J. Am. Chem. Soc.*, **1999**, *121*, 5846.